Thinking inside and outside the blood vessel: S1P-mediated control of vascular tone and the impact of CMV infection

By

Daniel Kerage

A thesis submitted in partial fulfillment of the requirements for the degree of

Doctor of Philosophy

In

Immunology

Department of Medical Microbiology and Immunology
University of Alberta

ABSTRACT

Sphingosine 1–phosphate (S1P), a bioactive lipid, has both endothelial barrier enhancing and disrupting effects, but also regulates vascular tone. The concepts of endothelial permeability and vascular tone have traditionally been studied separately. In this thesis, I demonstrate novel findings that these concepts are interconnected. Using a novel methodology I found that infusion of physiological concentrations of S1P (<1μmol/L) maintained endothelial barrier and had no significant effects on vascular tone in mouse uterine arteries. At a high physiological concentration, 1μmol/L, S1P-induced permeability permitted leakage of a co-infused vasoconstrictor (5 nmol/L U46619, a thromboxane A_2 mimetic analog) to the vascular smooth muscle cells (VSMCs) increasing vascular tone. Such endothelial permeability stimulated by S1P, was induced in an $S1P_3$ receptor–dependent manner. These findings reveal a new paradigm of vascular tone control by S1P, in which S1P maintains endothelial barrier that prevents leakage of circulating vasoactive agents to the VSMCs, but also high-end physiological concentrations of S1P (1 μmol/L) induces endothelial permeability that permits leakage of such vasoactive agents to the VSMCs maintaining normal vascular tone. These are important findings as the role of S1P in the control of endothelial barrier has only been previously investigated in cultured endothelial cells and venules. On the other hand, the S1P-induced endothelial permeability at pathophysiological concentrations (10 μmol/L), permitted its own leakage and/or that of co-infused U46619, strongly increasing vascular tone. Equally, endothelial permeability stimulated by thrombin, lipopolysaccharide (LPS) and cytomegalovirus glycoprotein B also facilitated leakage of U46619 to the VSMCs. These findings suggest that excessive increase in endothelial permeability can promote increased vascular tone in uterine arteries. Under pathological conditions, such increased vascular tone could have detrimental effects in reproduction and

pregnancy by limiting blood and nutrient supply to important organs for reproduction (ovaries, cervix etc) or to the fetus during pregnancy (leading to pregnancy disorders like intrauterine growth restriction that affect fetal growth). I also found that S1P (3 μmol/L) plays a potentiating role in U46619 (20 nmol/L)-induced vascular tone in mesenteric arteries from female mice. These arteries are however, less reactive to S1P or U46619 than uterine arteries. Such reduced reactivity implies that leakage of vasoconstrictors through the endothelium of systemic arteries is more tightly controlled, meaning that, leakage will likely occur only at pathological concentrations of S1P. Interestingly, I found that mesenteric arteries from male mice were remarkably different. First, their reactivity was similar to that of uterine arteries; secondly, infusion of U46619 (5 nmol/L) or S1P (1 μmol/L) alone, increased vascular tone, each of which was however, significantly lower compared to that induced when the two drugs were co-infused. This means that mesenteric arteries from male mice are likely leakier than those from female mice. This dichotomy of vascular responses found in males and females is not surprising as there are many examples of sex-based differences in vascular responses. Unexpectedly, U46619-induced vascular tone in the bath in mesenteric arteries from $S1P_3$ KO male mice was dramatically decreased compared to the wildtype control, suggesting that in these arteries, U46619-induced responses could be occurring partly through the S1P pathway. Consistent with these assumptions, I provided the first evidence that thromboxane A_2 (TXA_2) (using U46619), at pathophysiological concentrations (20 nmol/L) could increase endothelial permeability that was accompanied with increased vascular tone in a mechanism that depended on S1P signaling. While these results indicate that TXA_2 stimulates downstream S1P signaling, I also demonstrated novel data indicating that cytomegalovirus (CMV) infection enhances the vascular tone induced by TXA_2, but also decreases the dependence of TXA_2 on the S1P for downstream signaling.

CMV infection also opened up an alternative mechanism through which TXA_2 increased vascular tone in uterine arteries that was independent of the S1P pathway. Additional studies will be needed to uncover the details of the mechanisms through which CMV infection modulates the vascular tone induced by TXA_2.These results indicate that CMV infection can contribute to the pathogenesis of vascular-related complications such as hypertension or pregnancy-related disorders like intrauterine growth restriction Collectively, there is therapeutic promise in targeting the S1P pathway for treatment of vascular disorders caused by TXA_2-mediated actions, but also that of CMV infection.

PREFACE

The research output presented in this thesis involves a collaborative effort of experimental, intellectual and financial support. All experiments, analyses and results presented in Chapter 3: "A novel mechanism for vascular tone regulation in arteries by sphingosine 1-phosphate through endothelial barrier control" were conducted by Daniel Kerage with the exception of experimental support in the data presented in Figure 3.1A by Maggie Wang, Figure 3.1B, C by Meagan Brown and Figure 3.5C by Martina Mackova. All the experiments, analyses and results presented in Chapter 4: "Sphingosine 1-phosphate-induced nitric oxide production regulates endothelial permeability and vascular tone in mouse uterine arteries", Chapter 5: "Thromboxane A_2 increases endothelial permeability and vascular tone through a novel pathway stimulated by sphingosine 1-phosphate" and Chapter 6: "Cytomegalovirus infection dampens the vascular tone induced by thromboxane A_2 via the S1P pathway" were conducted by Daniel Kerage except in Chapter 6 where mice were infected by Dr. Denise Hemmings. In all the Chapters presented in this thesis Dr. Denise Hemmings provided intellectual, financial support from grants awarded to her from CIHR, NSERC and WCHRI as well as securing ethics approvals for the studies. The ethics approval regarding the procedures for humane mouse handling, euthanization and disposal, were granted by the University of Alberta's Animal Care and Use Committees under the guidelines outlined by the Canadian Council of Animal Care. The ethics approval for using umbilical cords from normal term pregnancies to isolate endothelial cells (HUVECs) was also sought and granted by the Research Ethics Board at the University of Alberta, the Royal Alexandria Hospital, and written consent from the donors. Permission to use Figures 1.7, 1.8 and 1.9 was granted by Morgan and Claypool publishers, whereas the use of Figures 1.14 and 1.15 was granted by the American Society for Microbiology. This thesis contains ideas and information from a previously published review by Kerage D, Brindley DN and Hemming DG (2014).

DEDICATION

This work is dedicated to my mum madam *Agnes Nyasuguta*, without whom I could not have been educated, Mama, you are the best!

ACKNOWLEDGEMENT

Well, finally the ship docks! I have sailed through the deep waters, but I passed through great hands, both big and small that helped me to remain on course and successfully get into the shore. I was privileged to work with my supervisor Dr. Denise G. Hemmings, your patience, guidance, critique, and many advises helped me to remain focussed. I can't thank you enough for the many local, national and international scientific meetings I was lucky to attend. Some of these were very expensive but your hand was exceptionally generous, and I had the pleasure of meeting senior investigators in the fields of S1P and vascular biology, and the experiences were very rewarding. My great appreciation also goes to my committee members Drs. Sandra Davidge and Deborah Burshtyn you were the best, the friendliest of committee members I could imagine of, your intellectual contributions to my work, your patience and support throughout my program will forever be remembered. Drs. Frances Plane and Viswanathan Natarajan, I know you have busy schedules; I truly thank you for sparing your time to be part of my examining committee. Dr. Troy Baldwin, thank you for accepting to chair my defence exam. Edan Foley for his great guidance and support during my PhD program. Lots of thanks too to Anne Giles at MMI for your support in many occasions during my program, your kindness is the best. I can't forget the many former and present members of Hemmings' Lab that I interacted with Martina Mackova, Meagan Brown, Maggie Wang, Shreya Amin, Meagan Timmons, Katie Kinaschuk, Hala Moraich, Amanda Cao, Veronika Berghold, Kelsey McCarroll, Clicia Rode de Oliveira, Samina Sana, Jennifer Stanfel, Ashley Davey, Randi Gombos, Nasim Boroumand, Robert Patry, Caroline Alexandria and Neil Brett, you all shaped my life at the U of A in many different ways, your critiques during the Hemmings' Writing Club/Meetings helped sharpen my thought process, and as you can imagine these skills will ever be with me. Maggie, Meagan, Shreya (data not included in the thesis) and Martina I can't thank you enough for contributing data to my thesis work. I also recognize that an intraluminal flow protocol previously generated by Randi Gombos and Denise Hemmings was important in helping me establish a novel technique for measuring endothelial permeability. I also appreciate the help I received from Denise Hemmings in infecting mice for experiments in chapter 6. In the Davidge Lab, Jude Morton, you may pass as an unsung hero but I greatly benefitted from your experiences in vascular biology, thank you. Subhadeep Chakrabarti, your generosity in sharing your cultured cells and your skills will always be remembered. I received many great ideas from the Hemmings/Davidge/ Bourque lab

members during Journal club/Lab meetings, those ideas are now finally part of my thesis, thank you guys. I will also thank the members of Mitchell and Olson Labs; you made my life at the U of A bearable in many different ways. While serving as the President of African Students' Association at the U of A, I interacted with some of the best souls around not only from the African community but also from other student groups, boy! those parties, BBQs, soccer competitions, cultural festivals, movie night, seminars etc, my social life could not have been any better.

Folks, you are the reason I have put together this great story. Through your hands, a scientist is born; I can now bend down and smell a flower! Your contributions will forever be cherished. Thank you!!!

TABLE OF CONTENTS

CHAPTER 1: INTRODUCTION 1

1.1. Summary and significance of study 1

1.2. Blood vessel structure and function: overview on vascular tone control 2

1.2.1 Vasodilation 3

1.2.1.1. Mechanisms for induction of vasodilation 3

1.2.1.2. Endothelial-derived vasodilators 5

1.2.1.2.1. PGI_2 and NO 5

1.2.1.2.2. Endothelial-derived hyperpolarization (EDH) 6

1.2.1.2.3. Carbon monoxide (CO) and hydrogen sulfide (H_2S) 7

1.2.1.3. Conducted vasodilation 8

1.2.2. Vasoconstriction 9

1.2.2.1. Mechanism for induction of vasoconstriction 9

1.2.2.2. Factors that stimulate vasoconstriction 10

1.2.2.2.1. Myogenic tone 10

1.2.2.2.2. Local and circulating factors 11

1.2.3. Factors with dual effects on vascular tone control 13

1.2.3.1. S1P 13

1.2.3.2. Endothelins 13

1.2.3.3. Membrane channels 14

1.2.3.4. Effect of blood flow on vascular tone 15

1.2.3.4.1. Blood flow–induced shear stress and vasodilation 15

1.2.3.4.2. Blood flow–induced mechanotransduction and vasoconstriction 15

1.2.3.5. The autonomic nervous system 16

1.3. Molecular passage across the endothelium 17

1.3.1. The transcellular pathway and molecular transport across endothelium 17

1.3.1.1. Mechanisms of caveolae-mediated transcytosis 18

1.3.1.2. Cav-1 in regulation of endothelial barrier 19

1.3.2. Paracellular or intercellular pathway in molecular transport between cells 20

1.3.2.1. The role of AJ in regulating endothelial barrier 21

1.3.2.2. The TJ as linkers of the cell-cell junctions 22
1.3.2.3. GJ as mediators of intercellular communication 23
1.3.2.4. Myoendothelial gap junctions in endothelial-smooth muscle communication 25
1.4. Extracellular anchors and their roles in the control of endothelial barrier 25
1.4.1. Focal adhesions as points of attachment for cellular stability 25
1.5. Endothelial cytoskeleton as a player in the control of endothelial barrier 26
1.5.1. The role of actin filaments 27
1.5.2. The role of actomyosin contractile machinery in the control of endothelial barrier 27
1.5.3. The role of microtubules in endothelial barrier control 28
1.5.4. The role of intermediate filaments in the control of endothelial barrier 29
1.6. Factors that generally increase endothelial permeability 29
1.7. S1P 30
1.7.1. Sphingolipid metabolism 30
1.7.1.1. S1P metabolizing enzymes 31
1.7.1.1.1. Sphingosine kinases: similarities and differences 31
1.7.1.1.1.1. SK-1 31
1.7.1.1.1.2. SK-2 and functional characterization 32
1.7.1.1.2. Phosphatases: SPPs and LPPs 34
1.7.1.1.3. SPL 35
1.7.1.2. Circulating S1P and its carriers 36
1.7.1.3. Intracellular S1P signaling 36
1.7.1.4. S1P transport out of cells 37
1.7.1.5. Extracellular and “inside-out” S1P signaling 37
1.7.2. S1P and endothelial permeability: effects on cell-cell junctions 38
1.7.2.1. S1P effects on AJ 48
1.7.2.2. S1P effects on TJ 40
1.7.2.3. S1P effects on GJ 40
1.7.3. S1P-mediated effects on endothelial cytoskeletal function and the impact on endothelial permeability 41

1.7.3.1. S1P effects on actin microfilaments 41
1.7.4. S1P and endothelial permeability in *in vivo* models 42
1.7.4.1. S1P and ALI 42
1.7.4.2. S1P and anaphylaxis 43
1.7.4.3. S1P and Ischemia–Reperfusion (I/R) Injury 44
1.7.5. S1P and vasodilation 45
1.7.6. S1P and vasoconstriction 46
1.7.7. Vascular tone control by S1P 48
1.8. AA metabolism 49
1.8.1. Regulation of the functions of COX-1 and COX-2 50
1.8.1.1. TXA_2 biosynthesis and related pathways 51
1.8.1.2. The biological functions of TXA_2 51
1.8.1.3. TXA_2 and vascular tone control 54
1.9. Infections, inflammation and vascular function 54
1.9.1. CMV infection 55
1.9.1.1. CMV infection: Clinical manifestations 56
1.9.1.2. CMV infection: Treatments 56
1.9.1.3. The CMV virion structure and overview on cell entry 58
1.9.1.3.1. Proposed entry mechanisms: role of CMV glycoproteins and cell receptors 58
1.9.1.3.2. Cytoplasmic–nuclear translocation of internalized CMV virion components 60
1.9.1.3.3. Post nuclear import events: viral replication, reassembly and egress 61
1.9.1.4. CMV infection: Modulation of vascular function 62
1.10. Overall rationale 65
1.11. Overall hypotheses 66

CHAPTER 2: MATERIALS AND METHODS 67
2.1 General materials and methods 67
2.1.1 Mouse handling and tissue isolation 67

2.1.2 Pressure myography: Justification for the use of the pressure myograph technique 67
2.1.2.1 Extraluminal experiments 68
2.1.2.2 Novel technique to simultaneously measure endothelial permeability and vascular tone in response to agonists infused into isolated intact arteries 69
2.1.3 Calculations and statistical analyses 72
2.2 Materials and methods for Chapter 3 72
2.2.1 Isolation of primary human umbilical vein endothelial cells (HUVECs) 72
2.2.1.1 Measurement of permeability using confluent endothelial cells 73
2.2.2 Immunohistochemistry 73
2.2.3 Western Analysis 75
2.2.4 Experimental protocol for vascular analysis 75
2.3 Materials and methods for Chapter 4 76
2.3.1 Experimental protocol 76
2.3.1.1 Experiments with S1P 76
2.3.1.2 Experiments with SNP 76
2.3.1.3 Denudation of arteries and treatment with SNP 77
2.4 Materials and methods for Chapter 5 77
2.4.1 Experimental protocol 77
2.5 Materials and methods for Chapter 6 78
2.5.1 Mouse CMV propagation 78
2.5.1.1 Evaluating the mCMV viral titre 79
2.5.2 Mouse infection and handing 79
2.5.3 Experimental protocol for vascular analysis 79

CHAPTER 3: A NOVEL MECHANISM FOR VASCULAR TONE REGULATION IN ARTERIES BY SPHINGOSINE 1-PHOSPHATE THROUGH ENDOTHELIAL BARRIER CONTROL 81
3.1 Introduction 81
3.2 Results 82
3.2.1 S1P-mediated control of endothelial barrier in cultured endothelial cells 82
3.2.2 Novel technique to simultaneously measure endothelial permeability and vascular

tone in response to agonists infused inside isolated intact arteries 83
3.2.3 S1P-induced permeability in intact uterine arteries contributes to increased vascular tone through leakage of a co-infused vasoconstrictor (U46619) 84
3.2.4 Role of thromboxane receptors in vascular tone induced by co-infused S1P and U46619 85
3.2.5 U46619-mediated induction of vascular tone after co-infusion with S1P depends on the $S1P_3$ receptor 85
3.2.6 Higher concentrations of S1P and U46619 were required to elicit responses in mesenteric arteries from female mice 86
3.2.7 Vascular tone induced in mesenteric arteries from male mice show dependence on the $S1P_3$ receptor 87
3.2.8 Co-infusion of U46619 with bacterial or viral components increased vascular tone 87
3.2.9 Co-infusion of U46619 with thrombin increased vascular tone in uterine arteries that was prevented by SEW2871 88
3.2.10 Discussion of results from Chapter 3 99

CHAPTER 4: SPHINGOSINE 1-PHOSPHATE-INDUCED NITRIC OXIDE PRODUCTION REGULATES ENDOTHELIAL PERMEABILITY AND VASCULAR TONE IN MOUSE UTERINE ARTERIES 105
4.1 Introduction 105
4.2 Results 106
4.2.1 S1P generated NO that regulated endothelial permeability and vascular tone 106
4.2.2 Vascular tone induced after co-infusion of U46619 and S1P is regulated by NO 107
4.2.3 SNP regulates endothelial barrier in isolated pressurized mouse uterine arteries 108
4.2.4 SNP-induced vasodilation is enhanced in the presence of L-NAME in arteries from eNOS KO and WT mice 108
4.2.5 Co-infusion of SNP and U46619 increased endothelial permeability and vascular tone: permeability, but not vascular tone, was inhibited in arteries from eNOS KO mice 109
4.2.6 Discussion of results from Chapter 4 121

CHAPTER 5: THROMBOXANE A_2 INCREASES ENDOTHELIAL PERMEABILITY AND VASCULAR TONE THROUGH A NOVEL PATHWAY STIMULATED BY SPHINGOSINE 1-PHOSPHATE 127

5.1 Introduction 127

5.2 Results 128

5.2.1 TXA_2 increases endothelial permeability and vascular tone when infused into uterine arteries 128

5.2.2 $S1P_1$ receptor agonist inhibits thromboxane A2-induced endothelial permeability and vascular tone in uterine arteries 128

5.2.3 TXA_2-induced vascular tone is inhibited by a TP receptor antagonist but not endothelial permeability 129

5.2.4 SK-1 mediates TXA_2-induced endothelial permeability and vascular tone in uterine arteries 130

5.2.5 ABC-type transporters promote TXA_2-mediated increase in endothelial permeability and vascular tone in uterine arteries 130

5.2.6 $S1P_1$/$S1P_3$ receptors promote the TXA_2-mediated induction in endothelial permeability and vascular tone 130

5.2.7 Increased vascular tone increases endothelial permeability of intact isolated pressurized uterine arteries 131

5.2.8 TXA_2-induced vascular tone in mesenteric arteries from male or female mice stimulates the activation of SK-1 or ABC-type transporters 132

5.2.9 Discussion of results of Chapter 5 141

CHAPTER 6: CYTOMEGALOVIRUS INFECTION SUBVERTS THE DEPENDENCE OF THROMBOXANE A_2 ON THE DOWNSTREAM SIGNALING BY SPHINGOSINE 1-PHOSPHATE IN INDUCING VASCULAR TONE 146

6.1 Introduction 146

6.2 Results 147

6.2.1 CMV infection enhances U46619 or S1P-induced vascular tone in part through Rho kinase 147

6.2.2 CMV infection blunts the dependence of U46619-induced vascular tone on SK activation or ABC transporters 148
6.2.3 U46619-induced vascular tone inhibited by VPC23019 or JTE013 is reversed by L-NAME 149
6.2.4 U46619 increased vascular tone via $S1P_3$ receptor in arteries from uninfected mice, but through $S1P_1$ receptor in CMV-infected mice 150
6.2.5 S1P-induced vascular tone is dependent on the $S1P_1$ and $S1P_3$ receptors in arteries from CMV infected mice 150
6.2.6 Phenylephrine-induced vascular tone inhibited by VPC23019 or JTE103 antagonism is relieved by pretreatment with L-NAME 151
6.2.7 The dependence of phenylephrine on the $S1P_3$ receptor to induce vascular tone in uterine arteries is lost in arteries from CMV-infected $S1P_3$ KO mice 151
6.2.8 Discussion of results from Chapter 6 161

CHAPTER 7: GENERAL DISCUSSION 167

CHAPTER 8: LIMITATIONS AND FUTURE DIRECTIONS 173

BIBLIOGRAPHY 178

APPENDIX 229

LIST OF TABLES

Table 1.1: CMV glycoproteins and cellular molecules involved in CMV entry into cells 60

Table 2.1: List of reagents (drugs) 71

LIST OF FIGURES

CHAPTER 1: INTRODUCTION

Figure 1.1: Longitudinal section of a blood vessel 3

Figure 1.2: Vascular tone control: the balance between vasoconstriction and vasodilation of the vessel 4

Figure 1.3: The pathway for generation of NO from arginine catalyzed by NOS, and the mechanism for NO-mediated vascular smooth muscle relaxation 6

Figure 1.4: The pathways, enzymes (boxed) and substrates involved in the biosynthesis of hydrogen sulphide (H_2S) that induces vasodilation 8

Figure 1.5: Ascending vasodilation and control of blood flow 10

Figure 1.6: The intracellular signaling pathways underlying vascular smooth muscle contraction 12

Figure 1.7: Role of Cav-1 in endocytosis 19

Figure 1.8: The role of AJ in endothelial barrier 23

Figure 1.9: The role of TJ on endothelial barrier function 24

Figure 1.10: Sphingolipid metabolism and S1P generation 33

Figure 1.11: Export of S1P out of a cell 39

Figure 1.12: S1P and vascular tone control 49

Figure 1.13: AA metabolism and TXA_2 synthesis 53

Figure 1.14: Proposed mechanisms for CMV cell entry 61

Figure 1.15: CMV infection in a human cell 63

CHAPTER 2: MATERIALS AND METHODS

Figure 2.1: Depiction of part of a pressure myograph 68

Figure 2.2: Experimental set-up for measurement of endothelial permeability in HUVECs using gelatin-coated inserts 74

CHAPTER 3: A NOVEL MECHANISM FOR VASCULAR TONE REGULATION IN ARTERIES BY SPHINGOSINE 1-PHOSPHATE THROUGH ENDOTHELIAL BARRIER CONTROL

Figure 3.1: Sphingosine 1-phosphate (S1P)-regulated leakage of fluorescent dextran through confluent endothelial cells 89
Figure 3.2: Vascular tone and dextran leakage in uterine arteries after treatment with sphingosine 1-phosphate (S1P) and/or U46619 90
Figure 3.3: Effect of thromboxane receptor antagonist on vascular tone induced by co-treatment of U46619 with S1P in uterine arteries 92
Figure 3.4: Vascular tone induced by co-treatment of U46619 with S1P in the presence of $S1P_{1/3}$ receptor antagonist or in uterine arteries from female $S1P_3$ KO and WT mice 93
Figure 3.5: Vascular tone after treatment with U46619 and S1P in mesenteric arteries and comparison of receptor expression in uterine and mesenteric arteries 94
Figure 3.6: Vascular tone after treatment with U46619 and S1P in mesenteric arteries from $S1P_3$ KO and WT male mice 95
Figure 3.7: Vascular tone induced by co-infusion of U46619 with LPS into uterine arteries 96
Figure 3.8: Vascular tone induced by co-infusion of U46619 with CMV glycoprotein B (gB) into uterine arteries 97
Figure 3.9: Vascular tone and dextran leakage in uterine arteries after treatment with U46619 and thrombin 98
Figure 3.10: Proposed mechanism for S1P-induced regulation of vascular tone 104

CHAPTER 4: SPHINGOSINE 1-PHOSPHATE-INDUCED NITRIC OXIDE PRODUCTION REGULATES ENDOTHELIAL PERMEABILITY AND VASCULAR TONE IN MOUSE UTERINE ARTERIES

Figure 4.1: Leakage of fluorescent dextran and vasoconstriction induced by S1P in the presence or absence of L-NAME 111
Figure 4.2: Vascular tone induced after co-infusion of sphingosine 1-phosphate (S1P) and U46619 into mouse uterine arteries 113
Figure 4.3: Dextran leakage and vascular tone stimulated after infusion of S1P alone, and vascular tone induced co-infusion of S1P with U46619 into uterine arteries from eNOS KO mice 114
Figure 4.4: Effect of SNP on dextran leakage in eNOS KO mice and WT mice 115

Figure 4.5: Dextran leakage following co-infusion of thrombin, LPS and gB with SNP, an NO donor 116
Figure 4.6: Induction of vasodilation by SNP in uterine arteries from eNOS KO and WT mice 117
Figure 4.7: Vascular tone induced after co-infusion of SNP and U46619 into uterine arteries 119
Figure 4.8: Dextran leakage and/or vascular tone induced after co-infusion of SNP and U46619 into uterine arteries from eNOS KO and WT mice 120
Figure 4.9: Proposed mechanism for S1P-mediated regulation of endothelial permeability and vascular tone via NO production in murine uterine arteries 125

CHAPTER 5: THROMBOXANE A_2 INCREASES ENDOTHELIAL PERMEABILITY AND VASCULAR TONE THROUGH A NOVEL PATHWAY STIMULATED BY SPHINGOSINE 1-PHOSPHATE

Figure 5.1: Infusion of U46619 at high concentration increased dextran leakage and vascular tone in uterine arteries. 133
Figure 5.2: $S1P_1$ agonist prevented U46619-induced endothelial permeability and vascular tone after infusion in uterine arteries 134
Figure 5.3: Enhanced dextran leakage and reduction in vascular tone in the presence of TP receptor antagonist following infusion of U46619 into uterine arteries 135
Figure 5.4: SK-1 mediated U46619-induced endothelial permeability and vascular tone in uterine arteries 136
Figure 5.5: The ABC transporters mediate U46619-induced endothelial permeability or vascular tone in uterine arteries 137
Figure 5.6: $S1P_1$/$S1P_3$ receptors promote U46619-induced endothelial permeability and vascular tone in uterine arteries 138
Figure 5.7: U46619-inducted dextran leakage and/or vascular tone after extraluminal stimulation of arteries is mediated via TP receptors, ABCC1 and endothelial SK-1 139
Figure 5.8: Vascular tone induced by U46619 is mediated by SK-1 or ABCC1 and ABCG2 transporters in mesenteric arteries from male and female mice 140

Figure 5.9: Induction of endothelial permeability and vascular tone by U46619 via an S1P pathway 145

CHAPTER 6: CYTOMEGALOVIRUS INFECTION SUBVERTS THE DEPENDENCE OF THROMBOXANE A_2 ON THE DOWNSTREAM SIGNALING BY SPHINGOSINE 1-PHOSPHATE IN INDUCING VASCULAR TONE

Figure 6.1: Effect of CMV infection on U46619 or S1P-induced vascular tone via Rho kinase pathway in uterine arteries in the bath 152

Figure 6.2: The impact of CMV infection on U46619-induced vascular tone mediated via sphingosine kinases in uterine arteries in the bath 153

Figure 6.3: The effects of CMV infection on the role of ABC transporters in promoting U46619-induced vascular tone in uterine arteries in the bath 154

Figure 6.4: CMV infection and its effects on the role of S1P receptors in mediating the U46619-induced vascular tone in uterine arteries in the bath 155

Figure 6.5: The effects of CMV infection on the $S1P_3$ or $S1P_2$ receptors in mediating the S1P-induced vascular tone in uterine arteries in the bath 156

Figure 6.6: The dependence of U46619-induced vascular tone on $S1P_3$ receptor in uterine arteries is impaired with CMV infection 157

Figure 6.7: The S1P-induced vascular tone in uterine arteries isolated from CMV infected mice is dependent on both $S1P_1$ and $S1P_3$ receptors 158

Figure 6.8: The dependence of phenylephrine-induced vascular tone on the S1P receptors in arteries from uninfected and CMV-infected mice 159

Figure 6.9: Phenylephrine-induced vascular tone in arteries from uninfected and CMV-infected C57Bl/6 KO and WT mice 160

Figure 6.10: Proposed model to account for the impact of CMV infection on the vascular tone induced by U46619 via an S1P pathway 165

CHAPTER 7: GENERAL DISCUSSION

Figure 7.1: Overall model for the thesis 172

ABBREVIATIONS

$[Ca^{2+}]i$	intracellular free Ca^{2+}
AA	arachidonic acid
ABC	ATP–binding cassette transporters
AJ	adherens junctions
ALI	acute lung injury
BH3	B-cell lymphoma 2 (Bcl-2) homology domain-3
BK_{Ca}	calcium-activated potassium channels (B=big subtype)
BST2	Bone Marrow Stromal Cell Antigen 2
CaM	calmodulin
cAMP	cyclic adenosine monophosphate
Cav	caveolin
cGMP	cyclic guanine monophosphate
CMV	cytomegalovirus
CO	carbonmonoxide
COX	cyclooxygenase
CRP	C–reactive protein
ECM	extracellular matrix
EDH	endothelium-derived hyperpolization
EDHFs	endothelium-dependent hyperpolization factors
EETs	epoxyeicosatrienoic acids
EGFR	epidermal growth factor receptor
eNOS	endothelial nitric oxide synthase
ER	endoplasmic reticulum
ET	endothelin
gB	CMV glycoprotein B
GC	guanylate cyclase
GJ	gap junctions
H_2S	hydrogen sulfide
HDL	high-density lipoproteins
HETEs	hydroxyeicosatetraenoic acids

HSPGs	heparan sulfate proteoglycans
HUVECs	human umbilical vein endothelial cells
I/R	Ischemia–Reperfusion
ICAM	intercellular adhesion molecule
IgE	immunoglobulin E
IK_{Ca}	calcium-activated potassium channels (I= intermediate subtype)
iNOS	inducible nitric oxide synthase
JAMs	junctional adhesion molecules
K_{ATP}	ATP-sensitive potassium channels
K_{Ca}	calcium-activated potassium channels
K_v	voltage-dependent K^+ channels
L-NAME	L–N^G–Nitroarginine methyl ester
LPPs	lipid phosphate phosphatases
LPS	lipopolysaccharide
LTA4	leukotriene A4
MLC	myosin light chain
MLCP	MLC phosphatase
MLK	MLC kinase
nNOS	neuronal nitric oxide synthase
NO	nitric oxide
NOS	NO synthase
PDGFRα	platelet–derived growth factor receptor–α
PGD2	prostaglandin D2
PGH_2	prostaglandin H_2
PGI_2	prostaglandin I2
PI3K	phosphatidylinositol 3-kinase
PKA	protein kinase A
PKC	protein kinase C
PKG	protein kinase G
PLC	phospholipase C
ROS	reactive oxygen species

S1P	sphingosine 1-phosphate
S1PP	S1P phosphatase
SK	sphingosine kinase
SK_{Ca}	calcium-activated potassium channels (S=small subtype)
SNP	sodium nitroprusside
SPL	S1P lyase
Spns2	spinster homolog 2
TJ	tight junctions
TNF–α	tumour necrosis factor alpha
TP	thromboxane/prostanoid receptors
TRP	transient receptor potential channels
t-SNARE	target-SNARE
TXA_2	thromboxane A_2
VCAM	vascular cell adhesion molecule
VE–cadherin	vascular endothelial cadherin
VEGF	vascular endothelial growth factor
VSMCs	vascular smooth muscle cells
v-SNARE	Vesicle-Soluble N-Ethylmaleimide-Sensitive Factor Attachment Protein Receptor
WT	wildtype
ZO	zona occludens

CHAPTER 1: INTRODUCTION

1.1 Summary and significance of study

In this thesis I present novel mechanisms through which sphingosine 1-phosphate (S1P)-mediated control of endothelial permeability and nitric oxide (NO) production regulates vascular tone in arteries. The findings from this study will extend our understanding of endothelial permeability from a physiological context, in that, finely regulated endothelial permeability could be part of the mechanisms through which normal vascular tone is controlled. This mechanism involves S1P maintaining endothelial barrier preventing the access of circulating vasoconstrictors to the underlying vascular smooth muscle cells (VSMCs), but also theS1P-induced endothelial permeability that can be tolerated physiologically, allows such vasoconstrictors to leak and access the VSMCs increasing vascular tone that is regulated by bioavailable NO. The study also establishes clinically-relevant information that provides ways to prevent hyperpermeability from contributing to an increase in vascular tone as mediated by S1P or other permeability-inducing agents like thrombin in arteries. Recently, the pharmaceutical agent, FTY720 (an S1P analog when phosphorylated) and its newly generated analogs approved for the treatment of multiple sclerosis, were shown to enhance pulmonary endothelial barrier and prevent vascular leakage [1-4]. This means that my findings will be important particularly in disease conditions associated with endothelial permeability such as acute lung injury (ALI), sepsis or anaphylaxis, but also in disorders associated with increased vascular tone such as hypertension. In these situations utilizing the endothelial barrier-enhancing properties of S1P or antagonizing its signaling capabilities will be helpful. Other novel findings indicate that thromboxane A_2 (TXA_2) predominantly signals through the S1P pathway to increase endothelial permeability and vascular tone in intact pressurized arteries. The findings from this study provide novel avenues for therapeutic targeting of the S1P pathway for treatment of disease conditions caused or contributed to by TXA_2 such as vascular leakage, atherosclerosis, hypertension or rheumatoid arthritis [5-8]. I also show that cytomegalovirus (CMV) infection enhances the vascular tone induced by S1P or TXA_2, indicating that CMV infection can exacerbate vascular-related complications like hypertension or intrauterine growth restriction. In fact, CMV infection has been shown to increase blood pressure in a rodent model, but also contribute to the pathogenesis of hypertension in humans. I now show that these complications could be potentiated by endogenous mediators of vascular tone like TXA_2 or S1P during CMV infection.

This means that targeting the S1P pathway may be an attractive alternative for treatment of vascular disorders associated with CMV infection, as demonstrated with FTY720 that reduces CMV disease in transplant patients [9]. I also show that the dependence of TXA_2-induced vascular tone on the S1P pathway is dampened in arteries isolated from mice infected with CMV, in which the virus opens up an alternative pathway for induction of vascular tone. Understanding fully the exact mechanism through which CMV infection contributes to the development of disease through increased vascular tone, could be important in finding therapeutic solutions against many vascular complications.

1.2 Blood vessel structure and function: overview on vascular tone control

Blood vessels consist of three main layers including the tunica intima, the media and adventitia. The tunica intima is the innermost layer containing the endothelium, which is a thin layer of cells that line the interior of blood vessels forming an interface between the circulating blood and the underlying VMSCs. The intima also contains the internal elastic lamina, also known as the internal elastic lamella, consisting of elastic tissues that forms the outermost part of the tunica intima that borders the tunica media [10]. The tunica media has thick layers of elastin, collagen and VSMCs. The tunica adventitia is the outermost layer composed of connective tissues, collagen and elastic fibers that provides arterial support [11,12].

Conduit arteries maintain a dilated phenotype in their steady-state conditions because of shear stress [13]. Compared to arteries, veins are thin-walled vessels with large and irregular lumens. Since they are low-pressure vessels, larger veins are commonly equipped with valves that promote unidirectional blood flow to the heart and prevent backflow. However, resistance arteries in a resting state exhibit partial constriction. This type of constriction generated from the vascular smooth muscle of unstimulated arteries is called basal vasomotor or vascular tone [14,15]. The increase or decrease in arterial diameter from the baseline value is referred to as a change in vasomotor or vascular tone, which constitutes the balance between vasodilation and vasoconstriction (Figure 1.1). Vascular tone is influenced by activation of specific receptors, opening and closing of membrane channels, or through mechanical stimuli. These factors can be broadly divided into three groups, namely the factors that cause only vasodilation, vasoconstriction or both. Factors that cause vasodilation include endothelial-derived factors (like NO, carbon monoxide) or blood flow, while those that stimulate vasoconstriction include

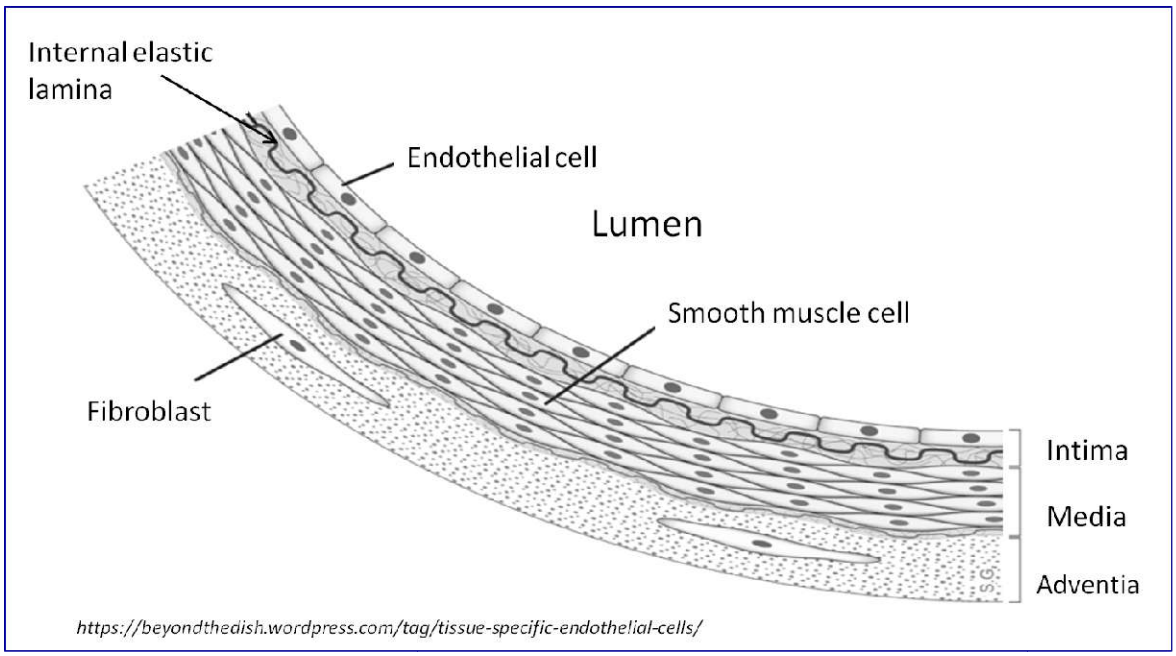

Figure 1.1: Longitudinal section of a blood vessel.

myogenic tone, local (e.g. thromboxane A_2) and circulating (e.g. S1P) factors. Endothelins, S1P, membrane channels, autonomic nervous system and blood flow are examples of factors that can induce both vasodilation and vasoconstriction [15,16].Increased vasoconstriction decreases vessel luminal diameter and blood flow. However, vasodilation increases internal diameter of blood vessels following vascular smooth muscle relaxation. Vasodilation increases blood flow due to decreased vascular resistance. Increased peripheral vascular resistance can lead to an increase in blood pressure. Vascular resistance is most experienced in small arteries and arterioles, and these types of blood vessels are of significant therapeutic value since they can be targeted to reduce vascular resistance. This is why this work focused on such arteries.

1.2.1 Vasodilation

1.2.1.1 Mechanisms for induction of vasodilation

The exact mechanism leading to vasodilation depends on the stimuli. Generally, endothelium-derived substances increase vasodilation via three main mechanisms involving the cyclic guanine monophosphate (cGMP) or cyclic adenosine monophosphate (cAMP)-dependent mechanisms, but also endothelium-dependent vascular smooth muscle hyperpolarization [17].

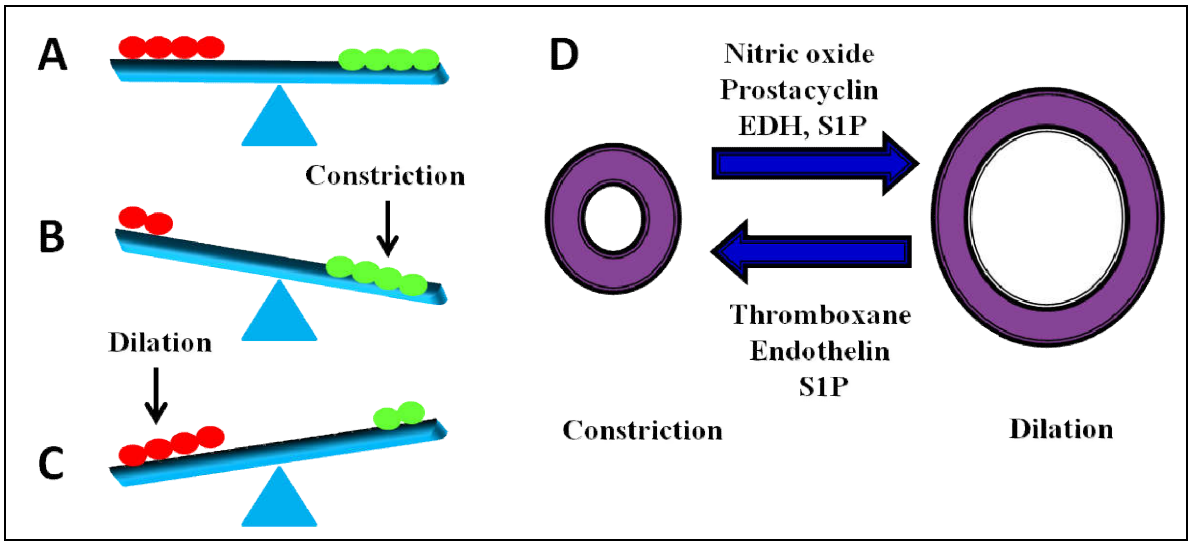

Figure 1.2: Vascular tone control: the balance between vasoconstriction and vasodilation of the vessel. In a steady state **(A)**, the vessel experiences equal stimuli from vasodilators (red) and vasoconstrictors (green) and thus maintains a specific vessel diameter that is considered to have a net change in vascular tone equivalent to zero. However, the increase in levels of vasoconstrictors compared to vasodilators leads to a prevailing vasoconstriction response which decreases the vessel diameter and this is termed as an increase in vascular tone **(B).** In contrast, higher levels of vasodilators increase vessel diameter which overcomes vasoconstriction leading to a decrease in vascular tone **(C)**. Different factors are involved in the control of vascular tone, and some have dual effects like S1P **(D)**.

NO is an example of an endothelium-derived molecule that increases vasodilation via guanylate cyclase (GC)-dependent generation of cGMP [18]. Secondly, prostaglandins like prostaglandin I_2 (PGI_2), also known as prostacyclin, activate adenylate cyclase which produces cAMP and this increases vasodilation by inhibiting phosphorylation of myosin light chains [17]. Thirdly, a family of vasoactive substances generally termed endothelium-dependent hyperpolarization factors (EDHFs) stimulates vasodilation by hyperpolarizing VSMCs following activation of potassium ion (K^+) channels or Na^+/K^+ ATPases. However, the specific molecule(s) defined as EDHFs remain to be determined [19-22]. Vasodilation can also be caused by a flow-mediated mechanism [23] or conducted vasodilation [24] as explained later. Described below are the various factors that cause vasodilation.

1.2.1.2 Endothelial-derived vasodilators

1.2.1.2.1 PGI_2 and NO

The vasodilator, PGI_2 is a prostanoid derived from arachidonic acid (AA) metabolism [25]. In its synthesis, endothelial cyclooxygenase-1, 2 (COX-1, 2) converts AA to prostaglandin H_2 (PGH_2). PGI_2 synthase converts PGH_2 to PGI_2 [26]. PGI_2 binds to endothelial G protein-coupled PGI_2 receptor (IP_1) activating adenylate cyclase, which converts ATP to cAMP. As a second messenger, cyclic AMP promotes vasodilation through the following mechanisms: (**1**) inhibiting an increase in intracellular Ca^{2+} concentration $[Ca^{2+}]i$ and (**2**) promoting protein kinase A (PKA)-dependent activation of phosphodiesterases which dephosphorylate and inactivate myosin light chain (MLC) kinase (MLCK). These events result in decreased MLC phosphorylation and increased vascular smooth muscle relaxation [27].

NO is produced from the amino acid, L-arginine, and molecular oxygen that requires the enzymatic activities of NO synthase (NOS) isoforms (Figure 1.2) including: endothelial NOS (eNOS), inducible NOS (iNOS) and neuronal NOS (nNOS) [28]. The NO formed has a very short half-life of only a few seconds, but it can also be quickly scavenged by reactive oxygen species (ROS) like superoxide anion thus reducing its bioavailability. NO also avidly binds to the heme moiety of hemoglobin and the heme moiety of GC in the VSMCs. Therefore, when NO is formed by the vascular endothelium, it rapidly diffuses to the VSMCs where it binds and activates GC [29]. This enzyme catalyzes the dephosphorylation and cyclization of GTP to cGMP. In the VSMCs, cGMP induces vasodilation by different mechanisms including: (**1**) inhibiting $[Ca^{2+}]i$ entry, but also decreasing the levels of Ca^{2+} inside the cells, (**2**) stimulation of cGMP-dependent protein kinase G which activates MLC phosphatase, the enzyme that dephosphorylates MLC leading to vasodilation, and (**3**) activation of K^+ channels resulting in VSMCs hyperpolarization and vasodilation [30].

NO is a highly versatile molecule that is induced by a wide range of factors or mechanisms to induce vasodilation. Some of these factors include adenosine, acetylcholine, norepinephrine and S1P which signal through their specific receptors: adenosine A_2, muscarinic, β_2-adrenergic, and $S1P_1$ and $S1P_3$ receptors, respectively [31-34]. The inflammatory molecules bradykinin, calcitonin gene-related peptide, and substance P also induce vasodilation in an eNOS/NO-dependent manner. In addition, the mechanical forces exerted on the endothelium by the flowing blood activate eNOS, in what is termed as flow- or shear-mediated vasodilation [35].

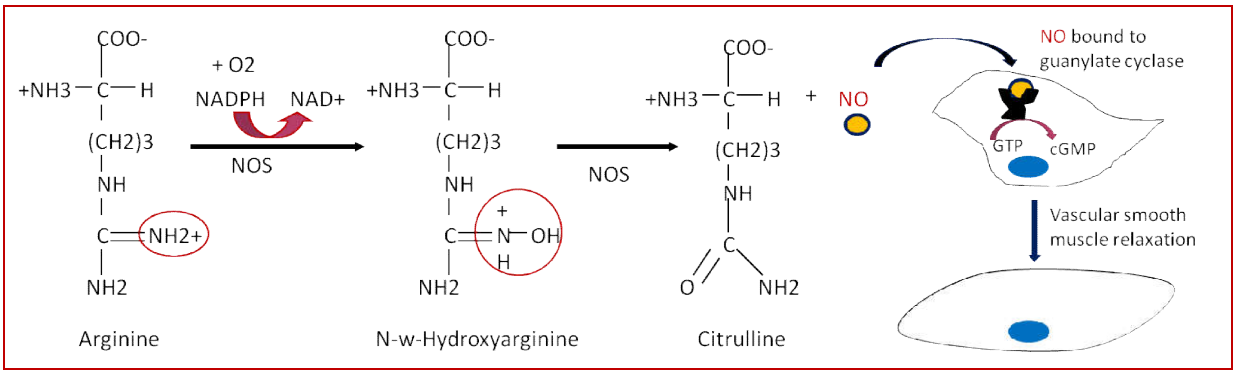

Figure 1.3: The pathway for generation of NO from arginine catalyzed by NOS, and the mechanism for NO-mediated vascular smooth muscle relaxation.

1.2.1.2.2 Endothelial-derived hyperpolarization (EDH)

Most endothelium-dependent receptor agonists that induce vasodilation and flow-mediated vasodilation are only partly inhibited after preventing NO/PGI_2 production. It is therefore believed that endothelial cells release other factors that also cause the vascular smooth muscle to relax [36,37]. The exact identity of the factor(s) that are associated with endothelium-dependent vascular smooth muscle hyperpolarization remains elusive. Even so, several candidates have been proposed which include: hydrogen peroxide, superoxide, extracellular K^+ ions, epoxyeicosatrienoic acids (EETs) or an electrical signal that is transmitted between endothelial cells through gap junctions (GJ) or myoendothelial gap junctions between the endothelium and VSMCs [20,22,37]. Of these factors, EETs have emerged as leading candidates. EETs are produced by endothelial cells from AA via the cytochrome P450/epoxygenase pathway in response to shear stress (dependent on blood flow), cyclical strain (vessel deformation), agonists like acetylcholine and bradykinin [20-22,36,38-41] or the mechanical stretch resulting from the pulsatile nature of blood flow [42-44].

EETs induce vasodilation via two major mechanisms; first, the EETs produced by endothelial cells are released to the vascular smooth muscle where they activate the calcium-activated K^+ channels (described later) BK_{Ca} (B=large subtype). The activation of BK_{Ca} channels cause efflux of K^+ ions leading to hyperpolarization of the VSMCs membrane. This hyperpolarization inhibits Ca^{2+}entry promoting vasodilation [20,45]. Second, the signaling mediated by endothelial EETs causes Ca^{2+} influx through transient receptor potential (TRP) channels in endothelial cells (described later) including the subtypes TRPV4, TRPC3 and

TRPC6. The Ca^{2+} entry promotes the activation of calcium-activated K^+ channel subtypes SK_{Ca} and IK_{Ca} (S=small, I=intermediate, respectively). This activation will cause an efflux of K^+ ions into the subendothelial space thereby hyperpolarizing the endothelial cell membrane. The leaked K^+ ions stimulate the Na^+/K^+-ATPase or the inwardly rectifying K^+ (K_{ir}) channels causing membrane hyperpolarization, and inhibition of Ca^{2+} influx in the VSMCs. K_{ir} are also activated by S1P leading to decreased rat myocyte contractility [46]. These events promote vasodilation. The myoendothelial gap junctions provide a pathway for electrical coupling for endothelial hyperpolarization to be transmitted to the VSMCs [21,22,38,39,45].

1.2.1.2.3 Carbon monoxide (CO) and hydrogen sulfide (H_2S)

CO, H_2S and NO belong to a family of endogenously generated gaseous signaling molecules loosely termed "gasotransmitters" with potent vasodilatory capabilities [47]. CO and H_2S are gaseous signaling molecules with vasodilatory properties that are formed in the endothelium and VSMCs [48,49]. CO is formed physiologically by the action of heme oxygenase-1 and 2, enzymes involved in heme metabolism [48-50]. Like NO, CO induces vasodilation through the cGMP/protein kinase G-dependent mechanism. Endogenous H_2S is produced during the normal metabolic processes particularly of amino acids. H_2S is synthesized by three enzymes: 3-mercaptopyruvate sulfurtransferase, cystathionine β-synthase and cystathionine γ-lyase [51]. By working collaboratively with cysteine aminotransferase, which metabolizes cysteine in the presence of alpha-ketoglutarate to glutamate and 3-mercaptopyruvate, 3-mercaptopyruvate sulfurtransferase converts the latter to H_2S and pyruvate [52]. H_2S can also be generated from a reaction involving homocysteine and serine catalyzed by cystathionine β-synthase to cystathionine and H_2S. Cystathionine γ-lyase then breaks down cystathionine to cysteine, ammonia and 2-ketobutyrate. H_2S can also be formed from a cystathionine γ-lyase-mediated activity resulting to β-elimination of cysteine to pyruvate, H_2S and NH_4^+, or γ-elimination of homocysteine to 2-ketobutyrate, H_2S and NH_4^+. Cystathionine γ-lyase is believed to be the primary source of H_2S in the vascular tissues [51,53-55]. To induce vasodilation, H_2S relaxes the vascular smooth muscle by stimulating the ATP-activated potassium (K_{ATP}) and BK_{Ca} channels. Furthermore, H_2S-induced activation of IK_{Ca} and SK_{Ca} channels cause vascular smooth muscle hyperpolarization and vasodilation (Figure 1.3) [55,56].

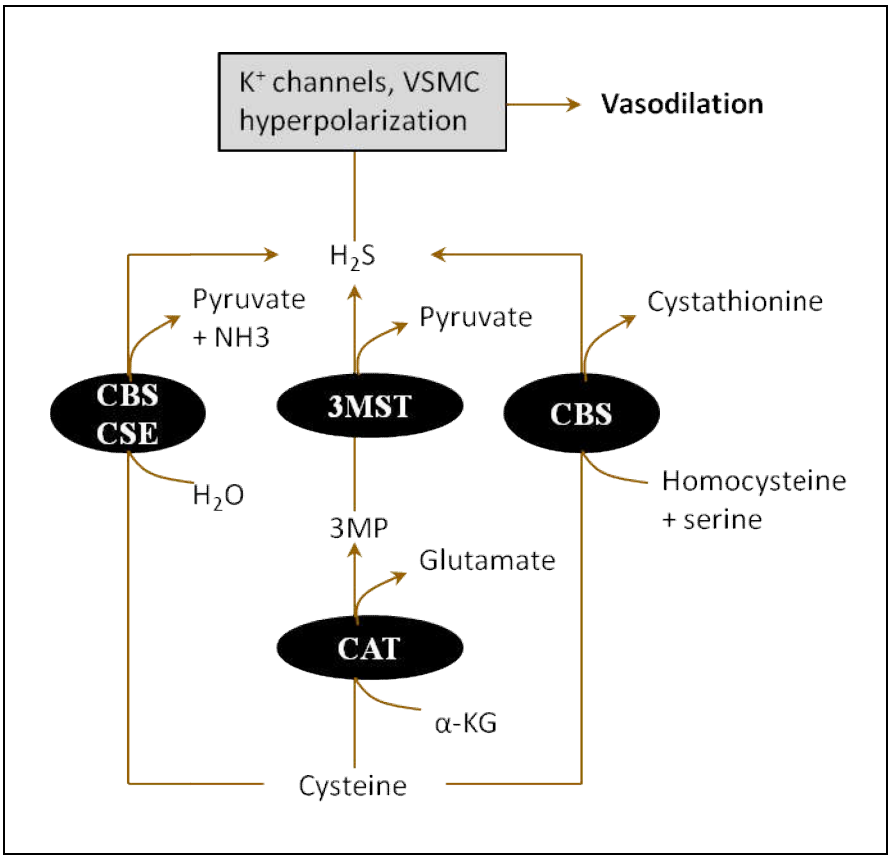

Figure 1.4: The pathways, enzymes (boxed) and substrates involved in the biosynthesis of H_2S that induces vasodilation. The abbreviations stand for: Cystathionine β-synthase (CBS), cystathionine γ-lyase (CSE), 3-mercaptopyruvate sulfurtransferase (3MST), cysteine aminotransferase (CAT), alpha-ketoglutarate (α-KG), 3-mercaptopyruvate (3MP).

1.2.1.3 Conducted vasodilation

Small arterioles initiate responses that are conducted along the endothelial and vascular smooth muscle interconnections by a mechanism that is independent of shear stress, also known as ascending vasodilation [24,57-59]. The responses are mainly generated by small arterioles and terminal arteries that branch into capillaries (Figure 1.4) [24]. In these arterioles, the endothelium sends projections through the underlying basement membrane that establish intimate association with the VSMCs [60]. These projections allow myoendothelial communication by signaling through specific pannexins (connexin-related proteins), K_{Ca} channels, inositol (1, 4, 5) triphosphate receptors, and plasminogen activator inhibitor-1 [60-65]. Myoendothelial are important in transmitting hyperpolarizing signals from endothelium to the VSMCs [64,65].

Myoendothelial junctions have also been proposed to provide a pathway for communication of signals from the abluminal vessel surface to the endothelium. These arguments are supported by the findings that pannexin-1 associated with α_1-adrenoreceptors regulate vasoconstriction induced by norepinephrine [66]. Most of the studies that have attempted to understand conducted vasodilation have utilized acetylcholine applied locally on the arteriolar wall and then observing responses upstream of the vascular tree from the point of application [67-70]. In these experiments, acetylcholine-induced vasodilation results from the trigger of a K_{Ca} channel-dependent wave of hyperpolarization that is communicated between adjacent endothelial cells and between the endothelium and the underlying VSMCs [71-73]. This communication involves different connexins and vasodilation is not prevented by NOS inhibitors [74], but by gap junction inhibitors between the locus of acetylcholine application and the distant upstream observation site of arteriole. Studies conducted in mice deficient in connexins support this conclusion [24]. These communications have important implications in our understanding of blood flow regulation in resistance arteries [24,70] .

1.2.2 Vasoconstriction

1.2.2.1 Mechanism for induction of vasoconstriction

In resistance arteries, the vascular smooth muscle contraction is mediated through two independent, but not mutually exclusive pathways; the Ca^{2+}-dependent and the Ca^{2+}-independent pathways. The constriction mediated by the Ca^{2+}-dependent pathway occurs through the rise in $[Ca^{2+}]i$ in response to a stimulus such as an agonist [75-77]. Increasing $[Ca^{2+}]i$ is mainly contributed by voltage-gated Ca^{2+} channels, store-operated Ca^{2+} channels (intracellular stores) such as from the sarcoplasmic reticulum or by the influx from the extracellular compartment [78-80]. The $[Ca^{2+}]i$ in turn complexes with calmodulin (CaM), and such a complex activates the enzyme MLCK. The activated MLCK phosphorylates MLC, which promotes cycling of cross-bridges between actin and myosin that produce a contractile force and therefore vasoconstriction [75-77]. The Ca^{2+}-independent pathway is mediated through a small G protein Rho. Rho proteins cycle between an inactive (GDP-binding) and an active (GTP-binding) state [81]. Guanine nucleotide exchange factors facilitate the exchange of GDP for GTP on Rho to generate the activated form, Rho-GTPase (RhoA) [82]. RhoA is activated via agonist signaling through specific receptors. RhoA in turn activates Rho-kinase, which inhibits the MLC phosphatase

(MLCP) activity by phosphorylating it at the myosin-binding subunit and thus augmenting vascular smooth muscle cell contraction [83]. Therefore, the main role of Rho-kinase is to keep MLCP phosphorylated and thus inactivated [83]. This significantly increases MLC phosphorylation and vasoconstriction (Figure 1.5). Vascular smooth muscle relaxation occurs when the MLC is dephosphorylated by MLCP [83]. In summary, vascular tone depends on the level of $[Ca^{2+}]i$ in the vascular smooth muscle which influences MLCK activity and the extent of MLC phosphorylation which is controlled by the relative activities of MLCK and MLCP [75-77].

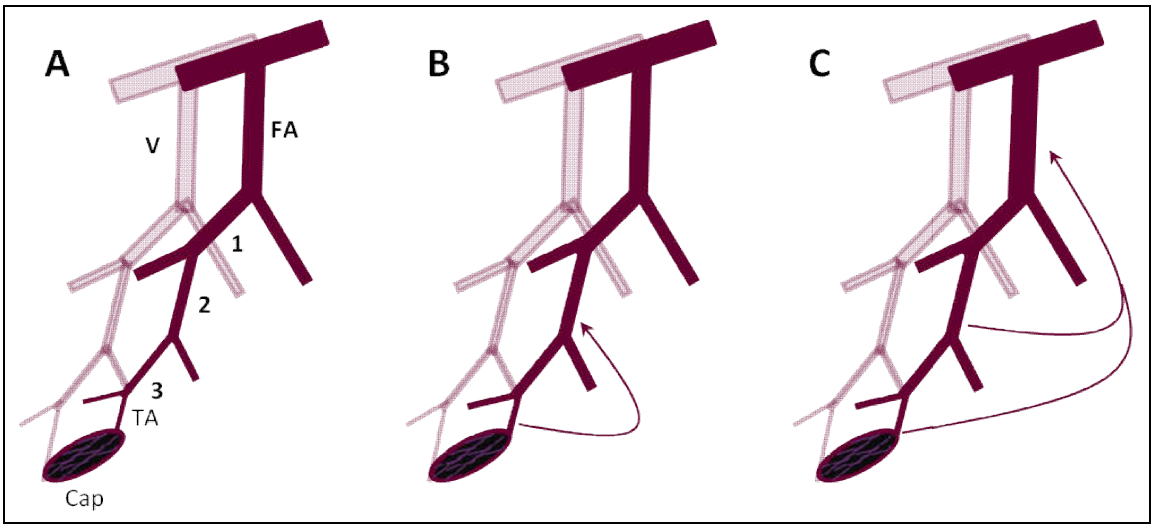

Figure 1.5: Ascending vasodilation and control of blood flow. Depiction of a conduit artery that could supply blood to the feed artery (FA) and which is collected back by the vein (V). The feed artery branches into 1st order (1), 2nd order (2), 3rd order (3), terminal arterioles (TA) and finally into the capillary network (cap), which feeds into the veins **(A)**.Vasodilation originating from the TA and 3rd order arterioles ascends into the proximal regions shown by the arrow (2nd order) contributing to an increase in local blood flow **(B)**. Vasodilation can also ascend from the downstream arterioles (arrows) into FA promoting an overall increase in blood flow **(C)**.

1.2.2.2 Factors that stimulate vasoconstriction

1.2.2.2.1 Myogenic tone

The constriction developed by resistance arteries in response to transmural pressure is referred to as myogenic tone. Transmural pressure is the difference between intraluminal (inside of a blood vessel) and extraluminal (outside) pressures experienced by the arteries. Increased

myogenic tone reduces the luminal diameter increasing the resistance to blood flow [14,84]. The change in vascular tone in response to intraluminal pressure changes is inherent in the vascular smooth muscle and is referred to as myogenic response. The importance of myogenic tone is to maintain an intermediate level of constriction in resistance arteries for optimal blood flow [14,85]. Evidence also supports the prominent role played by S1P [86-90] or TRP channels in the myogenic response, with TRPM4 and TRPC6 functioning as mechanosensitive ion channels mediating pressure-induced contraction of vascular smooth muscle. TRPP1 and TRPP2 regulate stretch-activated channels in the VSMCs membrane. It is suggested that a mechanosensitive Gq-coupled receptor may initiate downstream signaling that involves activation of TRPC and TRPM4 channels by a PLC-dependent mechanism [91-94].

1.2.2.2.2 Local and circulating factors

VSMCs can be influenced by factors produced by the endothelium and by circulating factors that affect what the endothelium produces as well as circulating factors that access the VSMCs through the endothelium. Endothelial cells communicate with the underlying VSMCs through myoendothelial gap junctions. These junctions allow molecular exchange such as ions or small molecules like cyclic nucleotides [95]. Endothelial cells produce different vasoactive agents that control vascular tone including vasodilators (described above) and vasoconstrictors like S1P, TXA_2 (both described later in more detail), endothelins, uridine adenosine tetraphosphate, isoprostanes, 20-hydoxyeicosatetraenoic acid, and angiotensin II [10]. Uridine adenosine tetraphosphate, is a novel endothelium-derived vasoconstrictor, which activates cyclooxygenases (COXs) that produces TXA_2 which ultimately stimulates vasoconstriction [96,97]. Uridine adenosine tetraphosphate induces its activities via purinergic receptors. These are receptors traditionally activated by purine nucleosides like adenosine (P1-type receptors) or purine nucleotides such as ATP, ADP, UTP or UDP (P2-type receptors) [98-100]. 20-hydoxyeicosatetraenoic acid is an endogenous vasoconstrictor produced following the metabolism of AA by cytochrome P450. 20-hydoxyeicosatetraenoic acid depolarizes the VSMCs, inhibits K^+ channel activity, and increases intracellular $[Ca^{2+}]i$ in VSMCs stimulating vasoconstriction [101,102]. Circulating factors like S1P, serotonin, acetylcholine and catecholamines (epinephrine, norepinephrine) increase vasoconstriction [34,102-106].

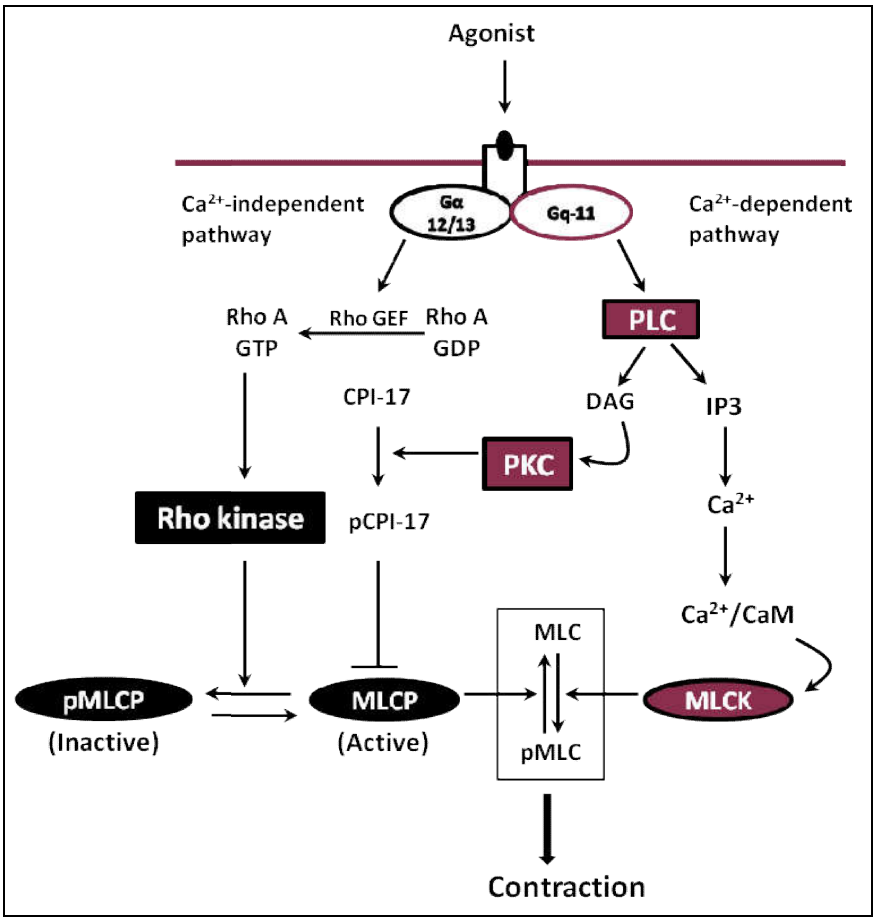

Figure 1.6: The intracellular signaling pathways underlying vascular smooth muscle contraction. Contraction is induced following increased phosphorylation of MLC in the vascular smooth muscle cells. Agonist-mediated activation of G protein-coupled receptors triggers the Ca^{2+}-dependent phosphorylation of MLC and/or Rho kinase-dependent inhibition of MLC dephosphorylation. Signaling via $G_{q\text{-}11}$ protein leads to the activation of phospholipase C (PLC) and rise in $[Ca^{2+}]i$ through inositol (1, 4, 5) triphosphate-sensitive endoplasmic reticulum stores. Then Ca^{2+} binds to CaM forming a complex (Ca^{2+}/CaM) that promotes phosphorylation and activation of MLCK. The second product of PLC, diacylglycerol, activates protein kinase C (PKC), which, through its substrate CPI-17, inhibits MLCP, and thus prevents MLC dephosphorylation. On the other hand, stimulation of $G\alpha_{12\text{-}13}$ activates Rho-guanine nucleotides exchange factor (Rho-GEF) that activates RhoA protein through GDP exchange to GTP. GTP-bound Rho activates Rho-kinase, which phosphorylates and inactivates MLCP, thereby inhibiting MLC dephosphorylation and promoting vascular smooth muscle contraction.

It has been proposed that circulating S1P can be transcytosed to the VSMCs to induce vasoconstriction [107], but also the VSMCs can endogenously produce S1P [89].Serotonin is one of the most extensively studied vasoconstrictors. Serotonin being a protonated molecule cannot diffuse across a hydrophobic lipid bilayer under physiological conditions; instead it is transported to the underlying VSMCs through specialized transporters called SERT. SERT is expressed in platelets which contribute to the circulating pool of serotonin, but also SERT is found on the luminal and abluminal sides of the vessels, including the arterial VSMCs [104,108-112]. Serotonin invokes vasoconstriction in different vascular beds (coronary, femoral, cerebral, mesentery, rat tail artery etc), but also exhibits synergistic effects on vasoconstriction with other vasoconstrictors like phenylephrine (an alpha-adrenergic receptor agonist), angiotensin-II, S1P, ATP, insulin, prostaglandin E_1 and E_2, TXA_2 and endothelin [113-120].

1.2.3 Factors with dual effects on vascular tone control

1.2.3.1 S1P

S1P is a signaling sphingolipid, also known as a lysosphingolipid with both vasodilating and vasoconstricting properties. Endothelial cells or VSMCs express each of the S1P receptor subtypes $S1P_1$, $S1P_2$, and $S1P_3$. Activation of endothelial $S1P_1$ or $S1P_3$ receptors stimulates vasodilation. Endothelial $S1P_2$ receptor which is only present in some vasculature has not been associated with vasodilation. Stimulation of $S1P_2$ or $S1P_3$ receptors on the VSMCs promote vasoconstriction [34,121,122]. The biology of S1P is explained in greater detail later.

1.2.3.2 Endothelins

Endothelins are peptides produced by the endothelium, but also from VSMCs [123,124], and they exhibit vasoconstricting or vasodilating properties depending on the receptors engaged. There are three isoforms of these peptides including endothelin-1 (ET-1), ET-2, and ET-3. Their activities are mediated through two G protein-coupled receptors, ET_A and ET_B [125]. Once produced by the endothelium, majority of ET-1 is released abluminally to the underlying VSMCs suggesting that ET-1 acts in an autocrine and paracrine manner. It does so through the ET receptors which are expressed on the endothelium and VSMCs in arteries and veins [126,127]. Since VSMCs cells also produce ET-1, the autocrine signaling can also occur in these cells, but it is unknown whether the ET-1 produced in the VSMCs impacts endothelial cell responses. In the

VSMCs ET-1 binds to Gq-coupled ET_A or ET_B, stimulating vasoconstriction. However, when ET-1 binds to ET_B receptors on the endothelium, it produces NO and PGI_2, which diffuse to the underlying VSMCs stimulating vasodilation. These findings confirm that ET-1 has a dual role in the regulation of vascular tone, by inducing vasodilation and vasoconstriction [126,128-131]. ET-1 also induces contraction of the myometrial strips through the S1P/$S1P_2$ receptor-dependent mechanisms [132].

Although ET-2 differs from ET-1 by two amino acid substitutions (Trp and Leu in ET-1, substituted for Leu and Met in ET-2), it has similar affinities for ET_A and ET_B as ET-1 [133]. The plasma levels of mature ET-2 peptide is ~0.5 pg/ml [134-136]. While ET-2 is a potent vasoconstrictor like ET-1 [137], the physiology and pathophysiology of ET-2 is not well understood. In addition to its vascular function, ET-2 is involved in ovarian physiology by stimulating contraction during ovulation, immunological responses as a chemokine and in cancer pathogenesis [134].

On the other hand, ET-3 has similar affinity for ET_B as ET-1 and ET-2, but has much lower affinity for ET_A compared to ET-1 or ET-2. The normal human plasma concentration of ET-3 is approximately 1.6 pg/ml [136]. ET-3 is mainly secreted by brain neurons, renal tubular epithelial cells, intestinal epithelial cells [138], and is the most poorly studied isoform.

1.2.3.3 Membrane channels

Membrane channels like K^+ channels are proteins that allow rapid and selective flow of K^+ ions in and out of the cell, and thus help generate electrical signals. Many K^+ channels are expressed on the endothelium and VSMCs and have been shown to control vascular tone. These channels include the calcium-activated (K_{Ca}), voltage-dependent (K_v), and K_{ATP} channels [139-142]. When these channels open, K^+ ions are transported extracellularly, producing a more negative membrane potential. This hyperpolarization in turn acts to close voltage-dependent Ca^{2+} channels, leading to decreased Ca^{2+} influx and vasodilation. Closing of K^+ channels leads to vasoconstriction [143-147].

1.2.3.4 Effect of blood flow on vascular tone

1.2.3.4.1 Blood flow–induced shear stress and vasodilation

Flow-induced vasodilation is a local or intrinsic mechanism for blood flow control that operates by mechanisms inherent to the blood vessel wall. Changes in blood flow induce alterations in vascular tone that are independent of transmural pressure, neural or humoral influences. This phenomenon has also been replicated in isolated perfused *ex-vivo* arteries [148-152]. Flow-induced vasodilation occurs in conduit vessels and resistance arteries, and serves as a mechanism to augment flow delivery to arterioles. Increase in flow-induced dilation at the arterioles also serves to balance blood flow and arterial pressure from the upstream conduit and resistance arteries supplying them. The increase in flow through these upstream vessels produces a shear stress that is sensed in the vessel wall and elicits vasodilation [153-156].
Removal or destruction of the endothelium abolishes flow-mediated vasodilation. Different molecules are believed to be involved in shear stress-induced vasodilation including NO since NOS inhibitors decrease flow-mediated dilation [157-160]. There is also evidence that increased shear stress elevates endothelial Ca^{2+} concentrations, which complexes with CaM to activate eNOS [149,161].

Further studies have proposed the role of endothelial-derived H_2O_2, and EDHF in flow-mediated vasodilation [20,23]. However, the identification of the flow/shear stress sensors in the endothelium remains challenging. A significant amount of evidence however, points to the importance of caveolae, endothelial cell cytoskeleton, focal adhesion complexes, the glycocalyx, endothelial junctional proteins, G protein-coupled receptors, primary cilia, and membrane ion channels which likely work together to induce vasodilation [23,161].

1.2.3.4.2 Blood flow–induced mechanotransduction and vasoconstriction

Shear stress arises from the frictional forces exerted directly on the endothelium from the blood flow, which is determined by the velocity, blood viscosity and vessel diameter. Shear stress can cause vasodilation as described above [153-156]. However, the pulsatile nature of blood flow can cause tensile stress (resulting from mechanical stretch), which mainly impacts the medial layers of the vasculature resulting in vasoconstriction [12,162]. Mechanical stretch can be detected and transduced by specific mechanoreceptors such as the stretch activated (SA) channel. SA channel is located on the plasma membrane and has been shown to promote Ca^{2+} influx in

response to mechanical stretch that later initiates phosphoinositide 3–kinase (PI3K) activation, Rho and Rho-associated kinase and vasoconstriction [42,163-165]. Studies on the role of SA channel on signal transduction have shown that TRP channels (such as TRPV4, TRPC1, and TRPP2) are responsible for the Ca^{2+} influx [42,163,166,167]. These reports collectively indicate that blood flow is part of the mechanism through which vascular tone can be controlled.

1.2.3.5 The autonomic nervous system

Vascular tone is also influenced by the autonomic nervous system through the parasympathetic and sympathetic systems that regulate cardiac output and vascular resistance [168]. The neurons of the parasympathetic system mainly regulate the heart rate, while those of the sympathetic system regulate the heart rate, cardiac contraction, vascular resistance, and venous compliance [168]. The changes in vascular tone induced by the sympathetic branch of the autonomic nervous system are mediated by catecholamines like norepinephrine and epinephrine [169]. The adrenal medulla produces the catecholamines which are transported to the VSMCs via the bloodstream. Norepinephrine is released in the perivascular space after activation of sympathetic nerve fibers in the medial layer of the blood vessel wall [170,171]. These catecholamines regulate vascular tone by exerting their effects on the endothelium or vascular smooth muscle by interacting with the α- or β-adrenergic receptors. Endothelial α2-adrenergic receptors promote vasodilation [171,172], whereas activation of α1or α2-adrenergic receptors on the VSMCs induce vasoconstriction [169,171,172]. In contrast, stimulation of the β1or β2-adrenergic receptors on the VSMCs causes vasodilation [173].

Moreover, stimulation of sympathetic nerves supplying the kidney activates the renin–angiotensin system, which results in the production of angiotensin II, a powerful vasoconstrictor [174]. This occurs following the release of renin, an enzyme that cleaves a ten-amino acid, inactive substrate angiotensinogen to angiotensin I. The angiotensin-converting enzyme cleaves two amino acids from angiotensin I to generate an active octapeptide angiotensin II [174,175]. Angiotensin II can then regulate vascular tone by amplifying the effects of norepinephrine on vasoconstriction, but also boost the release of S1P, or norepinephrine from the sympathetic nerve terminals [176-179]. Recently, the angiotensin II-induced hypertension was shown to be reduced following inhibition of sphingosine kinase -1 (SK-1), suggesting that S1P contributes to the pathogenesis of hypertension [179]. Angiotensin II can also induce superoxide formation which

can cause quenching of NO and/or eNOS uncoupling, thereby limiting flow-mediated vasodilation [180].

Collectively, evidence suggests that circulating or vasoactive factors released directly to the VSMCs from the endothelium or produced in the VSMCs modulate vascular tone. However, it is unknown how changes in endothelial permeability impacts vascular tone. One way permeability can affect vascular tone is by promoting leakage of substances to the VSMCs.

1.3 Molecular passage across the endothelium

Under normal physiological conditions, the endothelial barrier controls the exchange of substances between the blood and the sub-endothelial space. Substances like blood fluid, solutes, and even circulating cells can cross the endothelium, mainly through two different pathways, the transcellular and paracellular processes [10].

1.3.1 The transcellular pathway and molecular transport across endothelium

This pathway is also known as transcytosis and involves the transport of macromolecules through the endothelium [181-185]. During this process, the luminal endothelial membrane undergoes invagination to form vesicles that internalize plasma contents including fluid and solutes. The vesicle-mediated endocytosis is initiated when circulating albumin binds to the albumin-binding glycoprotein-60 receptors on the luminal side of the endothelium [186-188]. This is followed by transcytosis or shuttling of these vesicles across the endothelium from the apical to the basolateral membrane. Transcytosis is mediated by individual vesicles, or by a cluster of interconnected vesicles termed vesiculo-vacuolar organelles, which form channel-like structures that span endothelial cells. The vesicular content is delivered to the basolateral membrane by exocytosis [189,190]. Indeed, the processes of endocytosis and exocytosis have been visualized by electron microscopy in capillaries and in venules using gold conjugated to albumin [191], ferritin or horseradish peroxidase as molecular tracers [189]. In these micrographs, the authors showed albumin in various phases of transcytosis in endothelial cells, with open and closed vesicles on the luminal and abluminal side of the endothelium. In addition to albumin, blood immune cells such as leukocytes enveloped in endocytic vesicles can be moved by transcytosis across the endothelial cell interior. This argument has been supported by

the evidence showing fluorescently-labeled leukocytes in membrane invaginations or being enveloped [192,193].

1.3.1.1 Mechanisms of caveolae-mediated transcytosis

Endocytosis is mediated by the lipid raft microdomains known as caveolae, which form cave-like invaginations in the endothelial plasma membrane (Figure 1.6) [185,194,195]. Caveolae contain the protein caveolin (cav), which in mammalian cells consist of three homologs termed Cav-1, Cav-2 and Cav-3 [196]. These proteins are synthesized as monomers and transported to the Golgi complex from where they are externalized through the secretory pathway [196,197]. The caveolins then associate with lipid rafts, but also form oligomers of approximately 14 to 16 molecules. It is these oligomerized caveolins that form the caveolae. Caveolae also contain cholesterol and sphingolipids, as well as scaffolding and signaling molecules that modify caveolin function and initiate vesicle formation and trafficking [181,195,198].

During endocytosis cav-1 is recruited to the membrane forming an oligomer leading to a local change in morphology that give caveolae its characteristic shape and structure [185,199]. The formation of the vesicles is initiated when a family member of Src kinases phosphorylate cav-1 on the luminal side of endothelial cells. Cav-1 subunits aggregate in lipid rafts and oligomerize to form caveolae [200-203]. This is followed by recruitment of dynamin, a GTPase, and its binding partner intersectin-2 to form the elongated neck of caveolae invaginations [204]. The binding of Ras (belongs to a family of small GTPase proteins) to the dynamin-intersectin-2 complex triggers the pinching off of the caveolae invaginations forming enclosed vesicles [203]. These vesicles dock to the inner side of the apical membrane through attachment receptors called v-SNARE that bind to the membrane-bound ligand known as t-SNARE (Figure 1.6) [198,205,206]. Once the docked vesicles are disengaged, they may recycle back to the apical membrane or move across the cell interior to the basolateral side aided by cytoskeletal microtubules [183,207]. Upon arrival at the basolateral membrane, the vesicular v-SNARE bind to t-SNARE, fuse with the basolateral membrane and deliver the vesicular contents by exocytosis to the subendothelial space [185]. However, the specific substances deposited by these vesicles remain to be defined, and also the extent by which these solutes contribute to the basal or stimulated endothelial barrier control is unknown [189,208]. On the other hand, newly formed

undocked vesicles at the apical membrane may attach to microtubules such as kinesin or dynein that facilitate vesicular movement across the cell interior, and ultimately deliver the vesicular contents to the basolateral membrane [181,195,198].

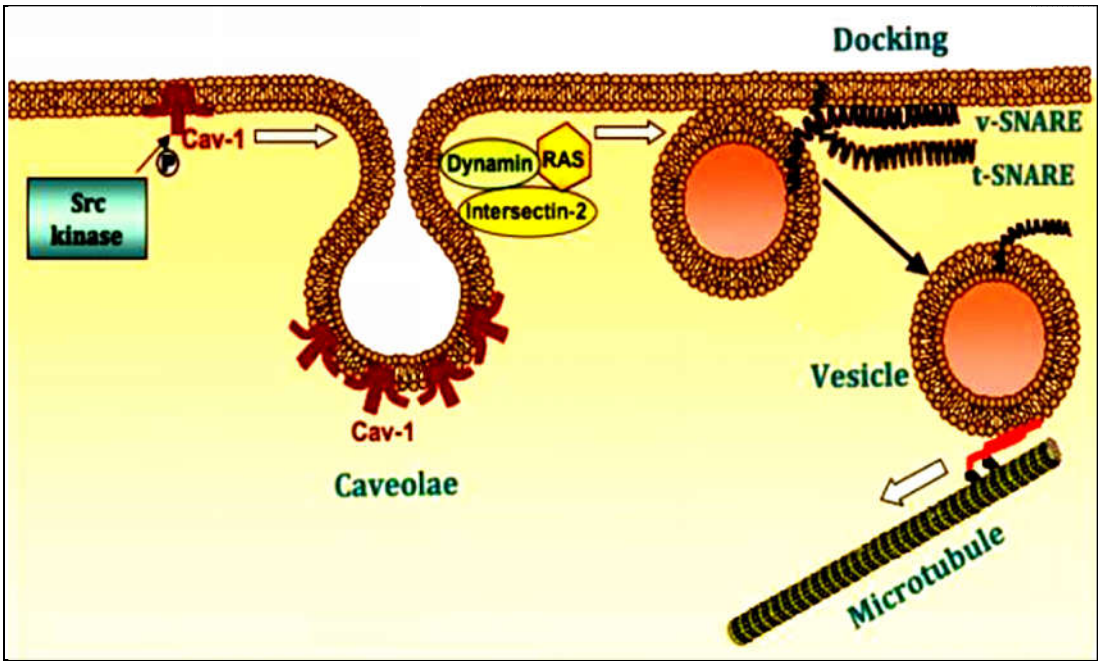

Figure 1.7: Role of Cav-1 in endocytosis. The phosphorylation and activation of cav-1 causes the invagination of the cell membrane, and the complete assembly of the dynamin-intersectin-2-Ras complex promotes the pinching off and formation of a new vesicle. Newly generated vesicles dock to the inside of the cell membrane following the ligation of the vesicular ligand v-SNARE to its cellular target, t-SNARE. Unbound or vesicles disengaged from the t-SNARES attach to motile microtubules which traffic the vesicles within the cell. Figure adapted from *Regulation of endothelial barrier function* by Yuan SY and Rigor RR, 2010. Permission was sought and granted by the primary author and the journal as outlined in Appendix.

1.3.1.2 Cav-1 in regulation of endothelial barrier

The role of cav-1 in regulating endothelial barrier has been shown using cav-1-/- mice or endothelial specific caveolin-expressing mice [209-211]. Cav-1-/- mice exhibited an increase in paracellular permeability in response to permeability-inducing agents [185,211]. In contrast, transgenic mice overexpressing endothelial specific cav-1 showed decreased permeability in response to vascular endothelial growth factor (VEGF) compared to wildtype mice. Thus, while cav-1 and transcytosis contribute to regulation of endothelial barrier under normal conditions,

transcytosis may not be necessary for permeability responses to occur. This argument is in part supported by findings showing that although albumin transcytosis occurs in the lungs, this transcellular albumin flux does not contribute to fluid passage to the subendothelial space [188]. Thus, the contribution of endothelial transcytosis to fluid homeostasis under physiological conditions or plasma leakage under pathophysiological conditions remains to be demonstrated. However, some studies have reported that transcellular water flux contributes a considerable amount of hydraulic conductivity (a measure of permeability) in some endothelial systems [212]. A possible explanation for these conclusions could be the contributions of the transmembrane water channels called aquaporins [213]. These channels are found on endothelial cells and they serve to permit movement of water across the cell membrane. Even so, the contribution of aquaporins in vascular fluid homeostasis is believed to be very minimal [214-217].

1.3.2 Paracellular or intercellular pathway in molecular transport between cells

Paracellular pathway accounts for most of the transport of substances through the intercellular junctions. In pathophysiological conditions, this pathway promotes endothelial leakage of blood fluids and protein molecules [182,186,196]. The control of transport of these substances through the paracellular pathway mainly depends on the structural integrity of intercellular junctions. However, there are exceptions where the cell-cell junctions do not play a role in regulating molecular transport via the paracellular process. In specialized tissues like kidneys, the liver, choroid plexus and the spleen, endothelial cell junctions exhibit discontinuities or fenestrations allowing large molecules and proteins to pass easily through these junctions [183,184]. These types of junctions are physiologically important in absorption of nutrients, detoxification and elimination of toxic waste products.

However, in most tissues and organs intercellular junctions in endothelial cells are tightly complexed allowing selective passage of molecules through these junctions [184,218]. There are mainly two types of intercellular junctions; the adherens junctions (AJ) and the tight junctions (TJ) [182,183]. AJ are widely expressed in most endothelial cells, and when closed, large molecules like albumin of molecular weight 69 kDa and molecular radius of 3.6 nm cannot pass between the cells. AJ, are therefore a major determinant of endothelial barrier in many organs and tissues [182,219]. TJ are less ubiquitous in the peripheral microvasculature compared to AJ. TJ are mainly found in specialized tissues like the blood-retinal or the blood-brain barriers [220].

TJ supply an additional seal to the endothelial barrier function, contributing to tighter restriction to molecular passage. This includes molecules less than 1 kDa and inorganic ions [217].

The tightness of the endothelial barrier is subject to disruption by different stimuli causing disassembly, internalization and/or degradation of junctional proteins (AJ, TJ), cytoskeletal reorganization or interference with extracellular matrix-mediated stabilization of the sealing efficiency of intercellular junctions. These changes cause increased endothelial permeability, and promote excessive leakage of plasma components [183,219,221]. The regulation of transport of substances through the paracellular pathway is very complex and multicomponent-mediated.

1.3.2.1 The role of AJ in regulating endothelial barrier

Endothelial cells are connected to each other by AJ, TJ and GJ, and to the VSMCs via the myoendothelial gap junctions. Extracellularly, the AJ and TJ form the cell-cell zipper-like adhesion complexes [182]. The AJ have been identified in nearly all types of vascular beds, especially in the peripheral microvasculature. Examples of AJ components include junctional adhesion molecules (JAMs), E–cadherin, the platelet-endothelial cell adhesion molecule-1 (PECAM-1) and vascular endothelial cadherin (VE–cadherin) (Figure 1.7). VE–cadherin is a transmembrane receptor and the major structural protein of AJ which has been studied extensively [222]. VE-cadherin binds directly to another VE–cadherin molecule expressed in the membrane of an adjacent endothelial cell. This way VE–cadherin forms a homotypic bond that glues neighboring cells together. The formation of this type of homotypic bond requires the availability of extracellular Ca^{2+} (Figure 1.7), which binds to negatively charged amino acid residues on the extracellular domain of VE–cadherin. This binding promotes a change in VE–cadherin protein conformation enabling the formation of a homotypic bond [223].

Intracellularly, VE–cadherin is linked to the cytoskeletal structures through a family of proteins called catenins. Evidence suggests that VE–cadherin binds directly to β–catenin and γ–catenin, which in turn bind to α–catenin, an actin binding protein. This way the α–catenin links the AJ (VE–cadherin) to the actin cytoskeleton [183,223]. Further stabilization of VE–cadherin to the cytoskeleton is enabled by the binding of α–catenin to additional proteins including the α–actinin, vinculin and formin. VE–cadherin is also stabilized downstream by another protein, p120-catenin, but its role in directly connecting AJ to the actin–cytoskeleton has not been shown.

However, p120-catenin serves an important role as a scaffold protein that brings other signaling molecules into close proximity to interact with VE–cadherin (Figure 1.7) [224]. Therefore this network of interaction between VE–cadherin, catenin and the cytoskeleton is essential not only for cell–cell communications, but also for the maintenance of endothelial barrier function [225-227]. Evidence shows that when the binding of VE–cadherin to β–catenin is disrupted, proper assembly of AJ is impaired decreasing the endothelial barrier function [222]. The functional role of VE–cadherin in promoting endothelial integrity has been demonstrated *in vivo*, in which mice injected with anti-VE–cadherin antibodies showed increased pulmonary vascular leakage [222].

1.3.2.2 The TJ as linkers of the cell-cell junctions

Endothelial TJ molecules include junctional adhesion molecule–A (JAM–A), claudin–3, 5 and occludin. JAM–A, is a member of the immunoglobulin superfamily of proteins; however, the role of JAM–A as a TJ molecule is not properly understood. Occludin and claudins are integral membrane proteins, each with four transmembrane domains and two extracellular loop domains. The extracellular loop domains bind homotypically to adjacent molecules in neighbouring cells. JAM–A, claudin–5 and occludin are further ligated intracellularly to zonula-occludens-1, 2 (ZO–1, 2) which is connected to α–catenin an important linker to actin-cytoskeletal system (Figure 1.8) [183,220,228]. Tight junctions are also present between adjacent endothelial cells and they not only restrict the movement of circulating molecules between endothelial cells to the sub-endothelial space, but they also prevent diffusion of plasma membrane proteins between the apical and basolateral compartments [182]. The binding of occludins, claudins, and JAMs with ZO proteins connects the TJ with the actin cytoskeleton, again promoting barrier integrity (Figure 1.8) [229].Whilst the AJ and TJ form intercellular bonds independently of each other on the extracellular domains, these junctional molecules interact intracellularly through their downstream components. For instance the endothelial TJ bind intracellularly to ZO-1, 2), which is a linker protein to α–catenin that connects VE–cadherin to the actin and the cytoskeleton. However, it is unknown, how such AJ-TJ interplay could regulate the endothelial barrier.

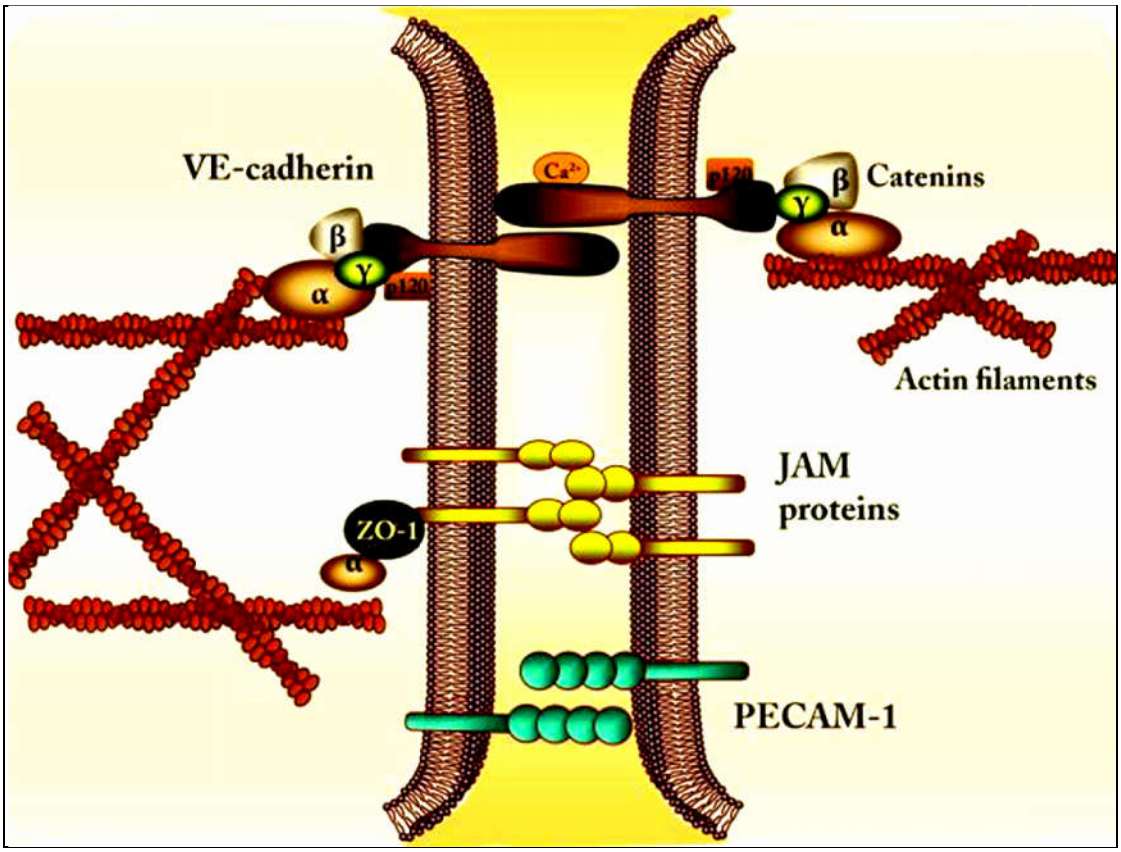

Figure 1.8: Role of AJ in luminal endothelial barrier. The VE-cadherin, JAM and PECAM-1 molecules form homotypic bonds at the cell to cell junctions. VE-cadherin binds to cellular p120, and catenins (α, β, γ) which connects VE-cadherin to the actin cytoskeletal elements via α-catenin. On the other hand, the JAM proteins are linked to the ZO-1 molecules which are further bound to α-catenin molecule connecting JAM molecules to the downstream actin filaments. Figure adapted from *Regulation of endothelial barrier function* by Yuan SY and Rigor RR, 2010. Permission was sought and granted by the primary author and the journal as outlined in Appendix.

1.3.2.3 GJ as mediators of intercellular communication

GJ are important in intercellular communication. They do this by forming channels that connect the cytosols of adjacent endothelial cells [230,231]. The molecular structure involves six connexin subunits that oligomerize to form a hemichannel in the plasma membrane, which can dock to another hemichannel in the plasma membrane of an adjacent cell, assembling a complete GJ channel. GJ allow intercellular transport of small molecules including Ca^{2+} and nucleotides [231]. It also remains to be demonstrated whether the gap junction–mediated molecular signaling

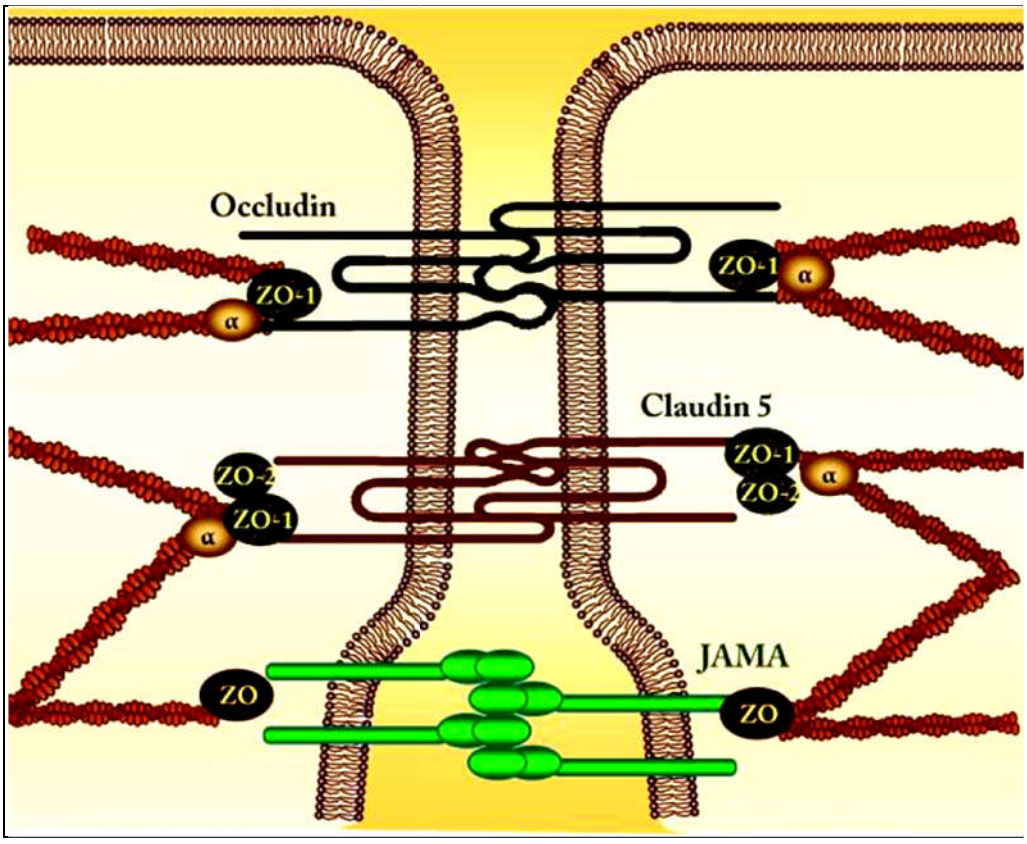

Figure 1.9: The role of TJ on luminal endothelial barrier function. The occludins, claudins and JAM-A enhance the sealing of intercellular junctions by forming homotypic bonds, but they are also further strengthened through ZO proteins which ligates TJ to the cytoskeleton. Figure adapted from *Regulation of endothelial barrier function* by Yuan SY and Rigor RR, 2010. Permission was sought and granted by the primary author and the journal as outlined in Appendix.

(e.g. Ca^{2+}) contributes to control of endothelial barrier. What is known however, is that GJ formed by connexin 43 have recently been linked to pregnancy adaptations involving $[Ca^{2+}]i$ signaling [230]. Activation of phosphorylated eNOS and subsequent production of NO to induce vasodilation, depends on increased $[Ca^{2+}]i$ [232]. NO and PGI_2 increase cAMP and GMP production respectively, which in turn increase connexin 43 expression and GJ. Using freshly isolated uterine artery endothelial cells from a pregnant sheep, Morschauser et al showed increased connexins 37 and 43 that correlated with increased eNOS expression [230]. Connexins, therefore, play an important role in regulating vascular tone through Ca^{2+}–mediated eNOS activation during pregnancy, but whether connexins are dysfunctional in complicated

pregnancies such as preeclampsia, is currently under investigation [230]. Indeed, Krupp et al have recently shown in umbilical vein endothelium isolated from pregnancies complicated by preeclampsia that reduced NO was accompanied by a failure of sustained Ca^{2+} bursting [233].

1.3.2.4 Myoendothelial gap junctions in endothelial-smooth muscle communication

In addition to the GJ between endothelial cells, myoendothelial gap junctions connect the endothelial cells to the underlying VSMCs [230]. The formation of myoendothelial gap junctions is inversely correlated with arterial diameter and the number of VSMCs [234]. These junctions could, therefore, play important physiological roles in smaller resistance vessels in the control of vascular tone [230,235].

1.4 Extracellular anchors and their roles in the control of the endothelial barrier

1.4.1 Focal adhesions as points of attachment for cellular stability

Endothelial cells are linked to the basolateral membrane and the surrounding extracellular matrix (ECM) of the vascular wall by focal adhesion molecules [236]. The major structural components of focal adhesions are transmembrane proteins called the integrins, which are a family of glycoproteins composed of α and β–subunits. Different subtypes of integrins are expressed on endothelial cells. The intracellular domains of integrins interact directly or indirectly with the cytoskeleton through linker proteins like α–actinin, paxillin, vinculin, and talin. Extracellular domains of integrins bind to ECM proteins, like fibrinogen, fibronectin, collagen, vitronectin and laminin [237-239].

The evidence that the integrin–ECM binding is essential for the stabilization of endothelial barriers [240], comes from studies showing that interference with the integrin–ECM binding can disengage focal adhesions, ultimately detaching the cells from ECM [237,241,242]. Recently, the S1P-induced activation of β_4 integrins was shown to enhance lung endothelial barrier [243]. Investigators have also shown that certain members of the integrin family can be located at endothelial cell junctions where they promote formation of lateral junctions. This means that interfering with the integrins function could alter the junctional connection, and the normal cytoskeletal tension leading to increased endothelial permeability. This has in part been shown using permeability-inducing agents like histamine, which increase the strength of integrin–ECM bonding (on either side of adjacent cells) leading to enhanced cytoskeletal

contractile forces and disruption of the cell-cell junctions. Angiopoietin-2 was also shown to destabilize endothelial cell through activation of β_1 integrins [244]. The ECM also maintains the endothelial barrier function by preventing extravasation of circulating cells into the extravascular tissues [245,246]. When antibodies are directed against the β_1 subunit of integrins, transendothelial flux of water and large solutes is dramatically increased. Direct evidence that integrin–matrix interactions is physiologically important has been shown in a study in which synthetic peptides that inhibit integrin binding to fibronectin or vitronectin were used which showed a dose–dependent increase in albumin permeability [247-250]. This response was time–dependent and reversible upon clearance of the peptides [248], consistent with the idea that endothelial cell–matrix adhesion is a dynamic process.

The β_5 subunit of integrins has been identified as a key molecule involved in the recruitment of kinases to focal adhesions in endothelial cells upon stimulation by permeability enhancing agents like VEGF [251]. Mice deficient in integrin β_5 expression display reduced vascular permeability in response to VEGF treatment [252]. Moreover, studies from *in vivo* experiments have demonstrated that plasma leakage across microvessels due to fibrinogen degradation is greatly attenuated in integrin β_1 KO (KO) mice [253], further supporting the role of integrins in regulating endothelial permeability. In pathophysiological conditions, such as inflammation or metastatic cancer, activated leukocytes [254] or invasive tumor cells secrete proteases and other enzymes capable of digesting ECM proteins and disengaging focal adhesions [255] leading to enhanced endothelial permeability. Collectively, these findings highlight the relevance of focal adhesions in the control of the endothelial barrier [256].

1.5 Endothelial cytoskeleton as a player in the control of the endothelial barrier

Apart from the extracellular components such as the endothelial junctions that regulate barrier function, endothelial cytoskeleton plays a central role in the regulation of cell morphology, adhesion and intercellular barrier [257]. Structurally, the endothelial cytoskeleton mainly consists of the actin filaments, microtubules and intermediate filaments [257,258]. Although, the structural support provided by all cytoskeletal components is important for maintenance of the barrier integrity, the actin cytoskeleton plays a significant role in control of endothelial barrier through linkage to AJ and TJ [259].

1.5.1 The role of actin filaments

The actin filaments are linear polymers of filamentous (F)–actin [257]. F–actin is formed from globular actin (G–actin) [258]. G–actin is found within the cell as small globules that polymerize to form and stabilize actin filaments. When the cell is in a resting state, the actin filaments are randomly distributed throughout the cell and at the cell periphery, which are also known as cortical actin [258]. When endothelial cells are stimulated by barrier disrupting agents such as thrombin or histamine via specific receptors and their downstream effectors like RhoA/Rho–kinase [260,261], the actin filaments reassemble into linear, parallel bundles across the cell interior forming what is known as stress fibers. The stress fibers cause the cells to assume a contractile morphology increasing tension between endothelial cells. This increasing tension results in the formation of gaps between adjacent endothelial cells (paracellular permeability) [10,236,257]. In contrast, when these cells are re–engaged with endothelial barrier–enhancing agents such as S1P, at physiological concentrations ≤ 1 μmol/L, the actin filaments rearrange and re–localize to the cell periphery strengthening the cell–cell junctions [262].

Different proteins are known to regulate actin polymerization through promotion of actin disassembly including heat shock proteins, actin depolymerizing factor (ADF), also known as cofilin, particularly non–muscle type cofilin–1 and gelsolin [257,263]. Molecules that activate the Rho family of small GTPases such as Rac1 and Cdc42 promote the formation of cortical actin [264], while those that activate RhoA lead to the formation of actin stress fibers [258]. Cytoskeletal rearrangement and stress fiber formation cause endothelial permeability, but the precise mechanisms and specific contribution of this process to permeability are not well established.

1.5.2 The role of actomyosin contractile machinery in the control of the endothelial barrier

The contraction mediated by actomyosin [265,266] and increased cytoskeletal tension [257,258] is a central mechanism for disruption of the endothelial barrier. Since endothelial cell junctions are connected to focal adhesions through the actin cytoskeleton, changes in cytoskeletal tension directly affect the barrier structure and function [236]. In endothelial cells, as in muscle cells, myosin is bound to actin, and cytoskeletal tension is increased following actomyosin contraction [265,266]. This contraction is initiated by phosphorylation of myosin

regulatory light chain (MLC) which causes an ATP–dependent change in the myosin protein folding and a shift in position relative to actin [263,267]. This shift produces actomyosin contractile force, increasing tension on the actin cytoskeleton. Because the actin cytoskeleton is connected both to cell junction proteins and to focal adhesions, the focal adhesions connection acts as a fulcrum [239], allowing cytoskeletal tension to physically pull apart the cell–cell junctions increasing endothelial paracellular permeability. Conversely, dephosphorylation of myosin light chain-2 (MLC–2) decreases actomyosin contractility, relaxing the actin cytoskeleton, and decreasing endothelial permeability [263,267].

MLC–2 is phosphorylated by MLCK [265,266] and is dephosphorylated by MLCP [268]. The normal endothelial barrier is regulated by the steady-state phosphorylation and dephosphorylation actions mediated by MLCK and MLCP, respectively [257,263]. Any stimulus that impacts any of these enzymes will affect endothelial barrier. Inflammatory agents and diseases associated with increased endothelial permeability have also been linked with the activation of MLC-2 [265,269].

1.5.3 The role of microtubules in endothelial barrier control

Microtubules are important for cell mitosis, morphology, and intracellular protein trafficking. Microtubules are tubular structures formed from α– and β–tubulin subunits [258]. One tubular structure is formed from 13 parallel polymeric filaments arranged in a ring. The stability of microtubules is determined by polymerization and depolymerization of component units. Microtubules can be further stabilized by capping or by other posttranslational modifications events. In endothelial cells, microtubules are cross–linked with actin filaments and can affect endothelial barrier through effects on actin filaments. Active rearrangements of microtubules affect the organization of other cytoskeletal components, and stabilization of microtubules protects the endothelium against actin stress fiber formation and barrier disruption [270]. Depolymerization of microtubules activates guanine nucleotide exchange factors, and signaling through Rho family GTPases, leading to actin stress fiber formation and endothelial barrier disruption [271]. The role of microtubules in the control of the endothelial barrier has been shown in experiments where microtubules were destabilized by treatment of endothelial cells with thrombin [272] or the inflammatory cytokine TNF–α [270,273], leading to barrier

dysfunction. Stabilization of microtubules in endothelial cells by agents such as cAMP [273], or activation of PKA enhances the endothelial barrier [274].

1.5.4 The role of intermediate filaments in the control of the endothelial barrier

The intermediate filaments are formed from heterogeneous proteins [275]. The major intermediate filament protein in most cells is vimentin. The intermediate filaments are important for cell structure, and are expressed mostly in cells exposed to shear stress, like endothelial cells. Intermediate filaments are connected to proteins at the cell–cell junctions (e.g. p120), and also connected to the focal adhesions at the basement membrane. Intermediate filaments transmit mechanical tension between cells joined by intercellular junctions [275]. The role of intermediate filaments in the control of endothelial barrier function is not fully understood. However, in endothelial cells, the intermediate filaments are believed to provide redundant structural support and stabilization of the actin filaments [275]. There are no vascular defects in vimentin gene knock-out mice [276], suggesting that vimentin filaments may not be necessary for the physiological functions of the endothelium. However, there is evidence that the connections of vimentin filaments to endothelial VE–cadherin are disrupted when endothelial cells are treated with histamine [277]. These data suggest the likelihood of an indirect involvement of the intermediate filaments in the control of the endothelial barrier. They may also serve as a scaffold for other proteins.

1.6 Factors that generally decrease or increase endothelial permeability

The barrier integrity is regulated by both circulating and endothelial–derived factors. The effectiveness of the barrier differs depending on the vascular bed; for example, it is greater in cerebral compared to the renal vasculature. One of the most studied signaling systems that maintains endothelial barrier integrity is angiopoietin–1, but also S1P (described later). Angiopoietin-1 enhances the barrier by signaling through its receptor, Tie2 regulating stress fiber formation [278], however, angiopoietin-2 disrupts the barrier by activating β_1-integrins [244]. The disruption of endothelial barrier function is common in vascular disorders like atherosclerosis [279], hypertension and cardiovascular disease [218]. Thrombin is an example of a relatively well known endothelial-barrier disrupting agents, which mediates its functions via the protease activated receptors (PARs). In addition to being a permeability factor, thrombin is

involved in the blood coagulation process in which it converts fibrinogen to fibrin, in a complex process involving the activation of transglutaminase (factor XIIIa) that catalyzes the formation of covalent bonds between lysine and glutamine residues in fibrin. These covalent bonds increase the stability of fibrin and blood clotting. Thrombin also promotes platelet activation and aggregation by activating PARs on the cell membrane of platelets as part of the clot formation process.

Other endothelial barrier-disrupting agents include TNF–α, IL–6 [280,281], C–reactive protein (CRP) [282], S1P, TXA_2 and VEGF [222,229]. The mechanisms through which these molecules cause endothelial permeability include promoting endocytosis of junctional molecules like VE–cadherin [227], PKC activation leading to phosphorylation of occludens and disruption of TJ [182,186,268], caveolae–mediated transcytosis [210] and activation of the eNOS pathway. While these mechanisms highlight the pathways through which inflammatory mediators cause endothelial permeability, it unknown whether and how endothelial permeability impacts vascular tone. S1P, a bioactive lipid that is part of the focus of this thesis controls endothelial barrier, but also vascular tone. However, the role of S1P in regulating endothelial permeability and vascular tone in arteries remains to be demonstrated.

1.7 S1P

1.7.1 Sphingolipid metabolism

Sphingolipids are structural components of the cell membrane; however, the sphingolipid metabolites including sphingomyelin, ceramide, ceramide 1–phosphate, sphingosine, and S1P exhibit cell signaling properties [283]. *De novo* synthesis of sphingolipids begins in the endoplasmic reticulum (ER), in which the amino acid serine and palmitoyl–CoA combine in the presence of serine palmitoyltransferase to form 3–ketodihydrosphingosine [284,285]. 3–ketodihydrosphingosine is then reduced through the actions of 3–ketodihydrosphingosine reductase to dihydrosphingosine. Dihydrosphingosine is rapidly N–acylated by a family of six dihydroceramide synthases (CerS1–6) to generate a precursor for ceramide, called dihydroceramide (Figure 1.9) [286]. Dihydroceramide undergoes desaturation (a double bond is introduced at C4 and C5) catalyzed by dihydroceramide desaturase, in which dihydroceramide becomes ceramide [287-289]. Ceramide is considered central to sphingolipid metabolism, and has several fates (Figure1.9): (**1**) ceramide can be converted to glycolipids such as

glucosylceramide or galactosylceramide which have glucose and galactose moieties, respectively. The transfer of these sugar units to ceramide is catalyzed by glucosylceramide or galactosylceramide synthase respectively. These glycolipids can be converted back to ceramide by cerebrosidase [285,290]. (**2**) Ceramide can also be phosphorylated by ceramide kinase to ceramide 1–phosphate or dephosphorylated by ceramide 1–phosphate phosphatase back to ceramide [285]. (**3**) The newly synthesized ceramide is transported from the ER to the Golgi complex aided by ceramide transfer protein or through specific vesicles [291]. In the Golgi complex, ceramide is converted by sphingomyelin synthase to sphingomyelin. Once formed, sphingomyelin is transported via Golgi complex–derived vesicles to the cell membrane. In the cell membrane, sphingomyelinase degrades sphingomyelin by cleaving the phosphocholine head group from phosphatidylcholine forming ceramide and diacylglycerol. Sphingomyelin hydrolysis also occurs in the Golgi complex and the lysosome [292]. (**4**) Ceramide can also be deacylated by ceramidase to form sphingosine, which can be recycled back to ceramide by the action of ceramide synthase [291]. Sphingosine is rapidly phosphorylated by SK-1 and SK-2 to form S1P [283,293]. S1P can itself be dephosphorylated by S1P phosphatases (S1PP)–1, 2 (S1PP1 and S1PP2) or lipid phosphate phosphatases (LPPs) in a reversible manner forming sphingosine [294]. S1P can also be irreversibly degraded by S1P lyase (SPL) to form ethanolamine 1–phosphate and hexadecenal [295,296].

1.7.1.1 S1P metabolizing enzymes

1.7.1.1.1 Sphingosine kinases: similarities and differences

SK-1 and SK-2 are structurally homologous, except that SK-2 has an extended N-terminal tail [297-299]. SK-1 is predominantly found in the cytoplasm, but also found in the plasma membrane portions of the cell, while SK-2 is located in the nucleus, ER or mitochondria [300,301]. SK-1 and SK-2 show different tissue distribution with SK-1 highly expressed in the lungs and spleen, and SK-2 in the liver and the heart. SK-1 and SK-2 are phosphorylated by ERK [302-305], and both show substrate specificity towards D-sphingosine and D-dihydrosphingosine [306,307]. However, SK-2 has broader substrate specificity, including phytosphingosine and the sphingosine analog FTY720. Pharmacologically inhibiting SK-1 or using SK-1 knock-out mice decreased plasma S1P to about 50% suggesting that both SK-1 and SK-2 are equally important in the production of circulating S1P [308,309]. However, as shown

in section 1.7.1.4, these experiments do not tell the entire story about the source of circulating S1P, and additional studies to provide further insights could be helpful. Interestingly, SK-1 and SK-2 also exhibit opposing functions, for example SK-1 has been shown to promote cell growth, while SK-2 inhibits it [290,293,303,310].

1.7.1.1.1.1 SK-1

SK-1 was initially cloned from yeast (in 1998) [311] and in the same year two splice variants were identified in mice (SK-1a, SK-1b) [306]. Eight years later three splice variants in human (SK-1a, SK-1b, and SK-1c) were identified [312]. There is high sequence homology between the human SK-1 and that from other organisms. SK-1 is highly regulated at all stages of expression including transcriptional and post–translational processes [313]. SK-1 is activated by direct phosphorylation of its serine residue 225 [314]. The cellular localization of SK-1 is important for its activity, where it needs to translocate to the cell membrane to interact with its substrate sphingosine [315]. SK-1 phosphorylation leads to conformational and/or electrostatic changes that enables SK-1 to translocate and localize at the cell membrane [316]. Such SK-1 translocation to the cell membrane is aided by CaM, PKC, calcium–and–integrin–binding protein 1 [315] and Ras [317]. SK-1 can also be deactivated by dephosphorylation by protein phosphatase 2A [318] or degraded permanently through the ubiquitin–proteasome complex–mediated pathway [319]. TNF-α also promotes downregulation of SK-1 through a cathepsin B–mediated process [320,321]. SK-1 is exported from endothelial cells [312,322], or monocytes [323] through ATP–binding cassette (ABC)–type transporters, indicating the possibility of a role played by extracellular SK-1 to generate S1P. Nevertheless, the S1P generated by SK-1 is important in different biological functions such as cell migration, angiogenesis, or lymphocyte trafficking [293,324,325].

1.7.1.1.1.2 SK-2 and functional characterization

SK-2 is poorly characterized compared to SK-1. Unlike SK-1 where plasma S1P is halved upon genetic deletion or pharmacological inhibition [326], subjecting SK-2 to the same treatment results in a dramatic increase in plasma S1P [308]. These results suggest that the control of plasma S1P levels is likely more complex than theoretically anticipated. It is possible to argue however, that such an exaggerated accumulation of plasma S1P results from

rephosphorylated sphingosine after degradation of S1P by ecto–LPPs. The re–phosphorylation of sphingosine is likely catalyzed by extracellular SK-1 [327].

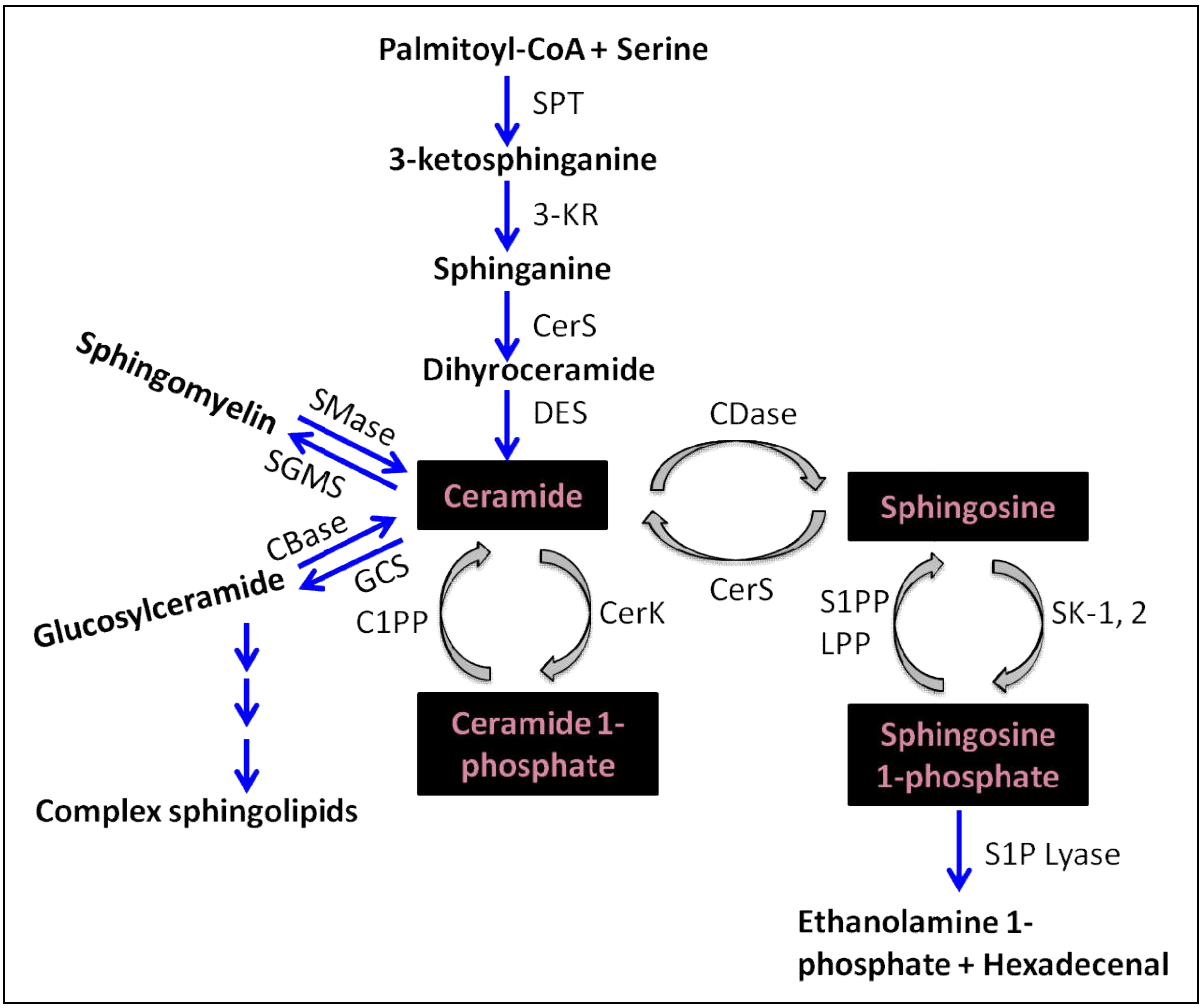

Figure 1.10: Sphingolipid metabolism and S1P generation. Ceramide is either synthesized *de novo* through the sequential action of serine palmitoyl transferase (SPT), ketosphinganine reductase (3-KR), ceramide synthase (CerS), and dihydroceramide desaturase (DES), or from the hydrolysis of sphingomyelin by sphingomyelinase (SMase) or glycolipids (like glucosylceramide) by cerebrosidase (CBase). Ceramide can further be metabolized as shown through different enzymatic steps. The abbreviations stand for: ceramidase (CDase), ceramide synthase (CerS), ceramide kinase (CerK), ceramide 1-phosphate phosphatise (C1PP), sphingosine kinase-1, 2 (SK-1, 2), and S1PP, lipid phosphate phosphatise (LPP), glucosylceramide synthase (GCS) and sphingomyelin synthase (SGMS).

Using SK-2-deficient mice or inhibitors, SK-2–derived S1P has been shown to be involved in

various biological functions including uterine deciduation [328], regulation of histone acetylation [329], macrophage polarization [330], regulation of cytokine expression [331], and protection from ischemia–induced renal and cerebral tissue injury [332]. Experiments from SK-2–generated S1P provided the first evidence for the existence of an intracellular S1P target, in which S1P directly deterred histone deacetylation. In these experiments, SK-2–generated nuclear S1P prevented the removal of acetyl groups from histone tails by directly interacting with and inhibiting histone deacetylases 1 and 2 [329]. In another study, hypoxia preconditioning–induced cerebral ischemia was associated with increased expression and activity of SK-2 in the cerebral microvasculature. In hypoxia preconditioning-induced cerebral ischemia, SK-1 was unchanged. Inhibiting SK-2 by N, N–dimethylsphingosine during hypoxia preconditioning blocked the infarct volume (a measure of brain injury) and hypoxia preconditioning–induced edema. These findings indicate that hypoxia preconditioning–induced ischemic tolerance is mediated by an increase in microvascular SK-2 activity. Even so, the use of the nonspecific inhibitor N, N–dimethylsphingosine leading to the abrogation of hypoxia preconditioning–induced tolerance may not preclude the participation of SK-1 [332].

In contrast, SK-2 also mediates biological events independently of the production of S1P. SK-2 appears to contribute to the regulation of $CD4^+$ T cell responses to interleukin 2 in an S1P–independent manner [333]. Further, SK-2 causes apoptosis independent of S1P activity that was linked to a 9–amino acid motif similar to that found in the BH3–only proteins (that is also present in SK-2), a pro–apoptotic subgroup of the B–cell lymphoma–2 (Bcl–2) family. Co–immunoprecipitation experiments revealed that indeed SK-2 directly ligates to Bcl–xL, and the SK-2–induced apoptosis was also associated with the release of cytochrome c and activation of caspase–3 [310]. Further evidence from site–directed mutagenesis targeting Leu–219 of SK-2, the conserved leucine amino acid present in all BH3 domains, showed that SK-2–induced apoptosis was linked to its BH3 domain [303,310].

1.7.1.1.2 Phosphatases: SPPs and LPPs

SPP1 and SPP2 belong to a family of phosphatases including the LPPs [295,334,335]. SPP1 and SPP2 are located in the ER, and they specifically dephosphorylate S1P to sphingosine [294,334,336]. SPP1 is also exported extracellularly by ABC transporters where it can access and dephosphorylate extracellular S1P [89]. The proinflammatory factors TNF–α and

lipopolysaccharide (LPS) increase the expression and activity of SPP2 in endothelial cells and neutrophils. Elevated levels of SPP1 and SPP2 have been implicated in the pathogenesis of inflammation-related diseases such as psoriasis and cancer [337,338].

Moreover, three broad–specificity LPPs (LPP1, LPP2, and LPP3) are normally found in the inner leaflet of the cell membrane, but also all three can function as ecto enzymes with their active site on the outer leaflet. These enzymes catalyze the dephosphorylation of S1P, ceramide 1–phosphate and FTY720–phosphate (FTY720–P), and lysophosphatidate (LPA) [335,338,339]. Interestingly, Ecto–LPP1 promotes the intracellular formation of S1P from internalized sphingosine in human lung endothelial cells [340]. This sphingosine is derived from LPP1-degraded S1P. Indeed overexpression, or siRNA–mediated knockdown of LPP1 results in increased, or decreased accumulation of intracellular S1P, respectively [340]. This means that LPP1 can contribute to intracellular S1P signaling. Since sphingosine or high levels of S1P can cause cell death, the fate of a cell depends on how the activities of SK-1 and SK-2 that control phosphorylation, and those of SPPs, SPL (see below) and LPPs that control dephosphorylation or degradation are balanced [341,342]. Furthermore, intracellular LPP2, but not LPP3, is functionally linked to phospholipase D1, which promotes recruitment of SK-1 to the perinuclear compartment (space between the inner and outer nuclear membranes) to catalyze formation of S1P [343]. Effectively, LPPs play a dual role that significantly regulates the levels of S1P.

1.7.1.1.3 SPL

SPL, an intracellular enzyme, degrades S1P irreversibly to hexadecenal and ethanolamine 1–phosphate [291]. The SPL activity was first described in 1969 [344], but it is in 1997 that the first SPL gene was cloned [344]. This discovery was followed by the cloning of *Sgpl1* genes encoding the murine and human SPL proteins [345]. The murine SPL is highly expressed in the intestine, the thymus and the olfactory (sensory system) mucosa. SPL is activated by the platelet–derived growth factor [346,347]. The SPL KO mice fail to survive beyond weaning and the mice suffer from myeloid cell hyperplasia, anemia, and exhibit pathological lesions in the lung, heart, urinary tract and bone [348]. These findings suggest that SPL is involved in development, likely by controlling the levels of S1P.

1.7.1.2 Circulating S1P and its carriers

S1P is an 18-carbon amino alcohol initially disregarded simply as an intermediate of sphingolipid metabolism [349]. Later, S1P was found to possess cell signaling capabilities, in particular $[Ca^{2+}]i$ release [350]. The discovery of the first S1P receptor previously termed endothelial differentiation gene (EDG)–1 [351] and later other EDG–related receptors [352] ushered in a new era of understanding the biology of S1P. Now, S1P is regarded as a multifaceted, bioactive signaling lipid [353]. S1P is a component of plasma [354], and is transported via high-density lipoproteins (HDL) (50–60%) bound to apolipoprotein M (apoM) in the HDL molecule [355]; [356], albumin (30–40%), low density lipoproteins (LDL) (~8%), and very low density lipoproteins (VLDL) (2–3%) [357-359]. The physiological concentration of S1P is ~ 0.1 to 1.1 μM [360], and the Kd values for the S1P receptors are ~2–30 nM [358]. This means that the circulating S1P in the plasma could induce a maximal response were it to interact with its receptors; however, evidence suggests that the amount of bioactive S1P in the plasma is only ~10 nmol/L [361]. This is in part because the metabolism and biological activity of plasma S1P depends on its carrier. For instance, the protection against myocardial ischemia/reperfusion injury is mediated by HDL or albumin–bound S1P, but not LDL–bound S1P [362]. Further, while HDL or albumin–bound S1P enhances the endothelial barrier, the duration of the barrier protection is much longer with HDL–bound S1P compared to albumin–bound S1P. This has been associated with the capacity of HDL to protect S1P against degradation by ecto–LPPs, particularly LPP1 [363]. The half–life of HDL–bound S1P when added to human umbilical vein endothelial cells (HUVECs) is four–fold longer compared to albumin–bound S1P [364]. The half–life of an albumin–bound 17–carbon analog of S1P (called C17–S1P) injected intravenously to mice is approximately 15 minutes [364]. S1P is more stable in isolated plasma, compared to whole blood or when added to HUVECs [365] or human pulmonary artery endothelial cells [340].

1.7.1.3 Intracellular S1P signaling

S1P has been regarded as an intracellular second messenger, but the intracellular targets have not been fully defined. Indeed, the lack of S1P receptors in lower order organisms like *Saccharomyces cerevisiae* [311] is a demonstration that S1P likely signals via intracellular targets. S1P also promotes growth and survival of mouse embryonic fibroblasts lacking S1P

receptors [366], and mobilizes [Ca^{2+}]i [367]. More compelling evidence came from studies showing that SK-2–produced S1P binds directly to histone deacetylases inhibiting their function [329]. A variety of studies performed in organisms lacking S1P receptors show that disrupting S1P metabolism can result in marked changes in cell migration, Ca^{2+} mobilization, stress responses, endocytosis, tissue homeostasis, and reproduction [291]. These effects could be explained by the direct interaction of S1P with intracellular targets.

1.7.1.4 S1P transport out of cells

SK-2 is located in the ER, nucleus or mitochondria and most of the S1P is likely degraded before it reaches the cytoplasm by SPP1 and SPP2 [294,334,336]. The S1P generated by SK-1 is secreted, and can activate S1P receptors ($S1P_{1–5}$) [293,324,325]. The ABC transporters including ABCC1 in breast cancer and mast cells [368,369], ABCA1 in astrocytes [370], and ABCG2 [369] in breast cancer cells are involved in S1P transport out of the cells. In addition, the two of hearts protein (TOH) also termed spinster homolog 2 (Spns2) previously identified as an S1P transporter in zebra fish [371], also exports S1P out of endothelial cells (Figure 1.10) [295,298]. Spns2 also externalizes phosphorylated FTY720, an S1P mimic that is used to control lymphocyte egress in multiple sclerosis [372].

1.7.1.4 Extracellular and “inside-out” S1P signaling

There are five S1P receptors ($S1P_{1–5}$), which are closely related. These receptors were originally named Edg for **E**ndothelial **d**ifferentiation **g**ene ($S1P_1$/Edg–1, $S1P_2$/Edg–5, $S1P_3$/Edg–3, $S1P_4$/Edg–6 and $S1P_5$/Edg–8). These S1P receptors are coupled to heterotrimeric G–proteins. $S1P_1$ is associated with G_i, (particularly subtypes $G_{i\alpha1}$ and $G_{i\alpha3}$); $S1P_2$ with G_i, $G_{12/13}$ and G_q;$S1P_3$ with G_i, G_q or $G_{12/13}$ subunits [341]. Various cell types express different combinations of these receptors. Endothelial cells primarily express $S1P_1$ and $S1P_3$ receptors, whereas $S1P_1$, $S1P_2$ and $S1P_3$ receptors are expressed on VSMCs. $S1P_4$ and $S1P_5$ receptors are normally expressed in the brain, lung and lymphoid tissues, but they are not normally detectable in the vascular system [373]. There have also been a number of putative S1P receptors described in the literature including Gpr_3, Gpr_6 and Gpr_{12}. These three receptors are coupled to $G_{\alpha s}$ and $G_{\alpha i}$ type of G proteins and are expressed in HUVECs and VSMCs [374-378]. The S1P signaling through the G

protein-coupled receptors results in downstream activation of different effector molecules like Rac, ERK, PI3K, PLC, Rho, and JNK, inducing different biological responses [293,325].

Intracellular S1P can be exported from inside to the outside of the cell through different transporters as noted above. This way S1P can access the cell surface receptors on the cell from which it was produced or on neighboring cells. The entire process leading to S1P export and activation of extracellular S1P receptors is loosely termed "inside-out" signaling [291,293,325,342,379,380]. Ligand–mediated activation of SK-1 is an example of an event that promotes *inside–out* S1P signaling. However, the subcellular compartment where S1P is produced is important for *inside–out* signaling. Most ligands that activate SK-1 promote its translocation to the plasma membrane bringing it into close proximity with its membrane–localized substrate, sphingosine [307,381]. S1P formed at the inner leaflet of the plasma membrane can then be immediately exported from the cell to act as a ligand for its own receptors [382]. In contrast, the S1P produced by the ER–resident SK-2 is subject to degradation by SPL and S1PP, both found in the ER [285]. This means that the chances of S1P to be exported from the ER to the cytoplasm, and then extracellularly to act as a ligand for S1P receptors are very minimal [307,381].

The major sources of circulating S1P include erythrocytes, platelets, leukocytes and the endothelium, but S1P is produced by virtually every cell [361,364,383]. At the cellular level, S1P activates its receptors to modulate different events including cell survival, proliferation, cytoskeletal structure and epigenetic regulation [293,352,384]. Physiologically, S1P contributes to vascular development, cardiovascular function, angiogenesis, heart rate, uterine implantation, lymphocyte recirculation, wound healing, vascular tone and endothelial integrity [32,293,352,373,385,386] among others. S1P also contributes to different pathologies including atherosclerosis, cancer and metastasis, multiple sclerosis [384,387,388], osteoporosis, inflammation and increased vascular leakage [389]. Part of this work focused on the role of S1P-induced endothelial permeability on vascular tone.

1.7.2 S1P and endothelial permeability: effects on cell-cell junctions

1.7.2.1 ***S1P effects on AJ:*** S1P-induced regulation of endothelial permeability depends on its concentration, the S1P receptors expressed and the vascular bed. Many studies demonstrate that signaling through $S1P_1$ enhances endothelial barrier function and blocking $S1P_1$ results in

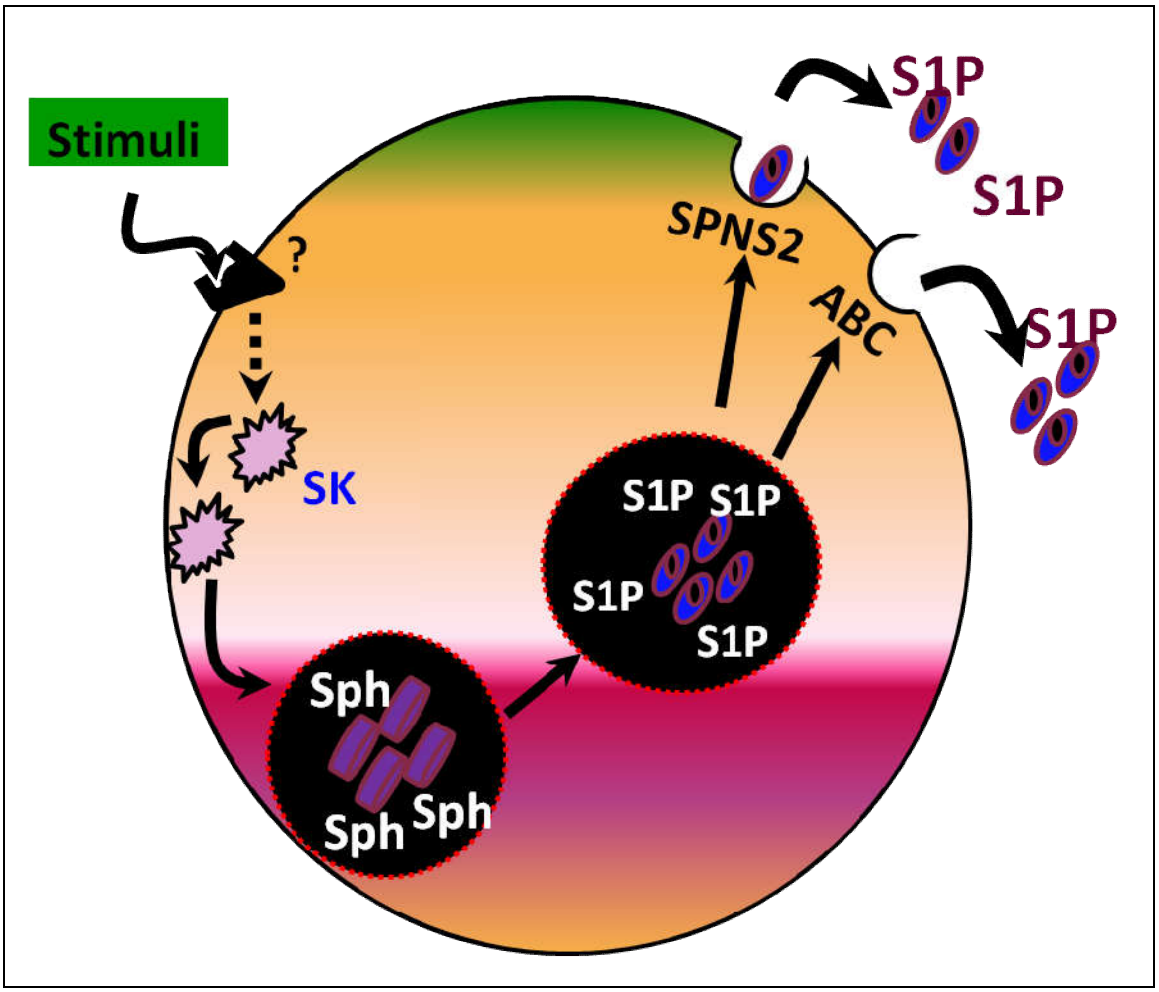

Figure 1.11: Export of S1P out of a cell. Depiction of stimuli-mediated activation of SK, intracellular generation and export of S1P through spns2 and/or ABC-type transporters.

vascular leakage [390]. S1P increases endothelial barrier function by reorganization of junctional proteins such as VE–cadherin and β–catenin at the cell–cell contacts [390]. Silencing of $S1P_1$ reduces VE–cadherin and platelet–endothelial cell adhesion molecule–1 expression [391]. S1P also promotes the formation of endothelial TJ through $S1P_1$ by redistributing ZO–1 to lamellipodia and cell–cell junctions [392]. These events are mediated through $S1P_1$ in a $G\alpha_i$/Rac/PI3K–dependent manner. Activation of $S1P_1$ stimulates Gαi–mediated activation of PLC, increases $[Ca^{2+}]i$ and activates Rac1 and Cdc42. This induces actin reorganization, stabilization and restoration of the cell–cell junctions [182,393]. Recently, the structure of ligand–bound $S1P_1$ was revealed, and the data suggest that S1P might engage with the receptor within the plasma membrane [394], indicating that lateral movements of S1P within the

membrane or ligand swapping between $S1P_1$ and other receptors might be possible. However, the effects of such S1P–$S1P_1$ interaction within the plasma membrane on endothelial barrier are not known. In contrast, the S1P signaling via $S1P_2$ and $S1P_3$ weakens the endothelial barrier by disrupting AJs and increasing paracellular permeability through Rho–A and phosphatase and tensin homolog (PTEN) activated pathways [390]. The disruption of cellular junctions through $S1P_2$ or $S1P_3$, occur by G_q activation of PLC and increased $[Ca^{2+}]i$ which is followed by induction of a cascade of events that ultimately disassemble the junctions. Activation of $G_{12/13}$ stimulates Rho–A and promotes actin cytoskeleton destabilization inducing disruption of cellular junctions [393].

1.7.2.2 ***S1P effects on TJ:*** In addition to increasing the tightening of AJ, S1P through S1P1 receptor enhances the assembly of endothelial tight TJ. The TJ are positioned in between the outer leaflets of the lateral membranes (the membrane bordering neighboring cells) of adjacent cells. The TJ are connected to the actin cytoskeleton by the interaction and binding of the occludins, claudins or junctional adhesion molecules to zona occludens proteins (ZO–1, ZO–2, or ZO–3) [395]. Following stimulation of cells by S1P, ZO–1 is translocated to the lamellipodia and the cell–cell junctions through the $S1P_1$/Gi/Rac/Akt pathway. The S1P–induced endothelial barrier stabilization is significantly attenuated by siRNA–mediated downregulation of ZO–1 expression [392]. Thus, like the AJ, the TJ also play an important role in S1P-mediated endothelial barrier control.

1.7.2.3 ***S1P effects on GJ:*** S1P impacts GJ in a cell–specific manner. S1P increases connexin 43 expression through p38–MAPK in skeletal muscle, stimulating differentiation [396]. S1P also inhibits GJ communication in astrocytes through dephosphorylation of connexin 43 [397]. S1P–induced phosphorylation of connexin 43 is PKC–dependent, and in cardiomyocytes was found to protect against ischemia reperfusion injury by decreasing GJ function [398]. The role of GJ in S1P–induced regulation of endothelial barrier function is unknown.

1.7.3 S1P-mediated effects on endothelial cytoskeletal function and the impact on endothelial permeability

1.7.3.1 ***S1P effects on actin microfilaments:*** The actin filaments are part of a network of cytoskeletal elements (described above) that regulate cell morphology and transduce signals within and between neighboring cells to maintain endothelial barrier [399]. S1P enhances polymerization of F–actin and MLC phosphorylation, increasing endothelial barrier function. The S1P–mediated effects on actin that lead to increased barrier function are disrupted by treatment of endothelial cells with an actin depolymerizing agent cytochalasin B, or an inhibitor of actin polymerization latrunculin B [400]. S1P also increases endothelial barrier via actin–associated cytoskeletal proteins like cortactin (name derived from cortical actin binding protein), a monomeric protein found in the cytoplasm involved in actin polymerization and cortical actin (actin found in the cell periphery) rearrangement [401,402]. S1P also enhances the barrier via MLCK which increases phosphorylation of MLC enabling actin–myosin interaction, stress fiber formation and cell contraction [403]. S1P–mediated stimulation of endothelial cells mobilizes cortactin translocation from the cytoplasm to the periphery, causing cortical actin redistribution. The role of S1P–induced cortactin activation and maintenance of endothelial barrier has been supported by cortactin depletion experiments using antisense oligonucleotides, which significantly attenuated S1P–mediated stabilization of endothelial barrier [404]. While exposure of endothelial cells to physiological levels of S1P stimulates activation of MLCK and phosphorylation of MLC, MLCK works cooperatively with cortactin to promote barrier–stabilization by S1P. This is supported by reports showing that MLCK directly binds to cortactin Src homology 3 domains, but also cortactin blocking peptides inhibit the S1P–induced MLC phosphorylation and barrier function [392,404].

The effect of S1P on the actin–dependent processes described above is mediated through a Rho family of small GTPases. The S1P signaling via $S1P_1$ results in the activation of Rac GTPases needed for S1P–induced cytoskeletal rearrangement [405,406]. This is followed by peripheral actin polymerization, formation of lamellipodia, cell ruffling, spreading of endothelial cells and increased barrier integrity [400,404]. Indeed inhibition of Rac GTPases increases endothelial permeability [407,408], but also microinjection of a dominative negative mutant of Rac into endothelial cells greatly decreases S1P–induced assembly of VE–cadherin and β–catenin at endothelial cell–cell junctions [406,409]. The S1P–induced cytoskeletal rearrangement

and barrier protection is dependent on the S1P concentration and the S1P receptors engaged. S1P at physiological concentrations (0.01–1 μmol/L) induces an $S1P_1$/Rac–dependent enhancement of barrier function, but at higher concentrations S1P stimulates $S1P_2$ or $S1P_3$/RhoA–dependent disruption of the barrier which overcomes the signals generated via $S1P_1$/Rac-pathway [410-413].The role of microtubule or intermediate filaments on the S1P–mediated endothelial barrier function is yet to be demonstrated.

In cultured endothelial cells S1P was shown to significantly decrease thrombin–induced permeability [414]. In tissues, such as intact perfused rat mesenteric venules, S1P or SEW2871 ($S1P_1$ agonist), were shown to inhibit endothelial permeability evoked by bradykinin or platelet activating factor [415,416], S1P exhibited barrier–enhancing properties in perfused rat mesenteric venules, but also erythrocyte–derived S1P tightens the barrier against basal permeability in rat mesenteric microvessels [415-417].

1.7.4 S1P and endothelial permeability in *in vivo* models

The role of S1P in protecting endothelial barrier function is becoming increasingly attractive for therapeutic application in endothelial–related pathologies. Vascular disorders are associated with increased permeability and they include inflammation, ALI, atherosclerosis, anaphylaxis and ischemia-reperfusion injury [418]. S1P enhances the endothelial barrier and one of the most compelling evidence is the demonstration that mice deliberately engineered to lack plasma S1P suffer from vascular leakage and restoration of S1P through erythrocyte transfusion dramatically decreased vascular leakage and improved mice survival [419].

1.7.4.1 *S1P and ALI*: ALI is an inflammatory lung disease associated with increased in vascular permeability [420]. Under laboratory conditions, to mimic the clinical presentation of ALI, researchers use LPS delivered intratracheally in experimental animal models. S1P decreases the inflammatory effects associated with ALI. In an ALI murine lung model, intravenous administration of S1P significantly reduced LPS–induced lung injury, but also lowered neutrophil infiltration in the lung parenchyma. The use of FTY720 (which is phosphorylated *in vivo*), a sphingosine analog delivered intraperitoneally, inhibited LPS-induced pulmonary vascular leakage [421,422]. Further, using a canine (beagle, i.e. dog) model of ALI, McVerry et al., showed that intravenous administration of S1P markedly attenuated alveolar and vascular

leakage [422]. Four years later Szczepaniak et al using the same animal model, demonstrated that S1P could decrease the LPS–induced pulmonary shunt (occurs when alveoli are filled with fluid, interfering with ventilation of the lungs), and accumulation of protein and neutrophils in the bronchoalveolar lavage fluid compared to vehicle–treated controls [423]. Moreover, the inhibition of SPL, which was associated with increased S1P levels in lung tissues and bronchoalveolar lavage fluids, was decreased in an ALI model [424].

As described above, S1P at physiological concentrations is barrier protective via the $S1P_1$ receptor and in an ALI murine model SEW2871 ($S1P_1$ receptor agonist) decreased the presence of protein in bronchoalveolar lavage, but also lowered leukocyte infiltration. In contrast, activation of $S1P_2$ or $S1P_3$ receptors, increases endothelial barrier disruption and alveolar leakage both of which were significantly decreased following targeted deletion of $S1P_2$ or silencing of the $S1P_3$ receptor in murine models of ALI. In these experiments, $S1P_2$ KO mice were used to evaluate the role of $S1P_2$ receptor, but $S1P_3$ receptors were silenced using nanocarriers injected into jugular veins of mice to deliver $S1P_3$ siRNA to the lung vessels. After 5 days, murine lung tissue homogenates were assessed for silencing of the $S1P_3$ receptors by immunoblot. Lung injury induced by LPS was significantly attenuated in $S1P_2$ KO mice, but also in mice whose $S1P_3$ receptors were selectively silenced by $S1P_3$ siRNA [421,422,425,426]. Collectively, these findings emphasize the role played by S1P in endothelial barrier regulation in *in vivo* models of lung permeability.

1.7.4.2 *S1P and anaphylaxis*: Anaphylaxis is a systemic often life–threatening allergic reaction [427,428]. Anaphylaxis is associated with exaggerated vasodilation and bronchoconstriction, severe laryngeal (voice box) edema, hypothermia and decreased cardiac pressure. Experimental models are normally generated in two different ways via: (1) passive anaphylaxis in nonimmunized animals, in which animals are injected with antibodies, or (2) active anaphylaxis in which animals are immunized with antigen(s). IgE–induced passive anaphylaxis is elicited by injecting mice with IgE antibodies 24–48 hours before an intravenous challenge with a specific antigen. The anaphylactic shock develops within minutes and can be assessed by monitoring the decline in body temperature. IgE–induced anaphylaxis can be abrogated in mice deficient in FcεRI, a high–affinity IgE receptor [429,430] or using histamine receptor antagonists [431,432]. This means that anaphylaxis can also be induced by intravenous injection of histamine [260], and

this method is widely used as a means of establishing anaphylactic reaction in experimental animals. Active systemic anaphylaxis is generated by an intravenous injection of antigen, into mice immunized with that antigen. Symptoms similar in kinetics to passive anaphylaxis develop post-immunization [433,434].

Anaphylaxis impairs the function of various organs, increases endothelial permeability and fluid extravasation [427]. S1P or histamine plasma concentrations are increased following anaphylaxis [435]. In experiments where SK-1–deficient mice were used, plasma S1P and mice survival sharply dropped. However, in SK–2 deficient mice which are usually associated with an increase in plasma S1P levels, better recovery and survival were reported after anaphylactic shock [435]. Also pS1Pless mice (mice lacking circulating S1P) exhibited increased vascular leakage, and poor survival following anaphylactic or histamine challenge. Vascular leakage and mice survival were improved upon restoration of S1P following wildtype erythrocytes transfusion (a rich source of plasma S1P) or intravenous delivery of $S1P_1$ receptor agonist (SEW2871) [419]. These findings highlight the role of plasma S1P and endothelial $S1P_1$ receptor interaction in maintaining endothelial barrier function.

Pharmacological blockade or genetic deletion of $S1P_2$ decreased histamine–induced vascular leakage or hypothermia in a mouse model of anaphylaxis [436,437]. However, evidence recently showed that $S1P_2$ prevents endothelial barrier disruption by suppressing eNOS activity in an anaphylaxis model [426]. While the S1P–endothelial $S1P_1$ signaling robustly ameliorates the symptoms of anaphylaxis, the *in vivo* role of $S1P_2$ in vascular–related complications arising from increased endothelial permeability such as in sepsis or anaphylaxis is yet to be fully understood. The role of $S1P_3$ in anaphylaxis has not been demonstrated.

1.7.4.3 ***S1P and Ischemia–Reperfusion (I/R) Injury*****:** Multiple disease–related conditions are associated with I/R injury including cardiopulmonary bypass, transplantation, aneurysm repair, stroke and hemorrhage. Ischemia is associated with decreased blood supply to the tissues, thus limiting oxygen and nutrient supply needed for cellular metabolism. So resupplying these "starved tissue" areas with blood (reperfusion) is associated with induction of oxidative stress, generation of ROS, increased endothelial permeability of arterioles and capillaries, which collectively can contribute to microvascular injury. In a rat model of orthotopic left lung transplantation (native lung replaced with a donor's), treatment of lung recipient rats with S1P

before graft reperfusion improved lung function. This was attributed to S1P–mediated reduction in tissue injury, endothelial permeability, cell infiltration, and endothelial cell apoptosis [438]. In a rat lung I/R injury model, rats were injected intravenously with S1P prior to pulmonary artery ligation and reperfusion. The rats that received S1P treatment displayed lower bronchoalveolar lavage albumin content, neutrophil infiltration and inflammatory cells compared to the controls [439]. In another study of mouse hepatic I/R injury which is known to complicate acute kidney injury, mice pretreated with S1P exhibit less systemic inflammation, permeability and endothelial injury (apoptosis) compared to mice that never received S1P treatment [402,440]. All these studies indicate the potential usefulness of S1P as therapeutic agent for I/R injury. Apart from the role of S1P on endothelial barrier, S1P also controls vascular tone by regulating vasodilation and vasoconstriction.

1.7.5 S1P and vasodilation

S1P–induced vasodilation is predominantly mediated via eNOS activation [33,34,121,122,441,442]. The pathway through which S1P activates the S1P receptors in endothelial cells leading to eNOS activation is relatively well defined. There are two major inter–related mechanisms through which eNOS activity is regulated by S1P: ***(a) phosphorylation of eNOS***, which involves multi–enzyme steps leading to the phosphorylation of serine 1177 residue in human cells (but ser1176 in a mouse). eNOS phosphorylation that occurs within the C terminus region leads to eNOS activation in the presence of $[Ca^{2+}]i$ [443]. S1P–induced eNOS activation via pertussis toxin–sensitive G protein (Gαi)–coupled S1P receptors/Rac1, results in downstream activation of PI3K, and ultimately protein kinase B (also known as Akt) which phosphorylates eNOS at the serine 1177 residue [33,442,444,445]. While $S1P_{1–3}$ receptors express Gαi–protein and have the potential to mediate eNOS activation, only $S1P_1$ and $S1P_3$ receptors promote eNOS activation [33]. In contrast, activation of $S1P_2$ receptors suppresses eNOS activation [426], suggesting that the induction of vasodilation by S1P depends on receptor subtype and/or the balance of the signals generated through S1P receptors. ***(b) The eNOS–caveolin regulatory cycle,*** in which eNOS is targeted to the invaginated domains of the cell membrane called caveolae (described above) where its activity is regulated by binding to caveolin [446-451]. In the caveolae, eNOS interacts with cav-1 in endothelial cells or cav3 as shown in cardiac myocytes [441,448-451]. This direct interaction between eNOS and caveolin

leads to inhibition of eNOS activity, in a process involving the binding of caveolin to eNOS which prevents interaction of eNOS with its co-factor tetrahydrobiopterin [452,453]. However, when endothelial cells are stimulated to increase $[Ca^{2+}]_i$, CaM stimulates activation of eNOS promoting NO production. The $S1P_1$ receptors are also targeted to caveolae, establishing an important physical proximity for S1P–induced eNOS activation. S1P–mediated activation of eNOS is associated with an increase in $[Ca^{2+}]_i$ in cultured endothelial cells [454-456] and chelation of $[Ca^{2+}]_i$ abrogates S1P–induced NO generation [33,457]. Overexpression of caveolin in cells co-expressing eNOS and $S1P_1$ receptors significantly decreased S1P–induced eNOS activation [441]. Taken together, the regulatory processes involving a caveolin/CaM switch or the S1P/S1P receptor–Rac1/PI3K/Akt signaling pathway play key roles in determining the eNOS activity.

S1P induces eNOS–dependent vasodilation of epinephrine–preconstricted mesenteric arterioles isolated from mice or rats [34,458,459]. Antagonizing the $S1P_1$ receptor promotes S1P–induced vasoconstriction in rodent cerebral arteries [460]. HDL (a carrier that is rich in S1P) stimulates vasodilation via the $S1P_3$ receptor and eNOS activation of phenylephrine–preconstricted thoracic aorta segments isolated from mice or rats [461]. Also FTY720 mediates eNOS–dependent vasodilation of phenylephrine–preconstricted mouse thoracic aorta preparations via the $S1P_3$ receptor [462,463].These studies, underscore the mechanisms through which S1P induces vasodilation, principally via eNOS activation and NO production. The mechanism through which NO stimulates vasodilation was described earlier. Although S1P [464] or HDL [465] have independently been linked to the increased release of PGI_2 in VSMCs, these events have not been linked with vasodilation.

1.7.6 S1P and vasoconstriction

S1P increases vasoconstriction via Rho kinase and Ca^{2+}-dependent mechanisms as previously described [466,467]. S1P mobilizes Ca^{2+} from intracellular stores in rat cerebral arteries, but also in cultured VSMCs derived from rat aorta [468-470]. The contraction induced by S1P via S1P receptors in the VSMCs occurs in part in a RhoA/Rho kinase–dependent manner. Using pharmacological agents C3 botulinum toxin, an inhibitor of RhoA, or Y–27632, a ROK inhibitor, the contraction elicited by S1P in cultured human coronary artery smooth muscle cells was significantly attenuated. S1P–induced vascular tone also occurs in human placental arteries

via Rho kinase [471-473]. Further, the dependence of RhoA by S1P in the induction of contraction has been shown in cultured VSMCs derived from rat cerebral arteries [469]. Y–27632 counteracts S1P–induced vasoconstriction in canine basilar arteries [474], and in hamster gracilis muscle small resistance arteries [475]. The role of PKC in S1P–induced contraction has also been demonstrated [476-479]. The S1P-induced Ca^{2+}–dependent mechanism for induction of vasoconstriction is mediated through the L–type voltage operated Ca^{2+} channels [476,480]. This means that both the Ca^{2+}–dependent and independent mechanisms are involved in S1P–induced vasoconstriction [476,480]. Even so, the induction of these downstream mechanisms depends on the S1P receptors activated.

S1P loses its vasoconstricting activity in basilar arteries from mice lacking the $S1P_3$ receptor, but vasoconstriction in arteries from $S1P_2$ receptor deficient mice was unchanged. The authors also showed that in rat basilar arteries pretreated with VPC23019 (an $S1P_1$/$S1P_3$ receptor antagonist), S1P–induced constriction was significantly decreased, suggesting that the $S1P_3$ receptor is important in the induction of vasoconstriction by S1P in these arteries [460,468]. The $S1P_3$ receptor is also involved in the induction of myogenic tone and vasoconstriction of rat or canine cerebral arteries, respectively [87,481]. On the other hand, the $S1P_2$ receptor KO mice display markedly decreased mesenteric and renal vascular resistance compared to their littermate controls, suggesting that the $S1P_2$ receptor is important in maintaining basal tone in these arteries [482]. Genetic inactivation of $S1P_2$ receptors with antisense oligonucleotides in isolated hamster gracilis muscle resistance arteries showed significantly decreased myogenic tone induced by S1P [472]. Another group demonstrated that S1P binding to $S1P_2$ receptors stimulates vasoconstriction in the pulmonary vasculature [472]. While S1P–mediated stimulation of $S1P_2$ or $S1P_3$ receptors have been attributed to vasoconstriction, emerging evidence suggests that the $S1P_1$ receptor, which is traditionally known to induce vasodilation when engaged on the endothelial cells, induces vasoconstriction when engaged on smooth muscle cells. Recently, SEW2871 was independently shown to constrict renal afferent arterioles via L–type voltage–dependent Ca^{2+} channels [480]. Also SEW2871 was shown by another group to potentiate the vasoconstriction induced by phenylephrine or serotonin in rat mesenteric and coronary arteries [118]. Further, pressure or S1P–induced myogenic tone was shown to be inhibited when rabbit posterior cerebral arteries were pretreated with an $S1P_1$ receptor antagonist (W146) [87]. Thus, S1P may differentially

evoke vasoconstriction depending on the S1P receptors expressed in different organs, and also the animal species being studied.

1.7.7 Vascular tone control by S1P

As described earlier, vascular tone is the balance between vasodilation and vasoconstriction, and S1P stimulates both. The S1P–mediated regulation of vascular tone depends on the balance of receptors activated on the endothelium compared to the VSMCs [34]. Simply put, the induction of an overriding response by S1P leading to vasodilation or vasoconstriction, depends on how strongly or weakly the S1P receptors that evoke either of these responses are stimulated. As described, S1P induces vasodilation primarily via $S1P_1$ or $S1P_3$ receptors on the endothelium through eNOS activation leading to NO production, but also induces vasoconstriction through $S1P_2$, $S1P_3$ and perhaps $S1P_1$ receptors on the VSMCs (Figure 1.11) [34,386]. S1P has been shown to constrict renal, mesenteric, cerebral and basilar arteries from mammals and human placental arteries. Large conduit arteries, like aortas, exhibit vasodilator effects to S1P after preconstruction [386]. Although signals through both $S1P_2$ and $S1P_3$ induce vasoconstriction, their importance differs depending on the vascular bed. While activation of $S1P_3$ induces constriction in cerebral arteries, $S1P_2$ activation has no effect [460].

Generally, higher S1P concentrations are needed to stimulate vasoconstriction ($\geq$ 0.1 μmol/L) compared to S1P–induced vasodilation, which typically shows an EC_{50} in the low nanomolar range [33,460,483-485].Taken all together, the regulation of vascular tone by S1P depends on different experimental variables: the S1P concentrations used, the S1P receptors expressed and stimulated, the vascular bed and animal species under investigation. The access of circulating S1P to the VSMCs to stimulate vascular tone will need to be transcytosed or pass in between endothelial junctions, however, the role of these mechanisms and their contribution to vascular tone remain to be demonstrated.

Like S1P, TXA_2, another bioactive lipid, controls vascular tone. TXA_2 has been shown to increase the release of S1P from cultured human platelets [486] but this relationship has not been developed any further. TXA_2 is generated from AA through a series of enzymatic actions.

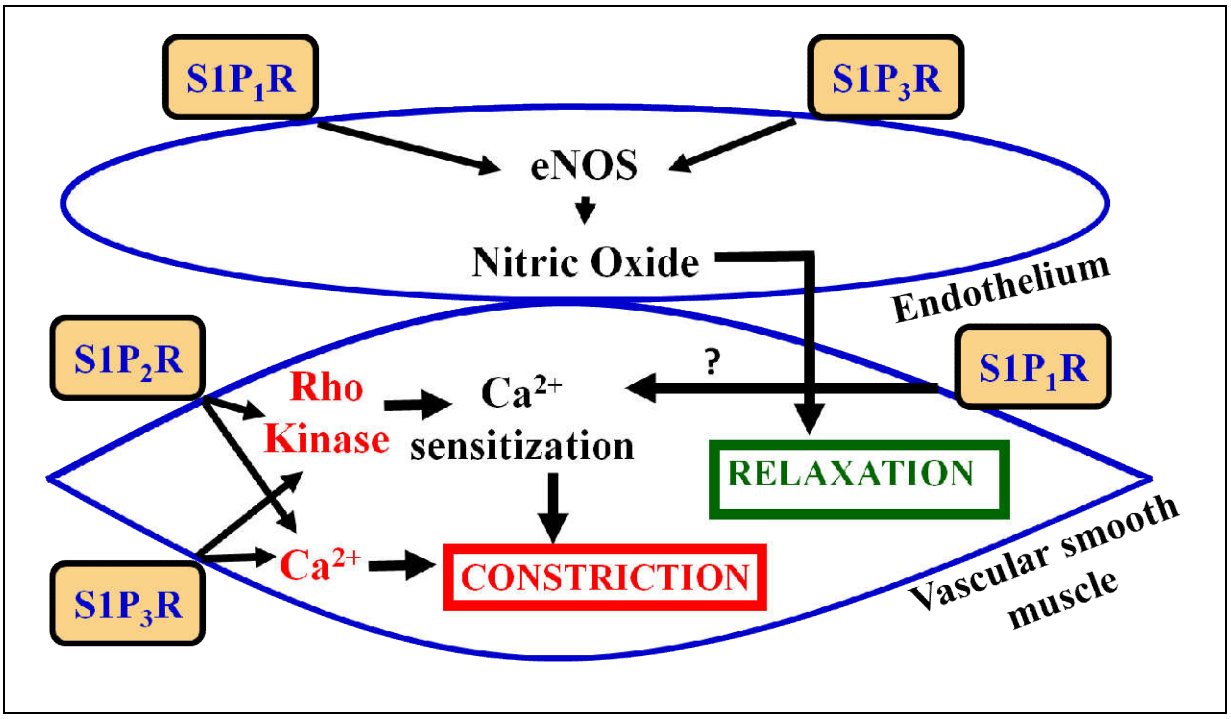

Figure 1.12: S1P and vascular tone control. Activation of the $S1P_1$ and $S1P_3$ receptors results in eNOS activation and generation of NO that causes vascular smooth muscle relaxation/vasodilation. On the other hand, activation of the vascular smooth muscle $S1P_2$ and/or $S1P_3$ receptors leads to Rho kinase and Ca^{2+}-dependent induction of vasoconstriction. There is now increasing evidence to support a vasoconstricting role for the $S1P_1$ receptor. Adapted from a figure previously generated by Dr. Denise Hemmings.

1.8 AA metabolism

AA which is 5, 8, 11, 14–eicosatetraenoic acid is a metabolic product of phospholipids or diacylglycerol [487]. AA is freed from phospholipids by phospholipase A_2 or from diacylglycerol by PLC (Figure 1.12) [488]. AA is metabolized by 5–lipoxygenase to 5–hydroperoxyicosatetraenoic acid. The activity of 5– lipoxygenase requires the presence of a helper protein 5– lipoxygenase activating protein (FLAP). 5–hydroperoxyicosatetraenoic acid is then converted to other eicosatetraenoic acids or to leukotrienes (Figure 1.12) [489].

5–hydroperoxyicosatetraenoic acid is reduced by cellular peroxidases to 5–hydroxyicosatetraenoic acid [490]. 5–hydroxyicosatetraenoic acid can further be metabolized by: (**1**) acyltransferases, generating different cellular phospholipid components including phosphatidylcholine, phosphatidylinositol, phosphatidylserine, phosphatidylethanolamine,

and glycerides [491-493] [494]; (**2**) microsome–bound nicotinamide adenine dinucleotide phosphate ($NADP^+$)–dependent dehydrogenase producing 5–oxo–6E,8Z,11Z,14Z–eicosatetraenoate [495]; (**3**) a C–20 hydroxylase forming 5, 20–dihydroxy–eicosatetraenoate [493]; (**4**) Arachidonate 15–lipoxygenase–1, 15–lipoxygenase–2, or 12–lipoxygenase to 5,15–dydroxy–eicosatetraenoate [490,496]; (**5**) 12–lipoxygenase to 5,12-dihydroxy-eicosatetraenoic acid [497]; and f) COX–2 to 5,15– dihydroxy-eicosatetraenoic acid and 5,11– dihydroxy-eicosatetraenoic acid [498].

Alternatively, 5–hydroperoxyicosatetraenoic acid can further be converted by 5–lipoxygenase to leukotriene intermediates (Figure 1.12) like leukotriene A4 (LTA4), which ultimately has two fates. First, LTA4 hydrolase cleaves the ether bond in LTA4 forming leukotriene B4. Second, glutathione–S–transferase catalyzes the conjugation of LTA4 with a tripeptide molecule, glutathione, forming leukotriene C4. Cleavage of the gamma–glutamyl moiety in leukotriene C4, by gamma–glutamyl transpeptidase generates leukotriene D4. Leukotriene D4 is degraded by a dipeptidase to Leukotriene E4 and a cysteinyl fatty acid backbone. Leukotrienes are powerful vasoconstricting and permeability enhancing agents [499].

AA can also be metabolized to different prostaglandin and thromboxane products by COXs as described below [500,501].

1.8.1 Regulation of the functions of COX-1 and COX-2

COX–1 and COX–2, also known as prostaglandin-endoperoxide synthase–1, 2, respectively, are highly homologous structurally, but their activity and expression are regulated differently, and these enzymes can function independently within the same cell type [502]. The activity of these enzymes depends on the presence of lipid peroxides; for example, the activation of COX–2 requires ten–fold lower concentrations of hydrogen peroxide compared to COX–1, suggesting that COX–2 can function in the presence of COX–1, while the activity of COX-1 remaining minimal [503,504]. AA is the preferred substrate for COX–1, while COX–2 can metabolize both AA and 2–arachidonyl glycerol. This means that COX–2 can generate products that COX–1 cannot synthesize [501]. ***Expression:*** COX–1 and COX–2 are both expressed in the endothelium and VSMCs of healthy blood vessels, with COX–1 being the dominant isoform [505,506]. COX–1 splice variant (enzymatically active), termed COX–3, is expressed in the heart and cerebral cortex, but it is not functional in humans [507]. COX–1 is constitutively

expressed in most tissues but it is overexpressed under conditions of shear stress [508]. COX–2 is normally induced during inflammation, but it is also constitutively expressed in some cells like endothelial cells [509]. The expression of COX–2 is also increased by viral infections such as CMV [510,511].

1.8.1.1 TXA_2 biosynthesis and related pathways

AA is sequentially broken down to TXA_2, a potent vasoconstrictor, initially described as a rabbit aorta–contracting substance [512]. In the synthesis of TXA_2, AA is metabolized by COX–1 and COX–2, to PGH_2. PGH_2 has several fates: (**1**) PGH_2 can be converted to prostaglandin (PG) D_2 (PGD_2) by PGD synthase [513,514]. (**2**) Prostaglandin E synthase also converts PGH_2 to prostaglandin E2, which is rapidly converted to prostaglandin F by PGE 9–ketoreductase. Alternatively, prostaglandin F can be synthesized through two additional pathways from PGD_2, or directly from PGH_2 by PGD 11–ketoreductase, or PGH 9–,11–endoperoxide reductase, respectively [515]. (**3**) Prostacylin synthase (also known as PGI_2 synthase) can also metabolize PGH_2 to PGI_2, which is further non–enzymatically converted to 6-keto PGF1α. 6–keto PGF1α serves a marker of PGI_2 biosynthesis *in vivo* [516,517]. (**4**) Finally, PGH_2 can also be converted to TXA_2 by thromboxane synthase [518]. Like PGI_2, TXA_2 is non–enzymatically converted to TXB_2 which is used a marker for *in vivo* biosynthesis of TXA_2. The conversion of PGH_2 to TXA_2 is accompanied with the production of other metabolic intermediates such as 12–hydroxy–5, 8, 10–heptadecatrienoic acid and malondialdehyde (Figure 1.12) [519,520]. However, it is unknown whether these intermediates have vascular–related effects. Thromboxane synthase has a molecular weight of 60 kDa and is found in platelets [518], the stomach, duodenum, colon, kidney and the spleen [521]. Other substrates for thromboxane synthase include AA, which is converted to TXA_2, but also 5, 8, 11, 14, 17–eicosapentaenoic acid which is converted to TXA_3. TXA_3 is less potent in platelet aggregation than TXA_2 and its vascular effects are not known [522]. Different cells produce TXA_2 including endothelial cells and smooth muscle cells [487,520].

1.8.1.2 The biological functions of TXA_2

TXA_2 is quite a labile molecule with a chemical half–life of approximately 30 seconds, and thus, TXA_2 acts locally as an autacoid in an autocrine or paracrine manner. TXA_2 exerts its

actions through two thromboxane/prostanoid (TP) receptors. The first human TP receptor was cloned from the placenta [523,524], and the second one from human endothelial cells [525].The TP receptor originally identified in the placenta is now called TPα, and the one from endothelial cells is called TPβ. The two receptors are structurally similar but they differ at the C–terminus with TPβ having an elongated cytoplasmic tail. Both of these receptors are coupled downstream to different G proteins including G_q [526] and $G_{12/13}$ [527], through which TXA_2 promotes different biological events. In humans, both TPα and TPβ receptors are expressed, but in rodents only TPα receptors are expressed [528]. While TXA_2 is the preferential ligand for TP receptors, PGH_2, isoprostanes and HETEs can also activate TP receptors [529]. In contrast, EETs function as endogenous antagonists of TP receptors [530,531].

TXA_2 causes platelet activation with changes in morphology and aggregation. These events promote thrombus formation and blood clotting, the most important known function of TXA_2 that prevents excessive bleeding [532]. However, thrombus formation and vasoconstriction mediated by TXA_2 have also been linked to fatal acute myocardial infarction and cerebral infarction [533]. As a negative feedback mechanism, TXA_2 produces PGI_2 which will reduce platelet aggregation [534]. TXA_2 is also associated with cardiovascular–related complications such as hypertension, atherosclerosis, and endothelial dysfunction [535].
In endothelial cells, TXA_2 increases endothelial permeability and surface expression of adhesion molecules associated with inflammation including intracellular adhesion molecule–1, vascular cell adhesion molecule–1 and endothelial leukocyte adhesion molecule–1 [536,537]. However, TXA_2 decreases the expression of leukocyte adhesion molecule [538]. TXA_2 also causes endothelial cell migration and angiogenesis [539]. In the smooth muscle, TXA_2 potently constricts various smooth muscles including the aorta [512], bronchial [540], intestinal [541], uterine [542] or urinary bladder [543]. TXA_2-induced constriction has been associated with hypertension [544], including pregnancy-induced hypertension [545], and asthma [546].The clinical relevance of TXA_2 has been shown, with the availability of thromboxane synthase inhibitors and TP antagonists which have the potential for treatment of several disorders like asthma and thrombosis [547-549].

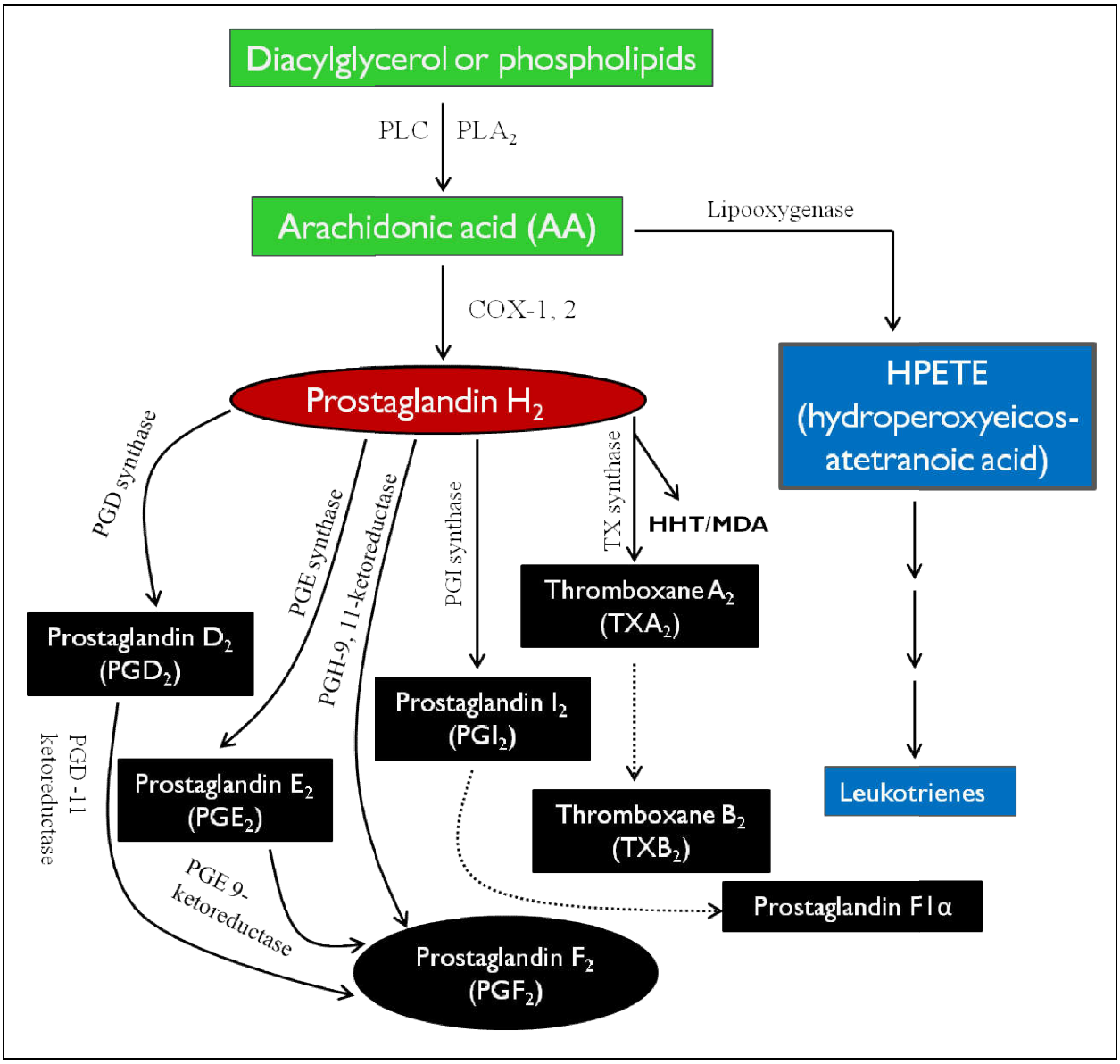

Figure 1.13: AA metabolism and TXA_2 synthesis. AA is generated from diacylglycerol and phospholipids, by the action of PLC or phospholipase A_2, respectively. AA is metabolized by COX-1 and 2 to PGH_2 from which various prostaglandin-related products and TXA_2 are released. AA can also be metabolized by lipooxygenase to HPETE which becomes the substrate from which different leukotrienes are produced in enzyme catalyzed reactions. Broken lines represent products generated spontaneously, and non-enzymatically. The abbreviations HHT, stand for 12–hydroxy–5, 8, 10–heptadecatrienoic acid, and MDA for malondialdehyde which are produced as part of TXA_2 synthase activity.

1.8.1.3 TXA_2 and vascular tone control

The endothelium regulates arterial tone by producing vasorelaxing and contracting factors. TXA_2 is a contracting factor produced in the endothelium from AA which in turn is released to the VSMC where it stimulates TP receptors inducing vasoconstriction [550,551]. Stimulation of TP receptors on the VSMCs leads to Ca^{2+}- or Rho kinase-dependent induction of vasoconstriction as already described [552,553]. Apart from directly inducing vasoconstriction, another mechanism through which TXA_2 controls vascular tone is by directly reducing vasorelaxation mediated by many vasodilators including NO, PGI_2, and EDHF [554]. Indeed, in piglet pulmonary arteries, relaxations to acetylcholine and the NO donor sodium nitroprusside (SNP) are reduced in U46619 (TXA_2 mimetic)-contracted arteries compared with those contracted with either noradrenaline or endothelin–1 [555]. Elevated levels of TXA_2 in human neutrophils is associated with increased hydrogen peroxide and superoxide generation [556], but also activation of TP receptors in bovine aortic endothelial cells increases peroxynitrite ROS generation [557]. ROS causes oxidation and reduces the bioavailability of the eNOS cofactor tetrahydrobiopterin [557], causing eNOS uncoupling [558], but they have also been shown to maintain the stability of TP receptors at the plasma membrane [559]. Collectively, these findings indicate a positive feedback loop through which TXA_2–induced ROS formation ultimately favors a contractile phenotype.

1.9 Infections, inflammation and vascular function

Infections such as those resulting from an obligate intracellular bacterium *Chlamydia pneumonia* contribute to the pathogenesis of atherosclerosis in healthy individuals [560] and in end–stage renal disease patients [279]. *C. pneumonia* infections have been linked to endothelial dysfunction in apolipoprotein E–KO mice [561]. Viral infections such as adenovirus trigger inflammatory responses that cause endothelial injury [562]. HIV infection causes endothelial injury rendering it dysfunctional, facilitating inflammation and development of cardiovascular disease [563]. Persistent infections have been associated with endothelial dysfunction in humans, in which prior infection with *C. pneumonia*, *Helicobacter pylori*, hepatitis A virus, herpes simplex virus type 1 and CMV are risk factors for the development of coronary endothelial dysfunction [564].

A number of studies have indicated that there is a link between infection–mediated

induction of inflammation and the risk for development of cardiovascular disease [565]. One of the ways infection can contribute to increased inflammation is by promoting increased production of pro-inflammatory cytokines. The exposure of endothelial cells to these type of cytokines increases the expression of cell–surface adhesion molecules associated with inflammation [566], and this has been associated with impaired endothelium–dependent vasodilation [567]. Increased CRP is associated with decreased forearm blood flow in response to acetylcholine in patients with coronary artery disease [282]. Other studies have also indicated that CRP can independently affect endothelium–dependent vascular function in healthy subjects [568] and in coronary heart disease patients [569]. These data show that chronic low-grade inflammation decreases basal endothelial NO synthesis. Studies by Hingorani *et al* demonstrated a link between inflammation and endothelial dysfunction in humans. In this study, 12 healthy subjects were vaccinated against *Salmonella typhi* and the mild inflammatory reaction that developed from vaccination caused a transient but profound dysfunction of the arterial endothelium (decreased vasodilation) [570]. Indirect evidence of a link between inflammation and endothelial dysfunction has also been shown in type–1 diabetic patients who show increased CRP and endothelium-derived proteins, such as von Willebrand factor and adhesion molecules (ICAM–1) [571]. Increased levels of ICAM–1 are also used as a marker of endothelial function, and has been shown to correlate with CRP in predialysis patients [281].

Collectively, these findings suggest that the inflammation induced by infections can contribute to endothelial dysfunction and ultimately impaired vascular function. Hemmings' Lab previously showed vascular dysfunction in arteries isolated from CMV–infected mice compared to uninfected controls (described later) [572-574].

1.9.1 CMV infection

The seroprevalence of CMV in the human population ranges between 30% and 90% in developed countries, and the seroprevalence increases with age [575,576]. CMV can be transmitted through saliva, placental transfer, sexual contact, breastfeeding, blood transfusion, or cell transplantation [577]. Primary CMV infection in immunocompetent hosts is normally asymptomatic except occasional cases of mononucleosis, after which the virus establishes lifelong infection within the host and is periodically reactivated [578]. The mechanism by which CMV establishes and maintains latency and is reactivated is still not fully understood,

particularly in humans. CMV viral latency is established in the haematopoietic progenitors in the bone marrow, while the cells of myeloid lineage (particularly monocytes) serve as a reservoir/carriers of the viral genome. However, reactivation occurs in the terminally differentiated myeloid macrophages and dendritic cells. Interestingly, the CMV viral genome is not carried in the lymphocyte population nor is there evidence for the establishment of viral latency in endothelial cells. Experimental data suggest that endothelial and neuronal progenitor cells may be sites of latency, but these findings remain unsupported by lack of data from natural latency in humans. Nevertheless, it is important to recognize that other sites of latency may still exist [578-580]. The virus is known to re–enter the lytic stage of the viral life cycle in the presence of certain environmental cues like weakened immunity or stress, which favours the production of viral progeny, causing an acute infection. In individuals who are immunocompromised or whose immune system is not fully developed CMV infection can cause morbidity and mortality [580-582].

1.9.1.1 CMV infection: Clinical manifestations

The clinical manifestations of CMV infections in those with weakened immunity (such as transplant patients who undergo bone marrow transplants) include increased fever, malaise, leucopenia, encephalitis, pneumonitis, hepatitis, uveitis (inflammation of the pigmented layer of the eye), retinitis, gastrointestinal disease and graft rejection [583,584]. If primary infection or reactivation of CMV occurs during pregnancy, this can be associated with serious fetal complications including microcephaly, mental retardation, anaemia, thrombocytopenia, deafness, and optic nerve atrophy which can cause blindness [583,585]. Although immunocompetent individuals are generally asymptomatic to CMV infection, CMV has been implicated in proliferative and inflammatory diseases [586] such as cancer (colon, breast, and prostate), atherosclerosis [586] and vascular dysfunction [572-574]. The proposed mechanism through which CMV contributes to atherosclerosis involves virus–induced vascular inflammation, smooth cell proliferation, uptake of low–density lipoproteins and narrowing of the vessel lumen [587,588].

1.9.1.2 CMV infection: Treatments

Currently there are no approved vaccines available against CMV infection [589,590].

One of the most characterized vaccine candidates is the attenuated Towne CMV strain, which has been shown to reduce CMV disease in healthy volunteers (who were challenged with viral infection) and transplant recipients, but it failed to prevent CMV infection [590-594]. Low–risk poxviral vectors have been used as vaccine carriers of recombinant gB and pp65 [590,595] and DNA vaccines have also been evaluated with the aim of eliciting both humoral and cell mediated immunity. However, limited success has been achieved [589,590,596]. Therefore, creating a successful vaccine against CMV remains a priority.

Anti–CMV drugs are available which can reduce/eliminate viremia or control CMV disease. These drugs include ganciclovir, valganciclovir, foscarnet, and cidofovir [597-600]. Ganciclovir is a nucleoside analog of 2'-deoxyguanosine that is activated by phosphorylation in CMV–infected cells and works by inhibiting viral DNA polymerase, and thus interfering with DNA replication. This prevents virus–specific polypeptide formation, interrupts cell–to–cell spread and virus–induced cytopathic effects [600,601]. Foscarnet also interferes with viral replication by binding to CMV DNA polymerase [599,602]. Cidofovir is an acyclic phosphonate analog of cytosine which inhibits CMV DNA synthesis by chain termination following incorporation of two consecutive cidofovir molecules at the 3'–end of the DNA chain [603]. Unfortunately, the use of these drugs has a number of drawbacks that limit their effectiveness. Many patients suffer from poor oral bioavailability, low potency, drug–resistant virus strains and various toxicities associated with these drugs including nephrotoxicity, neutropenia and bone marrow suppression [599,600,604,605]. This means that the search for better therapeutic agents is also needed.

Currently a panel of drugs are under investigation for treatment of CMV infection including: maribavir, an oral drug with specific activity as an inhibitor of CMV viral protein, UL97 protein kinase [605-607]. Letermovir is an inhibitor of CMV terminase enzyme [608,609] and is given orally or intravenously. Letermovir has been shown to be highly effective against wildtype and drug–resistant CMV *in vitro*, and is currently undergoing a phase III clinical trial [605,606,610]. Brincidofovir is a lipid-conjugated nucleotide, which is an analogue of cidofovir. Brincidofovir has been credited for its high oral bioavailability and long half–life, and broad spectrum antiviral activity against herpesviruses, polyomaviruses, adenoviruses, papillomaviruses, and variola virus [605,607]. The potential of brincidofovir as an anti–CMV therapy is currently being evaluated in phase III clinical trials [606]. Finally, artesunate, an

antimalarial drug exhibits antiviral activity *in vitro* against herpesviruses [611], hepatitis viruses, and HIV and is currently being investigated for its effectiveness as a therapeutic agent against CMV infection [605].

1.9.1.3 The CMV virion structure and overview on cell entry

CMV is a member of the *Herpesviridae* family [612,613]. The virion has an icosahedral (20 sides) protein nucleocapsid [614] that contains double–stranded DNA located in the central core of the virion [615,616]. The nucleocapsid is surrounded by a protein–rich tegument region, which is enclosed in a glycoprotein–rich lipid bilayer envelope [617]. CMV has a broad tropism and can infect different cell types including neutrophils, monocyte/macrophages/dendritic cells, VSMCs, endothelial cells, epithelial cells, hepatocytes, fibroblasts and neuronal cells [613,618,619]. CMV virions gain entry into host cells through a membrane fusion event, involving the interaction between the glycoproteins on the CMV envelope and the specific receptors on the outer membrane of the host cell [620]. This initial interaction promotes intracellular signaling, membrane fusion, and ultimately, the release of the viral genomic DNA and tegument into the host cell. The tegument proteins mediate the delivery of the DNA–containing nucleocapsid to the nuclear pore complex and the release of the viral DNA into the nucleus [621]. This initiates the lytic stage of the viral life cycle [620]. The viral gene expression occurs in the order (Immediate-Early, Early, Early–Late, and Late) during the viral life cycle. The tegument proteins also play additional roles including viral replication, gene expression, immune evasion, viral reassembly and egress of new infectious virions [621].

1.9.1.3.1 Proposed entry mechanisms: role of CMV glycoproteins and cell receptors

CMV can bind, enter and establish a productive infection in virtually all vertebrate cells [622]. This means that CMV likely utilizes multiple receptors to enter and infect different cell types. Various cellular molecules have been proposed as cell entry receptors (or as mediators) for CMV including: heparan sulfate proteoglycans (HSPGs), epidermal growth factor receptor (EGFR), platelet–derived growth factor receptor–α (PDGFRα), BST2 also known as tetherin, and integrins [623-626].

HSPGs/ EGFR: Initially it was proposed that cell entry by CMV involved the binding of CMV envelope glycoproteins gM/gN and/or gB to cellular HSPGs, and that gB interacted with

EGFR to stably dock the virus on the cell (Figure 1.13). EGFR was reported to promote CMV entry in fibroblasts and breast cancer cells [625,627]. The evidence that gB interacted with EGFR came from co–immunoprecipitation experiments. While gB lacks a EGF–like domain, studies demonstrated that it displayed an epitope homologous to a distinct region of EGF [625,628]. However, EGFR was subsequently found not to be activated by CMV in fibroblasts, and neither did antagonizing EGFR prevent CMV cell entry. Further, there was no correlation between EGFR expression and CMV infection, and the use of neutralizing antibodies against EGFR failed to prevent CMV entry into fibroblasts, epithelial or endothelial cells [629]. However, two years later another group provided evidence that EGFR expressed in human peripheral blood monocytes promoted CMV entry into monocytes. The binding of CMV to EGFR induced signalling that caused monocyte motility and transendothelial migration, a feature that is important for viral dissemination. EGFR was not found to be expressed in other circulating leukocytes [630]. Thus far, since gB binds to EGFR, EGFR could be functioning as a docking site for CMV and also as a receptor for viral entry but this is dependent on the cell type.

***PDGFR*α:** CMV infection of fibroblasts was also shown to activate PDGFRα signalling [624] which promoted CMV entry, and early stages of CMV replication. Inhibiting PDGFRα activity via siRNA–mediated silencing, use of PDGFRα inhibitor (Gleevec) or a PDGFRα–neutralizing monoclonal antibody all inhibited the production of CMV immediate early genes [624,627]. However, recent evidence thwarted the idea that PDGFRα may be a CMV entry receptor. In fact PDGFRα was demonstrated not to directly interact with CMV; instead the role of PDGFRα is simply “facilitative" by promoting a dynamin–dependent endocytosis of CMV [631].

BST2/tetherin: Recently, a study showed that transduction of a human monocytic cell line (THP–1 cells) with an interferon–inducible protein (BST2/tetherin) enhanced CMV (AD169, lab strain) cell entry [623]. However, BST2 has been shown not to be necessary for CMV infection, as infection occurs in the absence of BST2. While the mechanism through which BST2 enhances viral entry remains unclear, the authors suggested that BST2 may be acting as co–factor, or co–receptor that facilitates cell entry [623].

Integrins: Integrins play a prominent role in CMV cell entry by collaborating with innate immune responses (Figure 1.13) [632,633]. CMV gB protein contains a disintegrin domain that binds cellular integrin subunits α2β1, α6β1, and αVβ3 promoting intracellular signaling. CMV

entry is inhibited when gB disintegrin is targeted by binding peptides, or the cellular integrins targeted by specific antibodies [627,633]. gB interacts with β1 integrins facilitating CMV internalization. It is proposed that integrins serve as co-receptors (with other receptors) in the CMV entry process [627,634,635]. The binding of gB induces the release of type I interferons through interferon regulatory factor–3 [632]. The interaction between gB/gH and toll–like receptor–2, a host innate immune sensor that detect pathogen–associated molecular patterns displayed on CMV stimulates the activation of NF–κB/Sp1 and release of proinflammatory cytokines [632,636]. The intracellular signaling mechanisms promote CMV–cell fusion, internalization, and viral entry (Figure 1.13) [627,637].

HCMV envelope glycoprotein	Binding molecule on the cell	Role in HCMV entry process
1. gM/gN or gB	HSPGs	Tethering, signalling
2. gB	EGFR	Fusion, docking and signalling
3. gB	Integrins	Fusion, internalization and signalling
4. gB	TLR2	Innate immune response
5. gH/gL/gO	?	Fusion process

Table 1.1: CMV glycoproteins and cellular molecules involved in CMV entry into cells

1.9.1.3.2 Cytoplasmic–nuclear translocation of internalized CMV virion components

The events that follow viral internalization in permissive host cells, is the release of the capsid and tegument proteins to the host cell. The capsid then travels along the microtubule networks to the nucleus where the viral genome is released in order for viral DNA replication to occur. Along with the viral capsid, also transported to the nucleus are tegument proteins (such as pUL84, UL69, pp71) necessary to support viral DNA replication in the nucleus [638,639]. However, the transport of these tegument proteins is different from that of the capsid. The host cell importin–α proteins interact with viral tegument protein cargoes (pUL84, UL69, pp71) at specific regions of amino acids called nuclear localization signals [640]. The importin–α links the cargo to the β–karyopherin importin–β forming a trimeric complex that is translocated through the nuclear pore complex. Once the cargo is delivered in the nucleus, importin–β binds

to RanGTP (a GTP–binding, Ras–related nuclear protein (Ran)), inducing a conformation change that results in the release of the cargo. Importin–β complexed with RanGTP is recycled to the cytoplasm, whereas importin–α is exported complexed with β–karyopherin and RanGTP [640]. In the nucleus, the tegument proteins promote viral DNA replication.

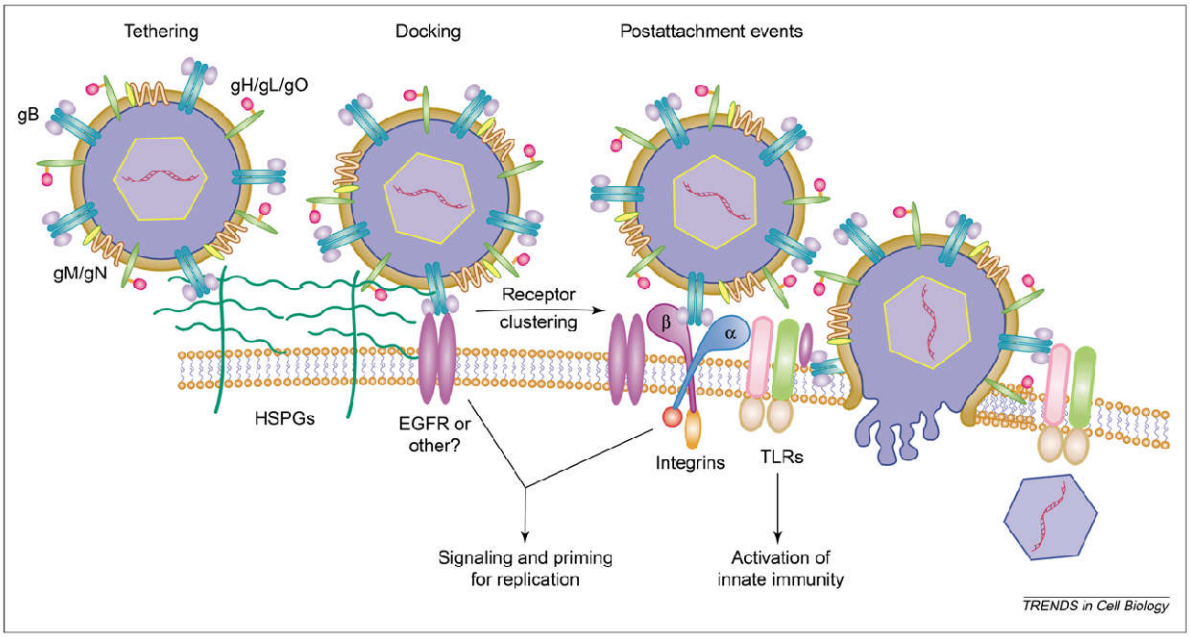

Figure 1.14: Proposed mechanisms for CMV cell entry. HCMV tethers to cellular HSPGs, and then docks by binding to EGFR, which depending on the cell type (e.g. monocytes), can promote CMV cell entry. The binding of CMV gB to cellular integrins or interaction with TLRs elicits downstream signaling mechanisms that promotes CMV internalization. Figure obtained from *Receptors and immune sensors: the complex entry path of human cytomegalovirus* by Compton, 2004. Permission was sought and granted by the primary author and the journal as outlined in Appendix.

1.9.1.3.3 Post nuclear import events: viral replication, reassembly and egress

Once the viral DNA genome enters the nucleus of the host cell, the virus uses the host cell machinery to replicate its DNA [641]. The CMV replication cycle, like that of many herpesviruses, involves nuclear and cytoplasmic phases. The nuclear phase involves viral capsid assembly, viral DNA synthesis, encapsulation and initial tegumentation [642]. The capsid is assembled from various viral proteins and the viral DNA is packaged inside it once replication is complete. Capsid reassembly begins outside the nucleus forming procapsid particles [643,644].

These procapsids undergo nuclear import where they are assembled into correctly organized capsids (Figure 1.14). This is followed by capsid maturation which includes the elimination of scaffolding proteins and packaging of viral DNA into nucleocapsids [642,645]. After viral DNA encapsulation, the nucleocapsids begin to egress from the nucleus to the cytoplasm in a complex process that must overcome the barriers of the nuclear lamina. This process involves primary envelopment of nucleocapsids at the inner nuclear membrane, followed by de–envelopment at the outer nuclear membrane [642,646] before release into the cytoplasm. The secondary and final envelopment occurs in the cytoplasm in a specialized compartment termed the cytoplasmic virus assembly compartment. Here, the nucleocapsids acquire the remaining tegument proteins and viral envelope [647,648]. Mature virion particles are then transported to the cell surface via the Golgi–derived vesicles (Figure 1.14) and are released into the extracellular compartment by exocytosis ~ 72 hours post–infection [645,649-651].

1.9.1.4 CMV infection: Modulation of vascular function

CMV infection is generally asymptomatic in immunocompetent hosts with no obvious clinical symptoms. However, there is increasing evidence that CMV infection in such individuals may contribute to cardiovascular–related disorders like hypertension and atherosclerosis [652-656]. The prevailing hypothesis is that CMV infection contributes to these diseases by stimulating inflammation [657-660] which is important for viral dissemination [661] and so it is a viral survival strategy in the host. CMV infects key cell types that are involved in cardiovascular function such as VSMCs and endothelial cells [573,662], but also increases the expression of molecules associated with inflammation like ICAM–1 [663,664], VCAM–1 [664], platelet–endothelial cell adhesion molecule–1 expression [661], and E–selectin [661]. CMV infection also increases leukocyte [665-668] and platelet adhesion [669] and cytokine release [670,671] which are also associated with inflammation and cardiovascular diseases. The microvasculature represents one of the sites where CMV infection could have a great impact on vascular function since it is the site that is predisposed to tissue injury following infection. Exposure to inflammatory stimuli or infection such as bacterial or viral infection is associated with a compromise in endothelial barrier function as this provides an avenue for transmigration of immune cells to the site of infection or injury. Upregulation of cell adhesion molecules support the trafficking of leukocytes and platelets to areas of demand by passing through the

post–capillary microvasculature [661,666-668,672]. These events contribute to inflammation and are believed to occur long before the disease manifests itself in large vessels or the appearance of clinical symptoms [667,668,672]. Indeed human CMV infection increases endothelial permeability by decreasing stress fibre formation and degrading endothelial junctional proteins [661].

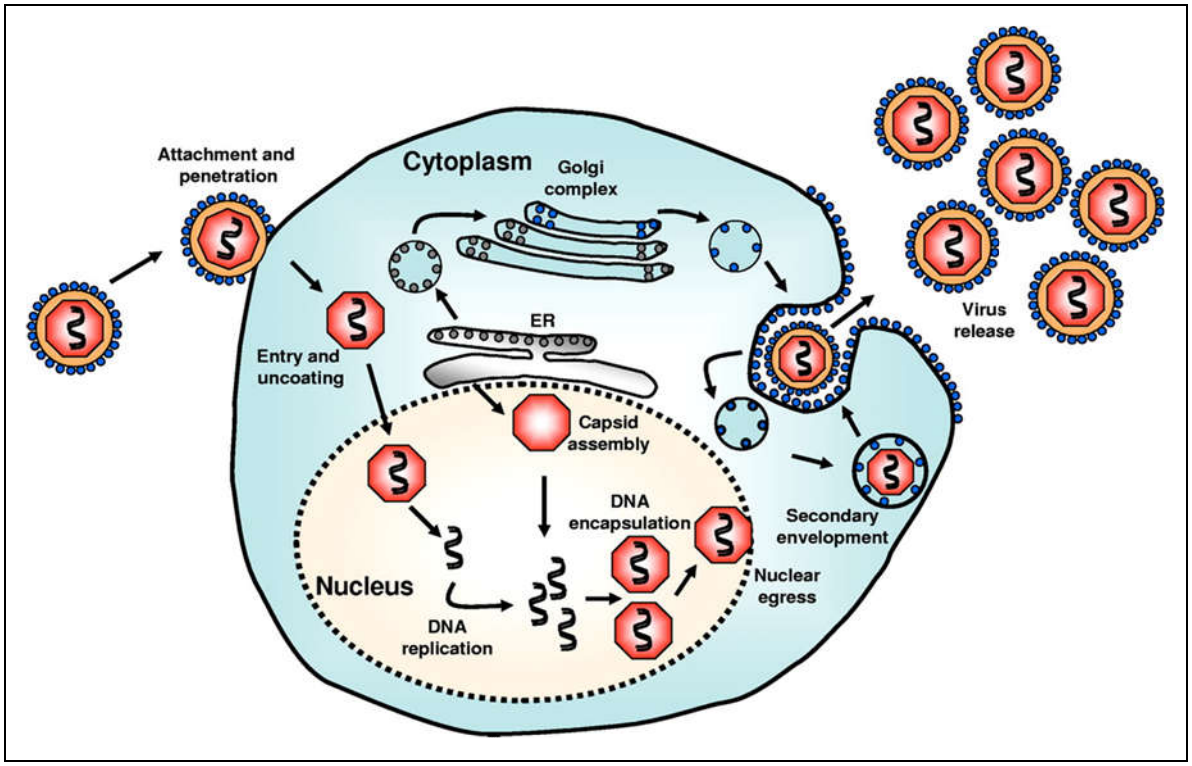

Figure 1.15: CMV infection in a human cell: The life cycle begins with CMV entry into the cell through direct fusion and endocytosis releasing nucleocapsids to the cytoplasm. These nucleocapsids are transported to the nucleus where viral DNA is delivered. This is followed by viral replication using host machinery, encapsulation of viral DNA, nuclear egress, maturation in the cytoplasm and exocytosis of mature virions. Figure obtained from *Immunobiology of Human Cytomegalovirus: from Bench to Bedside* by Tania and Khanna, 2009. Permission was sought and granted by the primary author and the journal as outlined in Appendix.

CMV infection also causes thickening of arterial walls [673], arteriopathy [662,673] and arteriolar dysfunction [674]. Khoretonenko et al demonstrated that mice infected with CMV exhibited decreased arteriolar vasodilation to acetylcholine, significantly increased leukocyte adhesion and migration, and platelet adhesion in the arterioles and post–capillary venules

compared to uninfected controls [675]. Recently, the same group showed the role of platelets in enhancing CMV-mediated vascular dysfunction in mice. First they showed that platelet depletion (using anti-platelet antibodies) was associated with decreased vasodilation of arterioles from CMV–infected compared to uninfected mice. Using bone marrow chimeric mice lacking P–selectin, vasodilation was normalized in arteries from CMV–infected mice compared to uninfected controls. These findings suggest that during CMV infection, P–selectin is involved in the suppression of vasodilation, although the exact mechanism remains to be defined [676].

The Hemmings' Lab has previously shown that mesenteric arteries isolated from young latently infected mice by CMV display decreased vasodilation to methacholine and increased vasoconstriction to phenylephrine. However, uterine arteries exhibited increased vasodilation and vasoconstriction compared to age-matched uninfected controls [677]. Hemmings' Lab also showed that active CMV infection directly infects endothelial and VSMCs in uterine arteries isolated from pregnant mice, and these effects were associated with significantly increased vasoconstriction to phenylephrine and decreased vasodilation to methacholine [572,573]. Mesenteric arteries isolated from CMV–infected nonpregnant mice, stimulated with the endothelium–dependent vasodilator (methacholine) or an NO donor (SNP) displayed significantly increased vasodilation compared to arteries from uninfected nonpregnant mice. Vasodilation in mesenteric arteries from CMV–infected pregnant and uninfected pregnant mice was not different. Further, uterine arteries isolated from CMV–infected nonpregnant mice, showed increased vasodilation in response to methacholine compared to arteries from uninfected mice. However, during pregnancy uterine arteries from CMV–infected mice showed significantly decreased vasodilation to methacholine, and increased vasoconstriction to phenylephrine compared to arteries from uninfected pregnant mice. These findings highlight the potential impact of CMV infection on the systemic vasculature that regulates blood pressure, but also in reproductive arteries which may compromise pregnancy outcomes or contribute to pregnancy–related disorders like intrauterine growth restriction [572-574].

These studies collectively highlight the negative impacts associated with CMV infection on the vasculature in immunocompetent hosts, and provide a rationale for continued investigation of the vascular effects of CMV infection in such hosts. The exact mechanisms through which CMV infection contributes to the aforementioned vascular disorders remains poorly understood. It also remains to be explained whether the CMV–induced changes in

molecular expression leading to increased vascular dysfunction is a direct or indirect effect. While a direct viral effect is a plausible explanation, it is likely that CMV infection greatly increases endogenous mediators such as lL–6, IL–8 and TNF–α [280], S1P (by increasing expression and activity of SK-1) [678,679] and TXA_2 (by increasing the expression and activity of COX-2) [680] that contributes to vasculopathy. However, there is no direct evidence that CMV infection and generation of these molecules cause vascular dysfunction.

1.10 Overall rationale

There are three major concepts arising from the literature regarding S1P, TXA_2 and CMV infection that this thesis focussed on. First, S1P has dual effects on the endothelial barrier, and in cultured endothelial cells, S1P at (≤ 1 μM) acts through the $S1P_1$ receptors increasing the endothelial barrier, but S1P at (≥ 1 μM) signalling via the $S1P_2$ or $S1P_3$ receptors weakens the barrier by overcoming signals originating from the $S1P_1$ receptor. S1P has been shown to decrease endothelial permeability in mesenteric microvenules at physiological concentrations, but this has not been reported in intact arteries. At physiological concentrations [0.1–1.1 μM], S1P induces vasodilation and vasoconstriction, the balance of which constitute vascular tone. Hemmings' Lab previously showed that infusion of S1P [0.1 μM] to preconstricted uterine arteries, vasodilation was increased which was lost at S1P [1 μM]. These findings suggested that at [1 μM], S1P likely induced endothelial permeability that allowed access of S1P to the VSMCs increasing vasoconstriction that was likely counterbalanced by the S1P-induced vasodilation. However, how the S1P–mediated control of endothelial barrier and access of circulating S1P to the VSMCs impacts vascular tone in intact isolated arteries remains uninvestigated.

The second important concept contributing to this thesis is that TXA_2, another bioactive lipid, also increases both endothelial permeability and vascular tone. There is limited evidence that TXA_2 and S1P may signal through similar pathways to effect vascular responses; however, the specific relationship between these two bioactive lipids remains to be explored. Part of this work focussed on understanding whether TXA_2 utilizes the S1P pathway to increase endothelial permeability and vascular tone.

Third, CMV infection appears to be linked with S1P or TXA_2 pathways. CMV infection increases the expression and activity of SK-1 that leads to the generation of S1P, but also that of COX–2 that produces TXA_2. CMV infection increases blood pressure in a rodent model or

hypertension in humans, both of which are associated with increased vascular tone. Whether the CMV–induced effects are mediated through the actions of S1P or TXA_2 is unknown. This thesis therefore aimed at addressing the following questions (**1**) whether S1P–stimulated changes in endothelial permeability regulates vascular tone in resistance arteries through NO, (**2**) whether TXA_2 signals via the S1P pathway to increase vascular tone and (**3**) finally the impact of CMV infection on the vascular tone induced by TXA_2 through the S1P-dependent responses in intact arteries. Unlike previous work which focussed on the role of S1P on the control of endothelial barrier in veins, studies in this thesis for the first time focussed on the arteries. Arteries used in this work were chosen as a model to study endothelial permeability and vascular tone, but also because they play key physiological functions. Uterine arteries are important in pregnancy, but these arteries also supply various reproductive organs including the ovaries (by the ovarian branch of uterine artery), cervix (vaginal branch of uterine artery), pelvis (internal iliac/hypogastric artery), and endometrium/uterus (spiral arteries) and are therefore crucial in reproduction. Mesenteric arteries branch from superior mesenteric arteries which are supplied by the abdominal aorta, and are therefore important in the regulation of blood pressure.

1.11 Overall hypotheses

Regulation of endothelial permeability in resistance arteries through S1P controls the access of S1P or of other circulating vasoconstrictors to the underlying vascular smooth muscle controlling vascular tone. This regulation occurs in part through endogenous and S1P-induced NO. TXA_2 signalling through the TP receptors leads to activation of sphingosine kinase generating S1P. S1P when exported extracellularly stimulates $S1P_1$, $S1P_2$ and/or $S1P_3$ receptors to increase vascular tone depending on the S1P receptors stimulated and the vascular bed. CMV infection enhances the vascular tone induced by S1P itself, and TXA_2 through its effects on the S1P pathway.

CHAPTER 2: MATERIALS AND METHODS

2.1 General materials and methods

2.1.1 Mouse handling and tissue isolation

Mice were housed and cared for in the Health Sciences Laboratory Animal Services (HSLAS) facilities at the University of Alberta. This study was approved by the University of Alberta's Animal Care and Use Committee under the guidelines outlined by the Canadian Council of Animal Care. Female C57Bl/6J which were used for the majority of experiments, and B6.129P2-*Nos3*^{tm1Unc}/J (eNOS KO) mice and wildtype (WT) littermate controls were obtained from Jackson Laboratories (Bar Harbor, ME, USA) and were used for experiments at 8–10 weeks of age. Male C57Bl/6J strain $S1P_3$ KO, female $S1P_2$ KO and $S1P_3$ KO mice and their WT littermates were provided by Dr. Jerold Chun (Scripps Research Institute) [681]. Male and female $S1P_3$ KO mice and WT littermates on a 129/S1SVIMJ background were generated in–house by multiple backcrossing and used at the age of 8–10 weeks. Mice were euthanized by cervical dislocation. Uterine horns or mesentery with associated vasculature were removed and placed in HEPES–buffered physiological saline solution (HPSS; 10 mM HEPES, 1.56 mM $CaCl_2$, 142 mM NaCl, 4.7 mM KCl, 1.18 mM KH_2PO_4, 1.17 mM $MgSO_4$, and 5.5 mM glucose at pH 7.5).

2.1.2 Pressure myography: Justification for the use of the pressure myograph technique

Pressure myography is a powerful tool in vascular biology, which offers opportunities to study vascular function and intrinsic properties (e.g. myogenic tone) of small resistance vessels in near physiological conditions [682]. Once the vessel is mounted on the pressure myograph and pressurized to an optimal luminal pressure, the vessel will maintain most of its *in vivo* characteristics. This is different from *ring vessel segments,* used for measuring vascular response, in conduit vessels in which ring segments are held on two hooks and connected to a force transducer allowing wall force to be measured. In *isometric or wire myography*, two wires are passed through the lumen of resistance vessels, and the wires are connected to a force transducer to measure tension in response to a stimulus (such as a drug) [683-686]. The use of pressure myography has several advantages over other existing techniques. These advantages include that: (**1**) can be used to study resistance arteries, unlike *ring vessel segments*, that is limited to large conduit arteries; (**2**) the risk of damaging the endothelium is minimized unlike in

wire myography where wires are passed through the vessel lumen; (**3**) the natural shape of the vessel is better maintained; (**4**) the vessels can respond to pressure and vessel dimensions can be studied over a wide range of pressures (myogenic responses) and (**5**) being a closed system, the role of the endothelium or VSMC on vascular function can be studied separately, unlike in wire myography where the drug can access both cell types simultaneously. However, the pressure myograph is also limited in evaluating the structural changes of intact resistance arteries, and the contribution of the abluminal component to vascular function.

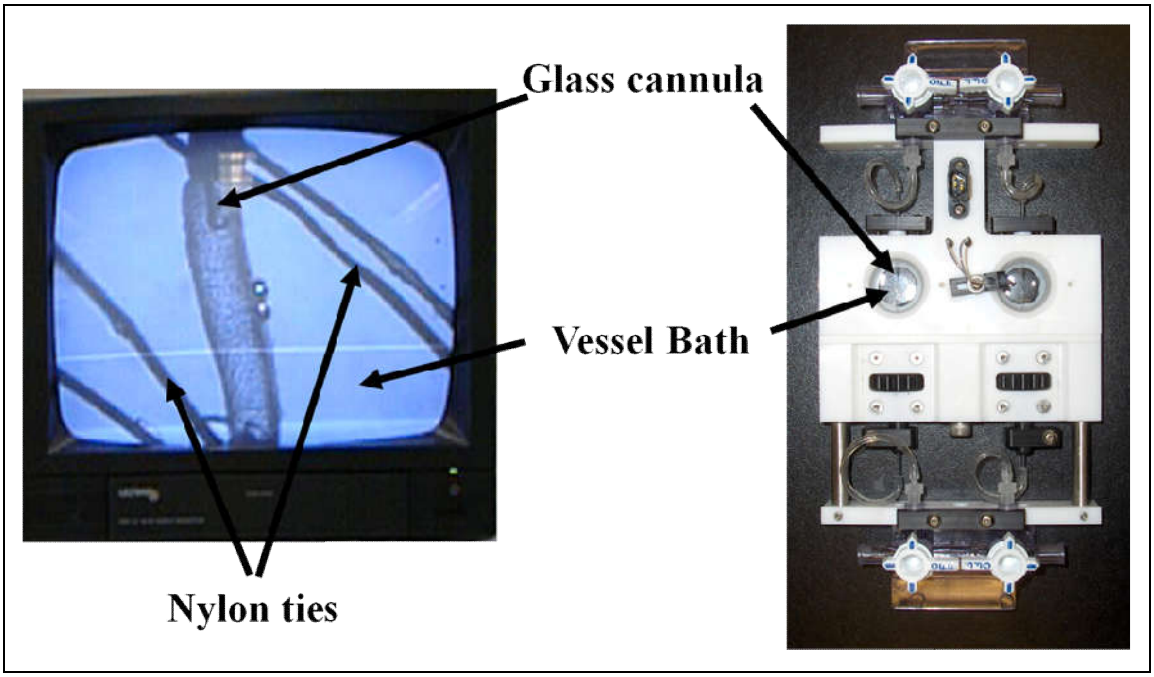

Figure 2.1: Depiction of part of a pressure myograph. The right component is a vessel bath where a vessel is mounted (arrows), tied to the glass cannulae (using nylon ties), pressurized and treated by either adding drugs to the bath (has HPSS solution) to interact with the VSMCs directly or drugs infused inside the vessel where they interact with the endothelium first. The vessel can then be projected on a screen (left component) from which changes in vascular function, can be observed visually and recorded. This picture was generated by Dr. Jude Morton.

2.1.2.1 Extraluminal experiments

Main uterine arteries and second order mesenteric arteries (with baseline diameters for both being approximately 130-200 nm) were used for experiments. These arteries were used as a model to study endothelial permeability and/or vascular tone, but also uterine arteries are important in pregnancy and mesenteric arteries in the regulation of blood pressure. The arteries

were dissected free of connective and fatty tissues in HPSS. After mounting and tying one end of the artery to a cannula on a single or double–bath pressure myograph (Living Systems Instrumentation, Burlington, VT), any residual luminal blood was flushed out by a low flow of < 10 µl/min before mounting the artery to the second cannula. Each artery was then optimally stretched every 10 minutes after pressurizing at each pressure point including 20, 40 and 50 mmHg (uterine) or 20, 40 and 60 mmHg for mesenteric arteries. These pressures are optimal for equilibration of these arteries *in vitro* [573,687-689]. Arteries not holding pressure were discarded and another one was mounted from the same animal. The arteries on the cannulae ligated to the tubing systems were connected to pressure transducers which measure intraluminal arterial pressure. This is maintained through a servo–enabled peristaltic pump. The arteries were maintained at 50 (uterine) or 60 mmHg (mesenteric arteries) pressures at 37^{o}C in a 2.5 ml double HPSS bath or 6 ml single bath while experiments were being conducted. The pressure at which uterine arteries are held for experiments is physiological (45-55 mmHg) [690], and while the 60 mmHg used for mesenteric arteries is slightly lower that physiological levels (75-110 mmHg) [691], the Hemmings' Lab had previously shown that using pressures more than 60 mmHg in arteries used in this study caused a lot of myogenic tone, but not at 60 mmHg.

In extraluminal experiments, one artery segment was used per *ex vivo* treatment and several segments were used per mouse for paired and related experiments. Drugs were added in vessel bath solutions (HPSS) where they could interact directly with the VSMCs. The drugs were added either as a single dose, a combination of doses between drugs or cumulatively. The changes in vascular responses after drug addition were measured every 4-5 min, and internal artery diameters were visualized using a video dimension analyzer (Living Systems Instrumentation, Burlington, VT) [687]. Addition of drugs to the bath was done in fatty acid-free 0.1% bovine serum albumin (0.1%BSA) (Akron Biotech, Boca Raton, FL).

2.1.2.2 Novel technique to simultaneously measure endothelial permeability and vascular tone in response to agonists infused into isolated intact arteries

We developed a novel technique for intraluminal infusion to measure endothelial permeability and vascular tone using intact isolated arteries mounted on the pressure myograph system. Using pressure myography Moss et al [692] published a method in which they used Evans Blue dye (EBD) to determine the amount of dye embedded in the vascular wall (a measure

of permeability) after infusion of permeability factors into human arteries. While this technique is useful for measurement of endothelial permeability in *ex vivo* vessels, it works best in Biopta PM–1 type of pressure myograph in which the equilibrating solutions and drugs can be delivered to the vessel through different compartments (micrometer syringes). However, for classical pressure myograph systems (Living System) it is difficult to properly equilibrate the vessels in the physiological saline solution, before infusing experimental treatments, without the possibility of mixing. Further, because of the opaqueness of EBD it is difficult to accurately visualize the vessel walls in our pressure myograph system. Building on the concepts published by these authors, we established a system that overcomes these difficulties in a Living System-type of pressure myograph.

In this technique, prior to mounting the artery on the first cannula, a "lead" solution (0.1% BSA in HPSS) was loaded into the tubing leading from the pump to the transducer and into the cannula. This was followed by 1.2 cm of air to prevent mixing of the lead solution from the experimental treatment (air does not reach the artery because this small volume is ultimately lost as it passes through the transducer). The use of the air also allowed us to properly equilibrate the arteries before infusion. The air was followed by loading a treatment of interest (such as a permeability factor) in the presence or absence of a 3 kDa dextran conjugated to rhodamine–green fluorescent dye (Invitrogen, Eugene, OR). Once the lead solution, air and experimental treatment were loaded into the tubing, flow was started until the lead solution reached the end of the cannula but the air bubble was still visible before reaching the transducer. Thus, the treatment did not mix with the lead solution during vessel equilibration. The artery was then mounted, pressurized and equilibrated. One artery segment was used per treatment and several segments were used per mouse for experiments. After a 20–min infusion at a flow rate of <20 µl/min to allow the experimental treatment to reach the vessel, the flow was stopped for 10-20 min to allow vessel equilibration with the experimental treatment. The incubation time was optimized for development of endothelial permeability by the agents used in the experiments. The tubing and the vessel bath systems were covered with light–proof aluminum foil to prevent photobleaching. Upon completion of each experiment, the whole vessel bath was transferred to light-proof tubes and dextran leakage as a measure of endothelial permeability, was assessed by quantifying the fluorescence at 502/527 nm corrected by arterial length. Changes in vascular diameters measured every five minutes were recorded as described above.

Type	Reagent	Target	Known effects on endothelial permeability	Known effects on vascular tone	Working Concentration	Company
Agonists	S1P	$S1P_1$ $S1P_2$ or $S1P_3$	Decreases via S1P1 Increases via S1P2/3	Decreases Increases	0.1–10 µmol/L [473,481,693]	Enzo Life Sciences
	U46619	TXA_2 mimetic	Increases	Increases	0.1–500 nmol/L [573,694,695]	Sigma
	SEW2871	$S1P_1$ agonist	Decreases	Decreases? Increases?	0.1 µmol/L [460,696]	Cedarlane
	Phenylephrine	α1-adrenergic receptor agonist	Unknown	Increases	0.1–10 µmol/L [573]	Sigma
Antagonists	VPC23019	$S1P_1$/$S1P_3$ receptor antagonist	Unknown	Enhances S1P-induced constriction	1 µmol/L [697,698]	Avanti Polar Lipids
	W146	$S1P_1$ receptor antagonist	Decreases	Decreases myogenic tone	1 µmol/L [87,699,700]	Avanti Polar Lipids
	JTE013	$S1P_2$ receptor antagonist	Decreases	Decreases	10 µmol/L [481,697]	Cedarlane
	SQ29548	TP receptor antagonist	Decreases	Decreases	10 µmol/L [97,534,546,695]	Cayman
Inhibitors	SK-II	SK-1 inhibitor	Decreases	Unknown	1 µmol/L [701]	Cayman
	ABC294640	SK-2 inhibitor	Unknown	Unknown	10 µmol/L [702]	MedKoo Biosciences
	MK571	ABCC1	Unknown	Unknown	10 µmol/L [368,703]	Sigma
	FTC	ABCG2	Unknown	Unknown	1 µmol/L [704]	Avanti Polar Lipids
	Y27632	Rho kinase Inhibitor	Decreases	Decreases	10 µmol/L [473]	Calbiochem
	L-NAME	NOS inhibitor	Decreases	Increases	100 µmol/L [572]	Sigma
	Papaverine	Phosphodiesterase inhibitor	Unknown	Decreases	100 µmol/L [572]	Sigma
Other Reagents	3 kDa fluorescent dextran	Permeability Tracer	None	None	100 µg/ml [705]	Invitrogen
	70 kDa fluorescent dextran	Permeability Tracer	None	None	1 µg/ml [706]	Invitrogen
	Thrombin (mouse)	Permeability factor	Increases	Can decrease or increase depending on concentration	1 U/ml [707]	Haematologic Technologies
	LPS	Permeability factor	Increases	None	50 ng/ml [708,709]	Sigma
	SNP	NO donor	Decreases, but also increases depending on concentration	Decreases	10–100 µmol/L [139,710,711]	Sigma

Table 2.1: List of reagents (drugs)

Measurement was done every 5 min to track the vascular responses for the entire 20 min of drug infusion. Drugs were infused in fatty acid-free 0.1% bovine serum albumin (0.1%BSA) (Akron Biotech). The drugs used for both extraluminal and intraluminal experiments are shown in table 2.1, and the rationale for using specific working concentrations was derived from the references provided.

2.1.3 Calculations and statistical analyses. The results are presented as means ± SEM and were analysed by Student's t–test, one-way or two-way ANOVA followed by the Tukey post hoc test as appropriate and as described in the figure legends. Tukey's test assumes that the responses being tested are independent within and among the groups, and the means obtained from the groups assumes a normal distribution. Percent decrease in diameter = (1– (d2/d1) × 100 whereby d1 is the initial arterial diameter after equilibration and d2 is the diameter after treatment. Change in lumen diameter from the baseline is reported as % decrease in diameter and reflects the outcome of both constrictor and dilator effects and so are generally referred to in the text as change in vascular tone. Percent vasodilation = (d2–d1/d1) × 100 whereby d1 is the preconstricted diameter value after equilibration and d2 is the arterial diameter after addition of vasodilator. Percent vasodilation was normalized to maximal arterial diameter obtained after the artery was incubated in the presence of Ca^{2+} free HPSS solution and 100 μmol/L papaverine for 10 min.

2.2 Materials and methods for Chapter 3

2.2.1 Isolation of primary human umbilical vein endothelial cells (HUVECs)

Human umbilical cords from normal term deliveries were obtained from the Royal Alexandra Hospital in Edmonton, Alberta, Canada. The study was approved by the Research Ethics Board at the University of Alberta and the Royal Alexandra Hospital and written consent was obtained from each donor. The cords were handled inside a sterile hood. HUVECs were isolated as previously described [712]. During cell isolation, the two ends of a cord were cut off using surgical blades. One end of the cord was clamped, and a butterfly needle (BD Biosciences, Bedford, MA) was inserted into the vein at the unclamped end and the vein was clamped. PBS was infused through the butterfly needle to flush out the blood by relieving the clamp on the end of the cord distal to the butterfly needle, which was again reclamped. To release the endothelial

cells, 0.1% collagenase (Worthington Biochemical Corporation, Lakewood, NJ) was infused into the vein through the butterfly needle and incubated by suspending the clamped cord in PBS for approximately 12 min at 37 C. Cells were then flushed out slowly into a centrifuge tube using an air–filled syringe. The cells were then centrifuged and resuspended in M199 medium supplemented with 10% fetal bovine serum (FBS), 2 mM L–glutamine and 1% penicillin–streptomycin (Gibco, Burlington, ON, Canada; $M199^{++}$ medium). The cells were incubated at 37 C + 5% CO_2 in $M199^{++}$ medium supplemented with 1% endothelial cell growth supplement (ECGS; BD Biosciences, Bedford, MA). The medium was changed the following day to remove residual red blood cells, and every 3 days thereafter as needed [712].

2.2.1.1 Measurement of permeability using confluent endothelial cells

Culture inserts (0.1 μm pores; BD Biosciences) were pre–coated with 0.1% gelatin (Sigma, St. Louis, MO) to facilitate HUVECs adherence and growth. HUVECs at less than three passages were seeded at 10^5 cells in 200 μl per insert and 800 μl of $M199^{++}$ media was added to the wells holding the inserts. Confluence was confirmed by staining 1–2 inserts per experiment with haematoxylin/eosin dye (Sigma). To measure permeability, inserts were gently rinsed inside and outside to remove excess phenol–red $M199^{++}$ medium. The inserts were then placed in new wells containing 400 μl of phenol–red free M199 medium supplemented with 1% FBS, 2mM L–glutamine and 1% penicillin–streptomycin (Q–media). S1P (Enzo Life Sciences, Inc., Farmingdale, NY) at various concentrations (0.01 – 10 μmol/L) was added simultaneously to individual inserts with 70 kDa dextran conjugated to Oregon–green fluorescent dye (Invitrogen, Eugene, OR) (Figure 2.2). Inserts were moved every 30 min for a total of 3 h to wells with fresh medium. Endothelial permeability was quantified by measuring fluorescent dextran (496/524 nm) flux to the bottom wells and calculating the cumulative flux over 3 h.

2.2.2 Immunohistochemistry

HUVECs were seeded onto 14 mm coverslips (Deutsch Deckgläser, Waldemar Knittel Glasbearbeitungs, GmbH, Germany) coated with 0.1% gelatin and grown to confluence overnight in $M199^{++}$ medium supplemented with 1% ECGS. After changing to Q media, cells were pretreated with 1 μmol/L of the $S1P_{1/3}$ receptor antagonist, VPC23019 (Avanti Polar Lipids, Alabaster, AL) for 20 min followed by treatment with 1 μmol/L S1P or 10 μmol/L S1P for 1 h in

the continued presence of VPC23019. Untreated cells were maintained in Q medium for an equivalent time. Cells grown on coverslips were fixed in ice-cold methanol for 20 min at –20°C, followed by blocking in 10% normal goat serum (Gibco) in PBS for 30 min. The coverslips were then incubated overnight with mouse anti–VE–cadherin antibody (Abcam Inc. Toronto, ON, Canada) added at 5 µg/ml in 1% normal goat serum. Coverslips were washed three times on the following day with PBS and further incubated for 2 h in the dark with 10 µg/ml Alexa Fluor 594 goat anti–mouse antibody (Invitrogen). The coverslips were again washed with PBS three times. To visualize actin, cells were fixed in 4% paraformaldehyde (Fisher Scientific, Ottawa, ON, Canada) in PBS for 10 min, washed three times in PBS and then permeabilized in 0.1% Triton

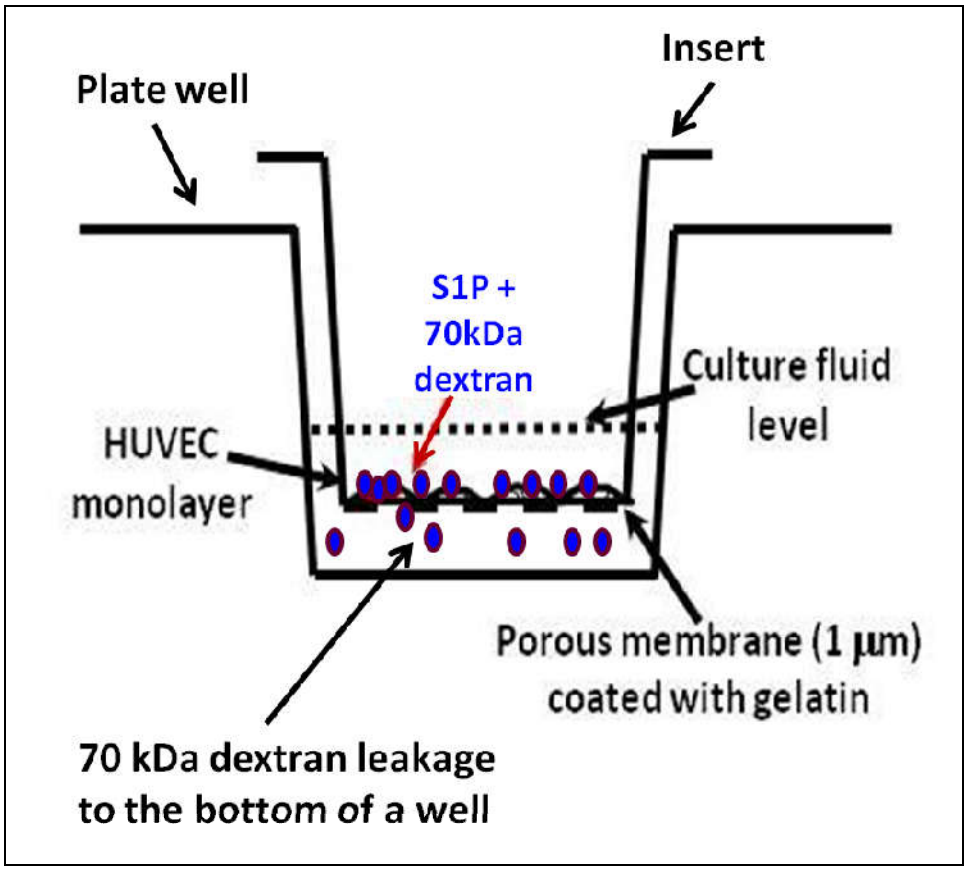

Figure 2.2: Experimental set-up for measurement of endothelial permeability in HUVECs using gelatin-coated inserts. HUVECs were grown to confluence using 1 µm pore inserts sitting inside the wells of a 24-well plate. S1P was added in the presence of a 70 kDa fluorescent dextran and any leakage of the dextran was detected in the bottom chamber of the well. The amount of the dextran at the bottom of the well was quantified as described in the methods to determine endothelial permeability.

X–100 in PBS for 5 min. After washing three times in PBS, cells were blocked in 1% normal goat serum for 30 min before addition of 0.165 μmol/L of Alexa Fluor 488 phalloidin (Invitrogen) in PBS. To visualize nuclei, cells were stained with a 10 μmol/L solution of 4', 6-diamidino-2–phenylindole (DAPI; Invitrogen) in PBS. Coverslips were inverted and mounted onto microscope slides with a drop of Vectashield (Li–Cor Biosciences, Lincoln, NE) and sealed. Images were taken using a Zeiss LSM 700 confocal microscope.

2.2.3 Western blot analysis

Uterine and mesenteric arteries from 10 mice were dissected as previously described and pooled. Protein concentrations of these homogenates (prepared by homogenization in protein lysis buffer and follow by sonication) were determined in duplicate with Micro BCA Reagent (PIERCE Chemical Company, Rockford, IL) using a serum albumin standard. Sample protein to be loaded (20 μg) was solubilized in 5×sample buffer (Sigma) by boiling for 5 min and stored at 20 °C until electrophoresis. SDS–PAGE was performed according to the procedure of Laemmli (1970) using 7.5% acrylamide (Mini-Protein II gel system, Bio–Rad Laboratories, Inc., Hercules, CA). Following electrophoresis, gels were equilibrated in transfer buffer (25 mM Tris, 190 mM glycine, and 20% methanol). Proteins were transferred onto nitrocellulose membranes (1 h, 100 V), which were then incubated with a 25% of blocking solution (Licor, Odyssey, Lincoln, NE) in PBS–Tween 20 for a minimum of 1 h. The blots were then incubated overnight at 4 °C with diluted primary rabbit polyclonal antibodies for $S1P_1$ (2.5 μg/ml), $S1P_3$ (10 μg/ml; Cayman Chemical Company, Ann Arbor, MI), β–actin (1 μg/ml; Abcam) or mouse monoclonal GAPDH (2 μg/ml; Santa Cruz Biotechnology Inc., Santa Cruz, CA). After washing 3x with PBS–Tween 20, the blots were incubated with Alexa Fluor 680 (red) or 750 (green) goat anti–mouse or Alexa Fluor 680 (red) or 750 (green) goat anti–rabbit (0.2 μg/ml; Invitrogen) secondary antibodies for 1 h in dark at room temperature. They were then washed extensively and developed using an infrared fluorescence imager (Licor, Odyssey). Results were quantified using densitometry measurements and analyzed by Image Studio Lite, normalized to β–actin and presented as the mean ± SEM from two–three separate blots using the same homogenates.

2.2.4 Experimental protocol for vascular analysis

Extraluminal experiments: A thromboxane mimetic, U46619 (5, 20 nmol/L; Sigma, St.

Louis, MO) was added to the bath with or without S1P (0.01, 1, 3, 10 μmol/L; Enzo Life Sciences Inc., Farmingdale, NY), thrombin (0.1 U/mL; Haematologic Technologies Inc. Essex, VT), LPS (50 ng/mL; Sigma) or gB, 0.5 μg/mL; ViroStat Inc., Portland, ME). The following antagonists, inhibitors or receptor agonists were preincubated in the bath for 10–30 min before adding other treatments: VPC23019 (1 μmol/L, Avanti Polar Lipids, Alabaster, AL), thromboxane receptor antagonist, SQ29548 (10 μmol/L; Enzo Life Sciences Inc.), NOS inhibitor, L–NAME (100 μmol/L; Sigma) or $S1P_1$ receptor agonist, SEW2871 (0.1 μmol/L; Cedarlane, Burlington, ON, Canada) [713].

Intraluminal experiments: Agonists that affect permeability including S1P, thrombin, LPS or gB were individually infused with or without U46619. Antagonists, inhibitors or receptor agonists as described above were co-infused with other treatments or added to the bath as outlined in the figure legends. Internal artery diameters were measured as described above.

2.3 Materials and methods for Chapter 4

2.3.1 Experimental protocol

2.3.1.1 *Experiments with S1P:* 0.01–10 μmol/L S1P (Enzo Life Sciences) in the presence of 3kDa fluorescent dextran (Invitrogen) was infused in single concentrations or added cumulatively to the bath containing untreated uterine arteries or those pretreated with 100 μmol/L L–N^G–Nitroarginine methyl ester (L-NAME) (Sigma, St. Louis, Missouri, USA) for 30 min in the bath. 1 or 10μmol/L S1P was also infused into arteries from eNOS KO and WT mice followed by determination of endothelial permeability and vascular tone as described. Next 1 μmol/L S1P, 5 nmol/L U46619 (Sigma, St. Louis, Missouri, USA) or a combination was infused into arteries from eNOS KO or WT mice. Infusion or addition of S1P, U46619 or a combination to the bath in arteries pretreated with or without L-NAME in the bath was repeated and vascular tone measured.

2.3.1.2 *Experiments with SNP:* Single doses of (10, 20, 50, 100 μmol/L) SNP, or 20 μmol/L SNP with or without thrombin, LPS or gB were infused together with a 3kDa fluorescent dextran into arteries, followed by determination of endothelial permeability. 20 μmol/L SNP, 5 nmol/L U46619 or a combination was also infused or added to the bath followed by measurement of

permeability and vascular tone. 0.01–100 μmol/L SNP was added to the bath cumulatively to arteries preconstricted with (5–10 nmol/L) U46619 to measure vasodilation.

2.3.1.3 *Denudation of arteries and treatment with SNP:* Arteries were denuded by passing an air bubble (3 inches) through arteries followed by HPSS solution (of 3 inches) and a second air bubble (3 inches) followed by HPSS solution. The successful removal of functional endothelium in arteries that had been used for SNP experiments was confirmed by testing for the lack of dilation in response to an endothelium–dependent vasodilator, methacholine added at 1 μmol/L. Methacholine was added to preconstricted denuded arteries. Denuded arteries were also infused with 1 or 20 μmol/L SNP into preconstricted arteries in the presence or absence of L-NAME to determine vasodilation. The internal diameters were measured as described above.
Where L-NAME was used to block endogenous NOS activity, it was added (or infused, for SNP experiments only) to the bath for 30 minutes before adding S1P, SNP, U46619 or a combination of either S1P or SNP with U46619.

2.4 Materials and methods for Chapter 5

2.4 .1 Experimental protocol

1, 5 or 20 nmol/L U46619 (Sigma, St. Louis, Missouri, USA) as single doses were infused inside pressurized arteries and endothelial permeability and vascular tone were determined as described. 20 nmol/L U46619 was co–infused with the following pharmaceutical agents:10 μmol/L SQ29548, a TPα/TPβ receptor antagonist (Cayman Chemical Company, Ann Arbor, Michigan, USA), 1 μmol/L SK–II (Cayman) a SK–1 inhibitor, 10 μmol/L MK571 (Sigma), an ABCC1 transporter inhibitor, 1 μmol/L FTC (Sigma), an ABCG2 transporter inhibitor, 1 μmol/L VPC23019 (Avanti Polar Lipids, Alabaster; Alabama, USA), an $S1P_1/S1P_3$ receptor antagonist, 0.1 μmol/L SEW2871 (Cedarlane, Burlington; Ontario, Canada), an $S1P_1$ receptor agonist. Each inhibitor or agonist was also preincubated in the arterial bath for 30 minutes before infusing 20 nmol/L U46619 inside the artery followed by determination of endothelial permeability and vascular tone. In some cases, arteries were pretreated with SQ29548 or MK571 in the bath before adding 20 nmol/L U46619 to the bath, followed by infusion of the dextran inside the artery from which permeability and vascular tone were measured. The arteries were also stimulated in the bath with 20 nmol/L U46619, before infusing SK–II inside the artery

followed by determination of vascular tone.

In extraluminal experiments, 1, 5 or 20 nmol/L U46619 was added as single doses to uterine arteries, whereas in mesenteric arteries, 0.1–500 nmol/L U46619 was added cumulatively to the arterial bath. The internal diameters were measured as described.

2.5 Materials and methods for Chapter 6

2.5.1 Mouse CMV Propagation

1. Mouse fibroblasts (NIH/3T3) were cultured in T75 culture flasks in DMEM (10% FBS) and grown to 90% confluence. The cultures were challenged with approximately 0.01 MOI of mouse CMV (RM427+) in 5 mL DMEM (2% FBS) overnight. An additional 5 mL of fresh DMEM (2% FBS) was added the next morning. The progression of infection was monitored every day.
2. When 90% of all cells visually demonstrated infection, the cultures were harvested by scraping and pipetting into 50 ml conical tubes followed by centrifugation at 4000 rpm for 30 min at 4^{o}C.
3. Supernatants were collected into new 50 ml tubes followed by centrifugation at 10000 x g for 2 hrs at 4^{o}C.
4. The pellets from Step 2 were resuspended and combined in 1 ml of DMEM and transferred to 15 ml conical tube. This solution was then frozen and thawed 3 times using an ethanol/dry ice bath and sonication in a water bath 3 times for 30 seconds with 15-second pauses. This solution was then centrifuged at 4000 rpm for 30 minutes at 4^{o}C.
5. The pellet from Step 3 was resuspended in the supernatant that was collected from Step 4 and kept on ice.
6. The pellet from Step 4 was resuspended in 0.5 ml of DMEM and sonicated in a water bath 3 times for 30 seconds with 15 second pauses. This solution was then centrifuged at 4000 rpm for 30 minutes at 4^{o}C.
7. The supernatant from Step 6 was added to already resuspended pellet that had been kept on ice from Step 5. This resulting solution was sonicated again 3 times 30 seconds with 15 second pauses. Finally, the solution was mixed well and aliquots of virus were stored at -80^{o}C.

2.5.1.1 Evaluating the mCMV viral titre

1. Mouse fibroblasts (NIH/3T3) were cultured in DMEM (10% FBS) in 24-well plates coated with 0.1% gelatin and grown to 90% confluence. The cultures were changed to DMEM (2% FBS) and challenged with increasing dilutions of the viral preparation to assess the viral titre, three wells per concentration.
2. After 24 hours in culture, the cells were fixed and a LacZ staining kit was used to assess β-galactosidase expression. Titre (plaque forming units) was evaluated by counting the number of positive cells (blue) per well volume and dilution of virus preparation.

2.5.2 Mouse infection and handling

Mice were challenged intraperitoneally with 10^6 plaque forming units (pfu) of $RM427^+$ mouse CMV which was provided as a gift by Dr. Edward Mocarski, Department of Microbiology and Immunology, Stanford University. The $RM427^+$ virus has a LacZ gene insertion in the non–essential immediate early gene 2 loci, for easy detection of the viral infection using β-galactosidase activity. Uninfected young female mice were infected or left uninfected at the age of 8–10 weeks. Experiments were done with infected mice during an active infection, 5–14 days after viral challenge. Mice were euthanized by cervical dislocation and uterine horns with associated vasculature removed and placed in HPSS solution

2.5.3 Experimental protocol for vascular analysis

In these experiments, I evaluated the potential pathological–related effects mediated by TXA_2, therefore, the concentrations were chosen based on normal compared to pathological concentrations [714-716]. I used U46619, a stable TXA_2 mimetic added to arteries as a single dose at (20 nmol/L) or cumulatively at (0.1–20 nmol/L). Responses to phenylephrine (Sigma, St. Louis, Missouri, USA), an alpha-1 adrenergic receptor agonist at (0.01–10 μmol/L) and S1P at a single dose of (1 μmol/L) or in a dose response curve (0.01–10 μmol/L) were also assessed. In experiments where inhibitors were used, the arteries were pretreated for 30 min before adding U46619, phenylephrine or S1P. The inhibitors used include SK–II [1 μM] (Cayman Chemical), 10 μmol/L ABC294640 (MedKoo Biosciences Inc); Fumitremorgin C, 1 μmol/L FTC (Sigma) [369,704]; 10 μmol/L MK571 (Sigma) [369,704]; 100 μmol/L L-NAME (Sigma); or 10 μmol/L Y27632, Rho kinase inhibitor, 1 μmol/L W146, $S1P_1$ receptor antagonist and 1 μmol/L

VPC23019 (Avanti Polar Lipids), and 10 μmol/L JTE013 (Cedarlane, Burlington; Ontario, Canada) $S1P_2$ receptor antagonist. Arteries from C57Bl/6 $S1P_2$ or $S1P_3$ KO mice and WT littermates were also used. In some cases, the inhibitors or antagonists were used in combination before adding the agonists. Changes in vascular diameters were analyzed as above.

CHAPTER 3

A NOVEL MECHANISM FOR VASCULAR TONE REGULATION IN ARTERIES BY SPHINGOSINE 1-PHOSPHATE THROUGH ENDOTHELIAL BARRIER CONTROL

Most of the results presented here were submitted to Nature Scientific Reports in November 2015 (Manuscript ID: SREP-15-32363) in an article entitled "A novel mechanism for vascular tone regulation in arteries by sphingosine 1-phosphate through endothelial barrier control" by Daniel Kerage, Martina Mackova, Randi Gombos and Denise Hemmings is currently under revision. The majority of data were generated by myself. Martina Mackova produced Figure 3.5C, and Randi Gombos was involved in establishing the intraluminal flow protocol and her unpublished preliminary results evaluating vasodilation after infusion of S1P contributed to the rationale for this chapter. Maggie Wang contributed to the data presented in Figure 3.1A and Meagan Brown was responsible for Figure 3.1B, C.

3.1 Introduction

The vascular endothelium plays an important role as a barrier between circulating factors and underlying tissues in addition to producing vasoconstrictors and vasodilators. The mechanisms through which circulating factors reach the underlying tissues are poorly understood. While endothelial permeability is largely viewed as pathophysiological, it is likely that endothelial permeability occurs within physiologically tolerable limits that permit circulating factors to access the VSMCs to maintain normal vascular tone. While increased endothelial permeability is often associated with vascular complications like diabetes mellitus [717], cardiovascular diseases [718] and pregnancy disorders [230,719,720], it is likely that this occurs when the physiologically regulated endothelial permeability is disrupted.

S1P enhances, but also disrupts the endothelial barrier depending on its concentration and the balance of the S1P receptors expressed, making it an ideal regulator of endothelial permeability [3,390,425,721,722]. At physiological concentrations (0.1-1 μmol/L), S1P signals through $S1P_1$ receptors to increase endothelial barrier function [400,721], but at higher concentrations, S1P disrupts the barrier via $S1P_2$ or $S1P_3$ receptors [425,722]. In addition, when S1P binds to $S1P_1$ or $S1P_3$ receptors on the endothelium it induces vasodilation [386], but it stimulates vasoconstriction when it interacts with $S1P_2$ or $S1P_3$ receptors on the VSMCs [386].

While the mechanisms by which S1P enhances endothelial barrier function are relatively well characterized using endothelial cell cultures, *in vivo* in animal models, and recently in isolated venules [416,417,723,724], no studies have examined the regulation of endothelial permeability by S1P in intact isolated arteries or the direct relationships between endothelial permeability and vascular tone.

In this study, I therefore proposed that S1P regulates endothelial permeability and thus controls leakage of circulating vasoconstrictors to the underlying VSMCs in arteries impacting vascular tone. High S1P concentrations or permeability enhancing agents will disrupt the endothelial barrier and promote an increase in vascular tone that can be reversed by engaging $S1P_1$ receptor. Building on the work of others [692,720,725], we established a novel technique to simultaneously measure endothelial permeability and vascular tone in intact arteries mounted on a pressure myograph system. Using this technique I studied this question in uterine arteries to assess the potential impact on reproduction and also in mesenteric arteries to evaluate the impact on systemic vascular function. In this Chapter, I therefore describe a novel link between S1P signaling, modulation of endothelial barrier function and the ensuing impact on vascular tone in resistance arteries.

3.2 RESULTS

3.2.1 S1P-mediated control of endothelial barrier in cultured endothelial cells

Using primary human umbilical vein endothelial cells (HUVECs) to model vascular endothelial cells, we assessed the role of S1P on endothelial permeability. Visual confluence of cultured cells was confirmed by a significant reduction in 70 kDa fluorescent dextran flux through untreated cell cultures compared to flux through cell–free gelatin–coated inserts (experiment by Maggie Wang) (Figure 3.1A). As expected, [400] addition of 0. 1 μmol/L S1P significantly decreased dextran flux 3 h after treatment compared to untreated cells. Treatment with 1 μmol/L S1P had no significant effect on dextran flux or disruption of cellular actin; however, this concentration showed relatively greater (as shown by arrows) VE–cadherin disorganization compared to untreated cells (Figure 3.1A, B, C). In contrast, 10 μmol/L S1P significantly increased dextran flux from 1.5 to 3 h (Figure 3.1A) and completely disrupted cellular actin (Figure 3.1B) and VE–cadherin (Figure 3.1C) compared to untreated or 1 μmol/L S1P–treated cells. Pretreatment of cells with 1 μmol/L VPC23019, an $S1P_1$/$S1P_3$ antagonist,

reduced the S1P–mediated effects on actin and VE–cadherin. VPC23019 treatment alone had no effect (experiments by Meagan Brown) (Figure 3.1B, C). These experiments suggest that S1P at low concentrations decreased endothelial permeability but high concentrations S1P increases endothelial permeability. I next investigated the role of S1P in the regulation of endothelial permeability, but also vascular tone in a more physiologically relevant model in mouse resistance arteries.

3.2.2 Novel technique to simultaneously measure endothelial permeability and vascular tone in response to agonists infused inside isolated intact arteries

To assess a dual role for S1P on endothelial permeability and vascular tone control, we developed a new method using the well-known and available Living Systems pressure myograph. A previously published method by Moss et al [692] used Evans Blue dye (EBD) to determine the amount of dye embedded in the vascular wall after infusion of human arteries with permeability factors. To ensure clear visualization and allow measurement of vascular tone of the arteries on the Living System myograph, we used leakage to the bath of a fluorescent-labeled low molecular weight (3kDa) dextran as a measure of permeability. As the Living Systems myograph does not have syringe pumps to inject solutions, we also established a new method to prevent mixing of solutions by incorporating a 1.2 cm air bubble between pre-loaded equilibration and experimental solutions in the distal tubing. This key component of our technique prevented mixing while the mounted artery equilibrated. Treatments were loaded in a total of 200 µl, and then infused for 20 min using a low flow rate to allow the experimental solution to reach the artery. The small air bubble was lost as it passed through the transducer prior to reaching the artery. The flow was then stopped for 10 or 20 min (I found some treatments like LPS or gB requires more time to increase endothelial permeability) to allow the treatments to equilibrate with the artery. After that, all the bath solution (6 ml) was harvested into light-proof tubes (I used aluminium foil to wrap the tube), and then distributed into 3 wells (2 ml each) of 24-well plate from which fluorescence was measured. The total fluorescence from the 3 wells divided by the arterial length was used as a measure of permeability after subtracting the background. I used this technique to assess endothelial permeability in response to different concentrations of infused S1P or other permeability factors by measuring leakage of co-infused fluorescent dextran to the bath. This technique also enabled me to simultaneously measure

changes in vascular tone to permeability-inducing agents infused in the presence and absence of U46619, a vasoconstrictor.

3.2.3 S1P-induced permeability in intact uterine arteries contributes to increased vascular tone through leakage of a co-infused vasoconstrictor (U46619)

Using the above method, I determined whether infusion of different concentrations of S1P alone would impact vascular tone. Neither intraluminal infusion nor extraluminal addition to the bath of 0.01 μmol/L S1P alone affected vascular tone (Figure 3.2A, B). However, while extraluminal addition of 1 μmol/L S1P alone increased vascular tone, intraluminal infusion of this concentration had no effect (Figure 3.2A, B). In contrast, both infusion and extraluminal addition of 10 μmol/L S1P increased vascular tone compared to the control or lower S1P concentrations (Figure 3.2A, B).

I then evaluated the effects of infusing different concentrations of S1P together with U46619 on vascular tone. Infusion of 5 nmol/L U46619 alone had no effect on vascular tone, but extraluminal addition of the same concentration effectively increased vascular tone (Figure 3.2 B). When 5 nmol/L U46619 was co-infused with 0.01 μmol/L S1P there continued to be no effect on vascular tone; however, vascular tone was increased after co-infusion of U46619 with 1 or 10 μmol/L S1P that was significantly greater than that induced by infused corresponding concentrations of S1P or U46619 alone (Figure 3.2A). The increased vascular tone after co-infusion of U46619 with 10 μmol/L S1P was significantly greater than that generated by co-infusion of U46619 with 1 μmol/L S1P (Figure 3.2A). Co-addition of S1P at any concentration with U46619 to the bath had no additive effect on vascular tone compared to that generated by U46619 alone. However, significant increases in vascular tone were found after co-addition of 0.01 or 1 μmol/L S1P with U46619 compared to 0.01 or 1 μmol/L S1P alone, respectively (Figure 3.2B).

Infusion of U46619 had no effect on dextran leakage (permeability) (Figure 3.2C). However, infusion of 1 or 10 μmol/L S1P alone significantly increased dextran leakage with a greater effect noted at 10 μmol/L S1P. The increased dextran leakage found with the combined S1P and U46619 infusion, did not differ from the individual S1P treatments (Figure 3.2C). To further investigate the mechanisms involved in the increased vascular tone generated by co-infusion of U46619 with S1P, I chose 1 μmol/L because this concentration is within the normal

physiological range, and 10 μmol/L S1P is pathophysiological. As well, the dual infusion (1 μmol/L S1P and 5nmol/L U46619) generated a constriction response that was absent with either treatment alone.

3.2.4 Role of thromboxane receptors in vascular tone induced by co-infused S1P and U46619

To investigate the contribution of U46619 both inside and outside the artery to the increased vascular tone when it was co-infused with S1P, I repeated the experiments in the presence of 10 μmol/L SQ29548 to block thromboxane receptors, and thus could inhibit U46619 activity. Co-infusion of SQ29548 with S1P and U46619 did not affect the vascular tone induced in its absence. However, the vascular tone induced following co-infusion of S1P and U46619, was completely blocked by pretreatment of arteries in the bath with SQ29548 (Figure 3.3A). Moreover, pretreatment with SQ29548 in the bath partially reduced vascular tone in response to simultaneous extraluminal addition of S1P and U46619 (Figure 3.3B), but completely blocked vascular tone induced by U46619 alone (Figure 3.3C).

3.2.5 U46619-mediated induction of vascular tone after co-infusion with S1P depends on the $S1P_3$ receptor

To determine the role of S1P in promoting the U46619-induced vascular tone, the results show that inhibition of the $S1P_1$ and $S1P_3$ receptors by co-infusing 1 μmol/L VPC23019 ($S1P_1$/$S1P_3$ receptor antagonist) with 1 μmol/L S1P and U46619 reduced vascular tone (Figure 3.4A). However, co-addition of VPC23019 with these same agonists to the artery bath also reduced vascular tone but to a lesser amount than that induced by co-infused S1P and U46619 in the presence of VPC23019 (Figure 3.4A). Infusion or extraluminal addition of 1 μmol/L VPC23019 alone had no effect on arterial diameter.

Since VPC23019 blocks both $S1P_1$ and $S1P_3$ receptors, I confirmed the importance of $S1P_3$ receptors by using uterine arteries from $S1P_3$ KO mice, which were available on a 129/S1SVIMJ background and their littermate WT controls. Unlike the previous infusion experiments in arteries from C57Bl/6J mice, infusion of 1 μmol/L S1P into arteries from WT control mice on the 129/S1SVIMJ background showed increased vascular tone similar to that found when added extraluminally to these arteries (Figure 3.4B, C) or extraluminally to arteries

from C57Bl/6J mice (Figure 3.2B). Importantly, no vascular tone was generated with infusion of U46619 alone or with either extraluminal addition of 1 μmol/L S1P alone to the bath or infusion inside uterine arteries from $S1P_3$ KO mice. Co-infusion of U46619 with S1P into arteries from WT controls generated significantly greater vascular tone than S1P alone while no vascular tone occurred after co-infusion in arteries from $S1P_3$ KO mice (Figure 3.4B). However, addition of U46619 or co-addition of U46619 with S1P to the bath significantly increased vascular tone similarly in arteries from both $S1P_3$ KO mice and their littermate controls (Figure 3.4C). Notably, vascular tone was greater overall after intraluminal infusion or extraluminal addition in arteries from WT compared to $S1P_3$ KO mice (Figure 3.4B, C).

3.2.6 Higher concentrations of S1P and U46619 were required to elicit responses in mesenteric arteries from female mice

I next determined whether infusion of S1P and U46619 could generate similar responses in mesenteric arteries from female C57Bl/6J mice. Intraluminal infusion or extraluminal addition of S1P or U46619 at the same concentrations used in uterine arteries, alone or in combination, showed minimal vascular effects in mesenteric arteries (Figure 3.5A). In contrast, co-infusion of 3 μmol/L S1P with 20 nmol/L U46619 increased vascular tone compared to the untreated control, 3 μmol/L S1P or 20 nmol/L U46619 alone. Similar to the lower concentrations in uterine arteries, infusion of 20 nmol/L U46619 alone had no effect on vascular tone in mesenteric arteries while addition of this same concentration to the bath induced significant vascular tone (Figure 3.5B). The co-addition of 3 μmol/L S1P and 20 nmol/L U46619 to the bath induced vascular tone that was significantly greater than that induced by S1P alone. However, there was no additive effect compared to U46619 alone (Figure 3.5B). Overall, vascular tone was higher after extraluminal addition compared to that induced by intraluminal infusion. These responses in mesenteric arteries at higher concentrations of S1P and U46619 were similar to those found in uterine arteries at lower concentrations (Figure 3.2B, C compared to Figure 3.5B). We then assessed the S1P receptor expression to determine whether differences between tissues could explain these results. The expression of $S1P_1$ was higher in uterine compared to mesenteric arteries, but the $S1P_3$ receptor expression was not different between the two vascular beds. Interestingly, we also found that expression of the housekeeping genes, β-actin or GAPDH, was consistently higher in uterine compared to mesenteric arteries (Figure 3.5C).

3.2.7 Vascular tone induced in mesenteric arteries from male mice show dependence on the $S1P_3$ receptor

I next determined whether co-infusion of S1P with U46619 could induce vascular tone in mesenteric arteries from male WT and $S1P_3$ KO mice. S1P, U46619 or a combination at the lower concentrations used in uterine arteries from female mice were infused into mesenteric arteries from WT male mice. Similar to the effects found in WT female mice on the 129/S1SVIMJ background, S1P alone generated significant and similar vascular tone whether infused or added to the bath (Figure 3.6A, B). As well, S1P alone also did not induce vascular tone infused or added to the bath in mesenteric arteries from male $S1P_3$ KO mice. Interestingly, infusion of U46619 alone induced a significant vascular tone unlike the lack of response found in arteries from females (Figure 3.6A). However, vascular tone induced by co-infusion of S1P and U46619 into arteries from WT mice was still significantly greater than that from individual treatments or that induced by co-infusion in arteries from $S1P_3$ KO mice (Figure 3.6A). Overall, responses to infused treatments in arteries from $S1P_3$ KO mice were significantly reduced compared to those from WT controls (Figure 3.6A). Extraluminal co-addition (Figure 3.6B) of S1P with U46619 induced vascular tone in arteries from WT male mice that was not significantly different from the individual treatments. The vascular tone induced after intraluminal infusion of S1P, U46619 or a combination in arteries from WT mice was not different from that induced when these treatments were added extraluminally (Figure 3.6A, B). Only the combined addition of S1P and U46619 to the bath of arteries from $S1P_3$ KO mice showed minimal yet significant vascular tone compared to no treatment. The vascular tone induced by the addition of S1P, U46619 or a combination to the bath of arteries from $S1P_3$ KO mice was significantly decreased overall compared to arteries from WT mice (Figure 3.6B).

3.2.8 Co-infusion of U46619 with bacterial or viral components increased vascular tone

I then asked whether co-infusion of U46619 with factors known to increase permeability under pathological conditions such as infections [661,726,727] could also increase vascular tone. I found that co-infusion of U46619 with either LPS (Figure 3.7A) or gB (Figure 3.8A) followed by incubation of the treatments for 10 min, vascular tone was increased compared to infusion of each component alone. By contrast, extraluminal co-addition of LPS did not affect U46619-induced vasoconstriction (Figure 3.7B). There was, however, a significant decrease in U46619-

induced vasoconstriction in the presence of gB which was reversed by L-NAME treatment (Figure 3.8B).

3.2.9 $S1P_1$ agonist (SEW2871) prevented increase in vascular tone induced by co-infusion of U46619 with thrombin into uterine arteries

Infusion of thrombin increased permeability in uterine arteries with no additive effect when U46619 was co-infused. Infusion of SEW2871, a specific $S1P_1$ receptor agonist, reduced thrombin-induced permeability in the presence or absence of U46619 (Figure 3.9A). U46619 co-infused with thrombin also led to increased vascular tone compared to arteries infused with either thrombin or U46619 alone. The increased vascular tone was completely blocked by co-infused SEW2871. There was an overall increase in vascular tone under flow conditions compared to when flow was stopped (Figure 3.9B). Neither thrombin nor SEW2871 added to the bath affected vascular tone induced by extraluminal addition of U46619 (Figure 3.9C).

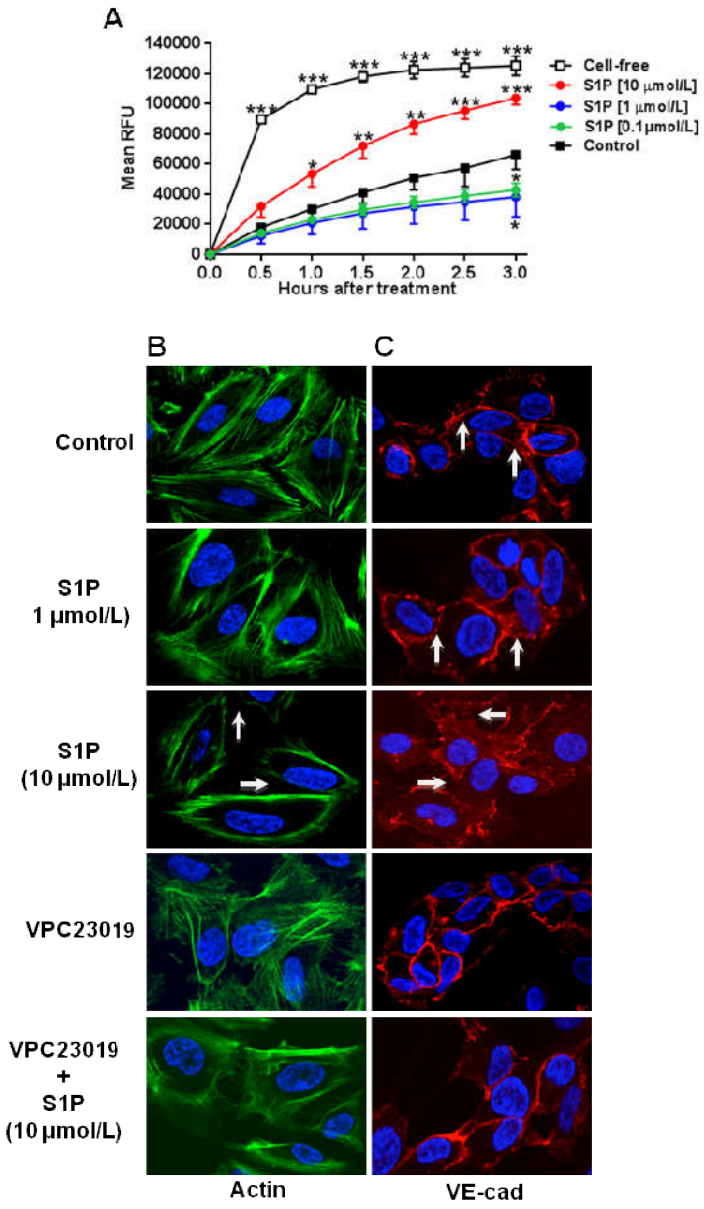

Figure 3.1: S1P-regulated leakage of fluorescent dextran through confluent endothelial cells. Fluorescent dextran leakage through cell-free inserts or those with confluent endothelial cells treated with S1P was compared to leakage through untreated cells. The cumulative mean ± SEM relative fluorescence units (RFU; n=3) were analyzed by two-way ANOVA and the Tukey post hoc test. *=p<0.05, **=p<0.01, ***=p<0.001 **(A)** (experiment by Maggie Wang). Cells treated with 1 or 10 µmol/L S1P +/- 1 µmol/L VPC23019 were stained for cellular actin **(B)** or VE-cadherin **(C)** (experiments by Meagan Brown). Representative images (the arrows indicate points of disruption) from one of three independent experiments are depicted.

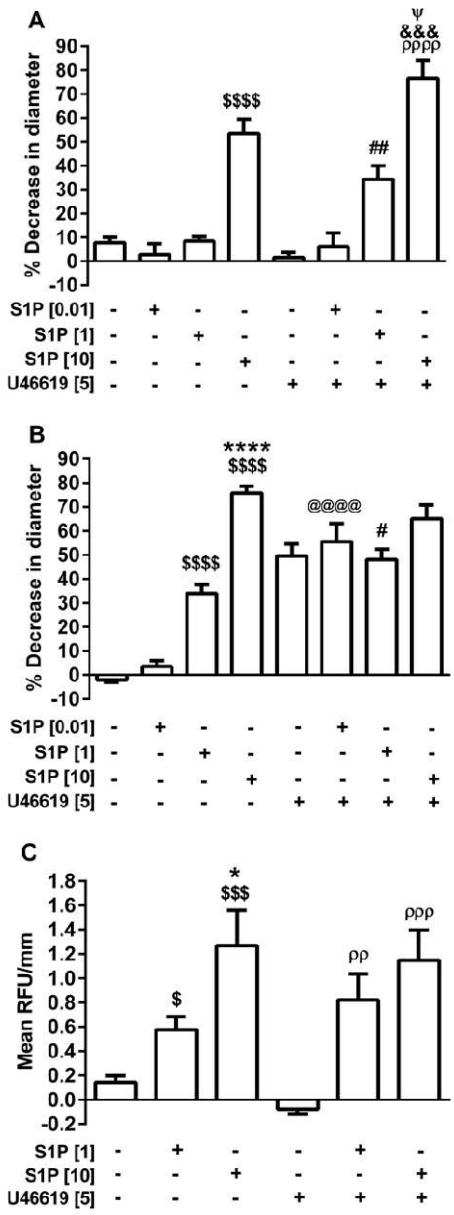
A
% Decrease in diameter
90
80
70
60
50
40
30
20
10
0
-10
$$$$
##
ψ
&&&
ρρρ
S1P [0.01] - + - - - + - -
S1P [1] - - + - - - + -
S1P [10] - - - + - - - +
U46619 [5] - - - - + + + +
B
% Decrease in diameter
90
80
70
60
50
40
30
20
10
0
-10
****
$$$$
$$$$
@@@@
#
S1P [0.01] - + - - - + - -
S1P [1] - - + - - - + -
S1P [10] - - - + - - - +
U46619 [5] - - - - + + + +
C
Mean RFU/mm
1.8
1.6
1.4
1.2
1.0
0.8
0.6
0.4
0.2
0.0
-0.2
*
$$$
$
ρρ
ρρρ
S1P [1] - + - - + -
S1P [10] - - + - - +
U46619 [5] - - - + + +

Figure 3.2: Vascular tone and dextran leakage in uterine arteries after treatment with S1P and/or U46619. The percent change in uterine artery diameters was assessed from the baseline after intraluminal infusion **(A)** or extraluminal addition **(B)** with 0.01, 1 or 10 μmol/L S1P, 5 nmol/L U46619 or U46619 combined with S1P (n = 3 to 16), where 'n' represents the number of arterial segments per mouse. The results are presented as mean ± SEM. Leakage of fluorescent dextran into the bath after co-infusion with the previous treatments was also measured and corrected by vessel length **(C)**. Statistical analysis was performed by one way ANOVA followed by Tukey's post hoc test. $ = compared to untreated control or lower S1P concentrations; * = compared to 1 μmol/L S1P; ψ = compared to 10 μmol/L S1P; ρ = compared to U46619; # = compared to 1 μmol/L S1P or U46619 in **(A)** or to 1 μmol/L S1P in **(B)**; & = compared to combined 1 μmol/L S1P and U46619; @ = compared to 0.01 μmol/L S1P. For all figures, the number of symbols depicts increasing levels of significance: 1 = $p<0.05$, 2 = $p<0.01$, 3 = $p<0.001$ and 4 = $p<0.0001$.

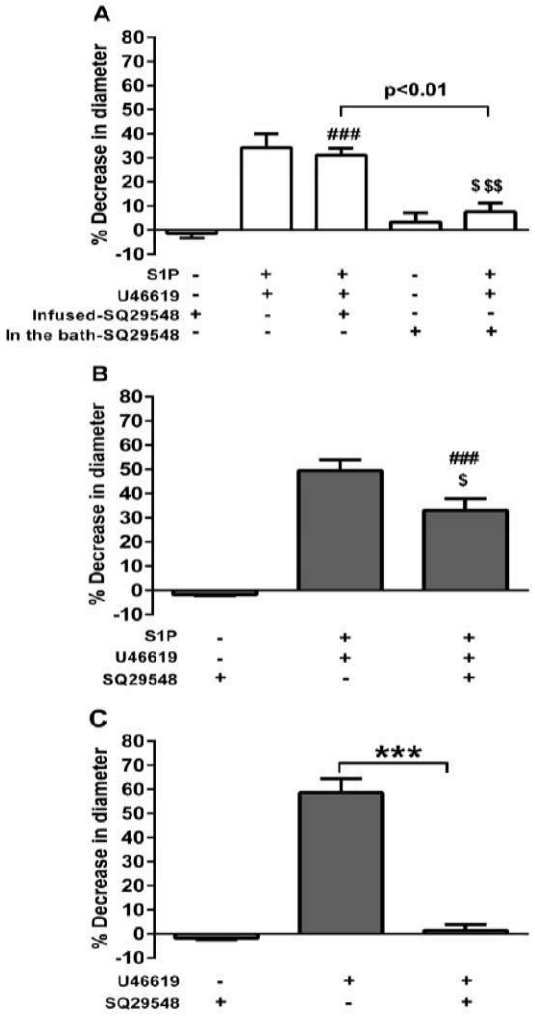

Figure 3.3: Effect of thromboxane receptor antagonist on vascular tone induced by co-treatment of U46619 with S1P in uterine arteries. The percent change in uterine artery diameters was assessed from the baseline after intraluminal co-infusion **(A)** or extraluminal co-addition **(B)** of 1 µmol/L S1P and 5 nmol/L U46619. 10 µmol/L SQ29548 was co-infused or added to the bath before co-infusing U46619 and S1P **(A)** or SQ29548 was added to the bath before co-addition of U46619 and S1P **(B)** or U46619 alone **(C)**. The results are presented as mean ± SEM and analyzed as described in Figure 3.2 (n = 3 to 9). # = compared to SQ29548; $ = compared to the combined U46619 and S1P treatment.

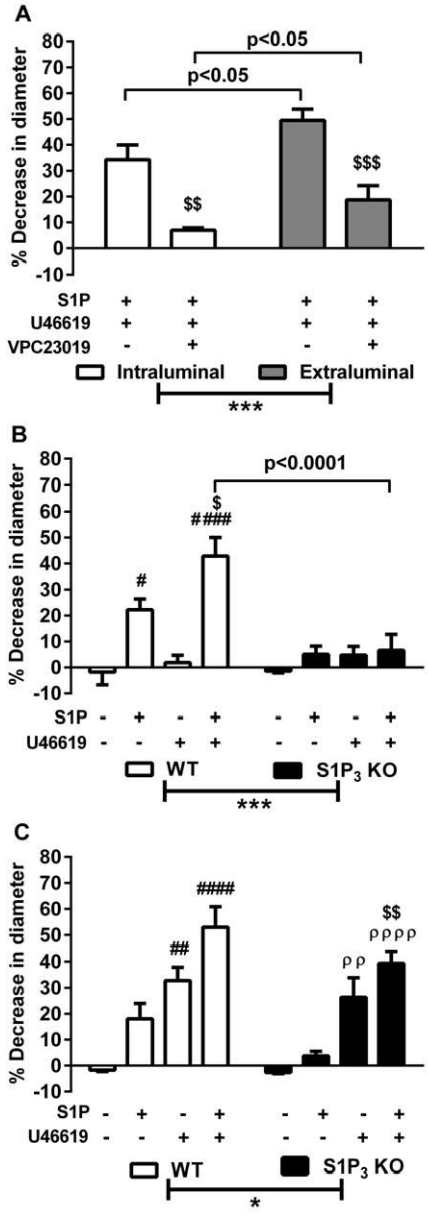

Figure 3.4: Vascular tone induced by co-treatment of U46619 with S1P in the presence of $S1P_{1/3}$ receptor antagonist or in uterine arteries from female $S1P_3$ KO and WT mice. The percent change in uterine artery diameters was assessed from the baseline, after intraluminal co-infusion **(A, B)**, extraluminal co-addition **(A, C)** of 5 nmol/L U46619 and 1 μmol/L S1P in the presence of 1 μmol/L VPC23019 **(A)** or in uterine arteries from $S1P_3$KO mice or littermate WT mice **(B, C)**. The results are presented as mean ± SEM and were analyzed by two-way ANOVA followed Tukey's post hoc test (n = 3 to 9). * = overall; $ = compared to combined S1P and U46619 **(A)** or S1P alone **(B, C)**; # or ρ = compared to untreated controls for WT or $S1P_3$ KO, respectively **(B, C)**.

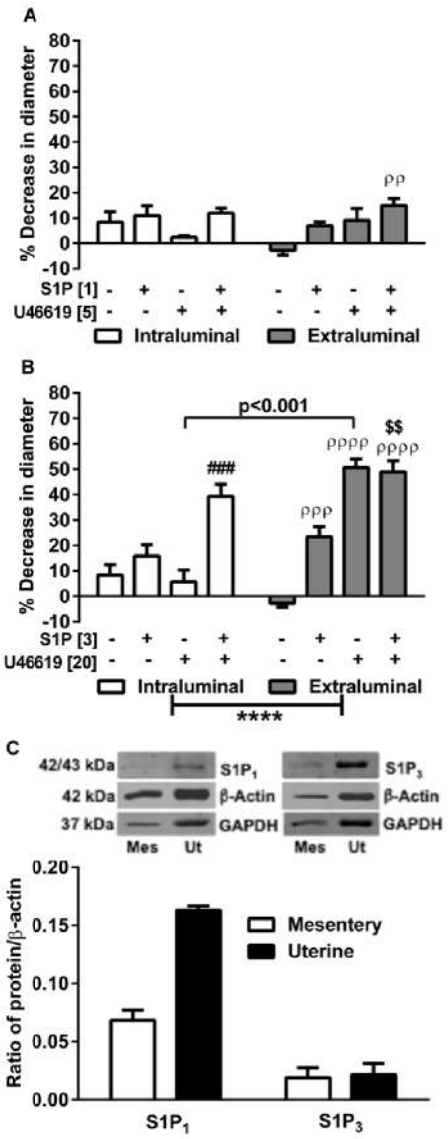

Figure 3.5: Vascular tone after treatment with U46619 and S1P in mesenteric arteries and comparison of receptor expression in uterine and mesenteric arteries. The percent change in mesenteric artery diameters was assessed from the baseline after intraluminal infusion or extraluminal addition of 5 nmol/L U46619, 1 μmol/L S1P, or the combination **(A)** or 20 nmol/L U46619, 3 μmol/L S1P, or the combination **(B)**. The results are presented as mean ± SEM and were analyzed as described in Figure 3 (n = 3 to 7). * = overall; # or ρ = compared to untreated controls for intraluminal or extraluminal, respectively; $ = compared to S1P alone. $S1P_1$ and $S1P_3$ receptor expression was assessed by Western blot from a tissue homogenate of arteries pooled from 10 mice. These results using these homogenates were repeated 2-3 times and were normalized to the housekeeping gene β-actin (experiment by Martina Mackova) **(C)**.

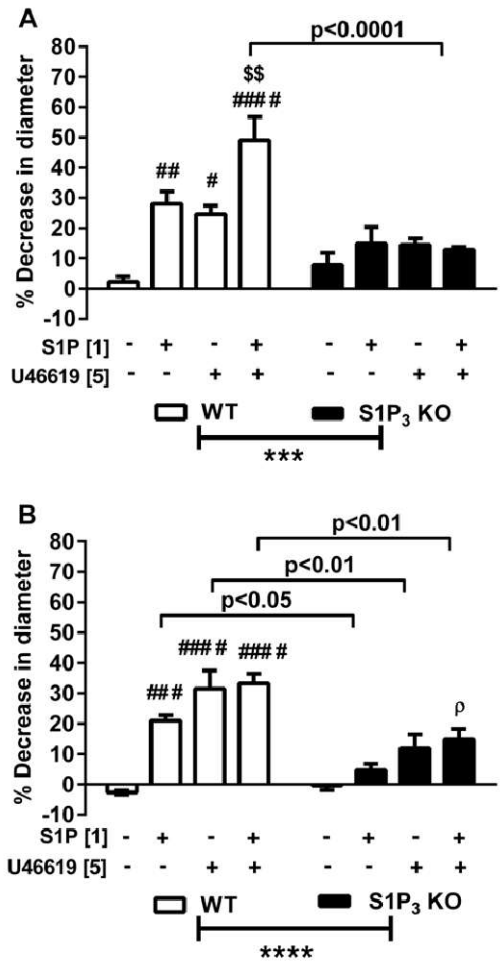

Figure 3.6: Vascular tone after treatment with U46619 and S1P in mesenteric arteries from $S1P_3$ KO and WT male mice. The percent change in mesenteric artery diameters was assessed from the baseline following intraluminal infusion **(A)** or extraluminal addition **(B)** of 5 nmol/L U46619, 1 µmol/L S1P or their combination to arteries from $S1P_3$ KO male mice or littermate WT mice. The results are presented as mean ± SEM and were analyzed as described in Figure 3.4 (n = 3 to 9). * = overall; # or ρ = compared to untreated controls for WT or $S1P_3$ KO, respectively; $ = compared to S1P or U46619 **(A)**.

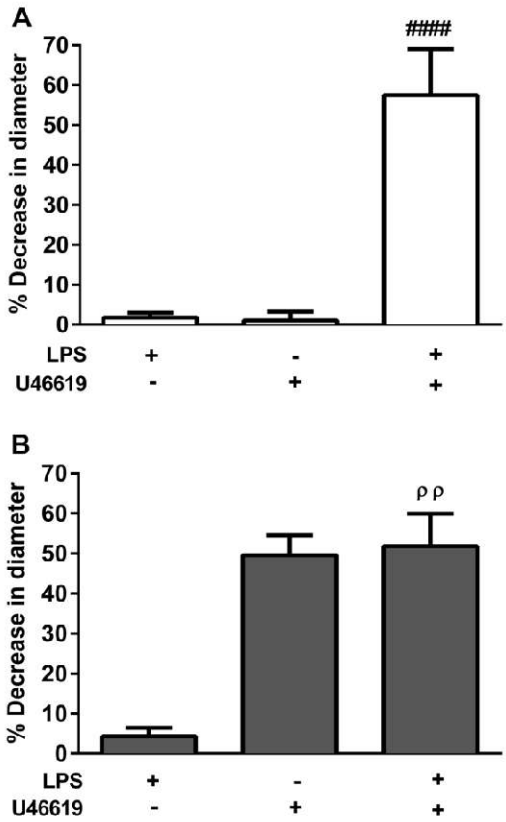

Figure 3.7: Vascular tone induced by co-infusion of U46619 with LPS into uterine arteries. The percent change in uterine artery diameters was assessed from the baseline following intraluminal infusion **(A)** or extraluminal addition **(B)** of 5 nmol/L U46619 alone or in combination with 50 ng/mL LPS. The results are presented as mean ± SEM and were analyzed as described in Figure 3.2 (n = 3 to 10). # = compared to LPS or U46619 treatment alone **(A)**; ρ = compared to LPS alone **(B)**.

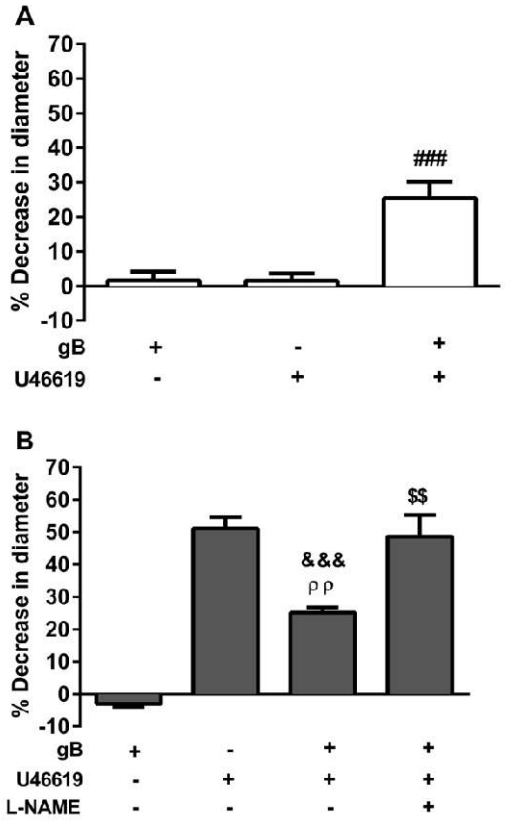

Figure 3.8: Vascular tone induced by co-infusion of U46619 with CMV glycoprotein B (gB) into uterine arteries. The percent change in uterine artery diameters was assessed from the baseline following intraluminal infusion **(A)** or extraluminal addition **(B)** of 5 nmol/L U46619 alone or in combination with 0.5 µg/mL gB. The results are presented as mean ± SEM and were analysed as described in Figure 3.2 (n = 3 to 10). # = compared to U46619 or gB treatment alone **(A)**; ρ = compared to gB alone; & = compared to U46619 alone; $ = compared to co-treatment with U46619 and gB **(B)**.

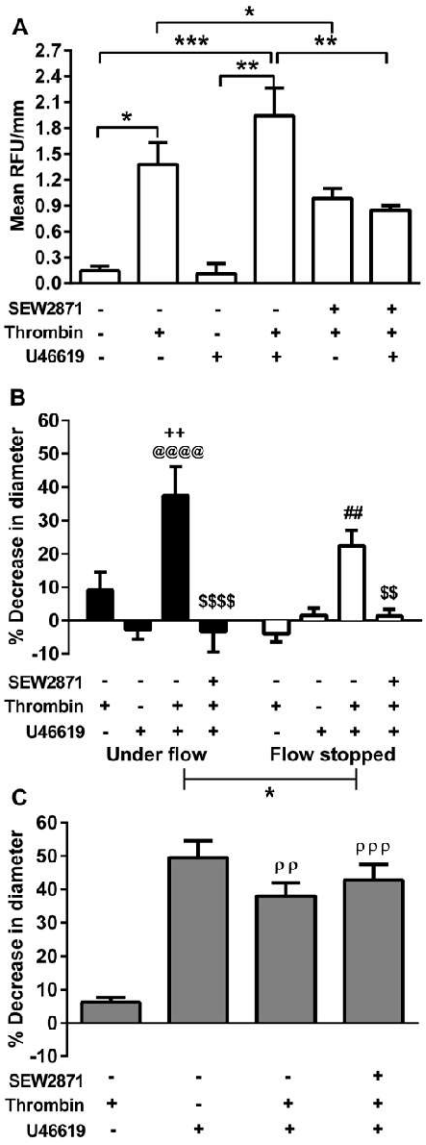

Figure 3.9: Vascular tone and dextran leakage in uterine arteries after treatment with U46619 and thrombin. 5 nmol/L U44619 in the presence or absence of 1 U/mL thrombin were co-infused with fluorescent dextran with or without the $S1P_1$ agonist, 0.1 μmol/L SEW2871. Dextran leakage was measured in the bath as described in Figure 3.2 **(A)**. The percent change in uterine artery diameters was assessed from the baseline under flow and no-flow conditions, following intraluminal infusion **(B)** or extraluminal addition **(C)**. The results are presented as mean ± SEM and were analysed as described in Figure 3.2 (n = 4 to 9). # = compared to U46619 or thrombin alone, @ = compared to U46619, + = compared to thrombin **(B)**; $ = compared to combined U46619 and thrombin treatment **(B)**; ρ = compared to thrombin alone **(C)**.

3.2.10 Discussion of results in Chapter 3

In this Chapter, I identified a new paradigm of vascular tone control in resistance arteries mediated by S1P through decreased or increased endothelial permeability. The role of S1P in maintaining endothelial barrier function has been shown in cultured endothelial cells [183,410,422,728], perfused venules [416,723,729] and models of lung permeability *in vivo* [3,425,722], but not in intact isolated arteries. Low S1P concentrations activate $S1P_1$ promoting signaling through the G_i-Rac1-pathway to increase endothelial barrier function. At high concentrations S1P activates both Rac and RhoA. However, the activation of Rac decreases after 5 to 10 minutes while the activation of RhoA remains sustained [410]. It is therefore likely that, at high S1P concentrations, $S1P_3$-mediated activation of RhoA via signaling through $G\alpha_q$ and $G\alpha_{12/13}$ predominates over Rac activation by $S1P_1$ leading to increased endothelial permeability [410,693,730]. In this Chapter, I show that in intact uterine arteries infusion of S1P dose-dependently regulates endothelial permeability. Infusion of physiological levels of 1 μmol/L S1P modestly increased permeability but did not appear to impact vascular tone while infusion of pathological levels (10 μmol/L) increased endothelial permeability allowing its own leakage to VSMCs, increasing vascular tone. Together, these findings emphasize the importance of S1P concentrations and S1P receptors in regulation of endothelial permeability.

A major finding of this study was that co-infusion of a high physiological concentration of 1 μmol/L S1P with 5 nmol/L U46619 increased vascular tone, even though infusion of each factor alone or co-infusion of U46619 with a lower concentration of 0.01 μmol/L S1P had no effect on vascular tone (Figure 3.10). The absence of vascular tone when U46619 was co-infused with 0.01 μmol/L S1P could be because S1P is maintaining the endothelial barrier preventing leakage of U46619 to the VSMCs. This argument is partly supported by the finding that S1P at a concentration that increases endothelial permeability permits leakage of U46619 to the VSMCs increasing vascular tone. The fact that 1 μmol/L S1P or 5 nmol/L U46619 at these concentrations each induce vascular tone when added extraluminally but not when infused, suggests that there is a barrier that prevents these molecules from accessing the VSMCs. This barrier is overcome when the two are co-infused. To further investigate why this might be occurring, I showed that the mechanism leading to increased vascular tone is leakage of U46619 through increased endothelial permeability induced by S1P. To support this argument, I demonstrated that co-infusion of the TXA_2 receptor antagonist, SQ29548 with S1P and U46619, did not reduce the

induced vascular tone. Since U46619 at the concentration used in this study had no effect on endothelial permeability, this rules out the possibility that U46619 could promote its own leakage. Interestingly, when I added SQ29548 to the bath followed by co-infusion of S1P and U46619 inside the artery, there was a complete blockade of vascular tone, suggesting that U46619 was reaching the VSMCs from the endothelium. Moreover, while the S1P-induced vascular tone when added extraluminally to arteries from the $S1P_3$ KO female mice was completely inhibited, the U46619-induced vascular tone was unaffected. This verifies that the loss of constriction after co-infusion of S1P and U46619 in arteries from $S1P_3$ KO mice was due to the loss of S1P-mediated permeability through $S1P_3$ that prevented the leakage of U46619. These results provide further evidence that the increase in vascular tone after co-infusion is mediated by U46619 through permeability generated by S1P at 1 μmol/L. I however, did not see any effect on vascular tone by infused individual treatments. Since U46619 alone does not induce permeability, it is not expected to leak; however S1P alone increased permeability yet had no effect on vascular tone. It is likely that S1P leaks to the VSMC and stimulates vasoconstriction but this is counterbalanced by S1P-induced NO production at this concentration. S1P activity is well known to cause eNOS activation and NO production [33,121,386,731]. This means that the U46619 leakage in the presence of 1 μmol/L S1P when co-infused induces additional vasoconstriction that overcomes the NO-mediated deterrence of S1P-induced constriction.

To support the role of S1P in facilitating access of infused U46619 to the underlying VSMC through increased endothelial leakage, I showed that when VPC23019 ($S1P_1$/$S1P_3$ receptor antagonist) was co-infused with S1P and U46619, there was a complete block of the induced vascular tone. Furthermore, the 1 μmol/L S1P-induced permeability was not different from that induced by the combined S1P and U46619, but also S1P at this concentration caused disruption of the endothelial junctional molecule, VE-cadherin in HUVECs. These results support the argument for the role of S1P in promoting leakage of U46619 through increased permeability. S1P at 0.1 μmol/L has been shown to increase endothelial permeability in HUVECs in an $S1P_2$ receptor-dependent manner [732]. Interestingly, the lack of vascular tone when U46619 was co-infused with the lower concentration of 0.01 μmol/L S1P indicates that S1P at this concentration likely contributes to the endogenous mechanisms for maintenance of the endothelial barrier thus preventing U46619 leakage to the VSMCs, but also that S1P does not

promote U46619-induced vascular tone except through increased endothelial permeability.

Maintenance of endothelial integrity requires the continuous engagement of $S1P_1$, and agents that induce permeability must overcome this protective signaling [419,436]. In contrast, signaling through $S1P_3$ exacerbates inflammation in sepsis by increasing endothelial permeability [733] and likely contributes to the lack of protection by S1P or SEW2871 at high concentrations in an *in vivo* LPS-induced acute inflammatory lung injury model [425]. I now show using an $S1P_1$/$S1P_3$ receptor antagonist and arteries from $S1P_3$ KO mice that ≥ 1 μmol/L S1P infused inside pressurized resistance arteries increases endothelial permeability largely through $S1P_3$. The differences in vascular response to S1P in arteries isolated from mice on a 129/S1SVIMJ compared to a C57Bl/6J background are likely associated with genetic differences such as S1P receptor expression. However, a potentiating effect of S1P on leakage of U46619 in uterine arteries was still observed in the WT littermates, which was absent in the $S1P_3$ KO mice, supporting an important role for $S1P_3$ in mediating the endothelial barrier disruption. Although I have not yet determined why there is an additive combined effect on vascular tone of co-infusing both S1P and U46619, I have demonstrated that the vascular tone is generated by leakage of U46619 and this leakage is mediated by S1P in an $S1P_3$-dependent manner.

I find that S1P also plays a role in potentiating U46619-induced vascular tone in mesenteric arteries from female mice. However, these arteries are less reactive to S1P or U46619 than uterine arteries. We examined whether the level and type of S1P receptors expressed in these two vascular beds could explain this finding. Unexpectedly, we found that the level of expression of $S1P_3$ is the same in uterine and mesenteric arteries. This suggests that differences in downstream signalling through $S1P_3$ on the endothelium in these two vascular beds may be the explanation, as there exists different subtypes of G-proteins that couples to S1P receptors in different cell types [734]. Alternatively, the ratio of $S1P_1$ to $S1P_3$ receptors may be higher in the mesenteric arteries leading to greater vasodilation that counters the induced vasoconstriction. However, interpretation of data from S1P receptors expression should be taken with caution as they were measured from whole arteries that included both endothelium and VSMCs. The higher expression of $S1P_1$, which is predominantly involved in vasodilation, in uterine compared to mesenteric arteries highlights its potential importance in reproduction. Increase in vasodilatory capacity is one of the major adaptations that occurs particularly in the uterine vasculature during pregnancy [735]. It is also possible that differential TP receptor expression on these arteries

could be an explanation. We also found that the expression of the housekeeping genes, β-actin and GAPDH, were lower in mesenteric compared to uterine arteries. This could be explained by the higher levels of non-cellular protein components not containing these housekeeping genes that have previously been reported in mesenteric arteries compared to other vessels [736]. Nevertheless, the reduced reactivity of mesenteric arteries from females implies that leakage of vasoconstrictors through the endothelium of systemic arteries is more tightly controlled in that it will only occur at pathological concentrations of S1P. An increase in circulating S1P concentrations as seen in coronary heart disease [737], could therefore negatively impact blood pressure.

I however, found that mesenteric arteries from male mice remarkably different. Infusion of U46619 by itself generates vascular tone unlike the lack of response in arteries from female mice, although S1P-induced potentiation still occurs after co-infusion similar to that found in mesenteric arteries from female mice. Mesenteric arteries from male mice are likely leakier than those from female mice, and they also exhibit constriction responses similar to uterine arteries. This dichotomy of vascular responses found in males and females is not surprising since there are many examples of sex-based differences in vascular responses [738,739]. Interestingly, U46619-induced vascular tone in the bath in mesenteric arteries from male mice was dramatically decreased in $S1P_3$ KO mice compared to the wildtype control, suggesting that in these arteries, U46619-induced responses could be occurring partly through the S1P pathway.

I then asked whether infectious agents known to increase endothelial permeability could also increase access of circulating vasoconstrictors to the VSMCs. Bacterial infections like *Escherichia coli* [726] or viral infections such as hantavirus [740] and CMV [661] increase endothelial permeability. By using only surface components of infectious agents, such as LPS from *K. pneumonia* or CMV gB protein co-infused with U46619 vascular tone was increased, suggesting that attachment of bacterial or viral particles is sufficient to potentiate vascular-related complications. Indeed, periodontal bacterial [741] and CMV [742] infections have been associated with hypertension. An interesting finding was that while co-infusion increased vascular tone, the addition of gB with U46619 to the bath decreased vascular tone. Restoration of the extraluminal U46619-induced vascular tone with L-NAME treatment indicates that gB induces NO production, consistent with our previously published findings showing increased vasodilation in response to infusion of gB [574].

Equally important was the finding that co-infusion of U46619 with thrombin, a well known permeability-inducing agent, promoted leakage of U46619 increasing vascular tone. The vascular tone generated by co-infusing thrombin with U46619 was greater under continuous flow conditions than when flow was stopped. This is typical of the rapid reversible nature of thrombin-induced permeability [743]. It has been proposed that this recovery is possibly mediated by cross-activation of SK-1 through the thrombin receptor leading to generation of S1P that signals through $S1P_1$ to decrease endothelial permeability[743]. This argument is partly supported by my experiments in which the vascular tone induced by co-infused thrombin and U46619 was fully inhibited by targeting $S1P_1$ with SEW2871, known to decrease endothelial permeability [414,744]. This provides further evidence that $S1P_1$ receptors can be therapeutically targeted to ameliorate the negative effects of vascular leakage [419]. None of these infectious or inflammatory agents added directly to the bath induced vasoconstriction, which supports the argument that the vasoconstriction was induced by leakage of the co-infused thromboxane mimetic (U46619).

In this Chapter, I demonstrate a novel mechanism where S1P controls vascular tone in resistance arteries by regulating endothelial permeability. Importantly, while signalling via the $S1P_1$ receptors has been shown to reduce permeability in cultured endothelial cells and veins, I now show that S1P signaling via $S1P_1$ decreases endothelial permeability and prevents leakage of circulating vasoconstrictors through the endothelium of resistance arteries regulating vascular tone (Figure 3:10). These findings have far reaching implications in understanding the impact of endothelial permeability generated under physiological, or abnormal conditions such as infection and inflammation. Using pharmacologic therapy, there is potential to utilize signaling through $S1P_1$ to treat hypertensive diseases and pregnancy-related complications like preeclampsia and intrauterine growth restriction.

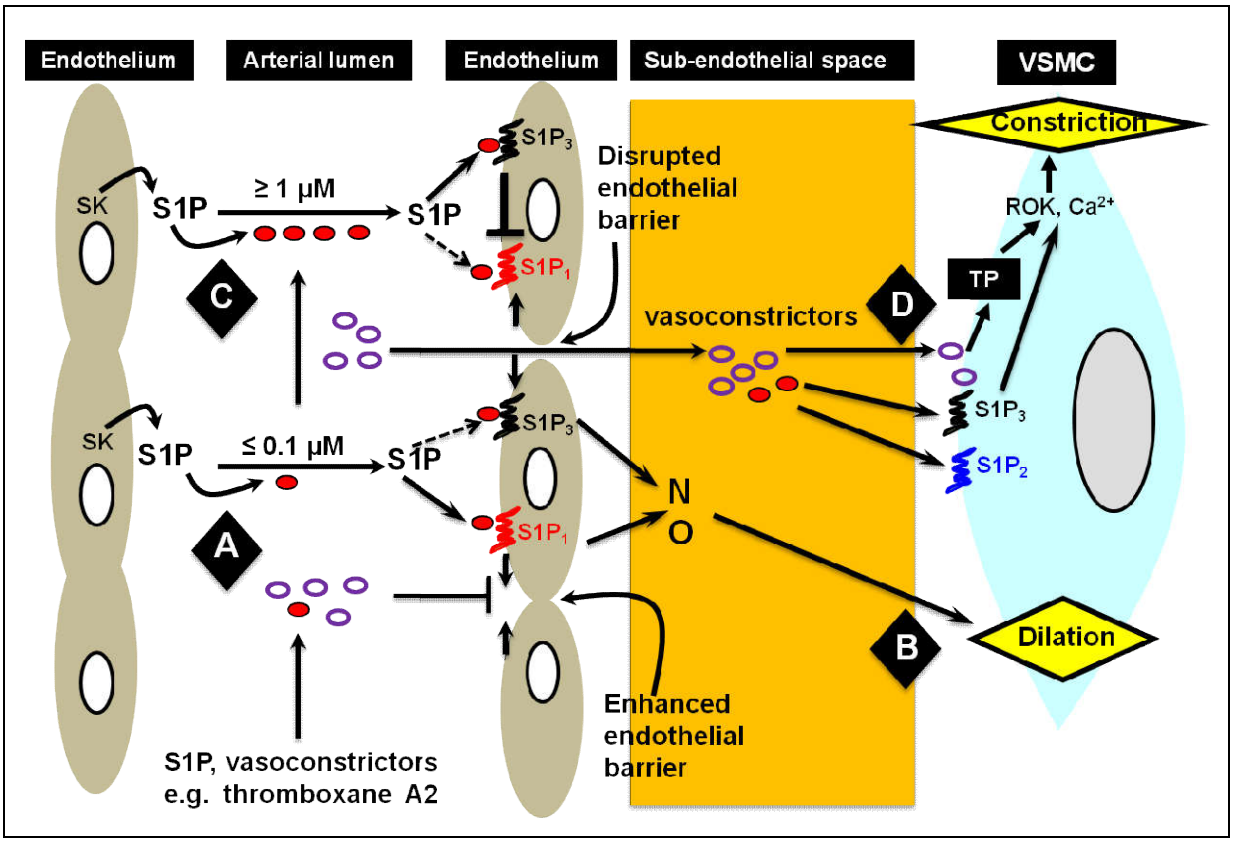

Figure 3.10: Proposed mechanism for S1P-induced regulation of vascular tone. Circulating S1P acts on endothelial cells. At low concentrations of ≤ 0.1 µmol/L S1P the prevailing response is produced by $S1P_1$ activation and this enhances the endothelial barrier, which blocks leakage of potential vasoconstrictors **(A)**. Activation of $S1P_1$ or $S1P_3$ on the endothelium also produces NO, which induces dilation **(B)**. At high concentrations ≥1 µmol/L S1P acts through S1P3 and counteracts the responses mediated through S1P1. This increases permeability (C) allowing leakage of vasoconstrictors (e.g. TXA_2 and S1P itself) to the sub-endothelial space, which increases the constriction of VSMCs through TXA_2/prostaglandin (TP) receptors and S1P2 and S1P3 receptors **(D)**. The figure depicts the extreme responses to low and high concentrations of S1P. There is a dynamic range between approximately 0.1 and 1 µmol/L where S1P dynamically regulates barrier function as a means of controlling vascular tone.

CHAPTER 4

SPHINGOSINE 1-PHOSPHATE-INDUCED NITRIC OXIDE PRODUCTION REGULATES ENDOTHELIAL PERMEABILITY AND VASCULAR TONE IN MOUSE UTERINE ARTERIES

All results in this Chapter were generated by myself, and have not yet been submitted for publication.

4.1 Introduction

In Chapter 3 I showed that ≥1 μmol/L S1P-induced endothelial permeability mediated via the $S1P_3$ receptor, promoted leakage of a co-infused vasoconstrictor (U46619) to the VSMCs increasing vascular tone. Such endothelial leakage and increase in vascular tone were prevented when U46619 was co-infused with a lower concentration of 0.01 μmol/L S1P that decreases permeability (Figure 3.2A). Further, an $S1P_1$ receptor agonist (SEW2871) prevented leakage of U46619 by decreasing endothelial permeability stimulated by thrombin. These results collectively emphasize the role of S1P in regulating endothelial barrier in mouse uterine arteries. However, the exact mechanisms through which S1P regulates the endothelial barrier in these arteries remain to be demonstrated. In this Chapter, I provide further mechanistic insights into how S1P controls the endothelial barrier and vascular tone in uterine arteries. As described earlier, S1P stimulates NO production when it engages the $S1P_1$ or $S1P_3$ receptors and NO has opposing effects on endothelial permeability. However, it is unknown whether the S1P-mediated enhancement or disruption of endothelial barrier in mouse uterine arteries is effected by NO.

Like S1P, NO has opposing effects on endothelial barrier function, whereby it increases or decreases the barrier, depending on the endothelial model system, the species, or vascular bed examined [745-750]. NO regulates endothelial barrier function depending on its concentration, in which low concentrations enhance the barrier and high concentrations disrupt the barrier [718,749-753]. NO exhibits barrier-protective effects in cultured endothelial cells and *in vivo* [752,753] by signaling through the GC/cGMP pathway [754]. NO has also been shown to increase endothelial permeability in cannulated coronary venules [755,756] and different microvascular beds in the rat kidney, stomach, intestine, pancreas, mouse paw and cat intestines [745-750]. Even so, the mechanisms through which NO increases endothelial permeability

remain poorly understood. Evidence suggests that eNOS-derived NO promotes activation of Rho GTPases/Rho kinase destabilizing the VE-cadherin complex and AJ [749]. The induction of eNOS activity by agonists like LPS or VEGF increases endothelial permeability [755,757].

Endothelial $S1P_2$ receptor plays a protective role against acute barrier disruption during anaphylaxis by suppressing eNOS activation and NO generation through inhibition of Akt *in vivo* [426]. Although this study sheds light on the potential relationship between S1P and NO in the control of endothelial barrier, the primary focus of the study was on lung permeability and it is likely that responses in this vascular bed are different from that of the uterine vasculature used in my study. While such *in vivo* experiments provide information that is physiologically relevant, examining *ex vivo* arteries canulated to a pressure myograph system provides an opportunity to investigate the effects of drugs on such arteries in a more controlled system devoid of other blood components.

Considering the aforementioned background, I hypothesized that S1P regulates endothelial permeability and thus leakage of circulating vasoactive factors to the underlying VSMCs in uterine arteries through production of NO. Using a novel method established in our hands with the capability to simultaneously measure endothelial permeability, vascular tone and modulation by NO (using SNP or L-NAME), in this Chapter, I describe a novel link between S1P signaling, regulation of endothelial barrier function and the ensuing vascular tone in uterine arteries mediated by NO. I show that infusion of low concentrations of 0.1-1 μmol/L S1P could be generating NO that maintains the endothelial barrier which prevents leakage of S1P to the VSMCs. At 10 μmol/L, it is likely that the NO induced by S1P increased endothelial permeability facilitating leakage of S1P to the VSMCs increasing vascular tone, which again could be attenuated by the available NO. These findings suggest that, mechanistically S1P utilizes NO to control endothelial barrier and leakage of substances to VSMCs that affect vascular tone.

4.2 RESULTS

4.2.1 S1P-generated NO regulates endothelial permeability and vascular tone

I examined the effect of NO on the S1P-induced endothelial permeability and vascular tone after intraluminal infusion of 0.01-10 μmol/L S1P. Permeability was not changed in intact uterine arteries infused with 0.01-1 μmol/L S1P compared to the untreated control (Figure 4.1A).

However, infusion of 10 μmol/L S1P increased permeability compared to other treatments. In the presence of L-NAME in the bath, permeability increased after infusion of 1 μmol/L S1P and was further increased after 10 μmol/L S1P compared to L-NAME alone or compared to these S1P concentrations in the absence of L-NAME. Permeability was also increased overall when S1P was infused into arteries in the presence of L-NAME compared to that induced when S1P was infused without L-NAME (Figure 4.1A).

Simultaneous measurement of arterial diameters showed that infusion of 10 μmol/L S1P without L-NAME inside uterine arteries increased vascular tone compared to all lower S1P concentrations or the untreated control (Figure 4.1B). Vascular tone also increased in the presence of L-NAME after infusion of 0.1, 1 or 10 μmol/L S1P compared to L-NAME alone. Furthermore, infusion of 0.1, 1 or 10 μmol/L S1P with L-NAME induced significantly greater vascular tone compared to that induced by these concentrations in the absence of L-NAME. Overall, vascular tone in response to infused S1P was significantly greater with L-NAME (Figure 4.1B).

Cumulative addition of S1P to the bath (extraluminal) increased vascular tone in a dose-dependent manner; however, pretreatment with L-NAME had no effect (Figure 4.1C). It is important to note, however, that 1 μmol/L S1P added extraluminally increased vascular tone significantly while the same concentration infused intraluminally in the absence of L-NAME had no effect ($p<0.001$; Figure 4.1B, C).

4.2.2 Vascular tone induced after co-infusion of U46619 and S1P is regulated by NO

In Chapter 3 I showed the S1P-induced endothelial permeability promotes leakage of U46619 to VSMCs increasing vascular tone in uterine arteries [696]. In this Chapter I show that infusion of 5 nmol/L U46619, 1 μmol/L S1P or the two combined in the presence of L-NAME led to increased vascular tone compared to the corresponding treatments without L-NAME and compared to the L-NAME control. The dramatic increase in vascular tone after infusion of U46619 in the presence of L-NAME suggests that U46619 is producing NO in these arteries (Figure 4.2A). L-NAME treatment alone did not significantly increase vascular tone compared to the untreated control. Vascular tone was increased in response to extraluminal addition of S1P, U46619 or the two combined with or without L-NAME compared to their respective controls. L-NAME treatment alone increased basal tone (Figure 4.2B). Overall, for intraluminal and

extraluminal treatments, vascular tone was increased in the presence of L-NAME.

Similar to arteries from WT mice, arteries from eNOS KO mice showed no effect on permeability after infusion of 1 μmol/L S1P; however, 10 μmol/L S1P induced similar levels of endothelial permeability (Figure 4.3A). Infusion of 1 μmol/L S1P significantly increased vascular tone in arteries from eNOS KO compared to the untreated control or arteries from WT mice. In contrast, infused 10 μmol/L S1P significantly increased vascular tone similarly in arteries from eNOS KO and WT mice (Figure 4.3B). Infusion of 5 nmol/L U46619 or 1 μmol/L S1P into arteries from eNOS KO mice increased vascular tone compared to the control or arteries from WT mice. However, co-infusion of S1P and U46619 into arteries from eNOS KO mice increased vascular tone similarly to that of individual treatments or the co-infused treatment in arteries from WT mice. Overall, vascular tone was increased in arteries from eNOS KO mice compared to WT mice (Figure 4.3C).

4.2.3 SNP regulates endothelial barrier in isolated pressurized mouse uterine arteries

S1P-induced endothelial permeability was enhanced in uterine arteries pretreated with L-NAME, suggesting an important barrier role for NO. I next directly examined the effects of NO on the control of endothelial barrier by infusing the NO donor SNP inside uterine arteries in the presence or absence of L-NAME. Infusion of SNP at 10 or 20 μmol/L had no effect on dextran leakage. However, infusion of 50 or 100 μmol/L SNP in the presence of L-NAME resulted in increased dextran leakage compared to the untreated control or lower concentrations. Such induced dextran leakage was completely absent in arteries from eNOS KO mice (Figure 4.4A, B). To assess the barrier-enhancing effects of SNP, I co-infused SNP with permeability-inducing agents (thrombin, LPS, gB). 1 U/ml thrombin or 0.5 μg/ml gB alone, but not 50 ng/ml LPS, increased permeability compared to the untreated control. 20 μmol/L SNP significantly decreased permeability compared to the untreated control and also decreased thrombin-induced permeability. SNP had no effect on LPS or gB-induced permeability (Figure 4.5A, B, C).

4.2.4 SNP-induced vasodilation is enhanced in the presence of L-NAME in arteries from eNOS KO and WT mice

So far, I have shown that endogenously and S1P-induced NO can enhance the endothelial barrier, but also NO disrupts the barrier at high concentrations. Such NO-induced permeability

could promote leakage of S1P or U46619 to the VSMCs increasing vascular tone that is attenuated with the same S1P-induced NO. Next, SNP was used to mimic the vasodilatory effects of NO. In arteries pretreated with L-NAME and preconstricted with U46619, cumulative addition of SNP to the bath, significantly increased vasodilation compared to arteries not treated with L-NAME (Figure 4.6A). The increased vasodilation was not affected by location of L-NAME, in the bath or inside the artery. SNP-induced vasodilation in arteries from eNOS KO mice was not different from WT mice. Pretreatment of arteries from eNOS KO mice with L-NAME significantly enhanced SNP-induced vasodilation similar to that found in arteries from WT mice (Figure 4.6B). When SNP at 1 μmol/L was added to the bath with preconstricted denuded arteries, vasodilation (41.2±6.4%) was significantly increased ($p<0.01$) compared to arteries with intact endothelium (14.8±7.0%) or denuded arteries treated with L-NAME (16.2±3.0%). Vasodilation to methacholine (1 μmol/L) in denuded arteries in the presence (8.4±6.9%) or absence of L-NAME (-2.2±1.0%) was greatly attenuated compared to intact arteries. Previous experiments from our lab using the same type of arteries showed that methacholine at (1 μmol/L) induced a vasodilation of ~ 70% [572]. In the above experiments, the dilation effect of SNP (NO donor) was assessed by addition to the bath, since NO induces vasodilation by signaling in the VSMCs. In contrast, infusion of SNP (1 or 20 μmol/L) into preconstricted arteries induced vasodilation that was not different in the presence or absence of L-NAME (Figure 4.6C).

4.2.5 Co-infusion of SNP and U46619 increased endothelial permeability and vascular tone: permeability, but not vascular tone, was inhibited in arteries from eNOS KO mice

Since S1P promotes leakage of U46619 to the VSMCs to stimulate vasoconstriction and S1P stimulates production of NO, the following experiments were conducted to determine whether NO itself promotes leakage of U46619 in a similar manner (Figure 4.2A, C). Co-infusion of SNP with U46619 into arteries not treated with L-NAME significantly increased vascular tone compared to individual treatments. The U46619-induced vascular tone after infusion in the presence of L-NAME was significantly decreased when U46619 was co-infused with SNP (Figure 4.7A). On the other hand, co-addition of SNP with U46619 to the bath significantly reduced the vascular tone induced by U46619 alone and this was not affected by the presence of L-NAME (Figure 4.7B). In arteries from eNOS KO mice, infusion of U46619

increased vascular tone (Figure 4.8A) that was not different from that found in arteries from WT mice with L-NAME treatment (Figure 4.7A). The vascular tone induced by U46619 in arteries from eNOS KO mice was unaffected when U46619 was co-infused with SNP (Figure 4.8A) unlike the reduced vascular tone in co-infused L-NAME-treated arteries from WT mice (Figure 4.7A). The vascular tone induced after co-infusion of SNP with U46619 was not different in arteries from eNOS KO and WT mice (Figure 4.8A). Co-addition of SNP and U46619 to the bath of arteries from eNOS KO mice increased vascular tone, but the vascular tone was significantly lower compared to U46619 alone (Figure 4.8B). Infusion or addition of SNP alone had no effect on vascular tone. Co-infusion of SNP with U46619 induced endothelial permeability compared to individual treatments, but this was completely absent in arteries from eNOS KO mice (Figure 4.8C).

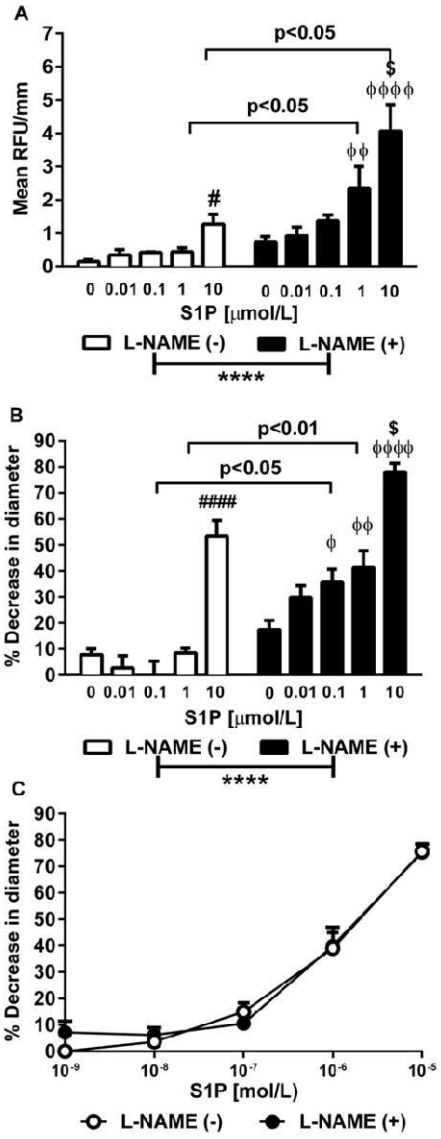
A
Mean RFU/mm
p<0.05
p<0.05
$
ϕϕϕϕ
ϕϕ
#
0 0.01 0.1 1 10 0 0.01 0.1 1 10
S1P [μmol/L]
L-NAME (-)
L-NAME (+)
****
B
% Decrease in diameter
p<0.01
p<0.05
$
ϕϕϕϕ
####
ϕ
ϕϕ
0 0.01 0.1 1 10 0 0.01 0.1 1 10
S1P [μmol/L]
L-NAME (-)
L-NAME (+)
****
C
% Decrease in diameter
10-9 10-8 10-7 10-6 10-5
S1P [mol/L]
L-NAME (-)
L-NAME (+)

Figure 4.1: Leakage of fluorescent dextran and vasoconstriction induced by S1P in the presence or absence of L-NAME. S1P was infused intraluminally into uterine arteries in the presence of 3 kDa fluorescent dextran conjugated to rhodamine green with or without 100 μmol/L L-NAME added to the bath. Leakage of dextran into the vessel bath was measured and normalized by artery length: RFU/mm = relative fluorescence units per millimetre of artery length **(A)**. To measure vasoconstriction, changes in artery diameter from the baseline were measured after intraluminal infusion **(B)** or extraluminal addition **(C)** of S1P with or without L-NAME added to the bath. Results were calculated as percent vasoconstriction of the initial arterial diameter at equilibration and presented as the mean ± SEM (n= 3 to 17). The results were analysed with a two-way ANOVA followed by the Tukey post-hoc test. * depicts an overall significant difference. # compared to no L-NAME controls. Φ compared to L-NAME only. $ compared to other treatments in L-NAME-treated vessels. For all figures, the number of symbols depicts increasing levels of significance: 1 = $p<0.05$, 2 = $p<0.01$, 3 = $p<0.001$ and 4 = $p<0.0001$.

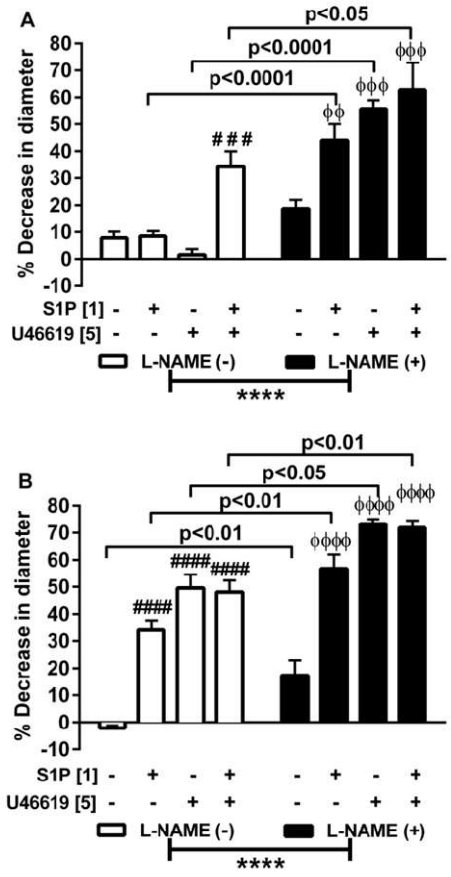

Figure 4.2: Vascular tone induced after co-infusion of S1P and U46619 into mouse uterine arteries. Uterine artery diameters from WT mice were measured after intraluminal infusion **(A)** or extraluminal addition **(B)** of 1 μmol/L S1P, 5 nmol/L U46619 or S1P combined with U46619 in the presence or absence of 100 μmol/L L-NAME added to the bath (n=3 to 16). The results were calculated and analyzed as for Figure 4.1. # compared to U46619 or S1P alone **(A)**. *overall, # compared to no L-NAME control, *Φ* compared to L-NAME control **(B)**. # compared to U46619 or S1P; $ compared to the control.

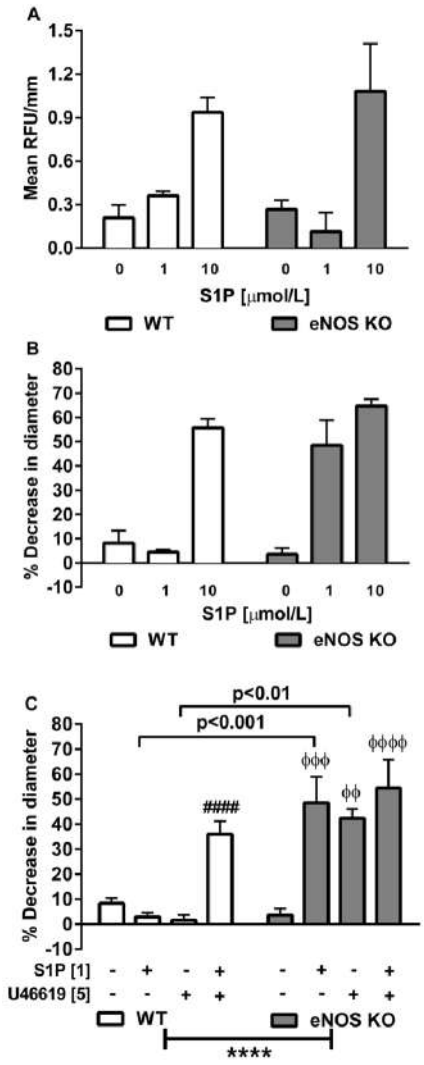

Figure 4.3: Dextran leakage and vascular tone stimulated after infusion of S1P alone, and vascular tone induced co-infusion of S1P with U46619 into uterine arteries from eNOS KO mice. 1 or 10 μmol/L S1P was infused in the presence of 3 kDa fluorescent dextran conjugated to rhodamine green, into uterine arteries isolated from eNOS KO or WT mice from which dextran leakage **(A)** and vascular tone were determined **(B).** 1 μmol/L S1P, 5 nmol/L U46619 or a combination of these, were also infused into arteries from eNOS KO or WT mice followed by measurement of vascular tone **(C)** as described in Figure 4.1. The results were calculated as percent vasoconstriction of the initial arterial diameter at equilibration and presented as the mean ± SEM (n= 2 to 3). The results were analysed using one-way ANOVA followed by the Tukey post-hoc test. * Overall, # compared to U46619 or S1P alone, *Φ* compared to no-treatment control. In **A** and **B**, some experiments have an "n" of 2, that is why statistics are not included.

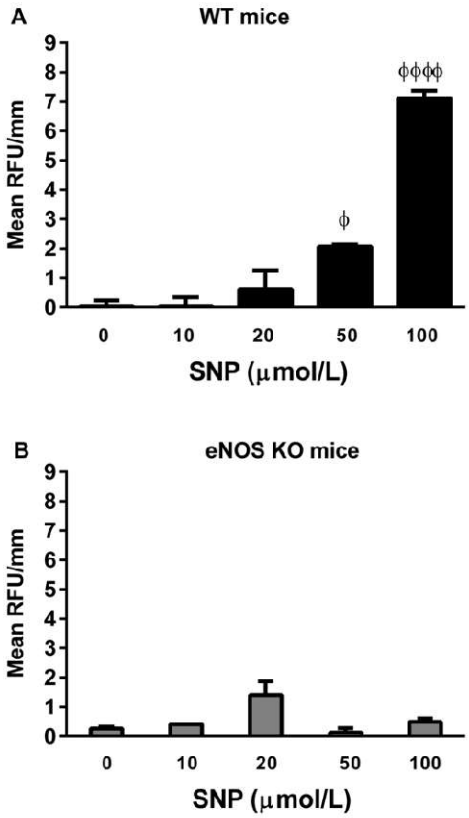

Figure 4.4: Effect of SNP on dextran leakage in eNOS KO mice and WT mice. SNP at different concentrations was infused in the presence of a 3kDa fluorescent dextran into uterine arteries pretreated with 100 μmol/L L-NAME in the bath, followed by determination of dextran leakage as in Figure 4.1. The mean ± SEM dextran leakage was analyzed by one-way ANOVA and the Tukey post-hoc test. *Φ* compared to the control or lower S1P concentrations.

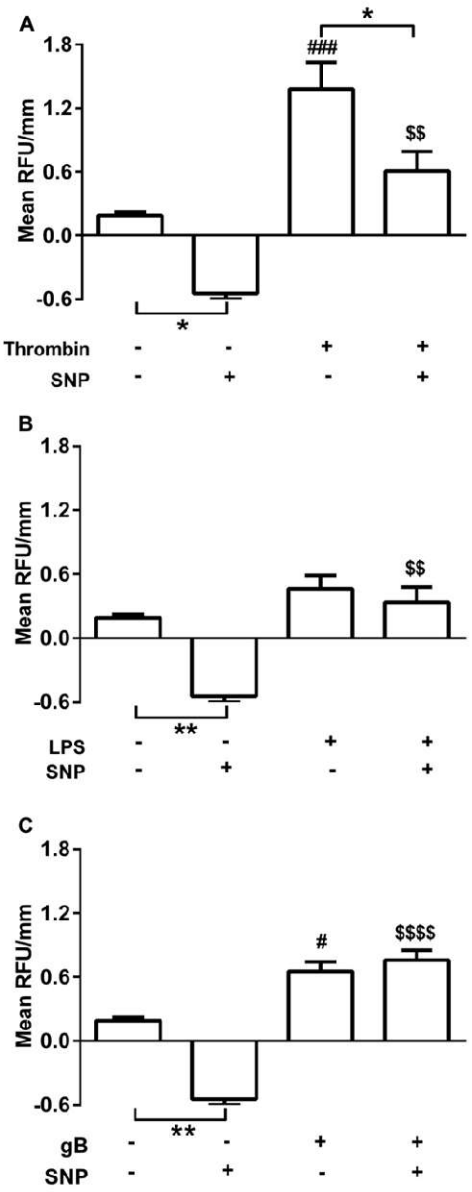

Figure 4.5: Dextran leakage following co-infusion of thrombin, LPS and gB with SNP. 20 µmol/L SNP was co-infused with 1 U/ml thrombin **(A)**, 50 ng/ml LPS **(B)** or 0.5 µg/ml gB **(C)** in the presence of 3 kDa fluorescent dextran conjugated to rhodamine green followed by measurement of dextran leakage as described in Figure 4.1. Results are as the mean ± SEM (n= 3 to 17). The results were analysed using one-way ANOVA followed by the Tukey post-hoc test. # = compared to the control; $ = compared to SNP.

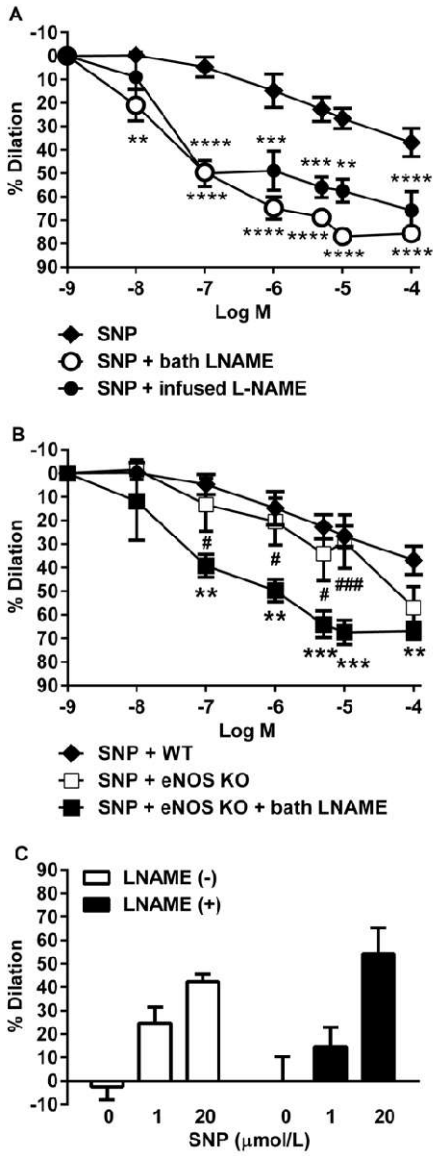
A
% Dilation
Log M
SNP
SNP + bath LNAME
SNP + infused L-NAME
B
% Dilation
Log M
SNP + WT
SNP + eNOS KO
SNP + eNOS KO + bath LNAME
C
LNAME (-)
LNAME (+)
% Dilation
SNP (μmol/L)

Figure 4.6: Induction of vasodilation by SNP in uterine arteries from eNOS KO and WT mice. In all experiments, arteries were preconstricted with U46619 before adding or infusing SNP and % vasodilation was measured from the preconstricted value. The arteries from eNOS KO mice required relatively lower concentrations of 1 ~ 5 nmol/L U46619 for preconstriction to approximately 50% compared to WT mice (5 ~ 10 nmol/L) **(A, B, C)**. Arteries pretreated with infused L-NAME or L-NAME added to the bath, were preconstricted and subjected to SNP added cumulatively to preconstricted arteries in the bath followed by determination of vasodilation **(A)**. SNP was also added cumulatively to the bath of arteries from eNOS KO mice in the presence or absence of L-NAME. The SNP-induced vasodilation was compared to arteries from WT mice with no L-NAME pretreatment **(B)**. 1 or 20 µmol/L SNP was infused into uterine arteries in the presence or absence of L-NAME followed by measurement of vasodilation **(C)**. The responses were normalized to maximal diameter obtained from the same arteries treated with 100 µmol/L papaverine and Ca^{2+} free solution. Results are presented as the mean ± SEM. The results were analysed using two-way ANOVA followed by the Tukey post-hoc test. * compared to SNP or SNP+WT, # SNP+WT compared to SNP+ eNOS KO. In **(C)**, SNP 0 µmol/L (for L-NAME) has n = 2, and therefore statistics were not conducted on this figure.

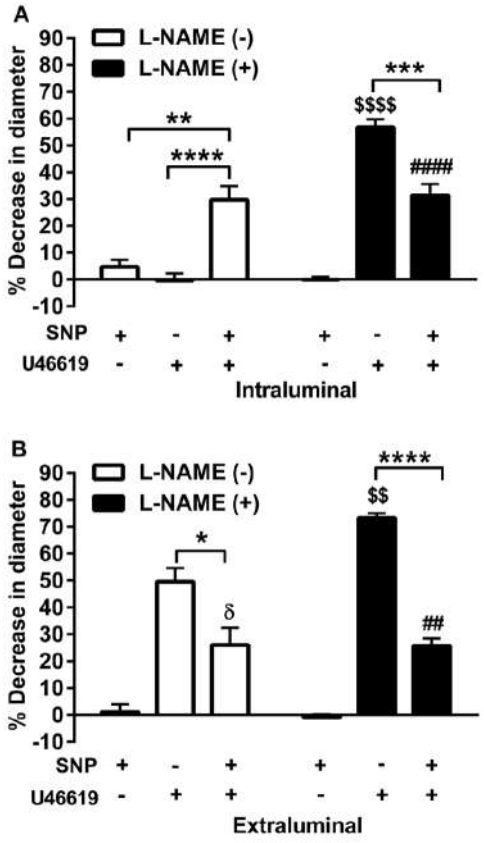

Figure 4.7: Vascular tone induced after co-infusion of SNP and U46619 into uterine arteries. 20 μmol/L SNP, 5 nmol/L U46619 or a combination were infused **(A)** or added to the bath **(B)** in arteries pretreated or not treated with L-NAME, followed by measurement of vascular tone as in Figure 4.1. Results are presented as the mean ± SEM. The results were analysed using two-way ANOVA followed by the Tukey post-hoc test. $ compared to U46619 (L-NAME (-)), # = compared to SNP (L-NAME (+)), δ = compared to SNP (L-NAME (-)).

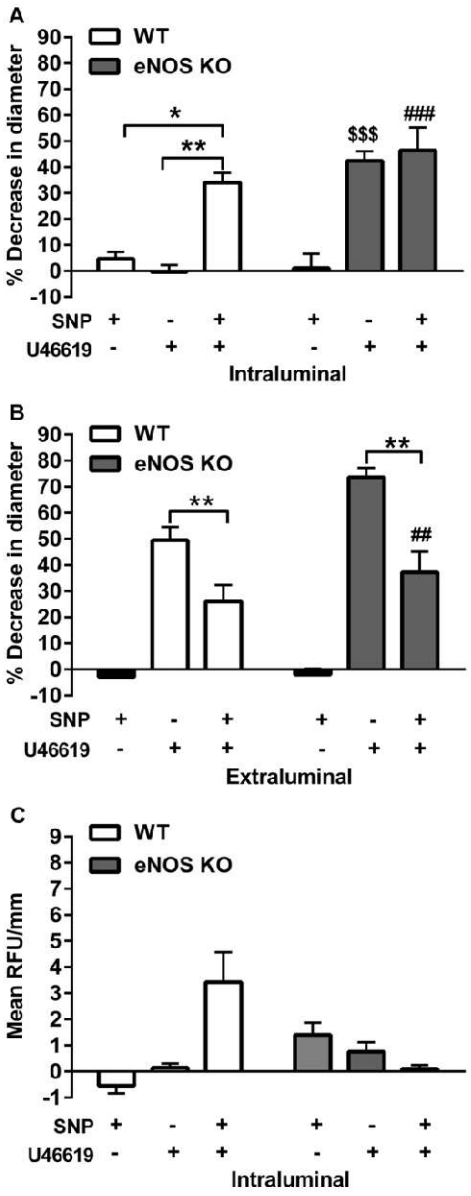

Figure 4.8: Dextran leakage and/or vascular tone induced after co-infusion of SNP and U46619 into uterine arteries from eNOS KO and WT mice. SNP, U46619 or a combination were infused or added to the bath of arteries from eNOS KO or WT mice. Vascular tone **(A, B)** and dextran leakage **(C)** were determined as in Figure 4.1. Results are presented as the mean ± SEM. The results were analysed using two-way ANOVA followed by the Tukey post-hoc test. $ compared to U46619 (WT), # compared to SNP (eNOS KO).

4.2.6 Discussion of results from Chapter 4

In Chapter 3, I showed that S1P at physiological concentrations induces endothelial permeability that permits access of circulating vasoconstrictors to the underlying VSMCs increasing vascular tone. Since NO has been shown to independently regulate permeability and S1P acting through $S1P_1$ or $S1P_3$ receptors leads to eNOS activation and NO production, I asked whether S1P utilizes NO in arteries used in this study to control the endothelial barrier. In this Chapter, I provide further mechanistic insights into how S1P regulates permeability in mouse uterine arteries likely mediated by NO (Figure 4.9). I show that infusion of S1P inside pressurized arteries at normal physiological concentrations (≤1 μmol/L) maintained the barrier function that was lost at 10 μmol/L S1P or when NOS was inhibited. The fact that S1P-induced endothelial permeability was profoundly increased when NOS was inhibited, suggests that at physiological concentrations S1P stimulates NO production that maintains the barrier. To emphasize the role of NO in maintaining the endothelial barrier, I further show that exogenously delivered NO (via SNP in the absence of L-NAME) inhibited endothelial permeability induced by thrombin, but not from LPS or gB.

The role of NO in promoting endothelial barrier function has been described in cell culture and in *in vivo* mouse models [752,753]. Predescu et al. showed that constitutively produced NO by eNOS is important in maintaining barrier integrity in venules. Using eNOS KO and L-NAME-treated mice they showed excessive postcapillary, muscle, diaphragm and cremaster venular leakage compared to controls. The authors concluded that maintenance of endothelial barrier function in a given vascular bed depends on the physiological concentration of NO [752]. While the S1P-induced endothelial permeability in arteries from eNOS KO and WT mice was not different in our study, it is likely that other NOS isoforms (iNOS and nNOS) present in the endothelium [758-760] may be important in the control of endothelial barrier by S1P.

In Chapter 3, I showed that S1P-induced permeability promotes leakage of co-infused U46619 to the VSMCs increasing vascular tone [696]. Here, I show that infusion or addition of 1 μmol/L S1P, 5 nmol/L U46619 or a combination to the bath induced vascular tone that was enhanced when NOS activity was inhibited. While S1P likely stimulated NO production, a novel finding is that infused U46619 also appears to generate NO in these arteries. The reduction in U46619-induced vascular tone in the presence of an NO donor in L-NAME-treated arteries and the significantly enhanced vascular tone induced by infused U46619 or S1P in arteries from

eNOS KO mice, highlight the role of NO in attenuating the vascular tone induced by S1P or U46619. Infusion of S1P or U46619 into arteries from eNOS KO mice increased vascular tone which was absent in WT mice, because sufficient NO is not generated from eNOS KO mice to overcome the induced vascular tone.

In the Chapter 3, I also showed that 10 μmol/L S1P increases endothelial permeability in cultured endothelial cells, and in intact pressurized uterine arteries [696]. In this Chapter, I now show that 10 μmol/L S1P-induced permeability in uterine arteries was enhanced following inhibition of NOS, suggesting that that the NO produced by 10 μmol/L S1P has opposing functions in the control of endothelial barrier. Given the increase in permeability induced by 10 μmol/L S1P, it is likely that the NO generated increases permeability by overcoming its own barrier-enhancing signals. This idea is supported by the results in which 20 μmol/L SNP decreased thrombin-induced permeability, but also SNP at high concentrations (50 or 100 μmol/L) increased endothelial permeability. The dual roles of NO in enhancing or weakening the endothelial barrier, has been described in cultured endothelial cells, veins and pulmonary arteries [745,749,750,752,753]. I found that SNP-induced permeability was eNOS-dependent, but these findings are not surprising as SNP (as low as 10 μmol/L) has been shown to activate eNOS [761]. This means that the mechanism through which high concentrations of SNP increases permeability involves both the NO produced by SNP and the endogenously generated NO. An additional reason why SNP-induced permeability was absent in arteries from eNOS KO mice could be because endothelial cells isolated from eNOS KO mice exhibit decreased active Rho, but increased active Rac [749]. These conditions can prevent endothelial barrier disruption including that mediated by SNP. In addition, phosphorylation of Ser1176 of eNOS determines its activity, and and a genetic mutation of this amino acid in knock-in mice, or a genetic deletion of eNOS significantly decreases VEGF or histamine-induced permeability, neutrophil recruitment and vascular function [749,762-765]. These findings support the argument that depending on the concentration, SNP increases endothelial permeability via eNOS activation, increasing the levels of NO available.

The role of NO in regulating the S1P-induced vascular tone is associated with its vasodilatory properties [572,766]. SNP (NO donor) was used to mimic the vasodilatory effects of NO, and I show that infusion or extraluminal addition of 20 μmol/L SNP to the bath of U46619-preconstricted arteries induced vasodilation. Interestingly however, extraluminally

induced vasodilation by SNP was enhanced in L-NAME-pretreated arteries. The idea of using L-NAME was to inhibit the endogenous NOS activity that could lead to NO production. However, L-NAME has been shown to increase the activity of NOS isoforms iNOS and eNOS in other systems like cultured astrocytes [767], bovine aortic endothelial cells [768], and *in vivo* in the heart, aorta and kidney of normal rats [769]. Further, LNA an active metabolite of L-NAME, also increases GC activity in mouse aortic homogenates [711]. SNP also independently activates GC and synergistically enhances GC activity in the presence of LNA, or YC-1, an allosteric activator (increases catalytic activity) of GC, leading to increased cGMP levels [711,770,771]. Collectively, these findings suggest that L-NAME pretreated arteries stimulated with SNP leads to increased production of NO through NOS, but also increased activation of downstream NO targets (GC) resulting in enhanced vasodilation. I also found that SNP-induced vasodilation was enhanced in L-NAME-pretreated arteries from eNOS KO mice compared to arteries from eNOS KO or WT mice treated with SNP only. It is possible that L-NAME activates iNOS as highlighted above [767], but studies by Brandes et al also showed increased GC activity in the aorta from eNOS KO compared WT mice, and SNP stimulation of aortic rings from eNOS KO mice increased cGMP levels compared to WT mice [711]. Thus far, my findings suggest that L-NAME enhances SNP activity through NO production or GC activity. However, the S1P-induced vascular tone in the presence of L-NAME is consistent with the inhibition of NOS, as vascular tone was dose-dependently increased. This means that the contribution of L-NAME in the activation of NOS in the arteries used in this study likely occurs in the presence of SNP, but not S1P. However, these differences between the way S1P and SNP induces vascular responses in the presence of L-NAME require further investigation.

Interestingly, SNP-induced vasodilation was enhanced in denuded arteries, suggesting that the endothelium is a source of endogenously produced vasoconstrictors that maintain resting tone. Similar findings have been reported in which SNP dose-dependently increased vasodilation in norepinephrine or 5-hydroxytryptamine preconstricted denuded mesenteric arteries from normotensive or hypertensive Wistar-Kyoto rats [772]. However, the normalization of SNP-induced vasodilation in denuded arteries in the presence of L-NAME suggests that the L-NAME-mediated activation of NOS described above is specific to those isoforms expressed on the endothelium (eNOS, iNOS, or nNOS) [759,760,766-769], and could not be activating GC on the VSMCs.

Another interesting finding was that co-infusion of SNP with U46619 led to an increase in endothelial permeability and vascular tone similar to that found with co-infusion of 1 μmol/L S1P with U46619. Since U46619 likely produces NO, the increase in endothelial permeability after co-infusion could be associated with increased levels of NO contributed by both SNP and U46619. This idea is supported by the results in which endothelial permeability was completely blocked when SNP and U46619 were co-infused into arteries from eNOS KO mice. This reduced permeability in arteries from eNOS KO mice did not affect the vascular tone induced by infused U46619 alone or when co-infused with SNP. Vascular tone induced by co-infusion or co-addition of SNP and U46619 to the bath was the same, but was significantly lower than U46619-induced vascular tone in L-NAME-treated arteries or when treatments were added to the bath in arteries from eNOS KO mice. It is therefore likely that induced endothelial permeability allows co-leakage of SNP/NO and U46619 to the VSMCs, where NO negatively controls U46619-induced vascular tone. It is noteworthy, that the SNP-mediated endothelial permeability was enhanced in the presence of U46619 and SNP, likely as a result of enhanced NO production. The fact that such induced permeability was completely absent in arteries from eNOS KO mice, suggests that signaling of both factors (SNP, U46619) through eNOS is the principal mechanism through which they increase permeability.

Thus far, I have demonstrated that S1P could be stimulating NO generation in arteries used in this study, which at low concentrations maintains endothelial barrier, but at high S1P concentrations disrupts the barrier predominantly through eNOS activation (Figure 4.9). Enhancement of endothelial barrier by NO could be preventing endothelial leakage of S1P, but the induced permeability facilitates leakage of S1P into the VSMCs increasing vascular tone.

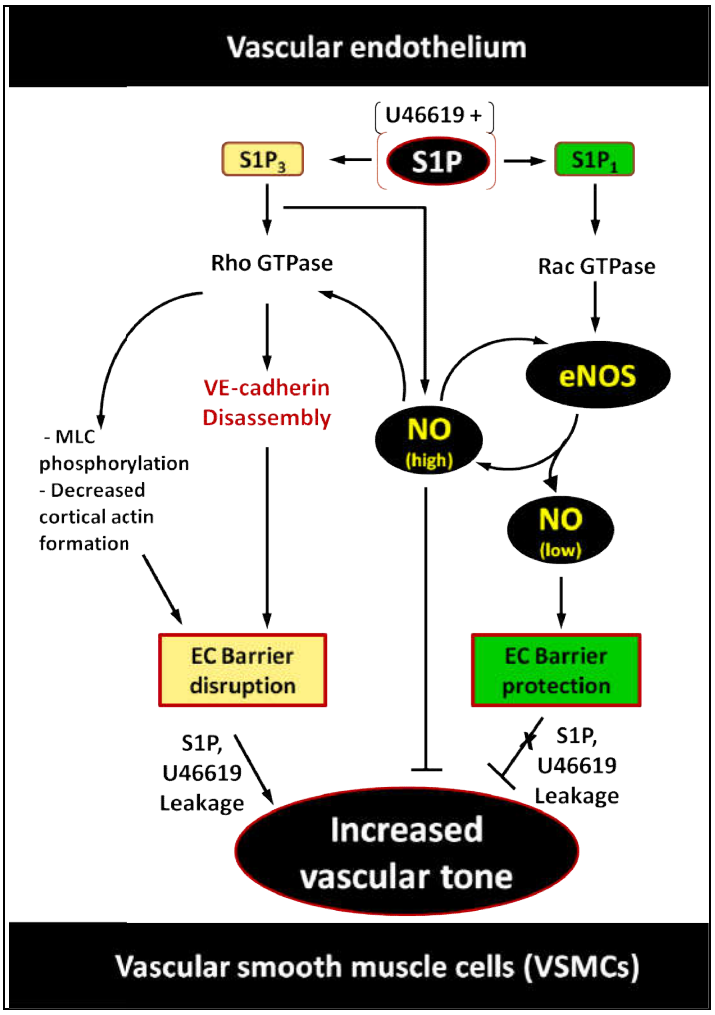

Figure 4.9: Proposed mechanism for S1P-mediated regulation of endothelial permeability and vascular tone via NO production in murine uterine arteries. Low S1P concentrations (≤1 μmol/L) activate endothelial $S1P_1$ receptor promoting a Rac-dependent activation of eNOS that generates nitric oxide (NO_{low}), which enhances endothelial cell (EC) barrier. Increased endothelial cell barrier indirectly prevents an increase in vascular tone by restraining the leakage of S1P and/or other circulating vasoconstrictors such as thromboxane A_2 (U46619) to the vascular smooth muscle cells (VSMCs). In contrast, S1P at high concentrations (≥5 μmol/L) can activate both $S1P_1$ and $S1P_3$ receptors, which leads to increased levels of $NO_{(high)}$. NO promotes a positive feedback program that replenishes NO via eNOS activation, but also stimulates a Rho-dependent disruption of VE-cadherin, and a decrease in cortical actin formation. These events cause increased endothelial permeability, permitting leakage of S1P and/or U46619 to VSMCs increasing vascular tone, which is also regulated by the vasodilatory actions of NO. However, the NO likely generated by S1P also

negatively regulates the vascular tone induced by S1P or any other circulating vasoconstrictors (U46619) that leaks to the VSMCs stimulating vascular tone (Figure 4.9). These findings indicate that pathological levels of NO can cause endothelial permeability in uterine arteries leading to increased vascular tone. Also under conditions of endothelial dysfunction where the levels of NO are greatly diminished, decreased barrier protection by NO can lead to increased endothelial permeability and vascular tone. Supplementation of arginine or anti-oxidants can help alleviate the vascular-related disorders associated with NO deficiency or overabundance, respectively.

CHAPTER 5

THROMBOXANE A_2 INCREASES ENDOTHELIAL PERMEABILITY AND VASCULAR TONE THROUGH A NOVEL PATHWAY STIMULATED BY SPHINGOSINE 1-PHOSPHATE

All results in this Chapter were generated by myself, and have not yet been submitted for publication.

5.1 Introduction

In Chapter 4, I showed that S1P utilizes NO to regulate endothelial barrier in uterine arteries, but I also showed that U46619, which likely generates NO, potentiates SNP-induced endothelial permeability in the same type of arteries. Both of these mechanisms signal through eNOS-dependent mechanisms to control endothelial barrier. These findings indicate that S1P and U46619 stimulate common downstream mechanisms. These results, together with those that I presented in Chapter 3, in figure 3-6B, which showed that U46619-induced vascular tone was completely blocked in mesenteric arteries from $S1P_3$ KO male mice [696], strongly suggested that the TXA_2 mimetic (U46619) could be signaling through the S1P/$S1P_3$ receptor-dependent pathways to increase endothelial permeability and vascular tone. Therefore this Chapter focused on determining whether the U46619-induced increase in endothelial permeability and/or vascular tone is mediated through the S1P pathway.

TXA_2, a lipid mediator, exerts its activity through two TP receptors, TPα and TPβ [525]. Activation of TP receptors contribute to various biological events including cell migration, angiogenesis, proliferation, platelet aggregation and vascular tone [8,573,694,773-775]. However, high levels of TXA_2 are implicated in the pathophysiology of different disease conditions like atherosclerosis, myocardial infarction, hypertension, vascular leakage and inflammatory lung disease [775,776]. Among other cells, VSMCs and endothelial cells express TP receptors [525,536,537,777,778], but the specific roles of these receptors in endothelial cells is poorly understood. There is a single reference in the literature that suggests a relationship exists between TXA_2 and S1P, that is, that TXA_2 activates SK-1 increasing the release of S1P from isolated and cultured human platelets [486]. However, this relationship has not been explored any further and has not been investigated in vascular cells

S1P controls the endothelial barrier as demonstrated in cell culture models, intact venules, *in vivo* [107,386,779] and in arteries as shown in my first two data Chapters [696]. Like S1P, TXA_2 (U46619 at 1 or 100 μmol/L as used in separate publications) increases endothelial permeability *in vitro* in cultured endothelial cells by causing disruption of endothelial VE-cadherin and PECAM-1, but also mice injected with 30 μmol/L U46619 showed leakage under the skin [8,694,780]. However, these are the only reports in the literature regarding the role of TXA_2 in the control of endothelial barrier.

While there appears to exist a link between the TXA_2 and S1P-mediated responses even in intact microvessels as shown in previous Chapters, it is unknown whether TXA_2-induced effects are S1P-mediated. In this Chapter, I sought to determine whether TXA_2-induced endothelial permeability and vascular tone are mediated through the S1P pathway. I hypothesized that TXA_2 will activate SK-1 increasing intracellular S1P, that will be exported extracellularly to stimulate an increase in endothelial permeability and/or vascular tone via the $S1P_3$ receptors. By targeting multiple steps within the S1P pathway, I demonstrate a novel mechanism through which TXA_2 increases endothelial permeability and vascular tone in uterine arteries. This also occurs in mesenteric arteries from male and female mice.

5.2 RESULTS

5.2.1 TXA_2 increases endothelial permeability and vascular tone when infused into uterine arteries

I found that infusion of 20 nmol/L U46619 inside uterine arteries significantly increased dextran leakage (Figure 5.1A) and vascular tone (Figure 5.1B) compared to control or lower U46619 concentrations. U46619 also increased vascular tone dose-dependently when added to the arterial bath (Figure 5.1C). These results indicate that U46619 at high concentration increased endothelial permeability permitting leakage of U46619 to the underlying VSMCs increasing vascular tone.

5.2.2 $S1P_1$ receptor agonist inhibits TXA_2-induced endothelial permeability and vascular tone in uterine arteries

To test the above hypothesis that U46619-induced permeability promotes its own leakage increasing vascular tone, I determined whether inhibiting the increase in endothelial permeability

using an $S1P_1$ agonist (known to decrease endothelial permeability) will prevent the vascular tone induced by infused U46619. When U46619 was co-infused with SEW2871, dextran leakage (Figure 5.2A) and vascular tone (Figure 5.2B) was significantly reduced. I next determined whether the reduction in vascular tone was because of vasodilatory effects mediated by co-infused SEW2871 on the VSMCs. The vascular tone induced by infusion of U46619 in the presence of SEW2871 in the bath (directly affecting the VSMCs) was unaffected (Figure 5.2C). These results suggest that SEW2871 has no vasodilatory effects on the VSMCs, but the reduction of vascular tone when co-infused with U46619 is more likely because SEW2871 enhanced the endothelial barrier.

5.2.3 TXA_2-induced vascular tone, but not TXA_2-induced endothelial permeability, is mediated through the TP receptors

I next sought to confirm whether the TXA_2-induced permeability and vascular tone are TP-receptor mediated. Unexpectedly, infusion of 20 nmol/L U46619 with addition of SQ29548 (a TP receptor antagonist) in the bath, or co-infusion with SQ29548 led to similar levels of dextran leakage that were dramatically greater compared to that observed with infusion or addition of SQ29548 or U46619 alone (Figure 5.3A). Considering that infused U46619 increased endothelial permeability, I determined whether the leakage of U46619 from the arterial lumen was reaching the underlying VSMCs by assessing the impact on vascular tone. When SQ29548 was added to the arterial bath before infusing U46619 inside the artery, the vascular tone was completely blocked. In contrast, when I co-infused U46619 with SQ29548 vascular tone was partially reduced compared to infused U46619 alone. The vascular tone resulting from co-infusion was still significantly greater compared to infused SQ29548 alone or the vascular tone induced by infused U46619 against SQ29548 in the bath (Figure 5.3B). These results suggest that U46619 increases endothelial permeability in arteries used in this study in a TP receptor-independent manner [781], possibly the mechanism may be nonreceptor mediated such as interfering with cell membrane integrity (e.g. membrane permeability) disrupting cell-cell junctions.

5.2.4 SK-1 mediates TXA_2-induced endothelial permeability and vascular tone in uterine arteries

In Figure 3- 5B, I showed that the vascular tone generated by U46619 was inhibited in mesenteric arteries from $S1P_3$ KO male mice, suggesting that this response involves activation of the $S1P_3$ receptor [696,779]. I therefore investigated the connection between the TXA_2 and S1P-mediated pathways. Co-infusion of U46619 with SK-II (SK-1 inhibitor) inside arteries completely inhibited dextran leakage (Figure 5.4A) and vascular tone (Figure 5.4B). However, the vascular tone induced by infused U46619 in the presence of SK-II in the bath was unaffected (Figure 5.4C). These findings suggest that endothelial permeability and vascular tone induced by infused U46619 is generated via SK-1 activity.

5.2.5 ABC-type transporters promote TXA_2-mediated increase in endothelial permeability and vascular tone in uterine arteries

Since TXA_2 increases endothelial permeability and vascular tone through SK-1, it is likely that this leads to intracellular generation of S1P and export. I next determined the transporters that could be involved in exporting S1P out of cells in uterine arteries infused with U46619. The ABCC1 and ABCG2 transporters are involved in S1P export in cancer cells, and rat myometrial smooth muscle cells [369,703]. U46619-induced dextran leakage remained unchanged in the presence of co-infused MK571 (ABCC1 inhibitor), but was completely blocked in the presence of FTC (ABCG2 inhibitor) (Figure 5.5A). However, the U46619-induced vascular tone was completely blocked in the presence of co-infused MK571 or FTC (Figure 5.5B). The vascular tone induced by infused U46619 against MK571 in the bath was significantly decreased, but not against FTC in the bath (Figure 5.5C). These results suggest that U46619-induced endothelial permeability involves the export of S1P through ABCG2 transporters likely in the endothelial cells, but vascular tone is induced by export of S1P from ABCC1 in the VSMCs.

5.2.6 $S1P_1$/$S1P_3$ receptors promote the TXA_2-mediated increase in endothelial permeability and vascular tone in uterine arteries

In Chapter 3, I showed that the S1P-induced endothelial permeability and vascular tone in uterine arteries occur via the $S1P_3$ receptor (Figs 3-3A,B and 3-5A, B) [696,779], I therefore

evaluated the role of this receptor (these experiments also simultaneously assessed the role of $S1P_1$ because VPC23019 is a dual antagonist) on the vascular tone induced by infused U46619. I show that the dextran leakage (Figure 5.6A) and vascular tone (Figure 5.6B) induced by infused U46619 in the presence of co-infused VPC23019 were significantly decreased. Further, vascular tone was also significantly decreased when U46619 was infused against VPC23019 in the bath (Figure 5.6C).

5.2.7 Increased vascular tone increases endothelial permeability of intact isolated pressurized uterine arteries

Since I demonstrated that 20 nmol/L U46619 increased endothelial permeability that promoted leakage of U46619 to the VSMCs increasing vascular tone, I next determined whether vasoconstriction could be part of the mechanism through which U46619 increased endothelial permeability. When U46619 was added to the bath of arteries pretreated extraluminally with SQ29548 there was complete reduction in dextran leakage and vascular tone. However, when arteries were pretreated intraluminally with SQ29548 before adding U46619, there were no significant differences in dextran leakage but there was complete reversal of vascular tone (Figure 5.7A, B). Given that vascular tone induced after infusion of U46619 inside arteries was completely blocked by co-infused SK-II, but not when SK-II was added to the bath against infused U46619 (Figure 5.4B, C), I used SK-II to block activation of sphingosine kinase on the endothelium before addition of U46619 to the bath. There was a trend in the reduction in permeability (not significantly different) and vascular tone was significantly reduced compared to U46619 alone (Figure 5.7C, D). Since, MK571 had no effect on U46619-induced endothelial permeability, but when added to the bath MK571 significantly decreased the vascular tone induced by infused U46619 (Figure 5.5C), I used MK571 to determine whether the S1P production in the VSMCs contributes to endothelial permeability induced by U46619 added to the bath. When U46619 was added to arteries pretreated with MK571 in the bath, dextran leakage and vascular tone were completely blocked (Figure 5.7E, F). These results suggest that U46619-induced vascular tone in the bath in part involves activation of endothelial SK-1, and S1P production in the VSMCs that stimulates an increase in endothelial permeability.

5.2.8 TXA_2-induced vascular tone in mesenteric arteries from male or female mice stimulates the activation of SK-1 or ABC-type transporters

In mesenteric arteries from male mice, the vascular tone induced by U46619 added cumulatively to the bath was completely blocked by SK-II or MK571, but partially by FTC (Figure 5.8A, B, C). In mesenteric arteries from female mice, U46619-induced vascular tone was completely blocked in the presence of SK-II, but partly in the presence of FTC or MK571. However, the U46619-induced vascular tone was completely blocked when FTC and MK571 were added in combination to the bath of mesenteric arteries from female mice (Figure 5.8D, E, F).

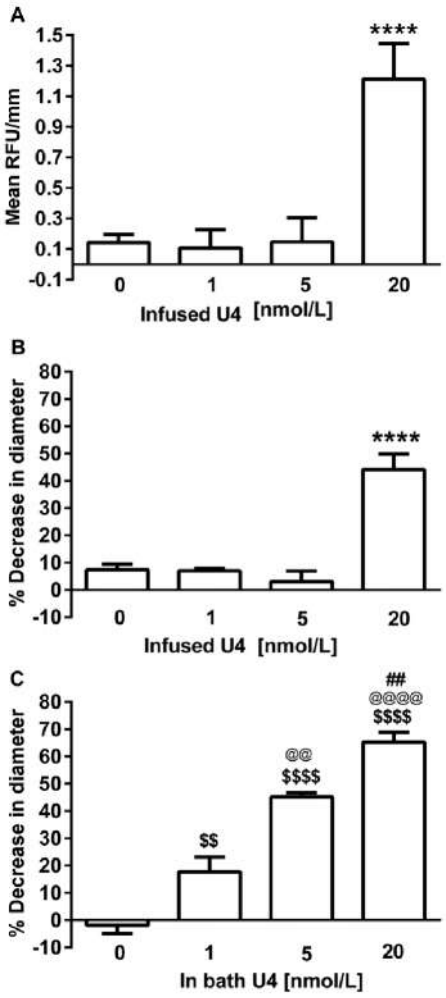

Figure 5.1: Infusion of U46619 at high concentration increased dextran leakage and vascular tone in uterine arteries. 20 nmol/L U46619 was infused inside uterine arteries in the presence of a 3kDa fluorescent dextran, followed by determination of dextran leakage **(A)** and vascular tone **(B)**. U46619 concentrations were also added individually to different arteries in the bath (directly to VSMCs) followed by measurement of vascular tone **(C)**. Dextran leakage to the bath corrected by arterial length was used as a measure of endothelial permeability, whereas vascular tone (% decrease in diameter) was determined as a change in vascular diameter from the baseline diameter after equilibration of arteries. The mean ± SEM percent decrease in diameter (n=3 to 13) were analyzed by one-way ANOVA and the Tukey post-hoc test. $ = compared to control; @ = compared to 1 nmol/L U46619; # = compared to 5 nmol/L U46619. For all figures, the number of symbols depicts increasing levels of significance: 1 = $p<0.05$, 2 = $p<0.01$, 3 = $p<0.001$ and 4 = $p<0.0001$.

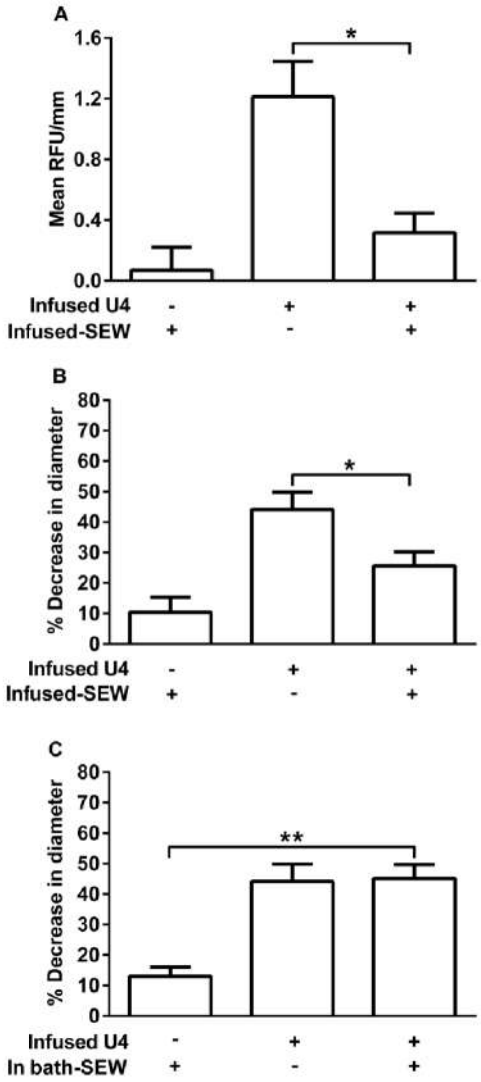

Figure 5.2: $S1P_1$ agonist prevented U46619-induced endothelial permeability and vascular tone after infusion in uterine arteries. 20 nmol/L U46619 was co-infused with 0.1 µmol/L SEW2871 ($S1P_1$ agonist) **(A, B)**, or SEW2871 was added to the bath against U46619 infused inside uterine arteries **(C)** followed by determination of dextran leakage **(A)** and vascular tone **(B, C)** as described in Figure 5.1. The results are presented as mean ± SEM (n=3 to 5) and were analyzed by one-way ANOVA and the Tukey post-hoc test.

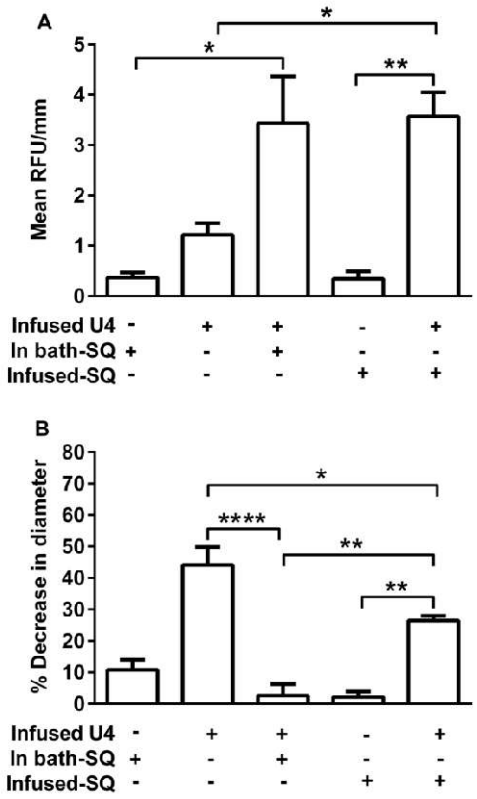

Figure 5.3: Enhanced dextran leakage and reduction in vascular tone in the presence of TP receptor antagonist following infusion of U46619 into uterine arteries. 20 nmol/L U46619 was infused inside uterine arteries against SQ29548 in the bath or in the presence of co-infused SQ29548 followed by determination of dextran leakage **(A)** or vascular tone **(B)** as in Figure 5.1. The results are presented as mean ± SEM (n=3 to 13) and were analyzed by one-way ANOVA and the Tukey post-hoc test.

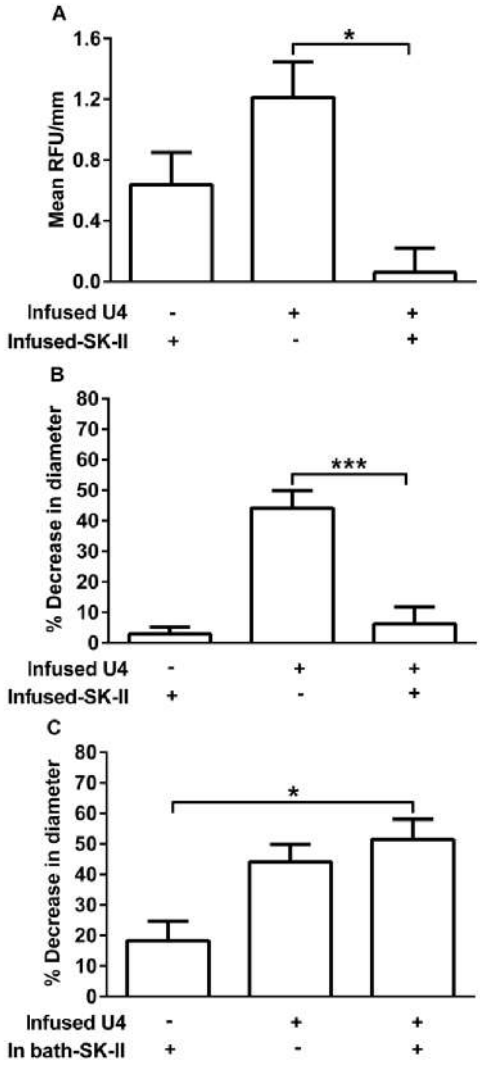

Figure 5.4: SK-1 mediated U46619-induced endothelial permeability and vascular tone in uterine arteries. 20 nmol/L U46619 was co-infused with 1 μmol/L SK-II **(A, B)** or infused in the presence of SK-II in the bath **(C)**, followed by determination of dextran leakage **(A)** and vascular tone **(B, C)** as in Figure 5.1. The results are presented as mean ± SEM (n=3 to 9) and were analyzed by one-way ANOVA and the Tukey post-hoc test.

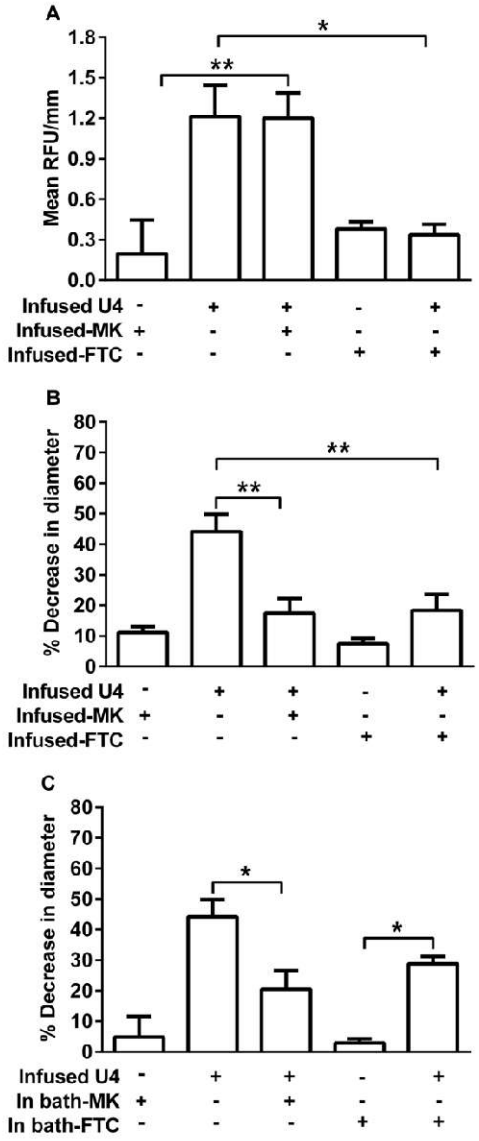

Figure 5.5: The ABC transporters mediate U46619-induced endothelial permeability or vascular tone in uterine arteries. 20 nmol/L U46619 was co-infused with 10 µmol/L MK571 or 1 µmol/L FTC **(A, B)**, or infused while MK571 or FTC **(C)** were added to the bath, followed by measurement of dextran leakage **(A)** or vascular tone **(B, C)** as in Figure 5.1. The results are presented as mean ± SEM (n=4 to 6) and were analyzed by one-way ANOVA and the Tukey post-hoc test.

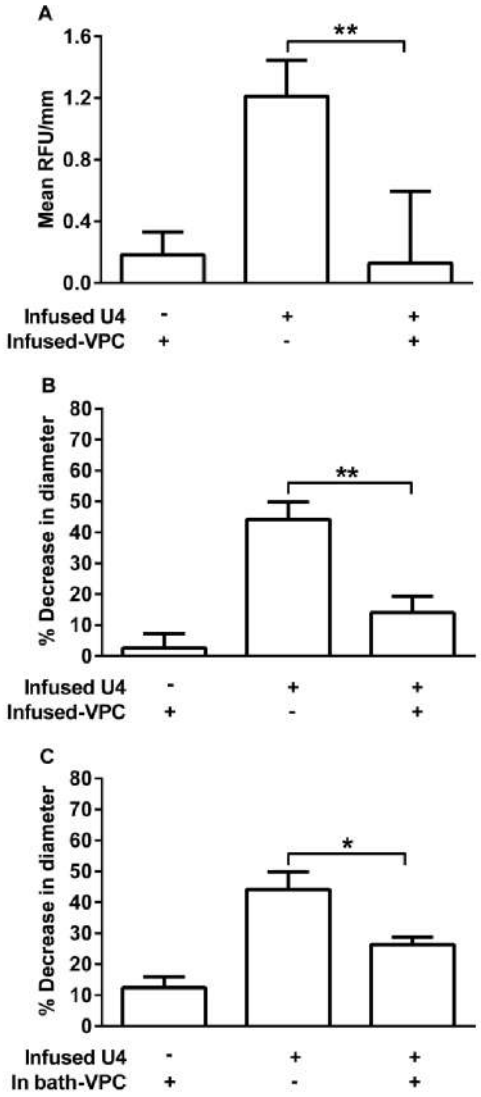

Figure 5.6: $S1P_1$/$S1P_3$ receptors promote U46619-induced endothelial permeability and vascular tone in uterine arteries. 20 nmol/L U46619 was co-infused with 1 μmol/L VPC23019, or infused while VPC23019 was added to the bath followed by determination of dextran leakage **(A)** and vascular tone **(B, C)** as in Figure 5.1. The results are presented as mean ± SEM (n=3 to 5) and were analyzed by one-way ANOVA and the Tukey post-hoc test.

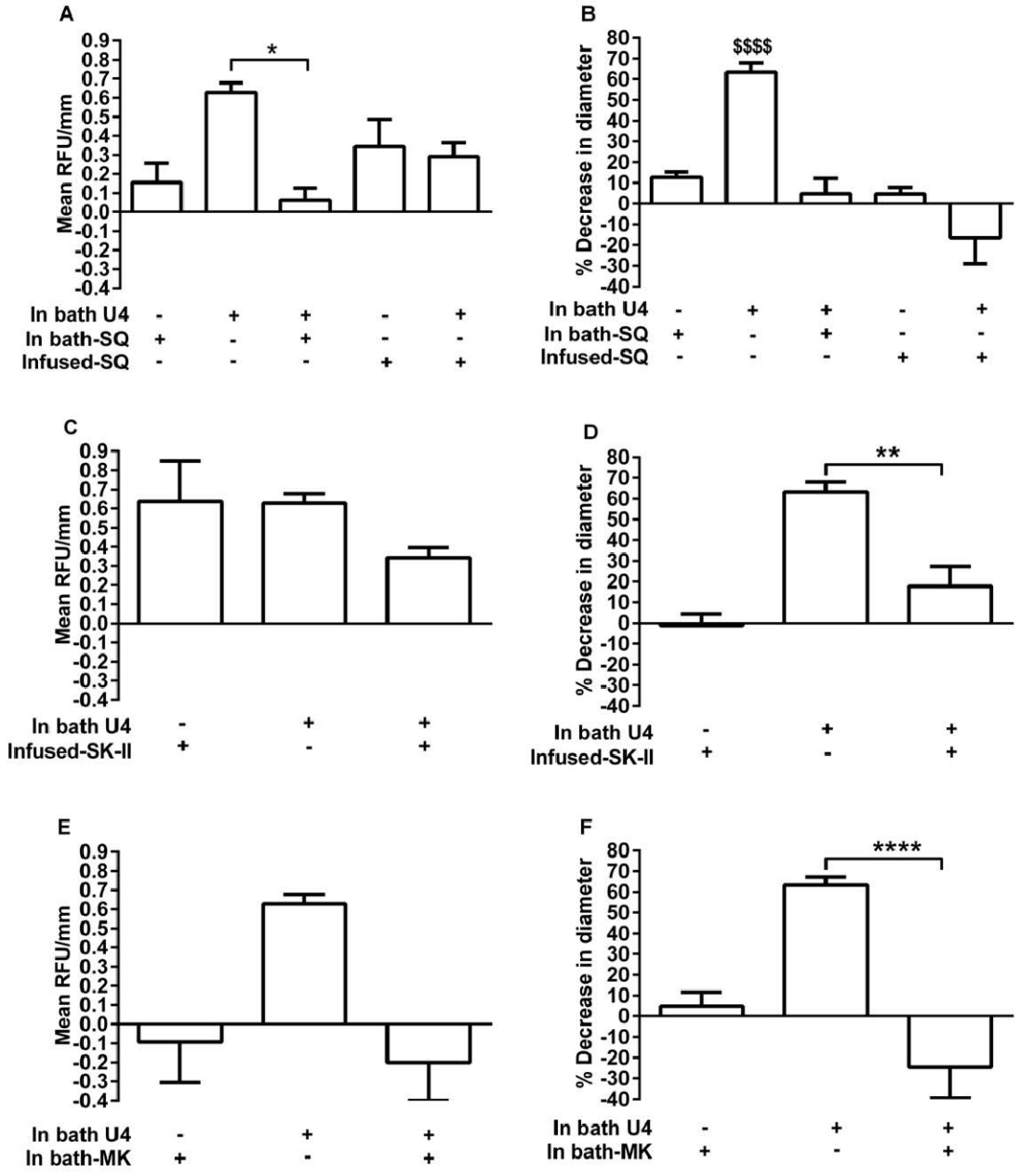

Figure 5.7: U46619-induced dextran leakage and/or vascular tone after extraluminal stimulation of arteries is mediated via TP receptors, ABCC1 and endothelial SK-1. Arteries were pretreated in the bath or infused with 10 µmol/L SQ29548 **(A, B)**, inside arteries with 1 µmol/L SK-II **(B, C)** or 10 µmol/L MK571 in the bath **(E, F)** before adding 20 nmol/L U46619 to the bath followed by determination of dextran leakage **(A, C, E)** and vascular tone **(B, D, F)** as in Figure 5.1. The results are presented as mean ± SEM (n=3 to 6) and were analyzed by one-way ANOVA and the Tukey post-hoc test.

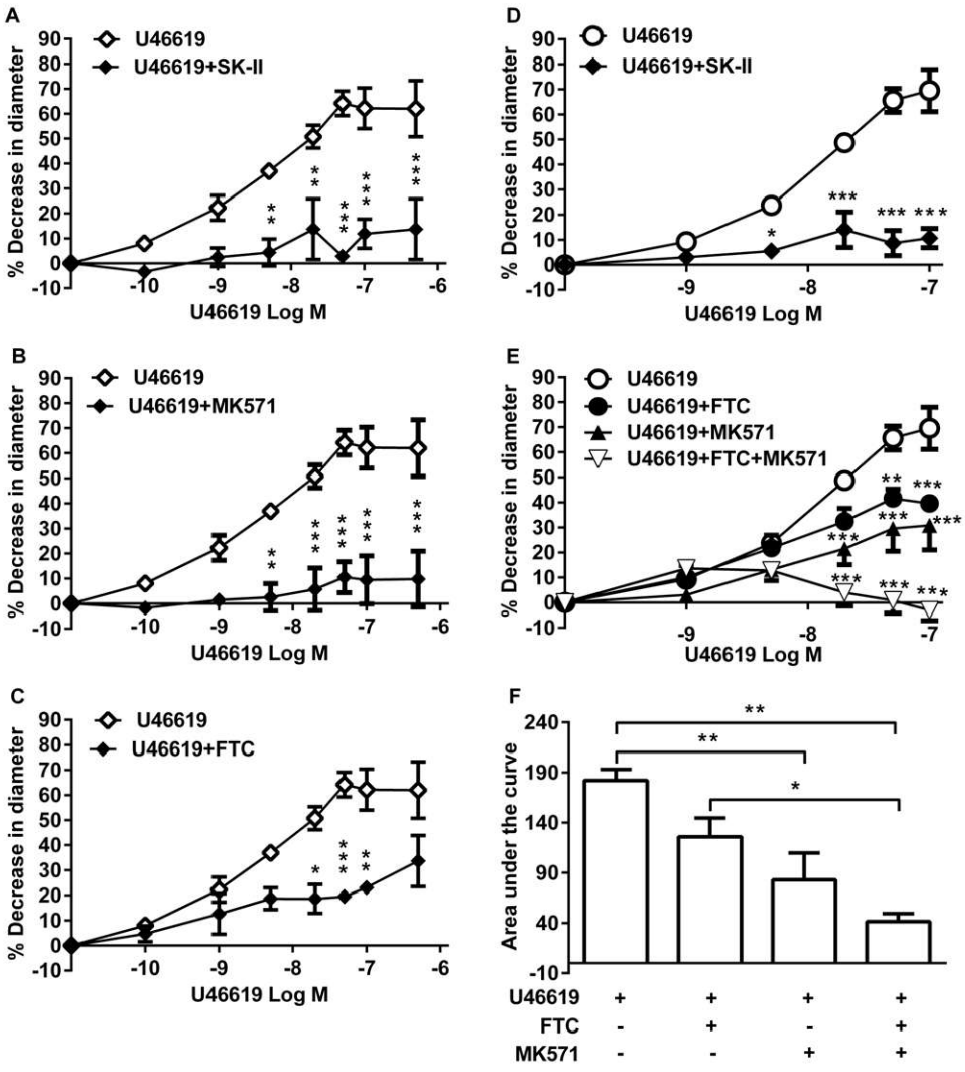

Figure 5.8: Vascular tone induced by U46619 is mediated by SK-1 or ABCC1 and ABCG2 transporters in mesenteric arteries from male and female mice. U46619 (0.1-500 nmol/L) was added cumulatively in the presence of 1 µmol/L SK-II, 10 µmol/L MK571 or 1 µmol/L FTC (**A, B, C**) to the bath containing mesenteric arteries isolated from male **(A, B, C)** or female (**D, E, F**) mice followed by determination of vascular tone. The area under the curve was determined from each of the curves induced by U46619 in the presence or absence of MK571, FTC or a combination (MK571+FTC) in arteries from female mice and the results presented as an average **(F)**. All results are presented as mean ± SEM (n=4 to 6) and were analyzed by Two-way ANOVA and the Tukey post-hoc test.

5.2.9 Discussion of results from Chapter 5

In Chapter 4, I showed that the S1P-induced endothelial barrier control was mediated by NO, through activation of eNOS. Although 5 nmol/L U46619 or 20 μmol/L SNP did not individually increase permeability, endothelial permeability was strongly increased when they were co-infused which was mediated via eNOS. Such increase in endothelial permeability was likely contributed by NO generated by both U46619 and SNP. These findings together with the results from Chapter 3, whereby the U46619-induced vascular tone was completely inhibited in mesenteric arteries from male $S1P_3$ KO mice, suggested that U46619 and S1P are closely related in their signaling mechanisms and that U46619 could be signaling through an S1P-mediated pathway. The normal human circulating levels of TXA_2 (U46619) is ~ [2.4 - 4.9 pM] [714], but these levels rise in pathological conditions like severe atherosclerosis to ~ [1.4 nM] [714]. TXA_2 is also increased to ~ [1.6 nM] in mice infected with *Trypanosoma cruzi* [715], or to ~ [24 nM] in rabbits experiencing renal resistance [716]. In this Chapter, I show novel findings whereby pathological levels of TXA_2 increases endothelial permeability and vascular tone in an S1P-dependent manner. I also show that TXA_2-induced permeability promoted endothelial leakage of TXA_2/S1P to the VSMCs increasing vascular tone.

S1P signals through the $S1P_1$ receptor enhance the endothelial barrier [782] so one of the best ways to increase the barrier is through specific activation of the $S1P_1$ receptor. The increase in U46619-induced permeability and vascular tone were prevented by co-infusion of an $S1P_1$ agonist (SEW2871). This experiment was done to show that TXA_2 itself was indeed increasing permeability in these arteries, which could be blocked by increasing the endothelial barrier. The fact that the vascular tone induced by infused U46619 against SEW2871 added to the bath was unchanged, suggests that the reduced vascular tone from U46619 co-infused with SEW2871, was because SEW2871 inhibited permeability and not because of a direct vasodilatory effect of SEW2871 on the VSMCs. SEW2871 or S1P itself has also been used to reverse vascular leakage upon anaphylactic, platelet activating factor (PAF) or histamine challenge. They have also been shown to improve mice survival under conditions where mice were engineered to deliberately lack plasma S1P [782]. These reports and the results in this Chapter are consistent with those in Chapter 3 where I showed that SEW2871 also inhibited thrombin-induced permeability in arteries used this study.

Previous studies showed that antagonizing TP receptors with SQ29548 decreased U46619-induced endothelial permeability in cell culture [8,694]. However, in my studies, SQ29548 promoted a 3-fold increase in endothelial permeability after co-infusion of U46619. These differences could be because of the vascular bed differences, but also as pointed out by the authors in these studies, the cell-based model used [694] does not necessarily reflect the vascular dynamics of intact microvessels as used in my study. In addition, both TPα and TPβ receptors couple downstream to adenylate cyclase with opposing effects: TPα activates while TPβ inhibits its activity [528]. Even so, the only receptor in the mouse is TPα [778]. Endothelial barrier is potently enhanced by cAMP generation [783-786], which means that antagonizing the TPα receptors, should disrupt the endogenous adenylate cyclase/cyclic AMP axis important for endothelial barrier control. It is likely that blocking TP receptors could predispose the endothelium to TXA_2-induced permeability through a yet to be identified mechanism. It is likely that the mechanism for mediating permeability after blocking TP receptors is non-receptor mediated, as previously proposed in pulmonary vessels in a study using a prostanoid-derivative. The lungs of patients with severe pulmonary hypertension were shown to have decreased expression of the prostacyclin receptor, but prostacyclin greatly improved the clinical outcome of patients with severe pulmonary hypertension. These effects of prostacyclin were mainly attributed to be non–receptor-mediated [781]; [787]TP receptor deficiency is also associated with exaggerated vasodilation [788] which may account in part for the increased permeability. Histamine-induced NO-dependent vasodilation has been shown to increase endothelial permeability [789].

In contrast, I show that the vascular tone induced after infusion of U46619 was completely blocked by antagonizing the TP receptors on the VSMCs in the bath, suggesting that U46619 was reaching VSMCs from the endothelium. In Chapter 3, I showed a similar type of leakage of 5 nmol/L U46619 mediated by S1P-induced permeability whereby the vascular tone generated following leakage of U46619 was completely blocked when SQ29548 was added to the bath against co-infused S1P and U46619. In Chapter 3, U46619 at the lower concentration used was unable to leak on its own, whereas in this Chapter, 20 nmol/L U46619-induced permeability promotes its own leakage. The partial reduction in vascular tone when SQ29548 and U46619 were co-infused could be due to co-leakage of both factors to the VSMCs, where SQ29548 can inhibit U46619-induced vascular tone.

An important novel finding in this Chapter is the demonstration that TXA_2 is signaling through an S1P-mediated pathway to generate endothelial permeability and vascular tone. I first show that TXA_2–induced endothelial permeability is dependent on SK-1. TXA_2 has been shown to stimulate the release of S1P from cultured human platelets in a TP-specific manner [486]. The authors isolated unactivated platelets from healthy volunteers, pretreated them with radiolabelled sphingosine, and then stimulated with U46619 for 10 minutes. The fact that radiolabelled S1P was released from radiolabelled sphingosine, suggests downstream activation of SK upon TP engagement [486]. Previous reports also show that thrombin or histamine induce endothelial permeability following SK-1 activation [790-792]. These findings collectively indicate that TXA_2-mediated activation of SK-1 can increase permeability.

The ATP binding cassette transporters, ABCG2 or ABCC1 are known to export S1P out of cells [369,486,793]. In this Chapter, I show that U46619-induced permeability is mediated via ABCG2 but not ABCC1 transporters. Although, both transporters promote induction of vascular tone by infused U46619, only ABCC1 has an additional direct role on the VSMCs to mediate U46619-induced tone. The fact that U46619-induced permeability was unaffected by blocking ABCC1, indicates that the reduction in vascular tone from co-infusion is likely due to co-leakage of the inhibitor, in which leaked MK571 inhibits U46619-induced vascular tone in the VSMCs. In contrast, inhibiting U46619-induced permeability by blocking ABCG2 decreased the vascular tone induced after infusion of U46619, suggesting that the enhanced endothelial barrier decreased the leakage of U46619/S1P to the VSMCs.

Antagonizing $S1P_1/S1P_3$ decreased endothelial permeability induced by co-infused 20 nmol/L U46619, which could limit endothelial leakage of infused U46619 to the VSMCs, and this could account for the decreased vascular tone. These results are supported by those from Chapter 3 where I showed that S1P-induced endothelial permeability and vascular tone occur through $S1P_3$. Interestingly, the vascular tone induced after infusion of U46619 was decreased by antagonizing $S1P_1/S1P_3$ on the VSMCs. Like ABCC1, $S1P_1/S1P_3$ appears to have an additional role on the VSMCs where it mediates S1P-induced vascular tone following infusion of U46619.

On the other hand, extraluminal stimulation of arteries by U46619 promoted VSMCs TP-specific induction of not only vascular tone, but also endothelial permeability. These results suggest that TXA_2 either evokes a stretch mechanism in the VSMCs or directly stimulates endothelial TP receptors to increase permeability. These ideas are supported by the finding that

U46619-induced vascular tone generated from the bath is partly mediated by ABCC1 on the VSMCs. Since ABCC1 had no effect on the endothelial permeability induced by infused U46619, these results suggest that U46619 in the bath stimulates S1P generation in the VSMCs likely through SK-2 that increases endothelial permeability. However, the exact mechanisms through which TXA_2 increases endothelial permeability via S1P produced in the VSMCs needs to be explored further. In mesenteric arteries from male or female mice, the U46619–induced vascular tone by direct stimulation of VSMCs in the bath is dependent on SK-1, ABCC1 or ABCG2. Again, these results support the argument for the dependence of TXA_2 on the S1P pathway to increase vascular tone.

In summary, I have shown that infusion of TXA_2 at pathological concentrations inside mouse uterine arteries increased endothelial permeability and vascular tone mediated through the S1P pathway. The increase in endothelial permeability and vascular tone were completely reversed by an $S1P_1$ agonist. Part of the mechanism leading to increased endothelial permeability involves increased vascular tone. The dependence of TXA_2 on the S1P pathway to increase vascular tone operates in the two vascular beds tested in this Chapter, including uterine and mesenteric arteries. These results provide novel insights into the potential mechanisms through which TXA_2 controls normal vascular tone, or contributes to disease conditions like vascular leakage, atherosclerosis or hypertension. Targeting the S1P pathway, particularly the $S1P_1$ or $S1P_3$ receptors could be therapeutically useful in reducing endothelial permeability and vascular tone mediated by TXA_2.

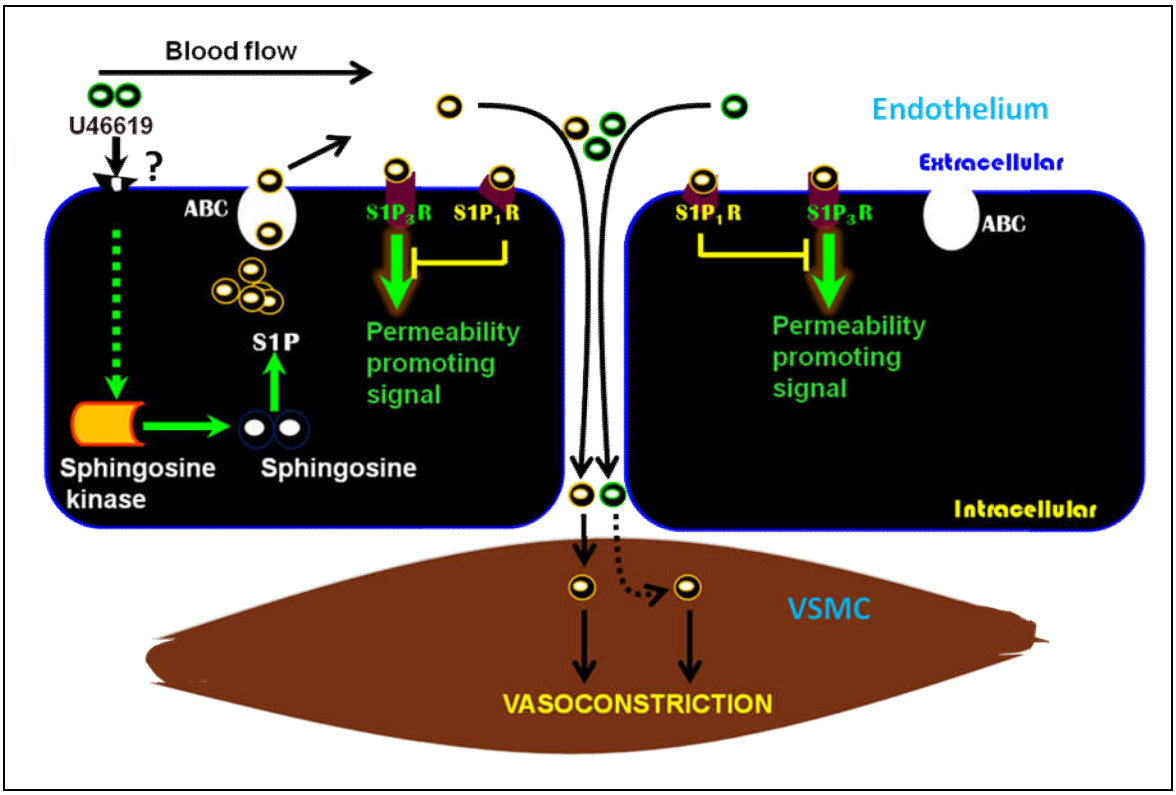

Figure 5.9: Induction of endothelial permeability and vascular tone by U46619 via an S1P pathway. Infusion of U46619 leads to sphingosine kinase-dependent generation of S1P, which is exported extracellularly leading to $S1P_3$ receptor-dependent increase in endothelial permeability and vascular tone in mouse uterine arteries. Direct stimulation of the $S1P_1$ receptor (using agonist SEW2871) prevented U46619-induced endothelial permeability and vascular tone indicating that the increase in endothelial permeability promoted leakage of U46619 and any S1P generated to the underlying vascular smooth muscle cells (VSMCs) increasing vascular tone. However, the U46619-induced permeability when infused inside the arteries was enhanced in the presence of TP receptor antagonist, indicating that the activation of the S1P pathway by U46619 at the level of the endothelium occurs through a yet to be identified mechanism

CHAPTER 6

CYTOMEGALOVIRUS INFECTION SUBVERTS THE DEPENDENCE OF THROMBOXANE A_2 ON THE DOWNSTREAM SIGNALING BY SPHINGOSINE 1-PHOSPHATE IN INDUCING VASCULAR TONE.

All results in this Chapter were generated by myself, and have not yet been submitted for publication.

6.1 Introduction

In Chapter 5, I showed that TXA_2 signals through the S1P pathway to increase endothelial permeability and the resulting vascular tone after infusion into uterine arteries. I also showed that direct stimulation of VSMCs by TXA_2 increased vascular tone by S1P-dependent mechanisms in mesenteric arteries from male and female mice. As well, the Hemmings laboratory has previously shown that inhibiting COX-1 and COX-2 activity or TP receptors, promotes methacholine-induced vasodilation in mesenteric arteries isolated from CMV-infected female mice [574]. These findings imply a significant contribution of prostanoids to the vascular changes that occur during CMV infection. In this Chapter, I focused on studying the impact of CMV infection on the vascular tone induced by TXA_2, one of the products of the COX pathway.

CMV a double-stranded DNA virus establishes a life-long latent infection, with potential for reactivation [613,794,795]. Healthy individuals infected with CMV generally do not suffer from overt clinical disease except for those who occasionally experience symptoms of mononucleosis. However, CMV infection contributes to vascular dysfunction [572-574,677] (please also refer section 1.9.1.4), cardiovascular-related disorders like atherosclerosis [796], fatal myocarditis [797], rheumatoid arthritis, cancer [798], morbidity and mortality in the elderly [799]. CMV infection potentiates the pathogenesis of these conditions partly through increased levels of various cytokines [670] including the activation of the COX pathway [680]. COX-1 is constitutively expressed in nearly all tissues, but COX-2 is normally only induced by a pathologic stimulus. Studies in human fibroblasts and retinal pigment epithelial cells show a relationship between CMV replication and COX-2 expression. In these studies COX-2 and prostaglandin E were increased in CMV-infected cells, and the activation of these pathways were shown to be important for CMV replication [511,680].

CMV infection also increases the expression and activity of SK-1 [679], one of the enzymes that generates S1P. Thus, CMV infection appears to impact the pathways that lead to TXA_2 [511,680] and S1P production [679]. Evidence also shows that TXA_2 increases the release of S1P from cultured human platelets through ABC transporters indicating the existence of a relationship between TXA_2 and S1P [486]. In chapter 5 I also showed that TXA_2 increases endothelial permeability and/or vascular tone via the S1P pathway.

In this Chapter, I sought to determine the impact of an *in vivo* CMV infection on the vascular tone induced by TXA_2 and the downstream S1P signaling pathway by directly stimulating the VSMCs of mouse uterine arteries. I hypothesized that CMV infection will increase SK-1 expression in VSMCs, and TXA_2 will in turn activate SK-1 increasing intracellular S1P which will be exported extracellularly to bind to $S1P_2$ or $S1P_3$ receptors increasing vascular tone. While I show that CMV infection enhances the vascular tone induced independently by either S1P or TXA_2 mediated partly through the Rho kinase pathway, CMV infection reduces the dependence of TXA_2 on the downstream S1P signaling pathway opening up alternative pathway(s) for induction of vascular tone.

6.2 RESULTS

6.2.1 CMV infection enhances U46619 or S1P-induced vascular tone in part through Rho kinase

I show that vascular tone is significantly increased in response to cumulative addition of U46619 (Fig 1A) or S1P (Fig 1B) to the bath containing arteries from CMV-infected mice compared to arteries from uninfected mice. Y27632 has no effect on U46619-induced vascular tone, but significantly decreased the vascular tone induced by S1P in arteries from uninfected mice. Y27632 also promoted a significant decrease in U46619 or S1P-induced vascular tone in arteries from CMV-infected mice (Fig 1C, D). These results suggest that S1P and U46619 share a common signaling pathway leading to Rho kinase activation in arteries isolated from CMV-infected mice. Considering this information, and given that I showed in Chapter 5 that U46619 increases endothelial permeability and vascular tone via the S1P pathway, I therefore investigated the relationship between these two bioactive lipids under conditions of CMV infection. In particular, the impact of CMV infection on the vascular tone induced by U46619 through the S1P pathway.

6.2.2 CMV infection blunts the dependence of U46619-induced vascular tone on SK-1 activation or ABC transporters

In Chapter 5, I showed that when U46619 was infused inside uterine arteries or added extraluminally to mesenteric arteries from male and female mice, the increased vascular tone was dependent on SK-1 activity (Figures 5-4B, 5-7D, 5-8D). In this Chapter I investigated whether U46619 acts via the S1P pathway to increase vascular tone upon direct stimulation of the VSMCs on intact uterine arteries, and whether this is altered by an *in vivo* CMV infection. Unlike the increased vascular tone induced by cumulative addition of U46619 to the bath (Figure 6.1A), addition of a single concentration of 20 nmol/L U46619 induced vascular tone that was not different in uterine arteries from CMV-infected compared to uninfected mice (Figure 6.2A). In arteries from uninfected mice, vascular tone induced by addition of 20 nmol/L U46619 to the bath was significantly decreased in the presence of a SK-1 inhibitor (SK-II), but this inhibition was completely absent in arteries from CMV-infected mice. Interestingly, the U46619-induced vascular tone was also completely blocked in the presence of ABC462940 (SK-2 inhibitor) in arteries from both uninfected and CMV infected mice (Figure 6.2B).

Activation of SK will lead to increased production of intracellular S1P that can be exported out of the cell to engage its receptors (S1P can also engage intracellular targets that were not under consideration in this study). I therefore determined the transporters that could be involved in exporting S1P out of the VSMCs, and the potential impact of CMV infection. In Chapter 5 I showed that MK571 inhibited the vascular tone induced following infusion of U46619 inside uterine arteries, but FTC did not. In contrast, FTC, MK571 or their combination strongly inhibited the vascular tone induced by U46619 added to the bath containing mesenteric arteries from male and female mice. In this Chapter, FTC partly (Figure 6.3A), and MK571 fully (Figure 6.3B) inhibited the U46619-induced vascular tone when added to the bath containing uterine arteries from uninfected mice. Results using arteries from CMV-infected mice showed a partial blunting of vascular tone in the presence of FTC that did not differ from that shown in arteries from uninfected mice; however, the complete inhibition by MK571 in arteries from uninfected mice was blunted in those from CMV-infected mice (Figure 6.3A, B). Surprisingly, while the vascular tone induced by U46619 in the presence of the combined FTC and MK571 treatment in uterine arteries from uninfected mice was halved, there was no effect on vascular tone by co-treatment of arteries from CMV-infected mice (Figure 6.3C). Further, the U46619-

induced vascular tone in arteries from CMV-infected mice in the presence of SK-II, MK571 or MK571 + FTC but not FTC alone, was significantly greater compared to the U46619-induced responses in the presence of these inhibitors in arteries from uninfected mice (Figure 6.2, and 6.3).

6.2.3 U46619-induced vascular tone inhibited by VPC23019 or JTE013 is reversed by L-NAME

In Chapter 3 (Figures 3-3A, B, 3-5A, B) and in Chapter 5 (Figures 5-6A, B, C) I showed that infusion of S1P or U46619, respectively, inside uterine arteries increased endothelial permeability and vascular tone through the $S1P_3$ or $S1P_1/S1P_3$ receptors, respectively. In this Chapter, I evaluated the S1P receptor dependence of U46619-induced vascular tone through direct effects on the VSMCs of intact arteries from CMV-infected and uninfected mice. U46619 increased vascular tone that was significantly reduced similarly by pretreatment with VPC23019 or JTE013 in arteries from uninfected mice (Figure 6.4A). Considering that VPC23019 has been shown to exhibit agonist activities [698] that could include the possibility of producing NO, and JTE013 is reported to inhibit constriction induced by several vasoconstrictors [800], I investigated whether these inhibitors could produce NO, a vasodilating factor, to promote their antagonistic activities on vascular tone. When I used VPC23019 or JTE013 in the presence of L-NAME, there was partial restoration of U46619-induced vascular tone in arteries from uninfected mice. L-NAME in combination with either receptor inhibitor partially restored the U46619-induced vascular tone in arteries from uninfected mice (Figure 6.4A). While VPC23019 or JTE013 also inhibited the vascular tone induced by U46619 in arteries from CMV-infected mice, the level of inhibition by VPC23019 was lower than that found in arteries from uninfected mice or that mediated by JTE013 (Figure 6.4B). Unexpectedly, the U46619-induced vascular tone in uterine arteries from CMV-infected mice was significantly decreased in the presence of L-NAME. L-NAME partly restored U46619-induced vascular tone in the presence of JTE013, but not VPC23019, in arteries from CMV-infected mice compared to those from uninfected mice (Figure 6.4B).

Similar to the results from U46619, S1P-induced vascular tone in arteries from uninfected mice was completely blocked by both VPC23019 and JTE013. However, while JTE013 continued to completely block S1P-induced vascular tone in arteries from CMV-infected

mice, VPC23019 had no effect on this response in arteries from CMV-infected mice (Figure 6.5A, B).

6.2.4 U46619 increased vascular tone via the $S1P_3$ receptor in arteries from uninfected mice, but through the $S1P_1$ receptor in CMV-infected mice

Since VPC23019 antagonizes both $S1P_1$ and $S1P_3$ receptors, JTE013 inhibits the $S1P_2$ receptors and both inhibitors appear to have additional effects on NO, I used $S1P_3$-/- or $S1P_2$-/- mice to further investigate the importance of these receptors in mediating U46619-induced vascular tone in arteries from CMV-infected mice. The U46619-induced vascular tone was significantly decreased in arteries from uninfected $S1P_3$-/- (Figure 6.6A), but remained unaffected in arteries from uninfected $S1P_2$-/- mice (Figure 6.6B) compared to arteries from their respective littermate WT controls. In contrast, U46619-induced vascular tone was unchanged in arteries from CMV-infected $S1P_3$-/- mice compared to arteries from littermate WT controls (Figure 6.6C) while the results in arteries from infected $S1P_2$-/- mice were similar to uninfected mice. In the presence of VPC23019, U46619-induced vascular tone was significantly decreased in arteries from CMV-infected $S1P_3$-/- mice compared to CMV-infected $S1P_3$+/+ or $S1P_3$-/- mice in the absence of VPC23019 (Figure 6.6C). Pretreatment of arteries from CMV-infected $S1P_2$-/- mice with W146 ($S1P_1$ receptor antagonist) also led to a significant reduction in U46619-induced vascular tone compared to untreated arteries from CMV-infected $S1P_2$+/+ or $S1P_2$-/- mice (Figure 6.6D).

6.2.5 S1P-induced vascular tone is dependent on the $S1P_1$ and $S1P_3$ receptors in arteries from CMV-infected mice

In Chapter 3 as cited above, I showed that S1P-induced vascular tone in uterine arteries from uninfected mice is dependent on the $S1P_3$ receptor [696], similar to the U46619-induced response in arteries from uninfected mice. Here I show that the S1P-induced vascular tone in arteries from CMV-infected $S1P_3$-/- mice was completely blocked, but was partially restored in the presence of VPC23019 (Figure 6.7A). The vascular tone induced by S1P in arteries from CMV-infected $S1P_2$+/+ or $S1P_2$-/- mice was similar. However, vascular tone was significantly reduced by pretreatment with W146 of arteries from CMV-infected $S1P_2$-/- mice compared to untreated arteries from CMV-infected $S1P_2$+/+ or $S1P_2$-/- mice (Figure 6.7B).

6.2.6 Phenylephrine-induced vascular tone inhibited by VPC23019 or JTE013 antagonism is relieved by pretreatment with L-NAME

S1P or U46619 share certain downstream pathways with phenylephrine including the $G\alpha_q$ or $G\alpha_{12/13}$ coupled to their receptors. I therefore asked whether phenylephrine-induced vascular tone could also occur via the S1P pathway and whether this was affected by CMV infection. VPC23019 or JTE013 significantly decreased or completely blocked, respectively, the vascular tone induced by phenylephrine in arteries from uninfected mice (Figure 6.8A, B) to a greater extent than in arteries from CMV-infected mice (Figure 6.8C, D). The phenylephrine-induced vascular tone in the combined presence of VPC23019 and L-NAME was unchanged, but was partially restored in the presence of JTE013 and L-NAME. Overall, L-NAME alone had no effect on phenylephrine-induced vascular tone (Figure 6.8C, D). Given that the phenylephrine-induced vascular tone was partially or completely restored in the presence of JTE013 and L-NAME or VPC23019 and L-NAME, respectively, plus the properties cited above (Figure 6.4) regarding JTE013 and VPC23019, I next evaluated whether VPC23019 or JTE013 on their own have vasodilation properties. When evaluated on preconstricted (by U46619) uterine arteries from uninfected mice, VCP23019 up to 50 μmol/L or JTE013 up to10 μmol/L had no dilatory effects. However at >10 μmol/L, JTE013 exhibited strong dilation responses which reached 80% at 100 μmol/L (Figure 6.8E). These results suggest that the concentrations used in my studies, 1 μmol/L VPC23019 or 10 μmol/L JTE013 likely do not generate dilation responses on their own.

6.2.7 The dependence of phenylephrine on the $S1P_3$ receptor to induce vascular tone in uterine arteries is lost in arteries from CMV-infected $S1P_3$ KO mice

Phenylephrine-mediated induction of vascular tone was completely blocked in uterine arteries from uninfected $S1P_3$-/- mice, but this inhibition was lost in arteries from CMV-infected $S1P_3$-/- mice (Figure 6.9A, B). There was no change in phenylephrine-induced vascular tone in arteries from uninfected or CMV-infected $S1P_2$-/- mice compared to arteries from their littermate WT controls (Figure 9C, D).

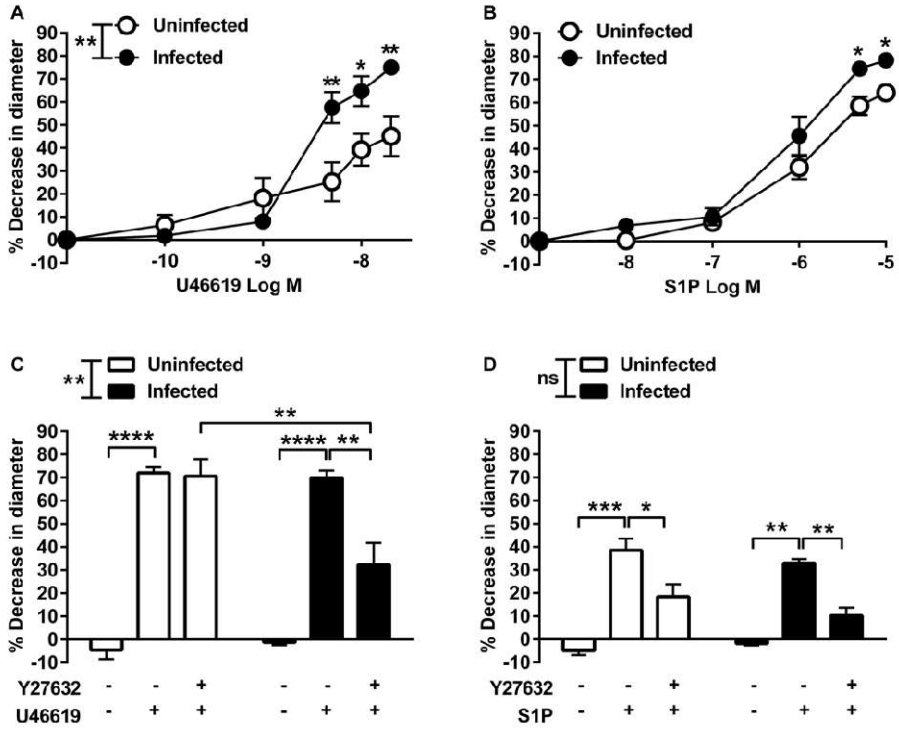

Figure 6.1: Effect of CMV infection on U46619 or S1P-induced vascular tone via Rho kinase pathway in uterine arteries in the bath. 1-20 nmol/L U46619 (**A**) or 0.01-10 µmol/L S1P (**B**) was added cumulatively to uterine arteries from uninfected or CMV-infected mice followed by measurement of changes in vascular diameter from the baseline diameter obtained after equilibration. Arteries from uninfected or CMV-infected mice were also treated with 20 nmol/L U46619 (**C**) or 1 µmol/L S1P (**D**) in the absence or presence of Y27632, all added to the bath, followed by measurement of changes in vascular diameter. The results are presented as the mean ± SEM percent decrease in diameter (n=4 to 6) and were analyzed by two-way ANOVA and the Tukey post-hoc test. For all the figures, the number of symbols depicts increasing levels of significance: 1 = $p<0.05$, 2 = $p<0.01$, 3 = $p<0.001$ and 4 = $p<0.0001$.

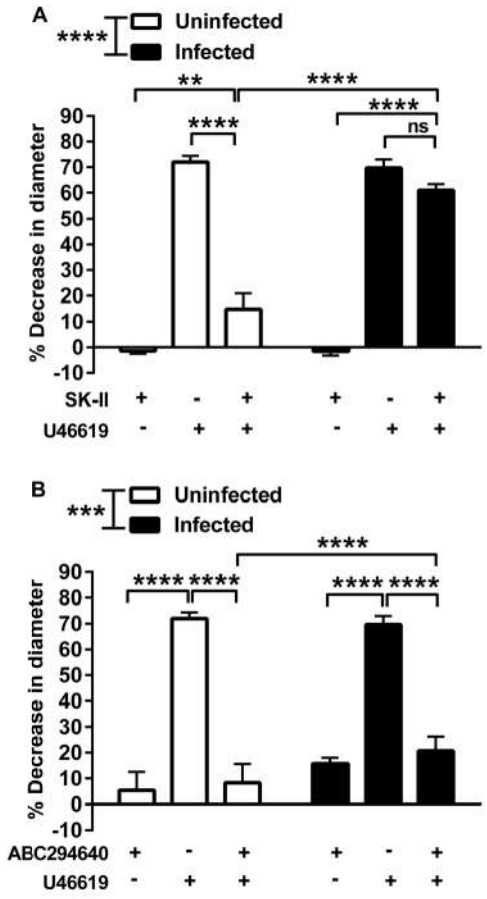

Figure 6.2: The impact of CMV infection on U46619-induced vascular tone mediated via sphingosine kinases in uterine arteries in the bath. 20 nmol/L U46619 was added to the bath of arteries from uninfected and CMV-infected mice in the presence or absence of SK-1 inhibitor (1 μmol/L SK-II) (**A**) or SK-2 inhibitor (10 μmol/L ABC294640) (**B**) followed by measurement of changes in vascular diameter from the baseline. The results are presented and analyzed as described in the legend for Figure 6.1 (n=4 to 10).

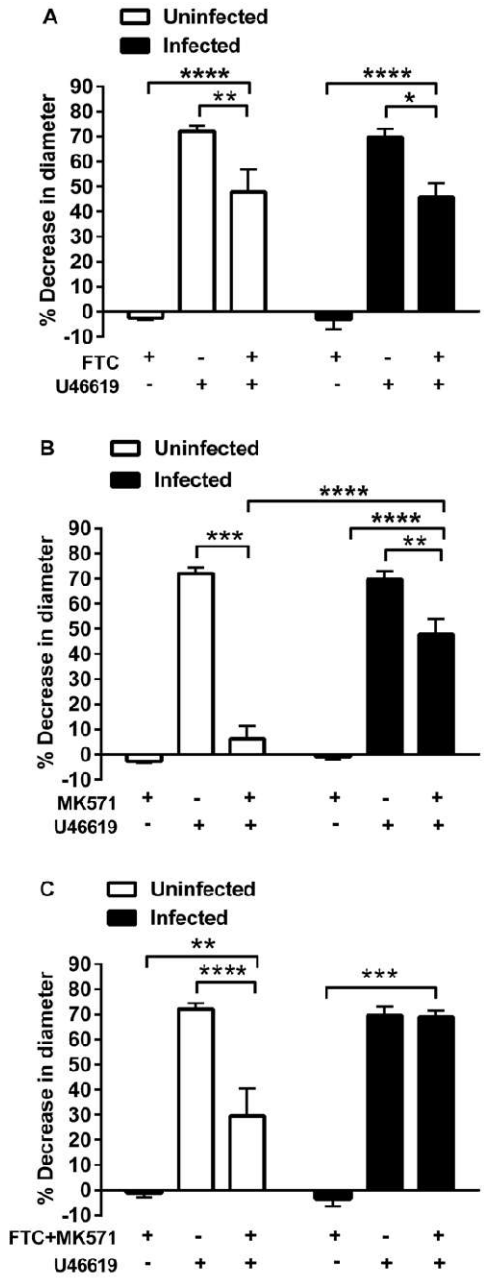

Figure 6.3: The effects of CMV infection on the role of ABC transporters in promoting U46619-induced vascular tone in uterine arteries in the bath. 20 nmol/L U46619 was added to uterine arteries from uninfected and CMV-infected mice in the presence or absence of ABCG2 inhibitor (1 μmol/L FTC) (**A**), ABCC1 inhibitor (10 μmol/L MK571) (**B**) or both inhibitors (**C**) followed by measurement of changes in vascular diameter from the baseline. The results are presented and analyzed as described in the legend for Figure 6.1 (n=4 to 6).

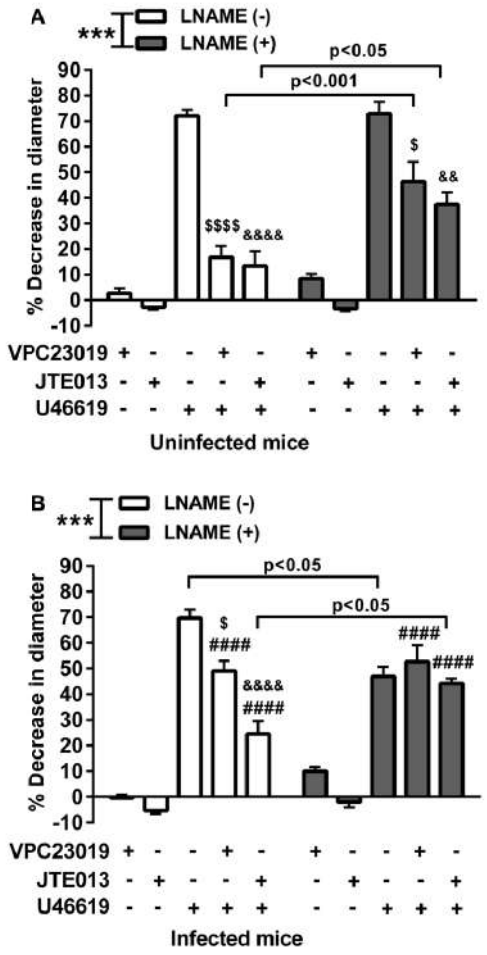

Figure 6.4: CMV infection and its effects on the role of S1P receptors in mediating the U46619-induced vascular tone in uterine arteries in the bath. 20 nmol/L U46619 was added to uterine arteries from uninfected and CMV-infected mice pretreated with $S1P_1/S1P_3$ antagonist (1 µmol/L VPC23019) (**A**) or $S1P_2$ antagonist (10 µmol/L JTE013) (**B**) in the presence or absence of NOS inhibitor 100 µmol/L L-NAME. The results are presented and analyzed as described in the legend for Figure 6.1 (n=4 to 6). $ or & compared to U46619 alone; # compared to VPC23019 or JTE013 alone.

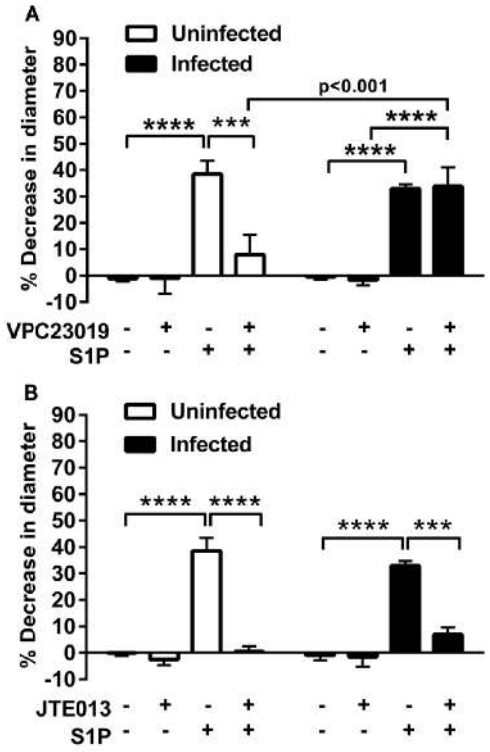

Figure 6.5: The effects of CMV infection on the $S1P_3$ or $S1P_2$ receptors in mediating the S1P-induced vascular tone in uterine arteries in the bath. 1 μmol/L S1P was added to arteries from uninfected and CMV-infected mice pretreated with 1 μmol/L VPC23019 (**A**) or 10 μmol/L JTE013 (**B**) followed by measurement of changes in vascular diameter from the baseline. The results are presented and analyzed as described in the legend for Figure 6.1 (n=4 to 6).

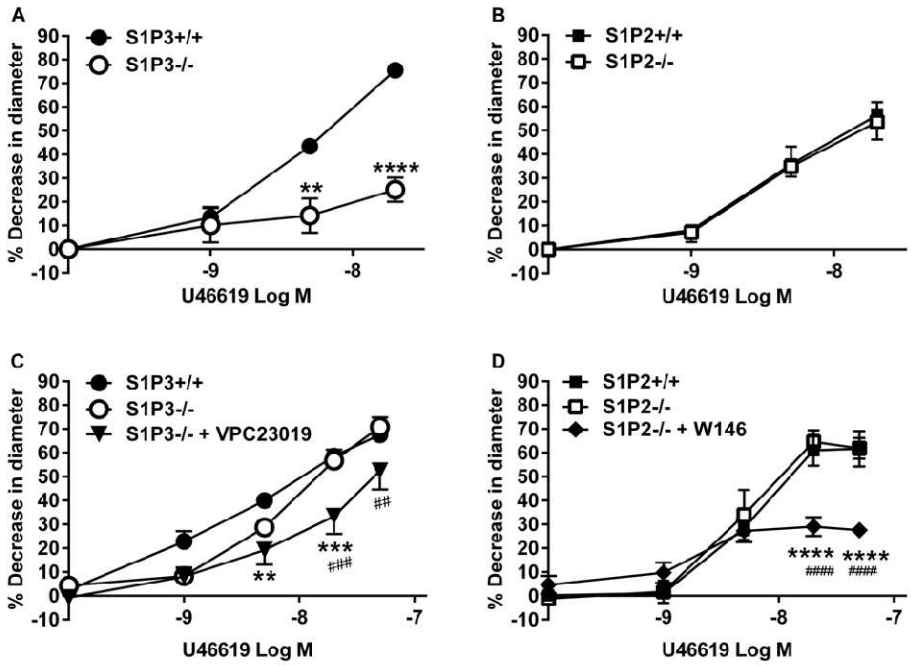

Figure 6.6: The dependence of U46619-induced vascular tone on $S1P_3$ receptor in uterine arteries is impaired with CMV infection. U46619 was added to arteries isolated from uninfected $S1P_3$ -/- **(A)**, $S1P_2$-/- **(B)** or CMV-infected $S1P_3$ -/- mice **(C)** and $S1P_2$ -/- mice **(D)** and their corresponding wildtype (WT) littermate controls. The mean ± SEM percent decrease in diameter (n=3 to 7) were analyzed by two-way ANOVA and the Tukey post-hoc test. # = $S1P_3$-/- compared to $S1P_3$-/- + VPC23019 **(C)** or $S1P_2$-/- compared to $S1P_2$-/-+ W146 **(D).** * compared to $S1P_3$+/+ (C).

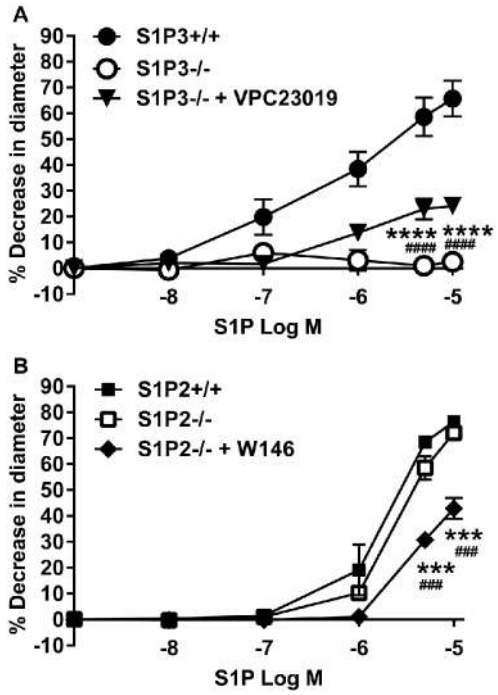

Figure 6.7: The S1P-induced vascular tone in uterine arteries isolated from CMV infected mice is dependent on both $S1P_1$ and $S1P_3$ receptors. 1 μmol/L S1P was also added to arteries isolated from CMV-infected $S1P_3$-/- **(A)** or $S1P_2$-/- **(B)** mice and their WT littermate controls, followed by measurement of changes in vascular diameter from the baseline. The mean ± SEM percent decrease in diameter (n=3 to 7) were analyzed by two-way ANOVA and the Tukey post-hoc test. # = $S1P_3$-/- compared to $S1P_3$-/- + VPC23019 **(A)** or $S1P_2$-/- compared to $S1P_2$-/-+ W146 **(B).** * compared to $S1P_3$+/+ or $S1P_2$-/-.

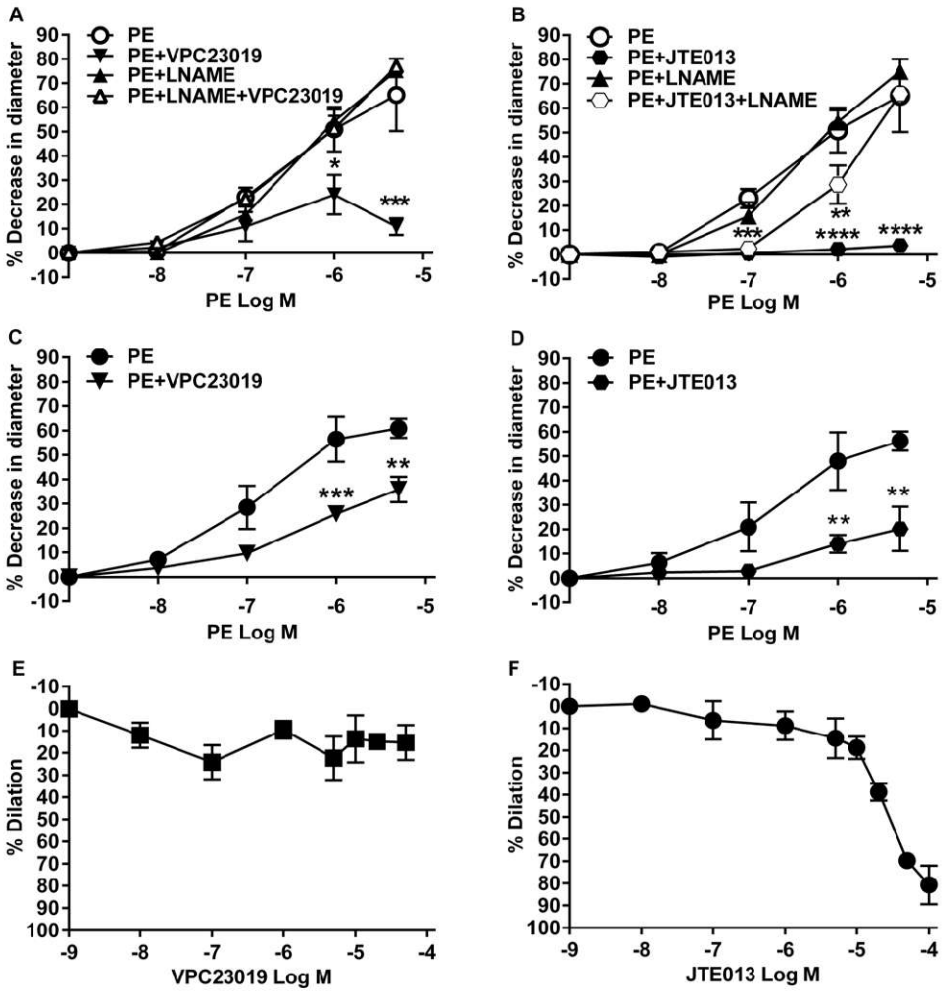

Figure 6.8: The dependence of phenylephrine-induced vascular tone on the S1P receptors in arteries from uninfected and CMV-infected mice. 0.01-10 μmol/L phenylephrine was added cumulatively to arteries from uninfected (**A, B**) and CMV-infected (**C, D**) mice pretreated with or without NOS inhibitor 100 μmol/L L-NAME and/or with or without 1 μmol/L VPC23019 (**A, C**) or 10 μmol/L JTE013 (**B, D**). Arteries were preconstricted with ~5-10 nmol/L U46619 followed by cumulative addition of increasing doses of VPC23019 or JTE013, to evaluate the dilatory properties of these inhibitors. Vasodilation was normalized to maximal arterial diameter induced by 100 μmol/L papaverine and Ca^{2+} free solution (**E, F)** followed by measurement of changes in vascular diameter from the baseline. The mean ± SEM percent decrease or increase in diameter (n=3 to 7) were analyzed by two-way ANOVA and the Tukey post-hoc test.

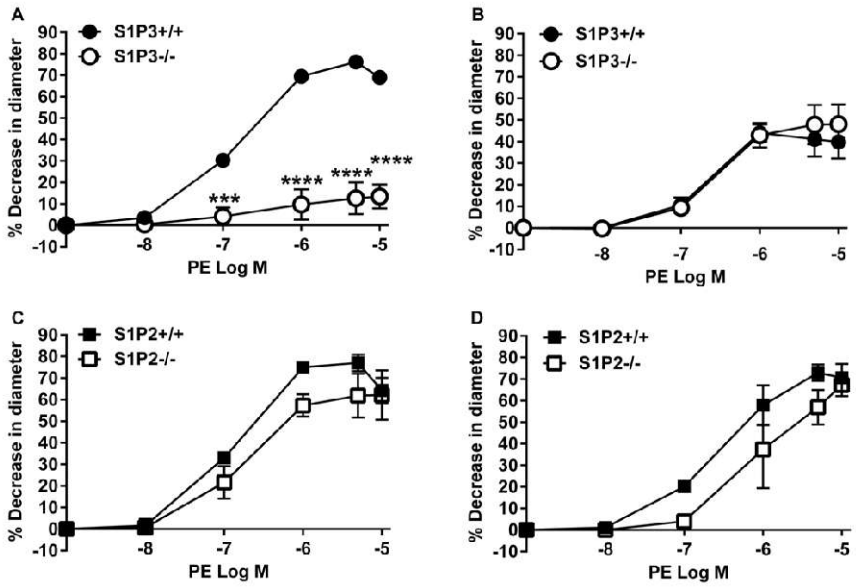

Figure 6.9: Phenylephrine-induced vascular tone in arteries from uninfected and CMV-infected C57Bl/6 KO and WT mice. 0.01-10 µmol/L phenylephrine was added cumulatively to arteries from uninfected (**A, C**) or CMV-infected **(B, D)** $S1P_3$ -/- mice and their littermate controls (A, **B**) or those from $S1P_2$ -/- mice and their littermate controls (**C, D**) followed by measurement of changes in vascular diameter from the baseline. The mean ± SEM percent decrease in diameter (n=3 to 4) were analyzed by two-way ANOVA and the Tukey post-hoc test.

6.2.8 Discussion of results from Chapter 6

In this Chapter, as already noted, I investigated the impact of CMV-infection on the vascular tone induced by TXA_2 via the S1P pathway. Indeed, I show that CMV infection enhances the vascular tone induced independently by TXA_2 and S1P in uterine arteries, likely resulting from CMV-mediated alteration of the downstream pathways of TP or S1P receptors. CMV infection increases the expression of MLC kinase 6-fold in primary human foreskin fibroblasts [801]. Further, CMV encodes G protein-coupled receptors (GPCRs) including US28 shown to promote PLC activation and inositol (1, 4, 5) triphosphate formation [802], which are key steps in TXA_2 or S1P-induced vascular tone. These CMV encoded G protein coupled receptors have been proposed to promote agonist-induced responses [803] which may also explain the enhanced TXA_2 or S1P-induced vascular tone in arteries from CMV-infected mice. Alternatively, since CMV infection has been associated with increased endothelial cell-cell gaps [661], and transmigration of immune cells like lymphocytes or monocytes [804], the presence of these cells in the subendothelial space could contribute to the enhanced vascular responses induced by TXA_2 or S1P. Indeed, activated macrophages under conditions of no- infection, contribute to the contraction of isolated rat pulmonary arteries in a mechanism that involves the generation of ROS. The contraction is blocked in the presence of ROS scavenger 4-hydroxy-TEMPO [805]. Since monocytes are known carriers of CMV [613,661,804], and CMV infection is associated with the release of ROS [806], when monocytes occupy the subendothelial space as macrophages, their activation following CMV infection could increase the basal levels of ROS. This means that the arteries stimulated by TXA_2 or S1P could exhibit enhanced constriction because of the addition role of ROS already available in arteries from CMV-infected mice.

The evidence that CMV increases the expression of MLC kinase [801], suggests that the TXA_2 or S1P-induced vascular tone in arteries from CMV-infected mice occur through the Ca^{2+}-dependent pathway. In this Chapter, I show that TXA_2-induced vascular tone occurs independent of the Rho kinase pathway under conditions of no infection, but via Rho-kinase/Ca^{2+}-dependent pathways following CMV infection. In contrast, the S1P-induced vascular tone is mediated through the Rho-kinase pathway with or without CMV infection (Figure 6.10). Although there are similarities, the differences between TXA_2 and S1P-induced responses could be due to the change in receptor dependence by S1P or alterations of the downstream signaling mechanisms during infection. CMV infection [679], and other viruses like influenza A virus [807,808] and

Epstein Barr virus [678,809] increase the expression and activity of SK-1. Moreover, CMV [806], TXA_2 [810] or S1P [811] promote the generation of ROS. This may also explain the lack of differences at the single doses used in U46619 or S1P-induced vascular tone in arteries from CMV-infected and uninfected mice. It is therefore likely that 20 nmol/L U46619 at this high concentration, added only at once and the response measured after a short time there could be more effect of ROS. In contrast, addition of U46619 cumulatively from low doses could have minimal effects on ROS generation, and since the responses were measured over a period of time, this could favor ROS disintegration. Thus, ROS likely contributes to increased vascular tone by decreasing NO bioavailability in arteries from uninfected and CMV-infected mice with no net difference. Indeed, in Chapter 3 I showed that at lower doses of 5 nmol/L U46619, the vascular tone induced was significantly enhanced in arteries pretreated with L-NAME, but not when 20 nmol/L U46619 was used in the presence of L-NAME as seen in this Chapter.

In Chapter 5, I showed that TXA_2 increases endothelial permeability or vascular tone in an S1P-dependent manner. In this Chapter, I show that in arteries from CMV-infected mice TXA_2-induced vascular tone occurs independently of SK-1, indicating a mechanistic shift in vascular tone control by TXA_2 during CMV infection to mainly utilize SK-2 (Figure 6.10). Evidence shows that signaling of TXA_2 through TP receptors activates SK-1 which phosphorylates radiolabelled sphingosine resulting in the release of S1P from cultured human platelets [486]. In Chapter 5, I reported a role for ABCG2 or ABCC1 transporters in the TXA_2-induced endothelial permeability and vascular tone, respectively. In this Chapter, the dependence by TXA_2 on ABCG2 in inducing vascular tone during CMV infection did not change compared to arteries from uninfected mice, suggesting CMV infection does not affect the activity of this transporter. However, the role of ABCC1 in mediating TXA_2-induced vascular tone was profoundly reduced following CMV-infection (Figure 6.10), suggesting that other transporters like spns2, not evaluated in this study, could be important during CMV infection [812]. Surprisingly, blocking the ABCC1 and ABCG2 simultaneously had no effect on TXA_2-induced vascular tone in arteries from CMV-infected mice. While these findings warrant further investigation, the results provide clinically important information that cautions against the use of a combination of these drugs to target the S1P pathway for therapeutic purposes under conditions of CMV infection, given that MK571 (as montelukast sodium) has been used in the treatment of asthma [813,814].

I have shown before that S1P (Chapter 3) and U46619 (Chapter 5) independently increases endothelial permeability or vascular tone in uterine arteries mediated through the $S1P_3$ receptor. In this Chapter, $S1P_3$ did not play a role in U46619-induced vascular tone following CMV infection, but instead U46619-induced vascular tone was mediated partly through the $S1P_1$ receptor, while the rest of the vascular response stimulated through a yet to be defined pathway. Interestingly, the S1P-induced vascular tone was mediated through both $S1P_1$ and $S1P_3$ receptors following CMV infection (Figure 6.10). These findings indicate that CMV infection changes the vascular tone induced by TXA_2 or S1P. While the role of $S1P_1$ inducing vasoconstriction is not fully characterized, emerging evidence suggests that $S1P_1$ could promote vasoconstriction via the Gi/PLC pathway that increases $[Ca^{2+}]i$ and MLCK activation [815]. $S1P_1$ and $S1P_3$ couples to Gi/o, and the S1P-induced vasoconstriction is significantly decreased in basilar arteries in the presence of Gi/o-specific inhibitor pertussis toxin [484]. $S1P_1$ (used W146 antagonist), and $S1P_1$ and $S1P_3$ (used VPC23019 dual inhibitor) have been shown to promote the S1P-induced contraction of excised tissue strips from porcine aortic valves, that was associated with an increase in $[Ca^{2+}]i$ [816]. In rabbit posterior cerebral arteries, the $S1P_1$ receptors (used W146) do contribute to myogenic tone induced by exogenously added S1P [87]. More recently, SEW2871 or FTY720 were shown to enhance phenylephrine or serotonin-induced vasoconstriction in rat mesenteric and coronary arteries [118], but also SEW2871 increased vasoconstriction in renal afferent arteries [480]. These findings suggest that $S1P_1$ could be involved in the induction of vasoconstriction as also demonstrated in my study using U46619 or S1P. Crosstalk exits between different G-proteins including $G_{i/o}$ and G_s, G_s and $G_{q/11}$, $G_{i/o}$ and $G_{q/11}$ in agonist stimulated responses [817,818]. In fact, a CMV-encoded $G_{q/11}$ GPCR hypersensitizes VSMCs responses to lysophosphatidic acid (LPA) [802].These findings collectively, indicate that CMV infection could alter the downstream receptor signaling capabilities, and may explain the switch in dependence of U46619 on $S1P_3$ in inducing vasoconstriction in arteries from uninfected mice to $S1P_1$ in arteries from CMV infected mice.

Although the vascular tone stimulated by U46619 or S1P is inhibited equally by JTE013 in arteries from uninfected and CMV-infected mice, vascular tone in arteries from $S1P_2$ KO mice was unaffected. JTE013 is reported to be nonselective [800], and VPC23019 exhibits agonist activities [698]. Considering these reports, and since I showed equal levels of inhibition of U46619 or S1P-induced vascular tone by JTE013 or VPC23019 in uninfected mice, I determined

whether these inhibitors produce vasodilatory factors which overcome TXA_2-induced tone. Indeed, L-NAME relieved the inhibition mediated by JTE013 or VPC23019 promoting partial restoration of U46619-induced vascular tone in uninfected mice. These findings imply that, JTE013 or VPC23019 act to antagonize the S1P receptors [800], but also cause vasodilatory effects through NOS activation. In arteries from CMV-infected mice blocking NOS activity significantly reduced the vascular tone induced by U46619. These findings are not surprising as L-NAME has been shown to increase the activity of NOS (iNOS or eNOS), both *in vitro* for instance in astrocytes [767] and bovine aortic endothelial cells [768], and *in vivo* in the heart, aorta and kidney of normotensive rats [769]. In Chapter 4, I showed that arteries pretreated with L-NAME exhibited enhanced vasodilation that was dependent on the activation of the endothelial isoforms of NOS. These findings indicate that under certain conditions L-NAME can stimulate NO activity leading to NO production.

Like U46619, phenylephrine also increased vascular tone through an S1P pathway. In the presence of L-NAME, VPC23019 lost its inhibitory potency, suggesting that VPC23019 mediates its effects through NO generation. Unexpectedly, VPC23019 did not generate vasodilation in preconstricted arteries. I have however consistently shown that the use of VPC23019 or arteries from $S1P_3$ null mice provides results consistent with the role of $S1P_3$ in mediating the increase in vascular tone. Phenylephrine-induced vascular tone was partially inhibited by VPC23019 in arteries from CMV-infected mice. Like U46619, phenylephrine-induced vascular tone was blocked in arteries from uninfected $S1P_3$-/- mice, but not with CMV infection, suggesting that the vascular tone likely occurs via the $S1P_1$ receptor.

JTE013 completely blocked phenylephrine-induced vascular tone which was partly restored in the presence of L-NAME. These results indicate that JTE013 functions as an antagonist but also promotes production of NO as an additional mechanism for preventing phenylephrine-induced vascular tone. Like with U46619, VPC23019 or JTE013 inhibited phenylephrine-induced vascular tone, but their inhibitory functions decreased with CMV infection. The lack of phenylephrine-induced vascular tone in arteries from CMV-infected $S1P_2$-/- or $S1P_3$-/- mice, suggests that the inhibition of phenylephrine-induced vascular tone by VPC23019 or JTE013 in CMV-infected mice is likely NO-mediated.

In summary, I have demonstrated that CMV infection enhances the vascular tone induced by TXA_2 or S1P which means that CMV infection can potentiate vascular complications leading

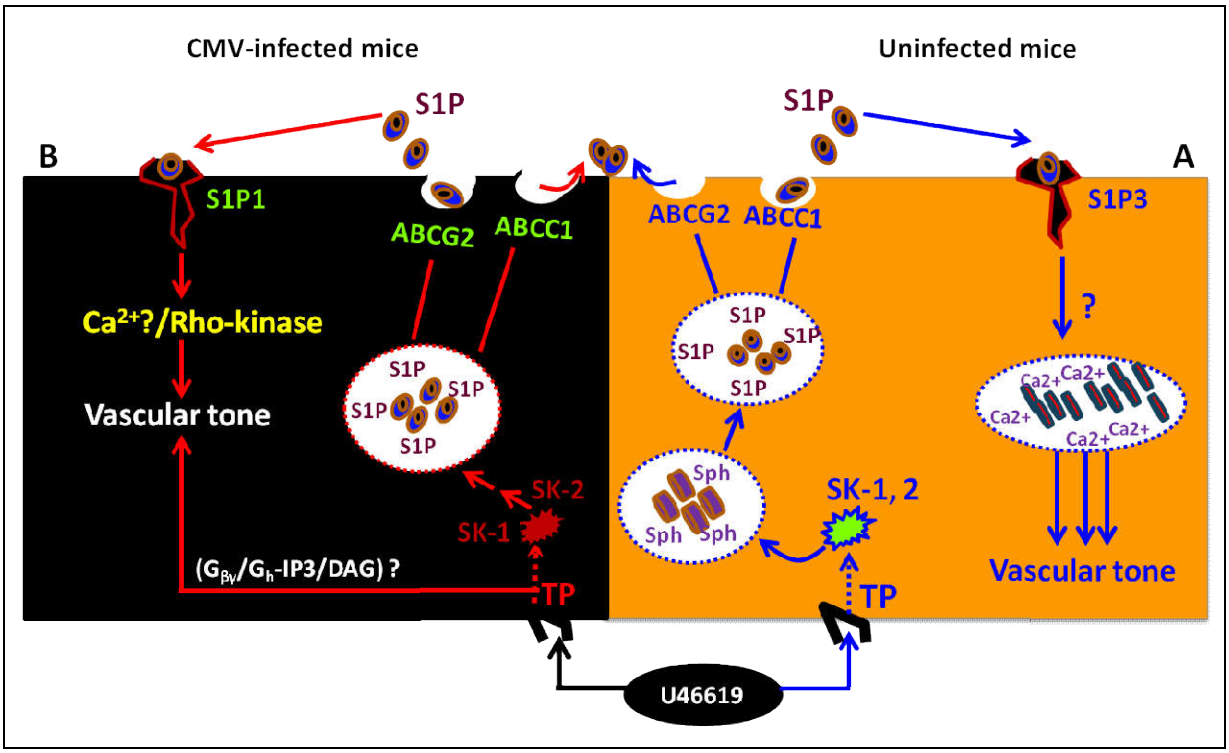

Figure 6.10: Proposed model to account for the impact of CMV infection on the vascular tone induced by U46619 via an S1P pathway. Under conditions of no infection U46619 increases vascular tone in murine uterine arteries predominantly through the S1P pathway mediated via the $S1P_3$ receptor, and likely downstream activation of the Ca^{2+}-dependent mechanism **(A).** Following CMV infection U46619 weakly stimulates vascular tone via the S1P pathway mediated through the $S1P_1$ receptor, downstream activation of Rho kinase and likely a Ca^{2+}-dependent pathway. However, the majority of the constriction response appears to be mediated through a yet to be identified mechanism that is independent of the S1P pathway. The width of arrows depicts the degree of activity **(B).**

to disorders like hypertension. Indeed, CMV infection increases blood pressure in a rodent model [655], and hypertension in humans [819]. I have also shown that the TXA_2–induced vascular tone through the S1P pathway is significantly attenuated following CMV infection, opening up alternative mechanisms through which TXA_2 increases vascular tone, for example, the $S1P_1$ receptor activation and the Rho kinase pathway. While targeting the S1P pathway will be valuable in ameliorating the clinical signs of vascular disorders caused by TXA_2 during CMV infection, identifying the additional mechanisms through which TXA_2 increases vascular tone in

arteries from CMV-infected mice will be essential for therapeutic purposes. These findings are important as one of the analogs of sphingosine (FTY720) approved for treatment of multiple sclerosis has been shown to reduce severe CMV disease in renal transplant patients [9].

CHAPTER 7: GENERAL DISCUSSION

Endothelial permeability and vascular tone have often been studied separately, but I now demonstrate that these concepts are interconnected. I show that S1P regulates endothelial barrier which has an impact on vascular tone. At physiological concentrations, that is, less than 1 μmol/L, S1P enhanced endothelial barrier limiting its own access to the VSMCs, and therefore had no effect on vascular tone although addition of 0.1-1 μmol/L S1P extraluminally increased vascular tone. The mechanisms through which S1P increases endothelial barrier are relatively well studied. In cultured endothelial cells, the S1P-mediated activation of the $S1P_1$ receptor and downstream stimulation of $G\alpha_i$/Rac/PI3K pathway results in decreased endothelial permeability. This mechanism involves the assembly of the VE–cadherin/β–catenin complex and redistribution of ZO–1 at the cellular junctions [390-392]. In isolated perfused rat mesenteric venules S1P was shown to enhance the endothelial barrier against barrier disrupting agents, platelet activating factor and bradykinin [415,416]. Further, mice engineered to deliberately lack circulating S1P were shown to suffer from vascular leakage and decreased survival, and resupplying S1P through transfusion of wildtype erythrocytes reversed vascular leakage and improved mice survival [419]. These findings emphasize the importance of S1P in maintaining endothelial barrier function. However, we are the first one to demonstrate the role of S1P in protecting endothelial barrier in isolated pressurized arteries as most previous studies have focussed on cultured endothelial cells and veins. We also further demonstrate novel findings in which S1P likely maintains endothelial barrier through NO-mediated activity (Figure 7.1). S1P-induced activation of $S1P_1$ or $S1P_3$ receptors stimulates eNOS activation and NO generation [33,34,121,122,386,441,442]. Such NO-stimulated endothelial barrier tightening likely prevented leakage of S1P to the VSMCs resulting in no effect on vascular tone. I also show that SNP (NO donor) at low concentrations enhanced the basal (unstimulated) barrier, but also decreased endothelial permeability generated by infusion of thrombin, but not LPS or gB, into uterine arteries. These differences in the capacity of SNP to enhance the barrier could be associated with the differences in the mechanisms utilized by these products from infectious agents compared to those produced physiologically.

The high-end physiological concentration of S1P (1 μmol/L) infused into uterine arteries had no effect on vascular tone despite having increased endothelial permeability. However, when the same concentration of S1P, was added extraluminally, vascular tone was increased. We have

shown that 0.01 μmol/L S1P or NO (SNP at 20 μmol/L) enhances the basal barrier, and these findings suggest that in isolated arteries whose blood components has been flushed out, these arteries exhibits some "low-level" leakiness. This idea is supported by studies showing that perfusion of rat mesenteric venules with erythrocyte-derived S1P led to a decrease in basal permeability [417]. It is therefore likely that the 1 μmol/L S1P-induced permeability promotes its own leakage to the VSMCs but the induced vasoconstriction is overcome by the likely S1P-generated NO. This argument is supported by the dramatic increase in vascular tone from infused 1 μmol/L S1P when NOS activity was inhibited by L-NAME. Furthermore, taking into account basal NO production, the level of constriction after infusion in the presence of L-NAME is still only approximately 50% for 1 μmol/L S1P of that found when added to the bath, suggesting the existence of partial functional barrier that can allow leakage of S1P to the VSMCs. These results are further supported by the results showing that infusion of 1 μmol/L S1P into arteries from eNOS KO mice increased vascular tone which was absent in arteries from WT mice. These results indicate that S1P does access the VSMCs but the NO produced in arteries from eNOS KO mice [820] was not sufficient to overcome the S1P-induced vasoconstriction.

The mechanism through which S1P increases endothelial permeability in uterine arteries may be NO-mediated (Figure 7.1). This idea is partly supported by results showing that high concentrations of NO donor 50 or 100 μmol/L SNP increased endothelial permeability compared to the control or lower SNP concentrations. In addition, co-infusion of SNP with U46619 (which we now know signals via the S1P pathway to increase permeability and vascular tone) increased endothelial permeability. Given the lack of SNP-induced permeability in arteries from eNOS KO mice, it is likely that the mechanism through which NO increases endothelial permeability in uterine arteries involves sustaining a positive feedback loop leading to eNOS activation, but it is also likely that the arteries from eNOS KO mice generates NO scavengers like apha-globin [821,822] which could take up most of the exogenously delivered NO via SNP inhibiting increase in endothelial permeability. NO has also been shown to activate Rho GTPases disrupting endothelial VE-cadherin [749]. Thus far, these findings indicate the role of S1P in regulating endothelial barrier mediated by the actions of NO. Such endothelial barrier control determines the outcome of vascular tone induced by S1P.

Another novel finding is that endothelial permeability induced by S1P at a physiological concentration (1 μmol/L) promotes leakage of circulating vasoconstrictors into the underlying

VSMCs increasing vascular tone. These S1P-mediated effects of endothelial permeability and vascular tone occur in at least two vascular beds: the uterine and mesenteric arteries. The co-infusion of S1P with U46619 into uterine arteries was associated with increased permeability mediated by S1P via $S1P_3$ allowing leakage of U46619 increasing vascular tone (Figure 7.1). The vascular tone induced by infused S1P, U46619 or their combination were markedly enhanced when NOS was inhibited by L-NAME, indicating that both of these drugs produce NO that blunts the vascular tone generated. Like S1P, co-infusion of NO donor (SNP) with U46619 was accompanied with increased endothelial permeability and vascular tone. While the 20 μmol/L SNP and U46619 independently had no effect on permeability it is more likely that the permeability was contributed by NO contributed by both SNP and U46619. Such co-induced permeability was completely abolished in arteries from eNOS KO mice, suggesting that the NO produced activates eNOS, which continually make NO available to increase permeability. This argument is supported by the evidence presented earlier that the 50 or 100 μmol/L SNP-induced endothelial permeability was completely inhibited in arteries from eNOS KO mice. Although U46619 does not appear to potentiate S1P-induced permeability, these differences could be associated with the way NO is generated by S1P and SNP, and ultimately activate eNOS. It was however, unexpected that co-infusion of the NO donor with U46619 could lead to an increase vascular tone (contributed by leakage of U46619 by co-induced permeability). However, as expected such vascular tone was lower (decreased by SNP-derived NO) compared to that induced by infused U46619 in the presence of L-NAME. Collectively, these findings indicate S1P at a physiological concentration increases endothelial permeability via eNOS/NO which is presumably within tolerable limits that allows circulating vasoactive agents to access the underlying VSMCs to maintain normal vascular tone.

The concept that increased endothelial permeability promotes leakage of circulating vasoconstrictors to the VSMCs increasing vascular tone is also demonstrated by the pathophysiological levels of S1P, permeability-inducing factors thrombin, LPS, gB and TXA_2. S1P at pathological levels (10 μmol/L) increased endothelial permeability, and promoted leakage of S1P to the VSMCs increasing vascular tone. Although inhibiting NOS dramatically increased S1P-induced permeability, it is likely that the permeability induced by10 μmol/L S1P in the absence of L-NAME experiences barrier enhancing signals generated by NO activity. Unlike 1 μmol/L S1P, the constriction induced by infused 10 μmol/L S1P was not different from that

obtained when added extraluminally. This is likely because 10 μmol/L being pathophysiological, S1P could stimulate other mechanisms that can interfere with NO bioavailability including the generation of ROS. While 10 μmol/L S1P contributes to the generation of ROS [823], it is unknown whether that is applicable in arteries used in this study. Like 10 μmol/L S1P, thrombin, LPS, gB-induced permeability also facilitated leakage of a co-infused vasoconstrictor (U46619) to the VSMCs increasing vascular tone. TXA_2 was used at high concentrations to investigate the potential effects of this lipid in promoting pathological-related effects on the vasculature. For the first time, I show that endothelial permeability and vascular tone generated by TXA_2 is mediated through an S1P pathway. TXA_2 increases permeability in cultured endothelial cells through disruption of VE-cadherin and PECAM-1 [8]. In my study, infusion of U46619 into mouse uterine arteries led to SK-1, ABCG2 (but not ABCC1), and $S1P_1$/$S1P_3$-dependent induction of permeability that was reversed by an $S1P_1$ receptor agonist, SEW2871. The SEW871-mediated reduction in permeability was accompanied with decreased vascular tone from infused U46619, suggesting that enhanced endothelial barrier prevented leakage of U46619 to the VSMCs. The role of SEW2871 as an endothelial barrier enhancing agent has been shown before [782], including in my study whereby SEW2871 reversed endothelial permeability induced by thrombin, but also prevented thrombin-mediated leakage of U46619 and induction of vascular tone. I also found that the vascular tone induced by infused U46619 was mediated by ABCC1 and $S1P_1$/$S1P_3$ on the VSMCs of uterine arteries. These results are consistent with the findings that I presented earlier in which S1P utilizes $S1P_3$ to increase vascular tone. Moreover, the vascular tone induced by U46619 in the bath containing mesenteric arteries from male and female mice was mediated via SK-1, ABCC1 and ABCG2. Interestingly, stimulation of arteries in the bath led to an increase in endothelial permeability that was approximately 50% of that induced when U46619 was infused. The induced permeability and vascular tone were mediated through TP receptors and ABCC1.These results suggest that vascular tone alone can contribute to increase in endothelial permeability. I therefore convincingly demonstrate that indeed TXA_2 utilizes the S1P pathway to increase endothelial permeability and/or vascular tone in mouse uterine and mesenteric arteries. Although, U46619 appears to induce the production of NO as already discussed, it is still not clear whether the permeability induced by TXA_2 is mediated through the S1P/eNOS/NO pathway.

While TXA_2 is clearly a stimulus that leads to S1P generation, I also found that CMV

infection enhances the vascular tone induced by S1P or TXA_2 in uterine arteries (potential contribution of immunological responses, please see section 6.2.8). The induced vascular tone was partly mediated through the Rho kinase pathway. While the TXA_2-induced vascular tone is mediated through the S1P pathway under conditions of no-infection, the role of SK-1, ABCC1 but not ABCG2, and the $S1P_3$ receptors were profoundly decimated following CMV infection. Instead, infection opened up a new avenue for induction of vascular tone by TXA_2 involving SK-2 and $S1P_1$ receptors, but also S1P-induced vascular tone was mediated through both $S1P_1$ and $S1P_3$ receptors. Although TXA_2 still stimulates vascular tone via the S1P pathway under condition of CMV infection, a large proposition of the response appear to be mediated through a different mechanism that is independent of the S1P pathway.

In summary, the findings presented here, will expand our understanding of the physiological control of endothelial barrier and vascular tone by S1P with potential for therapeutic applications. The results suggest that under pathological conditions, excessively increased endothelial permeability in reproductive arteries (like uterine) during pregnancy could increase vascular tone in these arteries limiting nutrient and blood supply to the fetus affecting fetal growth. This can lead to pregnancy disorders like intrauterine growth restriction. Moreover, increases in endothelial permeability and vascular tone in mesenteric arteries can interfere with systemic blood pressure. Therefore, therapeutic approaches aimed at reducing endothelial permeability via S1P-mediated actions, can be useful in the treatment of vascular complications associated with increased vascular tone like hypertension and intrauterine growth restriction. TXA_2 is associated with various disease-related conditions like vascular tone, vascular leakage, rheumatoid arthritis, atherosclerosis, inflammation, and preeclampsia. Considering the findings from this study, targeting the S1P pathway could ameliorate the clinical signs associated with vascular complications caused by elevated levels of TXA_2. CMV infection will likely potentiate the vascular complications mediated by TXA_2 or S1P and there is therapeutic potential in targeting the S1P pathway.

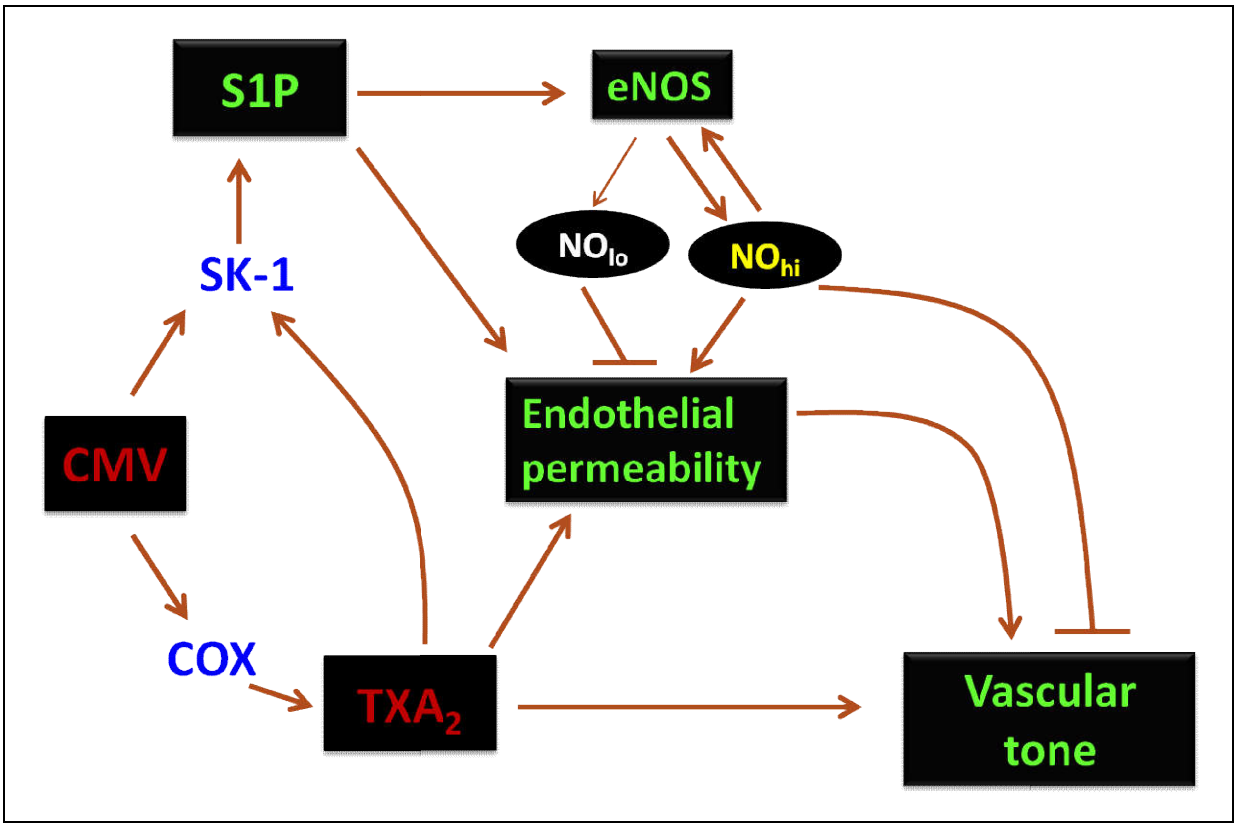

Figure 7.1: Overall model for the thesis. Infusion of S1P inside arteries enhanced, but also disrupted endothelial barrier. Mechanistically, I show that S1P stimulates eNOS, the enzyme that catalyzes the formation of NO. At low concentrations NO increases endothelial barrier, but high concentration it decreases the barrier. Increase in endothelial permeability promotes leakage of any available vasoconstrictor(s) increasing vascular tone. NO can also positively regulate eNOS activity or negatively control the establishment of vascular tone. The S1P pool can be replenished by other stimuli like CMV infection or TXA_2 activity. While TXA_2 increases endothelial permeability and vascular tone, I showed this is mediated via the S1P pathway. Although TXA_2 appeared to produce NO in uterine arteries, it remains to be determined whether TXA_2-induced endothelial permeability and vascular tone when infused, is mediated through the S1P-NO pathway.

CHAPTER 8: LIMITATIONS AND FUTURE DIRECTIONS

In this thesis, the use of pressure myography provided very useful information as it also helps to investigate vascular function in near physiological conditions. However, the physiological relevance of the findings can be corroborated with additional studies from *in vivo* models. The impact of vascular tone demonstrated in isolated arteries can be assessed *in vivo*, by delivering drugs into study animals and changes in blood pressure can be measured using tail cuff method or plethysmography. Endothelial permeability can also be assessed *in vivo* using miles assay. In this assay, Evans Blue dye (or fluorescent dextran of choice) is injected intravenously to the test animal (e.g. mice) followed by delivery of the experimental treatment (e.g. drugs). Evans Blue dye binds to albumin, and under physiological conditions albumin does not pass through an intact endothelium, and therefore the dye remains within the blood stream. When endothelial permeability is increased, the endothelium becomes permeable to albumin, allowing extravasation of Evans Blue dye to the tissues. Endothelial permeability can then be determined by visualization or quantitatively from the amount of dye embedded (in tissues) per tissue weight. The dye can be extracted using formamide. The advantage of this technique is that is it simple and also the ease with which results can be quantified. However, this technique is time consuming starting from the experiment itself, extraction of the dye and determination of optical density by spectrophotometry [824,825]. Alternatively, more advanced technologies to image vascular responses *in vivo* can be considered. The use of intravital microscopy provides tremendous opportunities to not only image vascular responses in live animals but also cellular and subcellular changes following treatment of the animals with drugs of interest [826].

In Chapter 3 of the thesis, I showed that S1P regulates normal vascular tone through endothelial permeability in mouse arteries. The S1P does this by promoting leakage of circulating vasoactive agents to the underlying VSMCs controlling vascular tone. However, the VPC23019 used as an S1P receptor antagonist binds to the $S1P_1$ and $S1P_3$ receptors simultaneously [698] making it difficult to accurately interpret the results. However, the use of the $S1P_3$ receptor KO mice which were available on a 129 (strain) background helped to streamline the interpretation. Although the $S1P_3$ KO mice do not display any growth-related defects [681], it is unknown whether any physiological compensations occurs in these mice that can affect the S1P responses. Future experiments should determine the levels of S1P receptor ($S1P_1$, $S1P_2$, because $S1P_{1-3}$ are the receptors mainly found on the vasculature) expression in

arteries from these type of $S1P_3$ KO mice. However, as already noted earlier, it is technically challenging to specifically measure the receptors on the endothelium or on VSMCs given that the arteries are very small. Although measuring the receptor expression by Western in a whole vessel as conducted in our study can provide useful information, the contribution of specific receptors to endothelial permeability or vascular tone (vascular function) will remain unclear. However, technologies like Laser Capture Microdissection with the capacity to isolate individual cells from tissues can be utilized, from which the cells can be stained for the receptors and analyzed by flow cytometry or imaged.

I couldn't analyze the role of the $S1P_2$ receptor in the S1P-induced responses in earlier experiments because we didn't have $S1P_2$ KO mice then, which are now available, but also the JTE013 an $S1P_2$ receptor antagonist available at the time was reported to be non-specific [800]. However, we interpreted the findings from this study that the compounds used (including U46619) were likely signaling through the S1P pathway to induce the responses, and indeed, as demonstrated in my thesis U46619 signals via the S1P pathway. Although I have shown that at high concentrations JTE013 increases vasodilation, at the concentrations used in my study JTE013 did not increase vasodilation on its own.

There were also limitations in the use of $S1P_1$ KO mice, as genetic deletion of this receptor is lethal; however, endothelial-specific $S1P_1$ KO mice have now been generated [827], which together with $S1P_1$-specific antagonists such as W146 [700,828,829], and those that are currently under evaluation [830], once they become commercially available, they will be valuable tools for analysis of vascular responses to S1P. It is noteworthy, that the responses of uterine arteries to infused 1 μmol/L S1P from 129 strain female mice induced vascular tone but those from C57Bl/6J mice didn't. Unlike uterine arteries from 129 strain, mesenteric arteries from the same strain showed increased vascular tone to infused S1P or U46619. These differences could be associated with vascular-bed, sex or genetic-related differences. To address these differences, vascular responses to infused S1P, U46619 or their combination should be repeated with uterine or mesenteric arteries isolated from our in-bred C57Bl/6 male and female (KO and WT) mice now available, but also determine the levels of S1P or TP receptor expression in these arteries.

In Chapter 3 and 4, I used the CMV glycoprotein gB at 0.5 μg/ml, which I showed increases endothelial permeability but also potentiates U46619-induced vascular tone in uterine

arteries. While these findings suggests that CMV viral attachment alone is sufficient to increase endothelial permeability and promote leakage of circulating vasoconstrictors to the VSMCs increasing vascular tone, using one viral protein alone does not mimic the effects of an intact virus. Future studies, should co-deliver an intact mouse CMV virus with U46619 or any other vasoconstrictor, and assess the effects on endothelial permeability and vascular tone. The protocol for delivering intact virus into arteries has already been established in our lab [574]. Since CMV infection has been shown to increase endothelial permeability in cultured cells [661], and high blood pressure in a rodent model [655], further experiments can now test whether an *in vivo* CMV infection contributes to an increase in vascular tone by promoting leakage of circulating vasoconstrictors to the VSMCs. This means that CMV infection will act as a permeability factor, and U46619 can be infused directly into arteries isolated from CMV-infected mice and vascular tone evaluated. However, *in vivo* experiments can also be conducted whereby fluorescently labeled U46619 or S1P (which we have) can be delivered into CMV infected mice, and permeability can be traced to specific arteries. Since I have already shown that CMV infection promotes an increase in vascular tone in an S1P-dependent manner, both of which increases endothelial permeability, further experiments should evaluate whether CMV-infection utilizes S1P signaling to increase endothelial permeability (and vascular tone-generated following infusion). These findings will be clinically important not only to CMV infection-induced pathologies, but also those induced by TXA_2 (which induces permeability and/or vascular tone via S1P pathway).

The inhibitors I used although some of them gave me specific responses, but some of them were useful in assessing general signal transduction mechanisms. L-NAME inhibits all of the NOS isoforms (eNOS, iNOS, nNOS) [831], but also L-NAME has been reported to activate NOS [767-769]. Although I used eNOS KO mice to determine the contribution of eNOS to the vascular responses, it was difficult to determine the contribution of other isoforms. To determine the role of each of these isoforms on vascular responses to S1P, U46619 or SNP, experiments in arteries from eNOS KO mice should be conducted in the presence of specific inhibitors to iNOS such as 1400W [832,833] or to nNOS like N-ω-propyl-L-arginine hydrochloride [834,835]. Although L-NAME did not appear to activate NOS in the presence of S1P, but with SNP, L-NAME enhanced the vasodilation induced by SNP. To find out whether L-NAME contributes to NOS activation, experiments can now be repeated by co-treating mouse uterine arteries with L-

NAME and SNP and determine eNOS phosphorylation at ser1176 or the experiments can be conducted using flourigenic NO probes (e.g. DAF-2, DAR-2) [836,837] that can detect NO generation.

Although I dissected the pathway through which TXA_2-induces endothelial permeability and/or vascular tone through the S1P pathway, there are three limitations (**1**) rodents express only one subtype of TXA_2/prostanoid receptors TPα, but humans express both TPα and TPβ receptors. These differences questions the applicability of my results in human situations, however, TPβ is easily downregulated in human cells at high TXA_2 concentrations including the concentration used in this study [524,528,778]. This means that my results mimics the pathophysiological conditions that occur in humans; (**2**) I mainly used inhibitors including those of ABC transporters, whose primary role (ABC) is to export ATP out of the cells. Since I targeted multiple steps of the S1P pathway, and demonstrated a high level of consistence of the message, the results generated using MK571 (ABCC1) or FTC (ABCG2) does not weaken the overall conclusion of my studies. However, if need be, additional transporters such as spns2 can be evaluated, and although the inhibitors for this transporter are not available, the siRNA-mediated silencing can be utilized, but also the spns2-specific KO mice have now been generated [371]; (**3**) Although I showed that U46619 signals through the S1P pathway to induce its responses, I did not quantitatively show that in the arteries I studied the S1P is released following U46619 treatment. We now have an S1P-specific antibody, and these experiments can be repeated for verification if need be. Experiments can also be conducted in cultured endothelial or VSMCs and the amount of S1P released following stimulation by U46619 can be determined using tin-layer chromatography or mass spectrometry.

While I used uterine arteries as a model to study the effects of S1P/TXA_2 on endothelial permeability and/or vascular tone, being reproductive arteries, further studies should look at such effects on normal pregnancy as this being one of the areas of focus of the Hemmings' Lab. S1P has been shown to play various roles in pregnancy including ovarian function. In pregnant rats, S1P was shown to prevent the apoptosis of luteal cells (cells in the corpus luteum) mediated by caspase or PGF2α. S1P also maintains normal blood vessel density (number of vessels per area) in the corpus luteum [699,838,839]. S1P is also involved in implantation, immune function during pregnancy, placentation and delivery [840,841]. We have also shown that S1P controls vascular tone mediated through the Rho-kinase and the NO-mediated pathways in human

placental arteries isolated from the chorionic plate and stem villi [473]. However, the role of S1P in controlling endothelial barrier and the impact on vascular tone in pregnancy remains to be demonstrated. While I showed that in mouse uterine and mesenteric arteries, TXA_2-induced endothelial permeability and/or vascular tone is mediated through the S1P pathway, because of the great vascular changes that occur during pregnancy, experiments will need to be repeated to confirm whether such a pathway still operates following pregnancy. Since this thesis also establishes a link between CMV infection and S1P/TXA_2-induced vascular tone, further studies should evaluate the impact of CMV infection on the S1P (TXA_2)-mediated control of endothelial barrier and vascular tone in pregnancy.

BIBLIOGRAPHY

1 Camp SM, Chiang ET, Sun C, Usatyuk PV, Bittman R, Natarajan V, Garcia JG, Dudek SM: Reprint of "Pulmonary endothelial cell barrier enhancement by novel fty720 analogs: Methoxy-fty720, fluoro-fty720, and beta-glucuronide-fty720". Chem Phys Lipids 2015.

2 Dudek SM, Camp SM, Chiang ET, Singleton PA, Usatyuk PV, Zhao Y, Natarajan V, Garcia JG: Pulmonary endothelial cell barrier enhancement by fty720 does not require the s1p1 receptor. Cell Signal 2007;19:1754-1764.

3 Natarajan V, Dudek SM, Jacobson JR, Moreno-Vinasco L, Huang LS, Abassi T, Mathew B, Zhao Y, Wang L, Bittman R, Weichselbaum R, Berdyshev E, Garcia JG: Sphingosine-1-phosphate, fty720, and sphingosine-1-phosphate receptors in the pathobiology of acute lung injury. Am J Respir Cell Mol Biol 2013;49:6-17.

4 Camp SM, Bittman R, Chiang ET, Moreno-Vinasco L, Mirzapoiazova T, Sammani S, Lu X, Sun C, Harbeck M, Roe M, Natarajan V, Garcia JG, Dudek SM: Synthetic analogs of fty720 [2-amino-2-(2-[4-octylphenyl]ethyl)-1,3-propanediol] differentially regulate pulmonary vascular permeability in vivo and in vitro. J Pharmacol Exp Ther 2009;331:54-64.

5 Wang MJ, Huang Y, Huang RY, Chen XM, Zhou YY, Yu WL, Chu YL, Huang QC: Determination of role of thromboxane a2 in rheumatoid arthritis. Discov Med 2015;19:23-32.

6 Montalescot G, Lowenstein E, Ogletree ML, Greene EM, Robinson DR, Hartl K, Zapol WM: Thromboxane receptor blockade prevents pulmonary hypertension induced by heparin-protamine reactions in awake sheep. Circulation 1990;82:1765-1777.

7 Egan KM, Wang M, Fries S, Lucitt MB, Zukas AM, Pure E, Lawson JA, FitzGerald GA: Cyclooxygenases, thromboxane, and atherosclerosis: Plaque destabilization by cyclooxygenase-2 inhibition combined with thromboxane receptor antagonism. Circulation 2005;111:334-342.

8 Kim SR, Bae SK, Park HJ, Kim MK, Kim K, Park SY, Jang HO, Yun I, Kim YJ, Yoo MA, Bae MK: Thromboxane a(2) increases endothelial permeability through upregulation of interleukin-8. Biochem Biophys Res Commun 2010;397:413-419.

9 Salvadori M, Budde K, Charpentier B, Klempnauer J, Nashan B, Pallardo LM, Eris J, Schena FP, Eisenberger U, Rostaing L, Hmissi A, Aradhye S: Fty720 versus mmf with cyclosporine in de novo renal transplantation: A 1-year, randomized controlled trial in europe and australasia. Am J Transplant 2006;6:2912-2921.

10 Deanfield JE, Halcox JP, Rabelink TJ: Endothelial function and dysfunction: Testing and clinical relevance. Circulation 2007;115:1285-1295.

11 Stenmark KR, Yeager ME, El Kasmi KC, Nozik-Grayck E, Gerasimovskaya EV, Li M, Riddle SR, Frid MG: The adventitia: Essential regulator of vascular wall structure and function. Annu Rev Physiol 2013;75:23-47.

12 Drummond HA, Grifoni SC, Jernigan NL: A new trick for an old dogma: Enac proteins as mechanotransducers in vascular smooth muscle. Physiology (Bethesda) 2008;23:23-31.

13 Dube S, Canty JM, Jr.: Shear stress-induced vasodilation in porcine coronary conduit arteries is independent of nitric oxide release. Am J Physiol Heart Circ Physiol 2001;280:H2581-2590.

14 Davis MJ: Myogenic response gradient in an arteriolar network. Am J Physiol 1993;264:H2168-2179.

15 Calo LA: Vascular tone control in humans: Insights from studies in bartter's/gitelman's syndromes. Kidney Int 2006;69:963-966.
16 Folkow B: Role of the nervous system in the control of vascular tone. Circulation 1960;21:760-768.
17 Durand MJ, Gutterman DD: Diversity in mechanisms of endothelium-dependent vasodilation in health and disease. Microcirculation 2013;20:239-247.
18 Mutchler SM, Straub AC: Compartmentalized nitric oxide signaling in the resistance vasculature. Nitric Oxide 2015;49:8-15.
19 Webb RC: Smooth muscle contraction and relaxation. Adv Physiol Educ 2003;27:201-206.
20 Campbell WB, Fleming I: Epoxyeicosatrienoic acids and endothelium-dependent responses. Pflugers Arch 2010;459:881-895.
21 Morton JS, Davidge ST: Arterial endothelium-derived hyperpolarization: Potential role in pregnancy adaptations and complications. J Cardiovasc Pharmacol 2013;61:197-203.
22 Ellinsworth DC, Shukla N, Fleming I, Jeremy JY: Interactions between thromboxane a(2), thromboxane/prostaglandin (tp) receptors, and endothelium-derived hyperpolarization. Cardiovasc Res 2014;102:9-16.
23 Stoner L, Erickson ML, Young JM, Fryer S, Sabatier MJ, Faulkner J, Lambrick DM, McCully KK: There's more to flow-mediated dilation than nitric oxide. J Atheroscler Thromb 2012;19:589-600.
24 Bagher P, Segal SS: Regulation of blood flow in the microcirculation: Role of conducted vasodilation. Acta Physiol (Oxf) 2011;202:271-284.
25 Norel X: Prostanoid receptors in the human vascular wall. ScientificWorldJournal 2007;7:1359-1374.
26 Baber SR, Deng W, Rodriguez J, Master RG, Bivalacqua TJ, Hyman AL, Kadowitz PJ: Vasoactive prostanoids are generated from arachidonic acid by cox-1 and cox-2 in the mouse. Am J Physiol Heart Circ Physiol 2005;289:H1476-1487.
27 Murray KJ: Cyclic amp and mechanisms of vasodilation. Pharmacol Ther 1990;47:329-345.
28 Albertini M, Vanelli G, Clement MG: Pgi2 and nitric oxide involvement in the regulation of systemic and pulmonary basal vascular tone in the pig. Prostaglandins Leukot Essent Fatty Acids 1996;54:273-278.
29 Palmer RM, Ashton DS, Moncada S: Vascular endothelial cells synthesize nitric oxide from l-arginine. Nature 1988;333:664-666.
30 Sessa WC: Molecular control of blood flow and angiogenesis: Role of nitric oxide. J Thromb Haemost 2009;7 Suppl 1:35-37.
31 Inazu M, Zhang H, Daniel EE: Properties of the lp-805-induced potassium currents in cultured bovine pulmonary artery endothelial cells. J Pharmacol Exp Ther 1994;268:403-408.
32 Morris AJ, Panchatcharam M, Cheng HY, Federico L, Fulkerson Z, Selim S, Miriyala S, Escalante-Alcalde D, Smyth SS: Regulation of blood and vascular cell function by bioactive lysophospholipids. J Thromb Haemost 2009;7 Suppl 1:38-43.
33 Igarashi J, Bernier SG, Michel T: Sphingosine 1-phosphate and activation of endothelial nitric-oxide synthase. Differential regulation of akt and map kinase pathways by edg and bradykinin receptors in vascular endothelial cells. J Biol Chem 2001;276:12420-12426.

34 Igarashi J, Michel T: Sphingosine-1-phosphate and modulation of vascular tone. Cardiovasc Res 2009;82:212-220.
35 Balligand JL, Feron O, Dessy C: Enos activation by physical forces: From short-term regulation of contraction to chronic remodeling of cardiovascular tissues. Physiol Rev 2009;89:481-534.
36 Cohen RA, Vanhoutte PM: Endothelium-dependent hyperpolarization. Beyond nitric oxide and cyclic gmp. Circulation 1995;92:3337-3349.
37 Hoepfl B, Rodenwaldt B, Pohl U, De Wit C: Edhf, but not no or prostaglandins, is critical to evoke a conducted dilation upon ach in hamster arterioles. Am J Physiol Heart Circ Physiol 2002;283:H996-H1004.
38 Fichtlscherer S, Dimmeler S, Breuer S, Busse R, Zeiher AM, Fleming I: Inhibition of cytochrome p450 2c9 improves endothelium-dependent, nitric oxide-mediated vasodilatation in patients with coronary artery disease. Circulation 2004;109:178-183.
39 Fleming I: Cytochrome p450 epoxygenases as edhf synthase(s). Pharmacol Res 2004;49:525-533.
40 Michaelis UR, Falck JR, Schmidt R, Busse R, Fleming I: Cytochrome p4502c9-derived epoxyeicosatrienoic acids induce the expression of cyclooxygenase-2 in endothelial cells. Arterioscler Thromb Vasc Biol 2005;25:321-326.
41 Papaioannou TG, Stefanadis C: Vascular wall shear stress: Basic principles and methods. Hellenic J Cardiol 2005;46:9-15.
42 Jufri NF, Mohamedali A, Avolio A, Baker MS: Mechanical stretch: Physiological and pathological implications for human vascular endothelial cells. Vasc Cell 2015;7:8.
43 Fisslthaler B, Popp R, Michaelis UR, Kiss L, Fleming I, Busse R: Cyclic stretch enhances the expression and activity of coronary endothelium-derived hyperpolarizing factor synthase. Hypertension 2001;38:1427-1432.
44 Popp R, Fleming I, Busse R: Pulsatile stretch in coronary arteries elicits release of endothelium-derived hyperpolarizing factor: A modulator of arterial compliance. Circ Res 1998;82:696-703.
45 Korthuis RJ: Skeletal muscle circulation. 2011.
46 Landeen LK, Dederko DA, Kondo CS, Hu BS, Aroonsakool N, Haga JH, Giles WR: Mechanisms of the negative inotropic effects of sphingosine-1-phosphate on adult mouse ventricular myocytes. Am J Physiol Heart Circ Physiol 2008;294:H736-749.
47 Wang R: Gasotransmitters: Growing pains and joys. Trends Biochem Sci 2014;39:227-232.
48 Durante W: Carbon monoxide and bile pigments: Surprising mediators of vascular function. Vasc Med 2002;7:195-202.
49 Durante W, Johnson FK, Johnson RA: Role of carbon monoxide in cardiovascular function. J Cell Mol Med 2006;10:672-686.
50 Durante W: Targeting heme oxygenase-1 in vascular disease. Curr Drug Targets 2010;11:1504-1516.
51 Kimura H: Hydrogen sulfide: Its production, release and functions. Amino Acids 2011;41:113-121.
52 Shibuya N, Tanaka M, Yoshida M, Ogasawara Y, Togawa T, Ishii K, Kimura H: 3-mercaptopyruvate sulfurtransferase produces hydrogen sulfide and bound sulfane sulfur in the brain. Antioxid Redox Signal 2009;11:703-714.

53 Chiku T, Padovani D, Zhu W, Singh S, Vitvitsky V, Banerjee R: H2s biogenesis by human cystathionine gamma-lyase leads to the novel sulfur metabolites lanthionine and homolanthionine and is responsive to the grade of hyperhomocysteinemia. J Biol Chem 2009;284:11601-11612.
54 Singh S, Padovani D, Leslie RA, Chiku T, Banerjee R: Relative contributions of cystathionine beta-synthase and gamma-cystathionase to h2s biogenesis via alternative trans-sulfuration reactions. J Biol Chem 2009;284:22457-22466.
55 Beltowski J, Jamroz-Wisniewska A: Hydrogen sulfide and endothelium-dependent vasorelaxation. Molecules 2014;19:21183-21199.
56 Wang R: Signaling pathways for the vascular effects of hydrogen sulfide. Curr Opin Nephrol Hypertens 2011;20:107-112.
57 Beach JM, McGahren ED, Duling BR: Capillaries and arterioles are electrically coupled in hamster cheek pouch. Am J Physiol 1998;275:H1489-1496.
58 De Wit C: Connexins pave the way for vascular communication. News Physiol Sci 2004;19:148-153.
59 de Wit C: Different pathways with distinct properties conduct dilations in the microcirculation in vivo. Cardiovasc Res 2010;85:604-613.
60 McSherry IN, Sandow SL, Campbell WB, Falck JR, Hill MA, Dora KA: A role for heterocellular coupling and eets in dilation of rat cremaster arteries. Microcirculation 2006;13:119-130.
61 Heberlein KR, Straub AC, Best AK, Greyson MA, Looft-Wilson RC, Sharma PR, Meher A, Leitinger N, Isakson BE: Plasminogen activator inhibitor-1 regulates myoendothelial junction formation. Circ Res 2010;106:1092-1102.
62 Isakson BE: Localized expression of an ins(1,4,5)p3 receptor at the myoendothelial junction selectively regulates heterocellular ca2+ communication. J Cell Sci 2008;121:3664-3673.
63 Isakson BE, Ramos SI, Duling BR: Ca2+ and inositol 1,4,5-trisphosphate-mediated signaling across the myoendothelial junction. Circ Res 2007;100:246-254.
64 Isakson BE, Damon DN, Day KH, Liao Y, Duling BR: Connexin40 and connexin43 in mouse aortic endothelium: Evidence for coordinated regulation. Am J Physiol Heart Circ Physiol 2006;290:H1199-1205.
65 Isakson BE, Duling BR: Heterocellular contact at the myoendothelial junction influences gap junction organization. Circ Res 2005;97:44-51.
66 Billaud M, Lohman AW, Straub AC, Looft-Wilson R, Johnstone SR, Araj CA, Best AK, Chekeni FB, Ravichandran KS, Penuela S, Laird DW, Isakson BE: Pannexin1 regulates alpha1-adrenergic receptor- mediated vasoconstriction. Circ Res 2011;109:80-85.
67 Emerson GG, Neild TO, Segal SS: Conduction of hyperpolarization along hamster feed arteries: Augmentation by acetylcholine. Am J Physiol Heart Circ Physiol 2002;283:H102-109.
68 Murrant CL, Sarelius IH: Multiple dilator pathways in skeletal muscle contraction-induced arteriolar dilations. Am J Physiol Regul Integr Comp Physiol 2002;282:R969-978.
69 Murrant CL, Sarelius IH: Local and remote arteriolar dilations initiated by skeletal muscle contraction. Am J Physiol Heart Circ Physiol 2000;279:H2285-2294.
70 Segal SS: Regulation of blood flow in the microcirculation. Microcirculation 2005;12:33-45.

71 Dora KA, Gallagher NT, McNeish A, Garland CJ: Modulation of endothelial cell kca3.1 channels during endothelium-derived hyperpolarizing factor signaling in mesenteric resistance arteries. Circ Res 2008;102:1247-1255.

72 Tallini YN, Brekke JF, Shui B, Doran R, Hwang SM, Nakai J, Salama G, Segal SS, Kotlikoff MI: Propagated endothelial ca2+ waves and arteriolar dilation in vivo: Measurements in cx40bac gcamp2 transgenic mice. Circ Res 2007;101:1300-1309.

73 Uhrenholt TR, Domeier TL, Segal SS: Propagation of calcium waves along endothelium of hamster feed arteries. Am J Physiol Heart Circ Physiol 2007;292:H1634-1640.

74 Emerson GG, Segal SS: Endothelial cell pathway for conduction of hyperpolarization and vasodilation along hamster feed artery. Circ Res 2000;86:94-100.

75 Lincoln TM, Dey N, Sellak H: Invited review: Cgmp-dependent protein kinase signaling mechanisms in smooth muscle: From the regulation of tone to gene expression. J Appl Physiol (1985) 2001;91:1421-1430.

76 Somlyo AP, Somlyo AV: Signal transduction and regulation in smooth muscle. Nature 1994;372:231-236.

77 Somlyo AV: New roads leading to ca2+ sensitization. Circ Res 2002;91:83-84.

78 Jackson WF: Ion channels and vascular tone. Hypertension 2000;35:173-178.

79 Forrest AS, Angermann JE, Raghunathan R, Lachendro C, Greenwood IA, Leblanc N: Intricate interaction between store-operated calcium entry and calcium-activated chloride channels in pulmonary artery smooth muscle cells. Adv Exp Med Biol 2010;661:31-55.

80 Jakoubek V, Bibova J, Hampl V: Voltage-gated calcium channels mediate hypoxic vasoconstriction in the human placenta. Placenta 2006;27:1030-1033.

81 Van Aelst L, D'Souza-Schorey C: Rho gtpases and signaling networks. Genes Dev 1997;11:2295-2322.

82 Schmidt A, Hall A: Guanine nucleotide exchange factors for rho gtpases: Turning on the switch. Genes Dev 2002;16:1587-1609.

83 Lai A, Frishman WH: Rho-kinase inhibition in the therapy of cardiovascular disease. Cardiol Rev 2005;13:285-292.

84 Bayliss WM: On the local reactions of the arterial wall to changes of internal pressure. J Physiol 1902;28:220-231.

85 Davis MJ, Hill MA: Signaling mechanisms underlying the vascular myogenic response. Physiol Rev 1999;79:387-423.

86 Yang J, Noyan-Ashraf MH, Meissner A, Voigtlaender-Bolz J, Kroetsch JT, Foltz W, Jaffray D, Kapoor A, Momen A, Heximer SP, Zhang H, van Eede M, Henkelman RM, Matthews SG, Lidington D, Husain M, Bolz SS: Proximal cerebral arteries develop myogenic responsiveness in heart failure via tumor necrosis factor-alpha-dependent activation of sphingosine-1-phosphate signaling. Circulation 2012;126:196-206.

87 Lim M, Choi SK, Cho YE, Yeon SI, Kim EC, Ahn DS, Lee YH: The role of sphingosine kinase 1/sphingosine-1-phosphate pathway in the myogenic tone of posterior cerebral arteries. PLoS One 2012;7:e35177.

88 Lidington D, Peter BF, Meissner A, Kroetsch JT, Pitson SM, Pohl U, Bolz SS: The phosphorylation motif at serine 225 governs the localization and function of sphingosine kinase 1 in resistance arteries. Arterioscler Thromb Vasc Biol 2009;29:1916-1922.

89 Peter BF, Lidington D, Harada A, Bolz HJ, Vogel L, Heximer S, Spiegel S, Pohl U, Bolz SS: Role of sphingosine-1-phosphate phosphohydrolase 1 in the regulation of resistance artery tone. Circ Res 2008;103:315-324.

90 Bolz SS, Vogel L, Sollinger D, Derwand R, Boer C, Pitson SM, Spiegel S, Pohl U: Sphingosine kinase modulates microvascular tone and myogenic responses through activation of rhoa/rho kinase. Circulation 2003;108:342-347.
91 Baylie RL, Brayden JE: Trpv channels and vascular function. Acta Physiol (Oxf) 2010;203:99-116.
92 Muraki K, Shigekawa M, Imaizumi Y: A new insight into the function of trpv2 in circulatory organs. 2007.
93 Patel A, Sharif-Naeini R, Folgering JR, Bichet D, Duprat F, Honore E: Canonical trp channels and mechanotransduction: From physiology to disease states. Pflugers Arch 2011;460:571-581.
94 Earley S, Brayden JE: Transient receptor potential channels and vascular function. Clin Sci (Lond) 2010;119:19-36.
95 Feletou M, Vanhoutte PM: Endothelium-derived hyperpolarizing factor: Where are we now? Arterioscler Thromb Vasc Biol 2006;26:1215-1225.
96 Durnin L, Hwang SJ, Kurahashi M, Drumm BT, Ward SM, Sasse KC, Sanders KM, Mutafova-Yambolieva VN: Uridine adenosine tetraphosphate is a novel neurogenic p2y1 receptor activator in the gut. Proc Natl Acad Sci U S A 2014;111:15821-15826.
97 Zhou Z, Sun C, Tilley SL, Mustafa SJ: Mechanisms underlying uridine adenosine tetraphosphate-induced vascular contraction in mouse aorta: Role of thromboxane and purinergic receptors. Vascul Pharmacol 2015;73:78-85.
98 Kaczmarek-Hajek K, Lorinczi E, Hausmann R, Nicke A: Molecular and functional properties of p2x receptors--recent progress and persisting challenges. Purinergic Signal 2012;8:375-417.
99 North RA: Molecular physiology of p2x receptors. Physiol Rev 2002;82:1013-1067.
100 Burnstock G: Introduction to purinergic signalling in the brain. Adv Exp Med Biol 2013;986:1-12.
101 Ma YH, Gebremedhin D, Schwartzman ML, Falck JR, Clark JE, Masters BS, Harder DR, Roman RJ: 20-hydroxyeicosatetraenoic acid is an endogenous vasoconstrictor of canine renal arcuate arteries. Circ Res 1993;72:126-136.
102 Hoopes SL, Garcia V, Edin ML, Schwartzman ML, Zeldin DC: Vascular actions of 20-hete. Prostaglandins Other Lipid Mediat 2015;120:9-16.
103 Brenner B, Harney JT, Ahmed BA, Jeffus BC, Unal R, Mehta JL, Kilic F: Plasma serotonin levels and the platelet serotonin transporter. J Neurochem 2007;102:206-215.
104 Mercado CP, Kilic F: Molecular mechanisms of sert in platelets: Regulation of plasma serotonin levels. Mol Interv 2010;10:231-241.
105 Nasa Y, Kume H, Takeo S: Acetylcholine-induced vasoconstrictor response of coronary vessels in rats: A possible contribution of m2 muscarinic receptor activation. Heart Vessels 1997;12:179-191.
106 Ton QV, Hammes SR: Recent insights on circulating catecholamines in hypertension. Curr Hypertens Rep 2014;16:498.
107 Levkau B: Sphingosine-1-phosphate in the regulation of vascular tone: A finely tuned integration system of s1p sources, receptors, and vascular responsiveness. Circ Res 2008;103:231-233.
108 Ni W, Geddes TJ, Priestley JR, Szasz T, Kuhn DM, Watts SW: The existence of a local 5-hydroxytryptaminergic system in peripheral arteries. Br J Pharmacol 2008;154:663-674.

109 Ni W, Thompson JM, Northcott CA, Lookingland K, Watts SW: The serotonin transporter is present and functional in peripheral arterial smooth muscle. J Cardiovasc Pharmacol 2004;43:770-781.
110 Ni W, Watts SW: 5-hydroxytryptamine in the cardiovascular system: Focus on the serotonin transporter (sert). Clin Exp Pharmacol Physiol 2006;33:575-583.
111 Wakayama K, Ohtsuki S, Takanaga H, Hosoya K, Terasaki T: Localization of norepinephrine and serotonin transporter in mouse brain capillary endothelial cells. Neurosci Res 2002;44:173-180.
112 MacLean MR, Dempsie Y: Serotonin and pulmonary hypertension--from bench to bedside? Curr Opin Pharmacol 2009;9:281-286.
113 Yildiz O, Smith JR, Purdy RE: Serotonin and vasoconstrictor synergism. Life Sci 1998;62:1723-1732.
114 Nakayama K, Ishigai Y, Uchida H, Tanaka Y: Synergistic coronary vasoconstriction produced by endothelin-1 in combination with 5-hydroxytryptamine. J Cardiovasc Pharmacol 1991;17 Suppl 7:S179-181.
115 Young MS, Iwanov V, Moulds RF: Interaction between platelet-released serotonin and thromboxane a2 on human digital arteries. Clin Exp Pharmacol Physiol 1986;13:143-152.
116 Xiao XH, Rand MJ: Amplification by serotonin of responses to other vasoconstrictor agents in the rat tail artery. Clin Exp Pharmacol Physiol 1989;16:725-736.
117 Bhaskaran S, Zaluski J, Banes-Berceli A: Molecular interactions of serotonin (5-ht) and endothelin-1 in vascular smooth muscle cells: In vitro and ex vivo analyses. Am J Physiol Cell Physiol 2014;306:C143-151.
118 Samarska IV, Bouma HR, Buikema H, Mungroop HE, Houwertjes MC, Absalom AR, Epema AH, Henning RH: S1p1 receptor modulation preserves vascular function in mesenteric and coronary arteries after cpb in the rat independent of depletion of lymphocytes. PLoS One 2014;9:e97196.
119 Watanabe S, Matsumoto T, Oda M, Yamada K, Takagi J, Taguchi K, Kobayashi T: Insulin augments serotonin-induced contraction via activation of the ir/pi3k/pdk1 pathway in the rat carotid artery. Pflugers Arch 2015.
120 Smid M, Husek P: Vasoconstrictor reaction to prostaglandins e1 and e2 in the isolated rat hindlimb mediated through serotonin release. Eur J Pharmacol 1993;230:69-76.
121 Hirafuji M, Hamaya Y, Matsumoto Y, Machida T, Minami M, Kohno T, Igarashi Y: [modulation of sphingosine 1-phosphate, a new lipid mediator, on nitric oxide production by vascular smooth muscle cells]. Nippon Yakurigaku Zasshi - Folia Pharmacologica Japonica 2002;120:70P-72P.
122 Dantas AP, Igarashi J, Michel T: Sphingosine 1-phosphate and control of vascular tone. American Journal of Physiology - Heart & Circulatory Physiology 2003;284:H2045-2052.
123 Sugo S, Minamino N, Shoji H, Isumi Y, Nakao K, Kangawa K, Matsuo H: Regulation of endothelin-1 production in cultured rat vascular smooth muscle cells. J Cardiovasc Pharmacol 2001;37:25-40.
124 Seol HJ, Oh MJ, Kim HJ: Endothelin-1 expression by vascular endothelial growth factor in human umbilical vein endothelial cells and aortic smooth muscle cells. Hypertens Pregnancy 2011;30:295-301.
125 Alexander SP, Mathie A, Peters JA: Guide to receptors and channels (grac), 5th edition. Br J Pharmacol 2011;164 Suppl 1:S1-324.

126 Rubanyi GM, Polokoff MA: Endothelins: Molecular biology, biochemistry, pharmacology, physiology, and pathophysiology. Pharmacol Rev 1994;46:325-415.
127 Korth P, Bohle RM, Corvol P, Pinet F: Cellular distribution of endothelin-converting enzyme-1 in human tissues. J Histochem Cytochem 1999;47:447-462.
128 Kawanabe Y, Nauli SM: Endothelin. Cell Mol Life Sci 2011;68:195-203.
129 Bourque SL, Davidge ST, Adams MA: The interaction between endothelin-1 and nitric oxide in the vasculature: New perspectives. Am J Physiol Regul Integr Comp Physiol 2011;300:R1288-1295.
130 Bourque SL, Whittingham HA, Brien SE, Davidge ST, Adams MA: Role of endothelin-1 in the hyper-responsiveness to nitrovasodilators following acute nos inhibition. Br J Pharmacol 2012;165:1992-1999.
131 Abdalvand A, Morton JS, Bourque SL, Quon AL, Davidge ST: Matrix metalloproteinase enhances big-endothelin-1 constriction in mesenteric vessels of pregnant rats with reduced uterine blood flow. Hypertension 2013;61:488-493.
132 Leiber D, Banno Y, Tanfin Z: Exogenous sphingosine 1-phosphate and sphingosine kinase activated by endothelin-1 induced myometrial contraction through differential mechanisms. Am J Physiol Cell Physiol 2007;292:C240-250.
133 Arvidsson K, Nemoto T, Mitsui Y, Ohashi S, Nakanishi H: The solution structure of human endothelin-2 a 1h-nmr and cd study. Eur J Biochem 1998;257:380-388.
134 Ling L, Maguire JJ, Davenport AP: Endothelin-2, the forgotten isoform: Emerging role in the cardiovascular system, ovarian development, immunology and cancer. Br J Pharmacol 2012;168:283-295.
135 Davenport AP, Maguire JJ: Endothelin. Handb Exp Pharmacol 2006:295-329.
136 Montani D, Souza R, Binkert C, Fischli W, Simonneau G, Clozel M, Humbert M: Endothelin-1/endothelin-3 ratio: A potential prognostic factor of pulmonary arterial hypertension. Chest 2007;131:101-108.
137 Maguire JJ, Davenport AP: Eta receptor-mediated constrictor responses to endothelin peptides in human blood vessels in vitro. Br J Pharmacol 1995;115:191-197.
138 Matsumoto H, Suzuki N, Onda H, Fujino M: Abundance of endothelin-3 in rat intestine, pituitary gland and brain. Biochem Biophys Res Commun 1989;164:74-80.
139 Carrier GO, Fuchs LC, Winecoff AP, Giulumian AD, White RE: Nitrovasodilators relax mesenteric microvessels by cgmp-induced stimulation of ca-activated k channels. Am J Physiol 1997;273:H76-84.
140 de Wit C, Wolfle SE: Edhf and gap junctions: Important regulators of vascular tone within the microcirculation. Curr Pharm Biotechnol 2007;8:11-25.
141 de Wit C, Wolfle SE, Hopfl B: Connexin-dependent communication within the vascular wall: Contribution to the control of arteriolar diameter. Adv Cardiol 2006;42:268-283.
142 Gutterman DD, Miura H, Liu Y: Redox modulation of vascular tone: Focus of potassium channel mechanisms of dilation. Arterioscler Thromb Vasc Biol 2005;25:671-678.
143 Hertel RF: Potassium channel activation improves blood flow pattern of conscious rats in cutaneous microcirculation. Clin Exp Pharmacol Physiol 1992;19:243-248.
144 Dellsperger KC: Potassium channels and the coronary circulation. Clin Exp Pharmacol Physiol 1996;23:1096-1101.
145 Jackson WF: Potassium channels in the peripheral microcirculation. Microcirculation 2005;12:113-127.

146 Brayden JE: Potassium channels in vascular smooth muscle. Clin Exp Pharmacol Physiol 1996;23:1069-1076.
147 Quayle JM, Nelson MT, Standen NB: Atp-sensitive and inwardly rectifying potassium channels in smooth muscle. Physiol Rev 1997;77:1165-1232.
148 Sinoway LI, Hendrickson C, Davidson WR, Jr., Prophet S, Zelis R: Characteristics of flow-mediated brachial artery vasodilation in human subjects. Circ Res 1989;64:32-42.
149 Falcone JC, Kuo L, Meininger GA: Endothelial cell calcium increases during flow-induced dilation in isolated arterioles. Am J Physiol 1993;264:H653-659.
150 Fujii K, Heistad DD, Faraci FM: Flow-mediated dilatation of the basilar artery in vivo. Circ Res 1991;69:697-705.
151 Smiesko V, Lang DJ, Johnson PC: Dilator response of rat mesenteric arcading arterioles to increased blood flow velocity. Am J Physiol 1989;257:H1958-1965.
152 Viswanathan M, Rivera O, Short BL: Heat shock protein 90 is involved in pulsatile flow-induced dilation of rat middle cerebral artery. J Vasc Res 1999;36:524-527.
153 Duncker DJ, Bache RJ: Regulation of coronary blood flow during exercise. Physiol Rev 2008;88:1009-1086.
154 Hudlicka O, Brown MD: Adaptation of skeletal muscle microvasculature to increased or decreased blood flow: Role of shear stress, nitric oxide and vascular endothelial growth factor. J Vasc Res 2009;46:504-512.
155 Koller A, Kaley G: Flow velocity-dependent regulation of microvascular resistance in vivo. Microcirc Endothelium Lymphatics 1989;5:519-529.
156 Koller A, Kaley G: Endothelial regulation of wall shear stress and blood flow in skeletal muscle microcirculation. Am J Physiol 1991;260:H862-868.
157 Hull SS, Jr., Kaiser L, Jaffe MD, Sparks HV, Jr.: Endothelium-dependent flow-induced dilation of canine femoral and saphenous arteries. Blood Vessels 1986;23:183-198.
158 Kuo L, Chilian WM, Davis MJ: Interaction of pressure- and flow-induced responses in porcine coronary resistance vessels. Am J Physiol 1991;261:H1706-1715.
159 Lie M, Sejersted OM, Kiil F: Local regulation of vascular cross section during changes in femoral arterial blood flow in dogs. Circ Res 1970;27:727-737.
160 Rubanyi GM, Romero JC, Vanhoutte PM: Flow-induced release of endothelium-derived relaxing factor. Am J Physiol 1986;250:H1145-1149.
161 Shi ZD, Tarbell JM: Fluid flow mechanotransduction in vascular smooth muscle cells and fibroblasts. Ann Biomed Eng 2011;39:1608-1619.
162 Nakayama K, Tanaka Y: Stretch-induced contraction and ca2+ mobilization in vascular smooth muscle. Biol Signals 1993;2:241-252.
163 Thodeti CK, Matthews B, Ravi A, Mammoto A, Ghosh K, Bracha AL, Ingber DE: Trpv4 channels mediate cyclic strain-induced endothelial cell reorientation through integrin-to-integrin signaling. Circ Res 2009;104:1123-1130.
164 Naruse K, Yamada T, Sokabe M: Involvement of sa channels in orienting response of cultured endothelial cells to cyclic stretch. Am J Physiol 1998;274:H1532-1538.
165 Franchi-Micheli S, Failli P, Mazzetti L, Bani D, Ciuffi M, Zilletti L: Mechanical stretch reveals different components of endothelial-mediated vascular tone in rat aortic strips. Br J Pharmacol 2000;131:1355-1362.

166 Adapala RK, Talasila PK, Bratz IN, Zhang DX, Suzuki M, Meszaros JG, Thodeti CK: Pkcalpha mediates acetylcholine-induced activation of trpv4-dependent calcium influx in endothelial cells. Am J Physiol Heart Circ Physiol 2011;301:H757-765.

167 Berrout J, Jin M, O'Neil RG: Critical role of trpp2 and trpc1 channels in stretch-induced injury of blood-brain barrier endothelial cells. Brain Res 2012;1436:1-12.

168 Guyenet PG: The sympathetic control of blood pressure. Nat Rev Neurosci 2006;7:335-346.

169 Dinenno FA, Joyner MJ: Alpha-adrenergic control of skeletal muscle circulation at rest and during exercise in aging humans. Microcirculation 2006;13:329-341.

170 Knight DS, Ellison JP, Hibbs RG, Hyman AL, Kadowitz PJ: A light and electron microscopic study of the innervation of pulmonary arteries in the cat. Anat Rec 1981;201:513-521.

171 Raven PB: Recent advances in baroreflex control of blood pressure during exercise in humans: An overview. Med Sci Sports Exerc 2008;40:2033-2036.

172 Petrof BJ: Molecular pathophysiology of myofiber injury in deficiencies of the dystrophin-glycoprotein complex. Am J Phys Med Rehabil 2002;81:S162-174.

173 Escourrou P, Raffestin B, Papelier Y, Pussard E, Rowell LB: Cardiopulmonary and carotid baroreflex control of splanchnic and forearm circulations. Am J Physiol 1993;264:H777-782.

174 Remuzzi G, Perico N, Macia M, Ruggenenti P: The role of renin-angiotensin-aldosterone system in the progression of chronic kidney disease. Kidney Int Suppl 2005:S57-65.

175 Thatcher S, Yiannikouris F, Gupte M, Cassis L: The adipose renin-angiotensin system: Role in cardiovascular disease. Mol Cell Endocrinol 2009;302:111-117.

176 Dendorfer A, Thornagel A, Raasch W, Grisk O, Tempel K, Dominiak P: Angiotensin ii induces catecholamine release by direct ganglionic excitation. Hypertension 2002;40:348-354.

177 Noshiro T, Shimizu K, Way D, Miura Y, McGrath BP: Angiotensin ii enhances norepinephrine spillover during sympathetic activation in conscious rabbits. Am J Physiol 1994;266:H1864-1871.

178 Fabiani ME, Sourial M, Thomas WG, Johnston CI, Johnston CI, Frauman AG: Angiotensin ii enhances noradrenaline release from sympathetic nerves of the rat prostate via a novel angiotensin receptor: Implications for the pathophysiology of benign prostatic hyperplasia. J Endocrinol 2001;171:97-108.

179 Wilson PC, Fitzgibbon WR, Garrett SM, Jaffa AA, Luttrell LM, Brands MW, El-Shewy HM: Inhibition of sphingosine kinase 1 ameliorates angiotensin ii-induced hypertension and inhibits transmembrane calcium entry via store-operated calcium channel. Mol Endocrinol 2015;29:896-908.

180 Lassegue B, Griendling KK: Nadph oxidases: Functions and pathologies in the vasculature. Arterioscler Thromb Vasc Biol 2010;30:653-661.

181 Chidlow JH, Jr., Sessa WC: Caveolae, caveolins, and cavins: Complex control of cellular signalling and inflammation. Cardiovasc Res 2010;86:219-225.

182 Komarova Y, Malik AB: Regulation of endothelial permeability via paracellular and transcellular transport pathways. Annu Rev Physiol 2010;72:463-493.

183 Mehta D, Malik AB: Signaling mechanisms regulating endothelial permeability. Physiol Rev 2006;86:279-367.

184 Michel CC, Curry FE: Microvascular permeability. Physiol Rev 1999;79:703-761.

185 Predescu SA, Predescu DN, Malik AB: Molecular determinants of endothelial transcytosis and their role in endothelial permeability. Am J Physiol Lung Cell Mol Physiol 2007;293:L823-842.

186 Hu G, Minshall RD: Regulation of transendothelial permeability by src kinase. Microvasc Res 2009;77:21-25.

187 Minshall RD, Tiruppathi C, Vogel SM, Niles WD, Gilchrist A, Hamm HE, Malik AB: Endothelial cell-surface gp60 activates vesicle formation and trafficking via g(i)-coupled src kinase signaling pathway. J Cell Biol 2000;150:1057-1070.

188 Vogel SM, Minshall RD, Pilipovic M, Tiruppathi C, Malik AB: Albumin uptake and transcytosis in endothelial cells in vivo induced by albumin-binding protein. Am J Physiol Lung Cell Mol Physiol 2001;281:L1512-1522.

189 Dvorak AM, Kohn S, Morgan ES, Fox P, Nagy JA, Dvorak HF: The vesiculo-vacuolar organelle (vvo): A distinct endothelial cell structure that provides a transcellular pathway for macromolecular extravasation. J Leukoc Biol 1996;59:100-115.

190 Kohn S, Nagy JA, Dvorak HF, Dvorak AM: Pathways of macromolecular tracer transport across venules and small veins. Structural basis for the hyperpermeability of tumor blood vessels. Lab Invest 1992;67:596-607.

191 Renkin EM: Cellular aspects of transvascular exchange: A 40-year perspective. Microcirculation 1994;1:157-167.

192 Carman CV, Sage PT, Sciuto TE, de la Fuente MA, Geha RS, Ochs HD, Dvorak HF, Dvorak AM, Springer TA: Transcellular diapedesis is initiated by invasive podosomes. Immunity 2007;26:784-797.

193 Carman CV, Springer TA: A transmigratory cup in leukocyte diapedesis both through individual vascular endothelial cells and between them. J Cell Biol 2004;167:377-388.

194 Predescu D, Palade GE: Plasmalemmal vesicles represent the large pore system of continuous microvascular endothelium. Am J Physiol 1993;265:H725-733.

195 Simons K, Ikonen E: Functional rafts in cell membranes. Nature 1997;387:569-572.

196 Boueiz A, Hassoun PM: Regulation of endothelial barrier function by reactive oxygen and nitrogen species. Microvasc Res 2009;77:26-34.

197 Rybin VO, Grabham PW, Elouardighi H, Steinberg SF: Caveolae-associated proteins in cardiomyocytes: Caveolin-2 expression and interactions with caveolin-3. Am J Physiol Heart Circ Physiol 2003;285:H325-332.

198 Predescu SA, Predescu DN, Palade GE: Endothelial transcytotic machinery involves supramolecular protein-lipid complexes. Mol Biol Cell 2001;12:1019-1033.

199 Sargiacomo M, Scherer PE, Tang Z, Kubler E, Song KS, Sanders MC, Lisanti MP: Oligomeric structure of caveolin: Implications for caveolae membrane organization. Proc Natl Acad Sci U S A 1995;92:9407-9411.

200 Lee H, Volonte D, Galbiati F, Iyengar P, Lublin DM, Bregman DB, Wilson MT, Campos-Gonzalez R, Bouzahzah B, Pestell RG, Scherer PE, Lisanti MP: Constitutive and growth factor-regulated phosphorylation of caveolin-1 occurs at the same site (tyr-14) in vivo: Identification of a c-src/cav-1/grb7 signaling cassette. Mol Endocrinol 2000;14:1750-1775.

201 Li S, Seitz R, Lisanti MP: Phosphorylation of caveolin by src tyrosine kinases. The alpha-isoform of caveolin is selectively phosphorylated by v-src in vivo. J Biol Chem 1996;271:3863-3868.

202 Minshall RD, Sessa WC, Stan RV, Anderson RG, Malik AB: Caveolin regulation of endothelial function. Am J Physiol Lung Cell Mol Physiol 2003;285:L1179-1183.

203 Shajahan AN, Timblin BK, Sandoval R, Tiruppathi C, Malik AB, Minshall RD: Role of src-induced dynamin-2 phosphorylation in caveolae-mediated endocytosis in endothelial cells. J Biol Chem 2004;279:20392-20400.

204 Predescu SA, Predescu DN, Timblin BK, Stan RV, Malik AB: Intersectin regulates fission and internalization of caveolae in endothelial cells. Mol Biol Cell 2003;14:4997-5010.

205 Predescu D, Horvat R, Predescu S, Palade GE: Transcytosis in the continuous endothelium of the myocardial microvasculature is inhibited by n-ethylmaleimide. Proc Natl Acad Sci U S A 1994;91:3014-3018.

206 Hu C, Ahmed M, Melia TJ, Sollner TH, Mayer T, Rothman JE: Fusion of cells by flipped snares. Science 2003;300:1745-1749.

207 Liu SM, Magnusson KE, Sundqvist T: Microtubules are involved in transport of macromolecules by vesicles in cultured bovine aortic endothelial cells. J Cell Physiol 1993;156:311-316.

208 Yui N, Lu HA, Chen Y, Nomura N, Bouley R, Brown D: Basolateral targeting and microtubule-dependent transcytosis of the aquaporin-2 water channel. Am J Physiol Cell Physiol 2013;304:C38-48.

209 Bauer PM, Yu J, Chen Y, Hickey R, Bernatchez PN, Looft-Wilson R, Huang Y, Giordano F, Stan RV, Sessa WC: Endothelial-specific expression of caveolin-1 impairs microvascular permeability and angiogenesis. Proc Natl Acad Sci U S A 2005;102:204-209.

210 Gratton JP, Bernatchez P, Sessa WC: Caveolae and caveolins in the cardiovascular system. Circ Res 2004;94:1408-1417.

211 Lin MI, Yu J, Murata T, Sessa WC: Caveolin-1-deficient mice have increased tumor microvascular permeability, angiogenesis, and growth. Cancer Res 2007;67:2849-2856.

212 Wolf MB, Watson PD: Measurement of osmotic reflection coefficient for small molecules in cat hindlimbs. Am J Physiol 1989;256:H282-290.

213 Levick JR, Michel CC: Microvascular fluid exchange and the revised starling principle. Cardiovasc Res 2010;87:198-210.

214 Fu BM, Adamson RH, Curry FE: Test of a two-pathway model for small-solute exchange across the capillary wall. Am J Physiol 1998;274:H2062-2073.

215 Tzeghai G, Weinbaum S, Pfeffer R: A steady-state filtration model for transluminal water movement in small and large blood vessels. J Biomech Eng 1985;107:123-130.

216 Mayes KR, Hodson S: Local osmotic coupling to the active trans-endothelial bicarbonate flux in the rabbit cornea. Biochim Biophys Acta 1978;514:286-293.

217 Curry FR: Microvascular solute and water transport. Microcirculation 2005;12:17-31.

218 Michiels C: Endothelial cell functions. J Cell Physiol 2003;196:430-443.

219 Simionescu N, Simionescu M, Palade GE: Open junctions in the endothelium of the postcapillary venules of the diaphragm. J Cell Biol 1978;79:27-44.

220 Hawkins BT, Davis TP: The blood-brain barrier/neurovascular unit in health and disease. Pharmacol Rev 2005;57:173-185.
221 Unterberg A, Wahl M, Baethmann A: Effects of bradykinin on permeability and diameter of pial vessels in vivo. J Cereb Blood Flow Metab 1984;4:574-585.
222 Dejana E, Giampietro C: Vascular endothelial-cadherin and vascular stability. Curr Opin Hematol 2012;19:218-223.
223 Rudini N, Dejana E: Adherens junctions. Curr Biol 2008;18:R1080-1082.
224 Piedra J, Miravet S, Castano J, Palmer HG, Heisterkamp N, Garcia de Herreros A, Dunach M: P120 catenin-associated fer and fyn tyrosine kinases regulate beta-catenin tyr-142 phosphorylation and beta-catenin-alpha-catenin interaction. Mol Cell Biol 2003;23:2287-2297.
225 Alcaide P, Newton G, Auerbach S, Sehrawat S, Mayadas TN, Golan DE, Yacono P, Vincent P, Kowalczyk A, Luscinskas FW: P120-catenin regulates leukocyte transmigration through an effect on ve-cadherin phosphorylation. Blood 2008;112:2770-2779.
226 Sallee JL, Wittchen ES, Burridge K: Regulation of cell adhesion by protein-tyrosine phosphatases: Ii. Cell-cell adhesion. J Biol Chem 2006;281:16189-16192.
227 Vincent PA, Xiao K, Buckley KM, Kowalczyk AP: Ve-cadherin: Adhesion at arm's length. Am J Physiol Cell Physiol 2004;286:C987-997.
228 Abbott NJ, Patabendige AA, Dolman DE, Yusof SR, Begley DJ: Structure and function of the blood-brain barrier. Neurobiol Dis 2010;37:13-25.
229 Vandenbroucke E, Mehta D, Minshall R, Malik AB: Regulation of endothelial junctional permeability. Ann N Y Acad Sci 2008;1123:134-145.
230 Bird IM, Boeldt DS, Krupp J, Grummer MA, Yi FX, Magness RR: Pregnancy, programming and preeclampsia: Gap junctions at the nexus of pregnancy-induced adaptation of endothelial function and endothelial adaptive failure in pe. Curr Vasc Pharmacol 2013;11:712-729.
231 Bosco D, Haefliger JA, Meda P: Connexins: Key mediators of endocrine function. Physiol Rev 2011;91:1393-1445.
232 Tran QK, Leonard J, Black DJ, Nadeau OW, Boulatnikov IG, Persechini A: Effects of combined phosphorylation at ser-617 and ser-1179 in endothelial nitric-oxide synthase on ec50(ca2+) values for calmodulin binding and enzyme activation. J Biol Chem 2009;284:11892-11899.
233 Krupp J, Boeldt DS, Yi FX, Grummer MA, Bankowski Anaya HA, Shah DM, Bird IM: The loss of sustained ca(2+) signaling underlies suppressed endothelial nitric oxide production in preeclamptic pregnancies: Implications for new therapy. Am J Physiol Heart Circ Physiol 2013;305:H969-979.
234 Segal SS, Bagher P: Regulation of myoendothelial junction formation: Bridging the gap. Circ Res 2010;106:1014-1016.
235 Senadheera S, Bertrand PP, Grayson TH, Leader L, Murphy TV, Sandow SL: Pregnancy-induced remodelling and enhanced endothelium-derived hyperpolarization-type vasodilator activity in rat uterine radial artery: Transient receptor potential vanilloid type 4 channels, caveolae and myoendothelial gap junctions. J Anat 2013;223:677-686.
236 Wu MH: Endothelial focal adhesions and barrier function. J Physiol 2005;569:359-366.
237 Dejana E, Lauri D: Biochemical and functional characteristics of integrins: A new family of adhesive receptors present in hematopoietic cells. Haematologica 1990;75:1-6.

238 Hodivala-Dilke KM, Reynolds AR, Reynolds LE: Integrins in angiogenesis: Multitalented molecules in a balancing act. Cell Tissue Res 2003;314:131-144.
239 Petit V, Thiery JP: Focal adhesions: Structure and dynamics. Biol Cell 2000;92:477-494.
240 del Zoppo GJ, Milner R: Integrin-matrix interactions in the cerebral microvasculature. Arterioscler Thromb Vasc Biol 2006;26:1966-1975.
241 Cheng YF, Clyman RI, Enenstein J, Waleh N, Pytela R, Kramer RH: The integrin complex alpha v beta 3 participates in the adhesion of microvascular endothelial cells to fibronectin. Exp Cell Res 1991;194:69-77.
242 Trache A, Trzeciakowski JP, Gardiner L, Sun Z, Muthuchamy M, Guo M, Yuan SY, Meininger GA: Histamine effects on endothelial cell fibronectin interaction studied by atomic force microscopy. Biophys J 2005;89:2888-2898.
243 Ni X, Epshtein Y, Chen W, Zhou T, Xie L, Garcia JG, Jacobson JR: Interaction of integrin beta4 with s1p receptors in s1p- and hgf-induced endothelial barrier enhancement. J Cell Biochem 2014;115:1187-1195.
244 Hakanpaa L, Sipila T, Leppanen VM, Gautam P, Nurmi H, Jacquemet G, Eklund L, Ivaska J, Alitalo K, Saharinen P: Endothelial destabilization by angiopoietin-2 via integrin beta1 activation. Nat Commun 2015;6:5962.
245 Kargozaran H, Yuan SY, Breslin JW, Watson KD, Gaudreault N, Breen A, Wu MH: A role for endothelial-derived matrix metalloproteinase-2 in breast cancer cell transmigration across the endothelial-basement membrane barrier. Clin Exp Metastasis 2007;24:495-502.
246 Wu C, Ivars F, Anderson P, Hallmann R, Vestweber D, Nilsson P, Robenek H, Tryggvason K, Song J, Korpos E, Loser K, Beissert S, Georges-Labouesse E, Sorokin LM: Endothelial basement membrane laminin alpha5 selectively inhibits t lymphocyte extravasation into the brain. Nat Med 2009;15:519-527.
247 Curtis TM, McKeown-Longo PJ, Vincent PA, Homan SM, Wheatley EM, Saba TM: Fibronectin attenuates increased endothelial monolayer permeability after rgd peptide, anti-alpha 5 beta 1, or tnf-alpha exposure. Am J Physiol 1995;269:L248-260.
248 Qiao RL, Yan W, Lum H, Malik AB: Arg-gly-asp peptide increases endothelial hydraulic conductivity: Comparison with thrombin response. Am J Physiol 1995;269:C110-117.
249 Wheatley EM, McKeown-Longo PJ, Vincent PA, Saba TM: Incorporation of fibronectin into matrix decreases tnf-induced increase in endothelial monolayer permeability. Am J Physiol 1993;265:L148-157.
250 Wu MH, Ustinova E, Granger HJ: Integrin binding to fibronectin and vitronectin maintains the barrier function of isolated porcine coronary venules. J Physiol 2001;532:785-791.
251 Avraham HK, Lee TH, Koh Y, Kim TA, Jiang S, Sussman M, Samarel AM, Avraham S: Vascular endothelial growth factor regulates focal adhesion assembly in human brain microvascular endothelial cells through activation of the focal adhesion kinase and related adhesion focal tyrosine kinase. J Biol Chem 2003;278:36661-36668.
252 Eliceiri BP, Puente XS, Hood JD, Stupack DG, Schlaepfer DD, Huang XZ, Sheppard D, Cheresh DA: Src-mediated coupling of focal adhesion kinase to integrin alpha(v)beta5 in vascular endothelial growth factor signaling. J Cell Biol 2002;157:149-160.
253 Guo M, Daines D, Tang J, Shen Q, Perrin RM, Takada Y, Yuan SY, Wu MH: Fibrinogen-gamma c-terminal fragments induce endothelial barrier dysfunction and

microvascular leak via integrin-mediated and rhoa-dependent mechanism. Arterioscler Thromb Vasc Biol 2009;29:394-400.

254 Bianchi E, Bender JR, Blasi F, Pardi R: Through and beyond the wall: Late steps in leukocyte transendothelial migration. Immunol Today 1997;18:586-591.

255 Zekovic DB, Kwiatkowski S, Vrvic MM, Jakovljevic D, Moran CA: Natural and modified (1-->3)-beta-d-glucans in health promotion and disease alleviation. Crit Rev Biotechnol 2005;25:205-230.

256 Rosenberg GA, Yang Y: Vasogenic edema due to tight junction disruption by matrix metalloproteinases in cerebral ischemia. Neurosurg Focus 2007;22:E4.

257 Shen Q, Wu MH, Yuan SY: Endothelial contractile cytoskeleton and microvascular permeability. Cell Health Cytoskelet 2009;2009:43-50.

258 Prasain N, Stevens T: The actin cytoskeleton in endothelial cell phenotypes. Microvasc Res 2009;77:53-63.

259 Hartsock A, Nelson WJ: Adherens and tight junctions: Structure, function and connections to the actin cytoskeleton. Biochim Biophys Acta 2008;1778:660-669.

260 Mikelis CM, Simaan M, Ando K, Fukuhara S, Sakurai A, Amornphimoltham P, Masedunskas A, Weigert R, Chavakis T, Adams RH, Offermanns S, Mochizuki N, Zheng Y, Gutkind JS: Rhoa and rock mediate histamine-induced vascular leakage and anaphylactic shock. Nat Commun 2015;6:6725.

261 van Nieuw Amerongen GP, van Delft S, Vermeer MA, Collard JG, van Hinsbergh VW: Activation of rhoa by thrombin in endothelial hyperpermeability: Role of rho kinase and protein tyrosine kinases. Circ Res 2000;87:335-340.

262 Wang L, Dudek SM: Regulation of vascular permeability by sphingosine 1-phosphate. Microvasc Res 2009;77:39-45.

263 Shen Q, Rigor RR, Pivetti CD, Wu MH, Yuan SY: Myosin light chain kinase in microvascular endothelial barrier function. Cardiovasc Res 2010;87:272-280.

264 Birukov KG: Small gtpases in mechanosensitive regulation of endothelial barrier. Microvasc Res 2009;77:46-52.

265 Garcia JG, Davis HW, Patterson CE: Regulation of endothelial cell gap formation and barrier dysfunction: Role of myosin light chain phosphorylation. J Cell Physiol 1995;163:510-522.

266 Goeckeler ZM, Wysolmerski RB: Myosin light chain kinase-regulated endothelial cell contraction: The relationship between isometric tension, actin polymerization, and myosin phosphorylation. J Cell Biol 1995;130:613-627.

267 Sheldon R, Moy A, Lindsley K, Shasby S, Shasby DM: Role of myosin light-chain phosphorylation in endothelial cell retraction. Am J Physiol 1993;265:L606-612.

268 Verin AD, Patterson CE, Day MA, Garcia JG: Regulation of endothelial cell gap formation and barrier function by myosin-associated phosphatase activities. Am J Physiol 1995;269:L99-108.

269 Hixenbaugh EA, Goeckeler ZM, Papaiya NN, Wysolmerski RB, Silverstein SC, Huang AJ: Stimulated neutrophils induce myosin light chain phosphorylation and isometric tension in endothelial cells. Am J Physiol 1997;273:H981-988.

270 Shivanna M, Srinivas SP: Microtubule stabilization opposes the (tnf-alpha)-induced loss in the barrier integrity of corneal endothelium. Exp Eye Res 2009;89:950-959.

271 Birukova AA, Smurova K, Birukov KG, Usatyuk P, Liu F, Kaibuchi K, Ricks-Cord A, Natarajan V, Alieva I, Garcia JG, Verin AD: Microtubule disassembly induces

cytoskeletal remodeling and lung vascular barrier dysfunction: Role of rho-dependent mechanisms. J Cell Physiol 2004;201:55-70.

272 Birukova AA, Birukov KG, Smurova K, Adyshev D, Kaibuchi K, Alieva I, Garcia JG, Verin AD: Novel role of microtubules in thrombin-induced endothelial barrier dysfunction. Faseb J 2004;18:1879-1890.

273 Shivanna M, Rajashekhar G, Srinivas SP: Barrier dysfunction of the corneal endothelium in response to tnf-alpha: Role of p38 map kinase. Invest Ophthalmol Vis Sci 2010;51:1575-1582.

274 Birukova AA, Liu F, Garcia JG, Verin AD: Protein kinase a attenuates endothelial cell barrier dysfunction induced by microtubule disassembly. Am J Physiol Lung Cell Mol Physiol 2004;287:L86-93.

275 Wang N, Stamenovic D: Mechanics of vimentin intermediate filaments. J Muscle Res Cell Motil 2002;23:535-540.

276 Colucci-Guyon E, Portier MM, Dunia I, Paulin D, Pournin S, Babinet C: Mice lacking vimentin develop and reproduce without an obvious phenotype. Cell 1994;79:679-694.

277 Shasby DM, Ries DR, Shasby SS, Winter MC: Histamine stimulates phosphorylation of adherens junction proteins and alters their link to vimentin. Am J Physiol Lung Cell Mol Physiol 2002;282:L1330-1338.

278 Mochizuki N: Vascular integrity mediated by vascular endothelial cadherin and regulated by sphingosine 1-phosphate and angiopoietin-1. Circ J 2009;73:2183-2191.

279 Zoccali C, Benedetto FA, Mallamaci F, Tripepi G, Fermo I, Foca A, Paroni R, Malatino LS: Inflammation is associated with carotid atherosclerosis in dialysis patients. Creed investigators. Cardiovascular risk extended evaluation in dialysis patients. J Hypertens 2000;18:1207-1213.

280 Humar A, St Louis P, Mazzulli T, McGeer A, Lipton J, Messner H, MacDonald KS: Elevated serum cytokines are associated with cytomegalovirus infection and disease in bone marrow transplant recipients. J Infect Dis 1999;179:484-488.

281 Stenvinkel P, Lindholm B, Heimburger M, Heimburger O: Elevated serum levels of soluble adhesion molecules predict death in pre-dialysis patients: Association with malnutrition, inflammation, and cardiovascular disease. Nephrol Dial Transplant 2000;15:1624-1630.

282 Fichtlscherer S, Rosenberger G, Walter DH, Breuer S, Dimmeler S, Zeiher AM: Elevated c-reactive protein levels and impaired endothelial vasoreactivity in patients with coronary artery disease. Circulation 2000;102:1000-1006.

283 Kolesnick R: Signal transduction through the sphingomyelin pathway. Mol Chem Neuropathol 1994;21:287-297.

284 Dolgachev V, Farooqui MS, Kulaeva OI, Tainsky MA, Nagy B, Hanada K, Separovic D: De novo ceramide accumulation due to inhibition of its conversion to complex sphingolipids in apoptotic photosensitized cells. J Biol Chem 2004;279:23238-23249.

285 Gault CR, Obeid LM, Hannun YA: An overview of sphingolipid metabolism: From synthesis to breakdown. Adv Exp Med Biol 2010;688:1-23.

286 Futerman AH, Hannun YA: The complex life of simple sphingolipids. EMBO Rep 2004;5:777-782.

287 Kraveka JM, Li L, Szulc ZM, Bielawski J, Ogretmen B, Hannun YA, Obeid LM, Bielawska A: Involvement of dihydroceramide desaturase in cell cycle progression in human neuroblastoma cells. J Biol Chem 2007;282:16718-16728.

288 Michel C, van Echten-Deckert G: Conversion of dihydroceramide to ceramide occurs at the cytosolic face of the endoplasmic reticulum. FEBS Lett 1997;416:153-155.
289 Michel C, van Echten-Deckert G, Rother J, Sandhoff K, Wang E, Merrill AH, Jr.: Characterization of ceramide synthesis. A dihydroceramide desaturase introduces the 4,5-trans-double bond of sphingosine at the level of dihydroceramide. J Biol Chem 1997;272:22432-22437.
290 Ponnusamy S, Meyers-Needham M, Senkal CE, Saddoughi SA, Sentelle D, Selvam SP, Salas A, Ogretmen B: Sphingolipids and cancer: Ceramide and sphingosine-1-phosphate in the regulation of cell death and drug resistance. Future Oncol 2010;6:1603-1624.
291 Fyrst H, Saba JD: An update on sphingosine-1-phosphate and other sphingolipid mediators. Nat Chem Biol 2010;6:489-497.
292 Bartke N, Hannun YA: Bioactive sphingolipids: Metabolism and function. J Lipid Res 2009;50 Suppl:S91-96.
293 Spiegel S, Milstien S: Sphingosine-1-phosphate: An enigmatic signalling lipid. Nat Rev Mol Cell Biol 2003;4:397-407.
294 Brindley DN, Pilquil C: Lipid phosphate phosphatases and signaling. J Lipid Res 2009;50 Suppl:S225-230.
295 Brindley DN: Lipid phosphate phosphatases and related proteins: Signaling functions in development, cell division, and cancer. J Cell Biochem 2004;92:900-912.
296 Kumar A, Saba JD: Lyase to live by: Sphingosine phosphate lyase as a therapeutic target. Expert Opin Ther Targets 2009;13:1013-1025.
297 Snider AJ, Orr Gandy KA, Obeid LM: Sphingosine kinase: Role in regulation of bioactive sphingolipid mediators in inflammation. Biochimie 2010;92:707-715.
298 Spiegel S, Milstien S: The outs and the ins of sphingosine-1-phosphate in immunity. Nat Rev Immunol 2011;11:403-415.
299 Alemany R, van Koppen CJ, Danneberg K, Ter Braak M, Meyer Zu Heringdorf D: Regulation and functional roles of sphingosine kinases. Naunyn Schmiedebergs Arch Pharmacol 2007;374:413-428.
300 Igarashi N, Okada T, Hayashi S, Fujita T, Jahangeer S, Nakamura S: Sphingosine kinase 2 is a nuclear protein and inhibits DNA synthesis. J Biol Chem 2003;278:46832-46839.
301 Strub GM, Paillard M, Liang J, Gomez L, Allegood JC, Hait NC, Maceyka M, Price MM, Chen Q, Simpson DC, Kordula T, Milstien S, Lesnefsky EJ, Spiegel S: Sphingosine-1-phosphate produced by sphingosine kinase 2 in mitochondria interacts with prohibitin 2 to regulate complex iv assembly and respiration. Faseb J 2011;25:600-612.
302 Sarkar S, Maceyka M, Hait NC, Paugh SW, Sankala H, Milstien S, Spiegel S: Sphingosine kinase 1 is required for migration, proliferation and survival of mcf-7 human breast cancer cells. FEBS Lett 2005;579:5313-5317.
303 Maceyka M, Sankala H, Hait NC, Le Stunff H, Liu H, Toman R, Collier C, Zhang M, Satin LS, Merrill AH, Jr., Milstien S, Spiegel S: Sphk1 and sphk2, sphingosine kinase isoenzymes with opposing functions in sphingolipid metabolism. J Biol Chem 2005;280:37118-37129.
304 Hait NC, Sarkar S, Le Stunff H, Mikami A, Maceyka M, Milstien S, Spiegel S: Role of sphingosine kinase 2 in cell migration toward epidermal growth factor. J Biol Chem 2005;280:29462-29469.
305 Hait NC, Bellamy A, Milstien S, Kordula T, Spiegel S: Sphingosine kinase type 2 activation by erk-mediated phosphorylation. J Biol Chem 2007;282:12058-12065.

306 Kohama T, Olivera A, Edsall L, Nagiec MM, Dickson R, Spiegel S: Molecular cloning and functional characterization of murine sphingosine kinase. J Biol Chem 1998;273:23722-23728.

307 Siow DL, Anderson CD, Berdyshev EV, Skobeleva A, Natarajan V, Pitson SM, Wattenberg BW: Sphingosine kinase localization in the control of sphingolipid metabolism. Adv Enzyme Regul 2011;51:229-244.

308 Kharel Y, Raje M, Gao M, Gellett AM, Tomsig JL, Lynch KR, Santos WL: Sphingosine kinase type 2 inhibition elevates circulating sphingosine 1-phosphate. Biochem J 2012;447:149-157.

309 Kharel Y, Mathews TP, Gellett AM, Tomsig JL, Kennedy PC, Moyer ML, Macdonald TL, Lynch KR: Sphingosine kinase type 1 inhibition reveals rapid turnover of circulating sphingosine 1-phosphate. Biochem J 2011;440:345-353.

310 Liu H, Toman RE, Goparaju SK, Maceyka M, Nava VE, Sankala H, Payne SG, Bektas M, Ishii I, Chun J, Milstien S, Spiegel S: Sphingosine kinase type 2 is a putative bh3-only protein that induces apoptosis. J Biol Chem 2003;278:40330-40336.

311 Lanterman MM, Saba JD: Characterization of sphingosine kinase (sk) activity in saccharomyces cerevisiae and isolation of sk-deficient mutants. Biochem J 1998;332 (Pt 2):525-531.

312 Venkataraman K, Thangada S, Michaud J, Oo ML, Ai Y, Lee YM, Wu M, Parikh NS, Khan F, Proia RL, Hla T: Extracellular export of sphingosine kinase-1a contributes to the vascular s1p gradient. Biochem J 2006;397:461-471.

313 Shida D, Takabe K, Kapitonov D, Milstien S, Spiegel S: Targeting sphk1 as a new strategy against cancer. Curr Drug Targets 2008;9:662-673.

314 Pitson SM, Moretti PA, Zebol JR, Lynn HE, Xia P, Vadas MA, Wattenberg BW: Activation of sphingosine kinase 1 by erk1/2-mediated phosphorylation. Embo J 2003;22:5491-5500.

315 Jarman KE, Moretti PA, Zebol JR, Pitson SM: Translocation of sphingosine kinase 1 to the plasma membrane is mediated by calcium- and integrin-binding protein 1. J Biol Chem 2010;285:483-492.

316 Gao P, Peterson YK, Smith RA, Smith CD: Characterization of isoenzyme-selective inhibitors of human sphingosine kinases. PLoS One 2012;7:e44543.

317 Gault CR, Eblen ST, Neumann CA, Hannun YA, Obeid LM: Oncogenic k-ras regulates bioactive sphingolipids in a sphingosine kinase 1-dependent manner. J Biol Chem 2012;287:31794-31803.

318 Pitman MR, Barr RK, Gliddon BL, Magarey AM, Moretti PA, Pitson SM: A critical role for the protein phosphatase 2a b'alpha regulatory subunit in dephosphorylation of sphingosine kinase 1. Int J Biochem Cell Biol 2011;43:342-347.

319 Thoms HC, Loveridge CJ, Simpson J, Clipson A, Reinhardt K, Dunlop MG, Stark LA: Nucleolar targeting of rela(p65) is regulated by commd1-dependent ubiquitination. Cancer Res 2010;70:139-149.

320 Taha TA, El-Alwani M, Hannun YA, Obeid LM: Sphingosine kinase-1 is cleaved by cathepsin b in vitro: Identification of the initial cleavage sites for the protease. FEBS Lett 2006;580:6047-6054.

321 Taha TA, Kitatani K, Bielawski J, Cho W, Hannun YA, Obeid LM: Tumor necrosis factor induces the loss of sphingosine kinase-1 by a cathepsin b-dependent mechanism. J Biol Chem 2005;280:17196-17202.

322 Venkataraman K, Lee YM, Michaud J, Thangada S, Ai Y, Bonkovsky HL, Parikh NS, Habrukowich C, Hla T: Vascular endothelium as a contributor of plasma sphingosine 1-phosphate. Circ Res 2008;102:669-676.

323 Hammad SM, Taha TA, Nareika A, Johnson KR, Lopes-Virella MF, Obeid LM: Oxidized ldl immune complexes induce release of sphingosine kinase in human u937 monocytic cells. Prostaglandins Other Lipid Mediat 2006;79:126-140.

324 Strub GM, Maceyka M, Hait NC, Milstien S, Spiegel S: Extracellular and intracellular actions of sphingosine-1-phosphate. Adv Exp Med Biol 2010;688:141-155.

325 Spiegel S, Milstien S: Exogenous and intracellularly generated sphingosine 1-phosphate can regulate cellular processes by divergent pathways. Biochem Soc Trans 2003;31:1216-1219.

326 Allende ML, Sasaki T, Kawai H, Olivera A, Mi Y, van Echten-Deckert G, Hajdu R, Rosenbach M, Keohane CA, Mandala S, Spiegel S, Proia RL: Mice deficient in sphingosine kinase 1 are rendered lymphopenic by fty720. J Biol Chem 2004;279:52487-52492.

327 Sensken SC, Bode C, Graler MH: Accumulation of fingolimod (fty720) in lymphoid tissues contributes to prolonged efficacy. J Pharmacol Exp Ther 2009;328:963-969.

328 Mizugishi K, Li C, Olivera A, Bielawski J, Bielawska A, Deng CX, Proia RL: Maternal disturbance in activated sphingolipid metabolism causes pregnancy loss in mice. J Clin Invest 2007;117:2993-3006.

329 Hait NC, Allegood J, Maceyka M, Strub GM, Harikumar KB, Singh SK, Luo C, Marmorstein R, Kordula T, Milstien S, Spiegel S: Regulation of histone acetylation in the nucleus by sphingosine-1-phosphate. Science 2009;325:1254-1257.

330 Weigert A, Schiffmann S, Sekar D, Ley S, Menrad H, Werno C, Grosch S, Geisslinger G, Brune B: Sphingosine kinase 2 deficient tumor xenografts show impaired growth and fail to polarize macrophages towards an anti-inflammatory phenotype. Int J Cancer 2009;125:2114-2121.

331 Lai WQ, Irwan AW, Goh HH, Melendez AJ, McInnes IB, Leung BP: Distinct roles of sphingosine kinase 1 and 2 in murine collagen-induced arthritis. J Immunol 2009;183:2097-2103.

332 Wacker BK, Park TS, Gidday JM: Hypoxic preconditioning-induced cerebral ischemic tolerance: Role of microvascular sphingosine kinase 2. Stroke 2009;40:3342-3348.

333 Samy ET, Meyer CA, Caplazi P, Langrish CL, Lora JM, Bluethmann H, Peng SL: Cutting edge: Modulation of intestinal autoimmunity and il-2 signaling by sphingosine kinase 2 independent of sphingosine 1-phosphate. J Immunol 2007;179:5644-5648.

334 Sigal YJ, McDermott MI, Morris AJ: Integral membrane lipid phosphatases/phosphotransferases: Common structure and diverse functions. Biochem J 2005;387:281-293.

335 Brindley DN, Waggoner DW: Mammalian lipid phosphate phosphohydrolases. J Biol Chem 1998;273:24281-24284.

336 Kirby RJ, Jin Y, Fu J, Cubillos J, Swertfeger D, Arend LJ: Dynamic regulation of sphingosine-1-phosphate homeostasis during development of mouse metanephric kidney. Am J Physiol Renal Physiol 2009;296:F634-641.

337 Mechtcheriakova D, Wlachos A, Sobanov J, Kopp T, Reuschel R, Bornancin F, Cai R, Zemann B, Urtz N, Stingl G, Zlabinger G, Woisetschlager M, Baumruker T, Billich A: Sphingosine 1-phosphate phosphatase 2 is induced during inflammatory responses. Cell Signal 2007;19:748-760.

338 Kok BP, Venkatraman G, Capatos D, Brindley DN: Unlike two peas in a pod: Lipid phosphate phosphatases and phosphatidate phosphatases. Chem Rev 2012;112:5121-5146.
339 Brindley DN, Lin FT, Tigyi GJ: Role of the autotaxin-lysophosphatidate axis in cancer resistance to chemotherapy and radiotherapy. Biochim Biophys Acta 2013;1831:74-85.
340 Zhao Y, Kalari SK, Usatyuk PV, Gorshkova I, He D, Watkins T, Brindley DN, Sun C, Bittman R, Garcia JG, Berdyshev EV, Natarajan V: Intracellular generation of sphingosine 1-phosphate in human lung endothelial cells: Role of lipid phosphate phosphatase-1 and sphingosine kinase 1. J Biol Chem 2007;282:14165-14177.
341 Hannun YA, Obeid LM: Principles of bioactive lipid signalling: Lessons from sphingolipids. Nat Rev Mol Cell Biol 2008;9:139-150.
342 Takabe K, Paugh SW, Milstien S, Spiegel S: "Inside-out" Signaling of sphingosine-1-phosphate: Therapeutic targets. Pharmacol Rev 2008;60:181-195.
343 Pyne S, Long JS, Ktistakis NT, Pyne NJ: Lipid phosphate phosphatases and lipid phosphate signalling. Biochem Soc Trans 2005;33:1370-1374.
344 Stoffel W, LeKim D, Sticht G: Distribution and properties of dihydrosphingosine-1-phosphate aldolase (sphinganine-1-phosphate alkanal-lyase). Hoppe Seylers Z Physiol Chem 1969;350:1233-1241.
345 Zhou J, Saba JD: Identification of the first mammalian sphingosine phosphate lyase gene and its functional expression in yeast. Biochem Biophys Res Commun 1998;242:502-507.
346 Zhan X, Desiderio DM: Nitroproteins from a human pituitary adenoma tissue discovered with a nitrotyrosine affinity column and tandem mass spectrometry. Anal Biochem 2006;354:279-289.
347 Mukhopadhyay D, Howell KS, Riezman H, Capitani G: Identifying key residues of sphinganine-1-phosphate lyase for function in vivo and in vitro. J Biol Chem 2008;283:20159-20169.
348 Vogel P, Donoviel MS, Read R, Hansen GM, Hazlewood J, Anderson SJ, Sun W, Swaffield J, Oravecz T: Incomplete inhibition of sphingosine 1-phosphate lyase modulates immune system function yet prevents early lethality and non-lymphoid lesions. PLoS One 2009;4:e4112.
349 Stoffel W: Studies on the biosynthesis and degradation of sphingosine bases. Chem Phys Lipids 1970;5:139-158.
350 Ghosh TK, Bian J, Gill DL: Intracellular calcium release mediated by sphingosine derivatives generated in cells. Science 1990;248:1653-1656.
351 Hla T, Maciag T: An abundant transcript induced in differentiating human endothelial cells encodes a polypeptide with structural similarities to g-protein-coupled receptors. J Biol Chem 1990;265:9308-9313.
352 Hla T: Sphingosine 1-phosphate receptors. Prostaglandins 2001;64:135-142.
353 Lamour NF, Chalfant CE: Ceramide-1-phosphate: The "Missing" Link in eicosanoid biosynthesis and inflammation. Mol Interv 2005;5:358-367.
354 Ikeda H, Ohkawa R, Watanabe N, Nakamura K, Kume Y, Nakagawa H, Yoshida H, Okubo S, Yokota H, Tomiya T, Inoue Y, Nishikawa T, Ohtomo N, Tanoue Y, Koike K, Yatomi Y: Plasma concentration of bioactive lipid mediator sphingosine 1-phosphate is reduced in patients with chronic hepatitis c. Clin Chim Acta 2010;411:765-770.

355 Blaho VA, Galvani S, Engelbrecht E, Liu C, Swendeman SL, Kono M, Proia RL, Steinman L, Han MH, Hla T: Hdl-bound sphingosine-1-phosphate restrains lymphopoiesis and neuroinflammation. Nature 2015;523:342-346.

356 Christoffersen C, Obinata H, Kumaraswamy SB, Galvani S, Ahnstrom J, Sevvana M, Egerer-Sieber C, Muller YA, Hla T, Nielsen LB, Dahlback B: Endothelium-protective sphingosine-1-phosphate provided by hdl-associated apolipoprotein m. Proc Natl Acad Sci U S A 2011;108:9613-9618.

357 Bode C, Sensken SC, Peest U, Beutel G, Thol F, Levkau B, Li Z, Bittman R, Huang T, Tolle M, van der Giet M, Graler MH: Erythrocytes serve as a reservoir for cellular and extracellular sphingosine 1-phosphate. J Cell Biochem 2010;109:1232-1243.

358 Okajima F: Plasma lipoproteins behave as carriers of extracellular sphingosine 1-phosphate: Is this an atherogenic mediator or an anti-atherogenic mediator? Biochim Biophys Acta 2002;1582:132-137.

359 Karuna R, Park R, Othman A, Holleboom AG, Motazacker MM, Sutter I, Kuivenhoven JA, Rohrer L, Matile H, Hornemann T, Stoffel M, Rentsch KM, von Eckardstein A: Plasma levels of sphingosine-1-phosphate and apolipoprotein m in patients with monogenic disorders of hdl metabolism. Atherosclerosis 2011;219:855-863.

360 Murata N, Sato K, Kon J, Tomura H, Yanagita M, Kuwabara A, Ui M, Okajima F: Interaction of sphingosine 1-phosphate with plasma components, including lipoproteins, regulates the lipid receptor-mediated actions. Biochem J 2000;352 Pt 3:809-815.

361 Hla T, Venkataraman K, Michaud J: The vascular s1p gradient-cellular sources and biological significance. Biochim Biophys Acta 2008;1781:477-482.

362 Theilmeier G, Schmidt C, Herrmann J, Keul P, Schafers M, Herrgott I, Mersmann J, Larmann J, Hermann S, Stypmann J, Schober O, Hildebrand R, Schulz R, Heusch G, Haude M, von Wnuck Lipinski K, Herzog C, Schmitz M, Erbel R, Chun J, Levkau B: High-density lipoproteins and their constituent, sphingosine-1-phosphate, directly protect the heart against ischemia/reperfusion injury in vivo via the s1p3 lysophospholipid receptor. Circulation 2006;114:1403-1409.

363 Wilkerson BA, Grass GD, Wing SB, Argraves WS, Argraves KM: Sphingosine 1-phosphate (s1p) carrier-dependent regulation of endothelial barrier: High density lipoprotein (hdl)-s1p prolongs endothelial barrier enhancement as compared with albumin-s1p via effects on levels, trafficking, and signaling of s1p1. J Biol Chem 2012;287:44645-44653.

364 Kimura T, Sato K, Kuwabara A, Tomura H, Ishiwara M, Kobayashi I, Ui M, Okajima F: Sphingosine 1-phosphate may be a major component of plasma lipoproteins responsible for the cytoprotective actions in human umbilical vein endothelial cells. J Biol Chem 2001;276:31780-31785.

365 Aoki S, Yatomi Y, Ohta M, Osada M, Kazama F, Satoh K, Nakahara K, Ozaki Y: Sphingosine 1-phosphate-related metabolism in the blood vessel. J Biochem 2005;138:47-55.

366 Olivera A, Rosenfeldt HM, Bektas M, Wang F, Ishii I, Chun J, Milstien S, Spiegel S: Sphingosine kinase type 1 induces g12/13-mediated stress fiber formation, yet promotes growth and survival independent of g protein-coupled receptors. J Biol Chem 2003;278:46452-46460.

367 van Koppen CJ, Meyer zu Heringdorf D, Alemany R, Jakobs KH: Sphingosine kinase-mediated calcium signaling by muscarinic acetylcholine receptors. Life Sci 2001;68:2535-2540.

368 Mitra P, Oskeritzian CA, Payne SG, Beaven MA, Milstien S, Spiegel S: Role of abcc1 in export of sphingosine-1-phosphate from mast cells. Proc Natl Acad Sci U S A 2006;103:16394-16399.

369 Takabe K, Kim RH, Allegood JC, Mitra P, Ramachandran S, Nagahashi M, Harikumar KB, Hait NC, Milstien S, Spiegel S: Estradiol induces export of sphingosine 1-phosphate from breast cancer cells via abcc1 and abcg2. J Biol Chem 2010;285:10477-10486.

370 Sato K, Malchinkhuu E, Horiuchi Y, Mogi C, Tomura H, Tosaka M, Yoshimoto Y, Kuwabara A, Okajima F: Critical role of abca1 transporter in sphingosine 1-phosphate release from astrocytes. J Neurochem 2007;103:2610-2619.

371 Fukuhara S, Simmons S, Kawamura S, Inoue A, Orba Y, Tokudome T, Sunden Y, Arai Y, Moriwaki K, Ishida J, Uemura A, Kiyonari H, Abe T, Fukamizu A, Hirashima M, Sawa H, Aoki J, Ishii M, Mochizuki N: The sphingosine-1-phosphate transporter spns2 expressed on endothelial cells regulates lymphocyte trafficking in mice. J Clin Invest 2012;122:1416-1426.

372 Hisano Y, Kobayashi N, Kawahara A, Yamaguchi A, Nishi T: The sphingosine 1-phosphate transporter, spns2, functions as a transporter of the phosphorylated form of the immunomodulating agent fty720. J Biol Chem 2011;286:1758-1766.

373 Skoura A, Hla T: Lysophospholipid receptors in vertebrate development, physiology, and pathology. J Lipid Res 2009;50 Suppl:S293-298.

374 Uhlenbrock K, Huber J, Ardati A, Busch AE, Kostenis E: Fluid shear stress differentially regulates gpr3, gpr6, and gpr12 expression in human umbilical vein endothelial cells. Cell Physiol Biochem 2003;13:75-84.

375 Uhlenbrock K, Gassenhuber H, Kostenis E: Sphingosine 1-phosphate is a ligand of the human gpr3, gpr6 and gpr12 family of constitutively active g protein-coupled receptors. Cell Signal 2002;14:941-953.

376 Niedernberg A, Tunaru S, Blaukat A, Ardati A, Kostenis E: Sphingosine 1-phosphate and dioleoylphosphatidic acid are low affinity agonists for the orphan receptor gpr63. Cell Signal 2003;15:435-446.

377 Niedernberg A, Tunaru S, Blaukat A, Harris B, Kostenis E: Comparative analysis of functional assays for characterization of agonist ligands at g protein-coupled receptors. J Biomol Screen 2003;8:500-510.

378 Zhang BL, Li Y, Ding JH, Dong FL, Hou YJ, Jiang BC, Shi FX, Xu YX: Sphingosine 1-phosphate acts as an activator for the porcine gpr3 of constitutively active g protein-coupled receptors. J Zhejiang Univ Sci B 2012;13:555-566.

379 Pyne S, Pyne N: Sphingosine 1-phosphate signalling via the endothelial differentiation gene family of g-protein-coupled receptors. Pharmacol Ther 2000;88:115-131.

380 Pyne S, Pyne NJ: Sphingosine 1-phosphate signalling in mammalian cells. Biochem J 2000;349:385-402.

381 Siow D, Wattenberg B: The compartmentalization and translocation of the sphingosine kinases: Mechanisms and functions in cell signaling and sphingolipid metabolism. Crit Rev Biochem Mol Biol 2011;46:365-375.

382 Nieuwenhuis B, Luth A, Kleuser B: Dexamethasone protects human fibroblasts from apoptosis via an s1p3-receptor subtype dependent activation of pkb/akt and bcl xl. Pharmacol Res 2010;61:449-459.

383 Pappu R, Schwab SR, Cornelissen I, Pereira JP, Regard JB, Xu Y, Camerer E, Zheng YW, Huang Y, Cyster JG, Coughlin SR: Promotion of lymphocyte egress into blood and lymph by distinct sources of sphingosine-1-phosphate. Science 2007;316:295-298.

384 Hla T, Brinkmann V: Sphingosine 1-phosphate (s1p): Physiology and the effects of s1p receptor modulation. Neurology 2011;76:S3-8.
385 Lucke S, Levkau B: Endothelial functions of sphingosine-1-phosphate. Cell Physiol Biochem 2010;26:87-96.
386 Hemmings DG: Signal transduction underlying the vascular effects of sphingosine 1-phosphate and sphingosylphosphorylcholine. Naunyn Schmiedebergs Arch Pharmacol 2006;373:18-29.
387 Pyne S, Pyne NJ: Translational aspects of sphingosine 1-phosphate biology. Trends Mol Med 2011;17:463-472.
388 Pyne S, Bittman R, Pyne NJ: Sphingosine kinase inhibitors and cancer: Seeking the golden sword of hercules. Cancer Res 2011;71:6576-6582.
389 Maceyka M, Harikumar KB, Milstien S, Spiegel S: Sphingosine-1-phosphate signaling and its role in disease. Trends Cell Biol 2012;22:50-60.
390 Abbasi T, Garcia JG: Sphingolipids in lung endothelial biology and regulation of vascular integrity. Handb Exp Pharmacol 2013:201-226.
391 Krump-Konvalinkova V, Yasuda S, Rubic T, Makarova N, Mages J, Erl W, Vosseler C, Kirkpatrick CJ, Tigyi G, Siess W: Stable knock-down of the sphingosine 1-phosphate receptor s1p1 influences multiple functions of human endothelial cells. Arterioscler Thromb Vasc Biol 2005;25:546-552.
392 Lee JF, Zeng Q, Ozaki H, Wang L, Hand AR, Hla T, Wang E, Lee MJ: Dual roles of tight junction-associated protein, zonula occludens-1, in sphingosine 1-phosphate-mediated endothelial chemotaxis and barrier integrity. J Biol Chem 2006;281:29190-29200.
393 Takuwa Y, Okamoto Y, Yoshioka K, Takuwa N: Sphingosine-1-phosphate signaling and biological activities in the cardiovascular system. Biochim Biophys Acta 2008;1781:483-488.
394 Hanson MA, Roth CB, Jo E, Griffith MT, Scott FL, Reinhart G, Desale H, Clemons B, Cahalan SM, Schuerer SC, Sanna MG, Han GW, Kuhn P, Rosen H, Stevens RC: Crystal structure of a lipid g protein-coupled receptor. Science 2012;335:851-855.
395 Dejana E: Endothelial cell-cell junctions: Happy together. Nat Rev Mol Cell Biol 2004;5:261-270.
396 Squecco R, Sassoli C, Nuti F, Martinesi M, Chellini F, Nosi D, Zecchi-Orlandini S, Francini F, Formigli L, Meacci E: Sphingosine 1-phosphate induces myoblast differentiation through cx43 protein expression: A role for a gap junction-dependent and -independent function. Mol Biol Cell 2006;17:4896-4910.
397 Tence M, Ezan P, Amigou E, Giaume C: Increased interaction of connexin43 with zonula occludens-1 during inhibition of gap junctions by g protein-coupled receptor agonists. Cell Signal 2012;24:86-98.
398 Morel S, Frias MA, Rosker C, James RW, Rohr S, Kwak BR: The natural cardioprotective particle hdl modulates connexin43 gap junction channels. Cardiovasc Res 2012;93:41-49.
399 Bogatcheva NV, Verin AD: Reprint of "The role of cytoskeleton in the regulation of vascular endothelial barrier function" [microvascular research 76 (2008) 202-207]. Microvasc Res 2009;77:64-69.
400 Garcia JG, Liu F, Verin AD, Birukova A, Dechert MA, Gerthoffer WT, Bamberg JR, English D: Sphingosine 1-phosphate promotes endothelial cell barrier integrity by edg-dependent cytoskeletal rearrangement. J Clin Invest 2001;108:689-701.

401 Owen KA, Pixley FJ, Thomas KS, Vicente-Manzanares M, Ray BJ, Horwitz AF, Parsons JT, Beggs HE, Stanley ER, Bouton AH: Regulation of lamellipodial persistence, adhesion turnover, and motility in macrophages by focal adhesion kinase. J Cell Biol 2007;179:1275-1287.

402 Belvitch P, Dudek SM: Role of fak in s1p-regulated endothelial permeability. Microvasc Res 2012;83:22-30.

403 Takashima S: Phosphorylation of myosin regulatory light chain by myosin light chain kinase, and muscle contraction. Circ J 2009;73:208-213.

404 Dudek SM, Jacobson JR, Chiang ET, Birukov KG, Wang P, Zhan X, Garcia JG: Pulmonary endothelial cell barrier enhancement by sphingosine 1-phosphate: Roles for cortactin and myosin light chain kinase. J Biol Chem 2004;279:24692-24700.

405 Singleton PA, Chatchavalvanich S, Fu P, Xing J, Birukova AA, Fortune JA, Klibanov AM, Garcia JG, Birukov KG: Akt-mediated transactivation of the s1p1 receptor in caveolin-enriched microdomains regulates endothelial barrier enhancement by oxidized phospholipids. Circ Res 2009;104:978-986.

406 Lee MJ, Thangada S, Claffey KP, Ancellin N, Liu CH, Kluk M, Volpi M, Sha'afi RI, Hla T: Vascular endothelial cell adherens junction assembly and morphogenesis induced by sphingosine-1-phosphate. Cell 1999;99:301-312.

407 Wojciak-Stothard B, Potempa S, Eichholtz T, Ridley AJ: Rho and rac but not cdc42 regulate endothelial cell permeability. J Cell Sci 2001;114:1343-1355.

408 Armstrong SM, Khajoee V, Wang C, Wang T, Tigdi J, Yin J, Kuebler WM, Gillrie M, Davis SP, Ho M, Lee WL: Co-regulation of transcellular and paracellular leak across microvascular endothelium by dynamin and rac. Am J Pathol 2012;180:1308-1323.

409 Sun X, Shikata Y, Wang L, Ohmori K, Watanabe N, Wada J, Shikata K, Birukov KG, Makino H, Jacobson JR, Dudek SM, Garcia JG: Enhanced interaction between focal adhesion and adherens junction proteins: Involvement in sphingosine 1-phosphate-induced endothelial barrier enhancement. Microvasc Res 2009;77:304-313.

410 Shikata Y, Birukov KG, Garcia JG: S1p induces fa remodeling in human pulmonary endothelial cells: Role of rac, git1, fak, and paxillin. Journal of applied physiology 2003;94:1193-1203.

411 Oo ML, Chang SH, Thangada S, Wu MT, Rezaul K, Blaho V, Hwang SI, Han DK, Hla T: Engagement of s1p(1)-degradative mechanisms leads to vascular leak in mice. J Clin Invest 2011;121:2290-2300.

412 Blaho VA, Hla T: An update on the biology of sphingosine 1-phosphate receptors. J Lipid Res 2014;55:1596-1608.

413 Hla T: Signaling and biological actions of sphingosine 1-phosphate. Pharmacol Res 2003;47:401-407.

414 Schaphorst KL, Chiang E, Jacobs KN, Zaiman A, Natarajan V, Wigley F, Garcia JG: Role of sphingosine-1 phosphate in the enhancement of endothelial barrier integrity by platelet-released products. American Journal of Physiology - Lung Cellular & Molecular Physiology 2003;285:258-267.

415 Adamson RH, Sarai RK, Altangerel A, Thirkill TL, Clark JF, Curry FR: Sphingosine-1-phosphate modulation of basal permeability and acute inflammatory responses in rat venular microvessels. Cardiovasc Res 2010;88:344-351.

416 Zhang G, Xu S, Qian Y, He P: Sphingosine-1-phosphate prevents permeability increases via activation of endothelial sphingosine-1-phosphate receptor 1 in rat venules. Am J Physiol Heart Circ Physiol 2010;299:H1494-1504.
417 Curry FE, Clark JF, Adamson RH: Erythrocyte-derived sphingosine-1-phosphate stabilizes basal hydraulic conductivity and solute permeability in rat microvessels. Am J Physiol Heart Circ Physiol 2012;303:H825-834.
418 Mullin JM, Agostino N, Rendon-Huerta E, Thornton JJ: Keynote review: Epithelial and endothelial barriers in human disease. Drug Discov Today 2005;10:395-408.
419 Camerer E, Regard JB, Cornelissen I, Srinivasan Y, Duong DN, Palmer D, Pham TH, Wong JS, Pappu R, Coughlin SR: Sphingosine-1-phosphate in the plasma compartment regulates basal and inflammation-induced vascular leak in mice. Journal of Clinical Investigation 2009;119:1871-1879.
420 Matthay MA, Ware LB, Zimmerman GA: The acute respiratory distress syndrome. J Clin Invest 2012;122:2731-2740.
421 Peng X, Hassoun PM, Sammani S, McVerry BJ, Burne MJ, Rabb H, Pearse D, Tuder RM, Garcia JG: Protective effects of sphingosine 1-phosphate in murine endotoxin-induced inflammatory lung injury. Am J Respir Crit Care Med 2004;169:1245-1251.
422 McVerry BJ, Garcia JG: Endothelial cell barrier regulation by sphingosine 1-phosphate. J Cell Biochem 2004;92:1075-1085.
423 Szczepaniak WS, Zhang Y, Hagerty S, Crow MT, Kesari P, Garcia JG, Choi AM, Simon BA, McVerry BJ: Sphingosine 1-phosphate rescues canine lps-induced acute lung injury and alters systemic inflammatory cytokine production in vivo. Transl Res 2008;152:213-224.
424 Zhao Y, Gorshkova IA, Berdyshev E, He D, Fu P, Ma W, Su Y, Usatyuk PV, Pendyala S, Oskouian B, Saba JD, Garcia JG, Natarajan V: Protection of lps-induced murine acute lung injury by sphingosine-1-phosphate lyase suppression. Am J Respir Cell Mol Biol 2011;45:426-435.
425 Sammani S, Moreno-Vinasco L, Mirzapoiazova T, Singleton PA, Chiang ET, Evenoski CL, Wang T, Mathew B, Husain A, Moitra J, Sun X, Nunez L, Jacobson JR, Dudek SM, Natarajan V, Garcia JG: Differential effects of sphingosine 1-phosphate receptors on airway and vascular barrier function in the murine lung. American Journal of Respiratory Cell & Molecular Biology 2010;43:394-402.
426 Cui H, Okamoto Y, Yoshioka K, Du W, Takuwa N, Zhang W, Asano M, Shibamoto T, Takuwa Y: Sphingosine-1-phosphate receptor 2 protects against anaphylactic shock through suppression of endothelial nitric oxide synthase in mice. J Allergy Clin Immunol 2013;132:1205-1214 e1209.
427 De Bisschop MB, Bellou A: Anaphylaxis. Curr Opin Crit Care 2012;18:308-317.
428 Galli SJ: Pathogenesis and management of anaphylaxis: Current status and future challenges. J Allergy Clin Immunol 2005;115:571-574.
429 Dombrowicz D, Flamand V, Brigman KK, Koller BH, Kinet JP: Abolition of anaphylaxis by targeted disruption of the high affinity immunoglobulin e receptor alpha chain gene. Cell 1993;75:969-976.
430 Li X, Kwon O, Kim DY, Taketomi Y, Murakami M, Chang HW: Necrox-5 suppresses ige/ag-stimulated anaphylaxis and mast cell activation by regulating the shp-1-syk signaling module. Allergy 2015.
431 Kimura S, Watanabe A, Takeuchi M, Nagata M, Harada M: Suppressive effects of antihistaminic and/or anti-paf agents on passive anaphylactic shock in mice sensitized with

allogeneic monoclonal ige and igg1 antibodies and hyperimmune serum. Immunol Invest 1998;27:379-393.

432 Pastorello EA, Stafylaraki C, Mirone C, Preziosi D, Aversano MG, Mascheri A, Losappio LM, Ortolani V, Nichelatti M, Farioli L: Anti-amoxicillin immunoglobulin e, histamine-2 receptor antagonist therapy and mast cell activation syndrome are risk factors for amoxicillin anaphylaxis. Int Arch Allergy Immunol 2015;166:280-286.

433 Oettgen HC, Martin TR, Wynshaw-Boris A, Deng C, Drazen JM, Leder P: Active anaphylaxis in ige-deficient mice. Nature 1994;370:367-370.

434 Shade KT, Platzer B, Washburn N, Mani V, Bartsch YC, Conroy M, Pagan JD, Bosques C, Mempel TR, Fiebiger E, Anthony RM: A single glycan on ige is indispensable for initiation of anaphylaxis. J Exp Med 2015;212:457-467.

435 Olivera A, Mizugishi K, Tikhonova A, Ciaccia L, Odom S, Proia RL, Rivera J: The sphingosine kinase-sphingosine-1-phosphate axis is a determinant of mast cell function and anaphylaxis. Immunity 2007;26:287-297.

436 Lee JF, Gordon S, Estrada R, Wang L, Siow DL, Wattenberg BW, Lominadze D, Lee MJ: Balance of s1p1 and s1p2 signaling regulates peripheral microvascular permeability in rat cremaster muscle vasculature. American Journal of Physiology - Heart & Circulatory Physiology 2009;296:H33-42.

437 Oskeritzian CA, Price MM, Hait NC, Kapitonov D, Falanga YT, Morales JK, Ryan JJ, Milstien S, Spiegel S: Essential roles of sphingosine-1-phosphate receptor 2 in human mast cell activation, anaphylaxis, and pulmonary edema. J Exp Med 2010;207:465-474.

438 Okazaki M, Kreisel F, Richardson SB, Kreisel D, Krupnick AS, Patterson GA, Gelman AE: Sphingosine 1-phosphate inhibits ischemia reperfusion injury following experimental lung transplantation. Am J Transplant 2007;7:751-758.

439 Moreno-Vinasco L, Gomberg-Maitland M, Maitland ML, Desai AA, Singleton PA, Sammani S, Sam L, Liu Y, Husain AN, Lang RM, Ratain MJ, Lussier YA, Garcia JG: Genomic assessment of a multikinase inhibitor, sorafenib, in a rodent model of pulmonary hypertension. Physiol Genomics 2008;33:278-291.

440 Lee SY, Kim DH, Sung SA, Kim MG, Cho WY, Kim HK, Jo SK: Sphingosine-1-phosphate reduces hepatic ischaemia/reperfusion-induced acute kidney injury through attenuation of endothelial injury in mice. Nephrology (Carlton) 2011;16:163-173.

441 Igarashi J, Michel T: Agonist-modulated targeting of the edg-1 receptor to plasmalemmal caveolae. Enos activation by sphingosine 1-phosphate and the role of caveolin-1 in sphingolipid signal transduction. J Biol Chem 2000;275:32363-32370.

442 Igarashi J, Michel T: Sphingosine 1-phosphate and isoform-specific activation of phosphoinositide 3-kinase beta. Evidence for divergence and convergence of receptor-regulated endothelial nitric-oxide synthase signaling pathways. J Biol Chem 2001;276:36281-36288.

443 McCabe TJ, Fulton D, Roman LJ, Sessa WC: Enhanced electron flux and reduced calmodulin dissociation may explain "Calcium-independent" Enos activation by phosphorylation. J Biol Chem 2000;275:6123-6128.

444 Levine YC, Li GK, Michel T: Agonist-modulated regulation of amp-activated protein kinase (ampk) in endothelial cells. Evidence for an ampk -> rac1 -> akt -> endothelial nitric-oxide synthase pathway. J Biol Chem 2007;282:20351-20364.

445 Gonzalez E, Kou R, Michel T: Rac1 modulates sphingosine 1-phosphate-mediated activation of phosphoinositide 3-kinase/akt signaling pathways in vascular endothelial cells. J Biol Chem 2006;281:3210-3216.

446 Shaul PW, Anderson RG: Role of plasmalemmal caveolae in signal transduction. Am J Physiol 1998;275:L843-851.
447 Williams JJ, Palmer TM: Cavin-1: Caveolae-dependent signalling and cardiovascular disease. Biochem Soc Trans 2014;42:284-288.
448 Capozza F, Cohen AW, Cheung MW, Sotgia F, Schubert W, Battista M, Lee H, Frank PG, Lisanti MP: Muscle-specific interaction of caveolin isoforms: Differential complex formation between caveolins in fibroblastic vs. Muscle cells. Am J Physiol Cell Physiol 2005;288:C677-691.
449 Feron O, Balligand JL: Caveolins and the regulation of endothelial nitric oxide synthase in the heart. Cardiovasc Res 2006;69:788-797.
450 Feron O, Belhassen L, Kobzik L, Smith TW, Kelly RA, Michel T: Endothelial nitric oxide synthase targeting to caveolae. Specific interactions with caveolin isoforms in cardiac myocytes and endothelial cells. J Biol Chem 1996;271:22810-22814.
451 Mineo C, Shaul PW: Regulation of enos in caveolae. Adv Exp Med Biol 2012;729:51-62.
452 Trane AE, Pavlov D, Sharma A, Saqib U, Lau K, van Petegem F, Minshall RD, Roman LJ, Bernatchez PN: Deciphering the binding of caveolin-1 to client protein endothelial nitric-oxide synthase (enos): Scaffolding subdomain identification, interaction modeling, and biological significance. J Biol Chem 2014;289:13273-13283.
453 Karuppiah K, Druhan LJ, Chen CA, Smith T, Zweier JL, Sessa WC, Cardounel AJ: Suppression of enos-derived superoxide by caveolin-1: A biopterin-dependent mechanism. Am J Physiol Heart Circ Physiol 2011;301:H903-911.
454 Lee H, Goetzl EJ, An S: Lysophosphatidic acid and sphingosine 1-phosphate stimulate endothelial cell wound healing. Am J Physiol Cell Physiol 2000;278:C612-618.
455 Muraki K, Imaizumi Y: A novel function of sphingosine-1-phosphate to activate a non-selective cation channel in human endothelial cells. J Physiol 2001;537:431-441.
456 Pulli I, Blom T, Lof C, Magnusson M, Rimessi A, Pinton P, Tornquist K: A novel chimeric aequorin fused with caveolin-1 reveals a sphingosine kinase 1-regulated ca(2)(+) microdomain in the caveolar compartment. Biochim Biophys Acta 2015;1853:2173-2182.
457 Egom EE, Mohamed TM, Mamas MA, Shi Y, Liu W, Chirico D, Stringer SE, Ke Y, Shaheen M, Wang T, Chacko S, Wang X, Solaro RJ, Fath-Ordoubadi F, Cartwright EJ, Lei M: Activation of pak1/akt/enos signaling following sphingosine-1-phosphate release as part of a mechanism protecting cardiomyocytes against ischemic cell injury. Am J Physiol Heart Circ Physiol 2011;301:H1487-1495.
458 Dantas AP, Igarashi J, Michel T: Sphingosine 1-phosphate and control of vascular tone. Am J Physiol Heart Circ Physiol 2003;284:H2045-2052.
459 Mulders AC, Mathy MJ, Meyer zu Heringdorf D, ter Braak M, Hajji N, Olthof DC, Michel MC, Alewijnse AE, Peters SL: Activation of sphingosine kinase by muscarinic receptors enhances no-mediated and attenuates edhf-mediated vasorelaxation. Basic Res Cardiol 2009;104:50-59.
460 Salomone S, Potts EM, Tyndall S, Ip PC, Chun J, Brinkmann V, Waeber C: Analysis of sphingosine 1-phosphate receptors involved in constriction of isolated cerebral arteries with receptor null mice and pharmacological tools. Br J Pharmacol 2008;153:140-147.
461 Nofer JR, van der Giet M, Tolle M, Wolinska I, von Wnuck Lipinski K, Baba HA, Tietge UJ, Godecke A, Ishii I, Kleuser B, Schafers M, Fobker M, Zidek W, Assmann G,

Chun J, Levkau B: Hdl induces no-dependent vasorelaxation via the lysophospholipid receptor s1p3. J Clin Invest 2004;113:569-581.

462 Tolle M, Levkau B, Keul P, Brinkmann V, Giebing G, Schonfelder G, Schafers M, von Wnuck Lipinski K, Jankowski J, Jankowski V, Chun J, Zidek W, Van der Giet M: Immunomodulator fty720 induces enos-dependent arterial vasodilatation via the lysophospholipid receptor s1p3. Circ Res 2005;96:913-920.

463 Westhoff TH, Schmidt S, Glander P, Liefeld L, Martini S, Offermann G, Neumayer HH, Zidek W, van der Giet M, Budde K: The impact of fty720 (fingolimod) on vasodilatory function and arterial elasticity in renal transplant patients. Nephrol Dial Transplant 2007;22:2354-2358.

464 Damirin A, Tomura H, Komachi M, Tobo M, Sato K, Mogi C, Nochi H, Tamoto K, Okajima F: Sphingosine 1-phosphate receptors mediate the lipid-induced camp accumulation through cyclooxygenase-2/prostaglandin i2 pathway in human coronary artery smooth muscle cells. Mol Pharmacol 2005;67:1177-1185.

465 Gonzalez-Diez M, Rodriguez C, Badimon L, Martinez-Gonzalez J: Prostacyclin induction by high-density lipoprotein (hdl) in vascular smooth muscle cells depends on sphingosine 1-phosphate receptors: Effect of simvastatin. Thromb Haemost 2008;100:119-126.

466 Somlyo AP, Somlyo AV: Ca2+ sensitivity of smooth muscle and nonmuscle myosin ii: Modulated by g proteins, kinases, and myosin phosphatase. Physiol Rev 2003;83:1325-1358.

467 Moreno-Dominguez A, Colinas O, El-Yazbi A, Walsh EJ, Hill MA, Walsh MP, Cole WC: Ca2+ sensitization due to myosin light chain phosphatase inhibition and cytoskeletal reorganization in the myogenic response of skeletal muscle resistance arteries. J Physiol 2013;591:1235-1250.

468 Fujii K, Machida T, Iizuka K, Hirafuji M: Sphingosine 1-phosphate increases an intracellular ca(2+) concentration via s1p3 receptor in cultured vascular smooth muscle cells. J Pharm Pharmacol 2014;66:802-810.

469 Coussin F, Scott RH, Wise A, Nixon GF: Comparison of sphingosine 1-phosphate-induced intracellular signaling pathways in vascular smooth muscles: Differential role in vasoconstriction. Circ Res 2002;91:151-157.

470 Bischoff A, Czyborra P, Fetscher C, Meyer Zu Heringdorf D, Jakobs KH, Michel MC: Sphingosine-1-phosphate and sphingosylphosphorylcholine constrict renal and mesenteric microvessels in vitro. Br J Pharmacol 2000;130:1871-1877.

471 Ohmori T, Yatomi Y, Osada M, Ozaki Y: Platelet-derived sphingosine 1-phosphate induces contraction of coronary artery smooth muscle cells via s1p2. J Thromb Haemost 2004;2:203-205.

472 Szczepaniak WS, Pitt BR, McVerry BJ: S1p2 receptor-dependent rho-kinase activation mediates vasoconstriction in the murine pulmonary circulation induced by sphingosine 1-phosphate. Am J Physiol Lung Cell Mol Physiol 2010;299:L137-145.

473 Hemmings DG, Hudson NK, Halliday D, O'Hara M, Baker PN, Davidge ST, Taggart MJ: Sphingosine-1-phosphate acts via rho-associated kinase and nitric oxide to regulate human placental vascular tone. Biol Reprod 2006;74:88-94.

474 Tosaka M, Okajima F, Hashiba Y, Saito N, Nagano T, Watanabe T, Kimura T, Sasaki T: Sphingosine 1-phosphate contracts canine basilar arteries in vitro and in vivo: Possible role in pathogenesis of cerebral vasospasm. Stroke 2001;32:2913-2919.

475 Bolz SS, Vogel L, Sollinger D, Derwand R, de Wit C, Loirand G, Pohl U: Nitric oxide-induced decrease in calcium sensitivity of resistance arteries is attributable to activation of the myosin light chain phosphatase and antagonized by the rhoa/rho kinase pathway. Circulation 2003;107:3081-3087.

476 Kamiya T, Nagaoka T, Omae T, Yoshioka T, Ono S, Tanano I, Yoshida A: Role of ca2+ -dependent and ca2+ -sensitive mechanisms in sphingosine 1-phosphate-induced constriction of isolated porcine retinal arterioles in vitro. Exp Eye Res 2014;121:94-101.

477 Chung FY, Song HJ, Park SY, Jang HS, Kim DS, Sim SS, Sohn UD: Signaling mechanisms of sphingosine 1-phosphate-induced erk1/2 activation in cultured feline esophageal smooth muscle cells. Arch Pharm Res 2008;31:1437-1445.

478 Song HJ, Choi TS, Chung FY, Park SY, Ryu JS, Woo JG, Min YS, Shin CY, Sohn UD: Sphingosine 1-phosphate-induced signal transduction in cat esophagus smooth muscle cells. Mol Cells 2006;21:42-51.

479 Zhou H, Murthy KS: Distinctive g protein-dependent signaling in smooth muscle by sphingosine 1-phosphate receptors s1p1 and s1p2. Am J Physiol Cell Physiol 2004;286:C1130-1138.

480 Guan Z, Singletary ST, Cook AK, Hobbs JL, Pollock JS, Inscho EW: Sphingosine-1-phosphate evokes unique segment-specific vasoconstriction of the renal microvasculature. J Am Soc Nephrol 2014;25:1774-1785.

481 Murakami A, Takasugi H, Ohnuma S, Koide Y, Sakurai A, Takeda S, Hasegawa T, Sasamori J, Konno T, Hayashi K, Watanabe Y, Mori K, Sato Y, Takahashi A, Mochizuki N, Takakura N: Sphingosine 1-phosphate (s1p) regulates vascular contraction via s1p3 receptor: Investigation based on a new s1p3 receptor antagonist. Mol Pharmacol 2010;77:704-713.

482 Lorenz JN, Arend LJ, Robitz R, Paul RJ, MacLennan AJ: Vascular dysfunction in s1p2 sphingosine 1-phosphate receptor knockout mice. Am J Physiol Regul Integr Comp Physiol 2007;292:R440-446.

483 Alewijnse AE, Peters SL: Sphingolipid signalling in the cardiovascular system: Good, bad or both? Eur J Pharmacol 2008;585:292-302.

484 Salomone S, Yoshimura S, Reuter U, Foley M, Thomas SS, Moskowitz MA, Waeber C: S1p3 receptors mediate the potent constriction of cerebral arteries by sphingosine-1-phosphate. Eur J Pharmacol 2003;469:125-134.

485 Ohmori T, Yatomi Y, Osada M, Kazama F, Takafuta T, Ikeda H, Ozaki Y: Sphingosine 1-phosphate induces contraction of coronary artery smooth muscle cells via s1p2. Cardiovasc Res 2003;58:170-177.

486 Ulrych T, Bohm A, Polzin A, Daum G, Nusing RM, Geisslinger G, Hohlfeld T, Schror K, Rauch BH: Release of sphingosine-1-phosphate from human platelets is dependent on thromboxane formation. J Thromb Haemost 2011;9:790-798.

487 Hamberg M, Svensson J, Samuelsson B: Thromboxanes: A new group of biologically active compounds derived from prostaglandin endoperoxides. Proc Natl Acad Sci U S A 1975;72:2994-2998.

488 Borgeat P, Samuelsson B: Arachidonic acid metabolism in polymorphonuclear leukocytes: Effects of ionophore a23187. Proc Natl Acad Sci U S A 1979;76:2148-2152.

489 Brash AR: Lipoxygenases: Occurrence, functions, catalysis, and acquisition of substrate. J Biol Chem 1999;274:23679-23682.

490 Chavis C, Godard P, Crastes de Paulet A, Damon M: Formation of lipoxins and leukotrienes by human alveolar macrophages incubated with 15(s)-hete: A model for cellular cooperation between macrophages and airway epithelial cells. Eicosanoids 1992;5:203-211.

491 Stenson WF, Parker CW: Metabolism of arachidonic acid in ionophore-stimulated neutrophils. Esterification of a hydroxylated metabolite into phospholipids. J Clin Invest 1979;64:1457-1465.

492 Bonser RW, Siegel MI, Chung SM, McConnell RT, Cuatrecasas P: Esterification of an endogenously synthesized lipoxygenase product into granulocyte cellular lipids. Biochemistry 1981;20:5297-5301.

493 O'Flaherty JT, Wykle RL, Redman J, Samuel M, Thomas M: Metabolism of 5-hydroxyicosatetraenoate by human neutrophils: Production of a novel omega-oxidized derivative. J Immunol 1986;137:3277-3283.

494 Arai M, Imai H, Metori A, Nakagawa Y: Preferential esterification of endogenously formed 5-hydroxyeicosatetraenoic acid to phospholipids in activated polymorphonuclear leukocytes. Eur J Biochem 1997;244:513-519.

495 Powell WS, Gravelle F, Gravel S: Metabolism of 5(s)-hydroxy-6,8,11,14-eicosatetraenoic acid and other 5(s)-hydroxyeicosanoids by a specific dehydrogenase in human polymorphonuclear leukocytes. J Biol Chem 1992;267:19233-19241.

496 Serhan CN: On the relationship between leukotriene and lipoxin production by human neutrophils: Evidence for differential metabolism of 15-hete and 5-hete. Biochim Biophys Acta 1989;1004:158-168.

497 Borgeat P, Picard S, Vallerand P, Sirois P: Transformation of arachidonic acid in leukocytes. Isolation and structural analysis of a novel dihydroxy derivative. Prostaglandins Med 1981;6:557-570.

498 Tejera N, Boeglin WE, Suzuki T, Schneider C: Cox-2-dependent and -independent biosynthesis of dihydroxy-arachidonic acids in activated human leukocytes. J Lipid Res 2012;53:87-94.

499 Powell WS, Rokach J: Biosynthesis, biological effects, and receptors of hydroxyeicosatetraenoic acids (hetes) and oxoeicosatetraenoic acids (oxo-etes) derived from arachidonic acid. Biochim Biophys Acta 2015;1851:340-355.

500 Wlodawer P, Samuelsson B: On the organization and mechanism of prostaglandin synthetase. J Biol Chem 1973;248:5673-5678.

501 Smith WL, Song I: The enzymology of prostaglandin endoperoxide h synthases-1 and -2. Prostaglandins Other Lipid Mediat 2002;68-69:115-128.

502 Davidge ST: Prostaglandin h synthase and vascular function. Circ Res 2001;89:650-660.

503 Eligini S, Arenaz I, Barbieri SS, Faleri ML, Crisci M, Tremoli E, Colli S: Cyclooxygenase-2 mediates hydrogen peroxide-induced wound repair in human endothelial cells. Free Radic Biol Med 2009;46:1428-1436.

504 Morita I: Distinct functions of cox-1 and cox-2. Prostaglandins Other Lipid Mediat 2002;68-69:165-175.

505 DeWitt DL, Day JS, Sonnenburg WK, Smith WL: Concentrations of prostaglandin endoperoxide synthase and prostaglandin i2 synthase in the endothelium and smooth muscle of bovine aorta. J Clin Invest 1983;72:1882-1888.

506 Tang EH, Vanhoutte PM: Gene expression changes of prostanoid synthases in endothelial cells and prostanoid receptors in vascular smooth muscle cells caused by aging and hypertension. Physiol Genomics 2008;32:409-418.
507 Park JY, Pillinger MH, Abramson SB: Prostaglandin e2 synthesis and secretion: The role of pge2 synthases. Clin Immunol 2006;119:229-240.
508 Doroudi R, Gan LM, Selin Sjogren L, Jern S: Effects of shear stress on eicosanoid gene expression and metabolite production in vascular endothelium as studied in a novel biomechanical perfusion model. Biochem Biophys Res Commun 2000;269:257-264.
509 Funk CD, FitzGerald GA: Cox-2 inhibitors and cardiovascular risk. J Cardiovasc Pharmacol 2007;50:470-479.
510 Schroer J, Shenk T: Inhibition of cyclooxygenase activity blocks cell-to-cell spread of human cytomegalovirus. Proc Natl Acad Sci U S A 2008;105:19468-19473.
511 Zhu H, Cong JP, Yu D, Bresnahan WA, Shenk TE: Inhibition of cyclooxygenase 2 blocks human cytomegalovirus replication. Proc Natl Acad Sci U S A 2002;99:3932-3937.
512 Palmer MA, Piper PJ, Vane JR: The release of rabbit aorta contracting substance (rcs) from chopped lung and its antagonism by anti-inflammatory drugs. Br J Pharmacol 1970;40:581P-582P.
513 Hayaishi O: [prostaglandins and sleep]. Nihon Rinsho 1998;56:285-289.
514 Onoe H: [molecular and neuroanatomical mechanisms of sleep-wakefulness regulation by prostaglandins d2 and e2]. Nihon Yakurigaku Zasshi 1998;112:343-349.
515 Watanabe K: Prostaglandin f synthase. Prostaglandins Other Lipid Mediat 2002;68-69:401-407.
516 Brash AR, Jackson EK, Lawson JA, Branch RA, Oates JA, FitzGerald GA: Quantitative aspects of prostacyclin metabolism in humans. Adv Prostaglandin Thromboxane Leukot Res 1983;11:119-122.
517 Brash AR, Jackson EK, Saggese CA, Lawson JA, Oates JA, FitzGerald GA: Metabolic disposition of prostacyclin in humans. J Pharmacol Exp Ther 1983;226:78-87.
518 Needleman P, Moncada S, Bunting S, Vane JR, Hamberg M, Samuelsson B: Identification of an enzyme in platelet microsomes which generates thromboxane a2 from prostaglandin endoperoxides. Nature 1976;261:558-560.
519 Haurand M, Ullrich V: Isolation and characterization of thromboxane synthase from human platelets as a cytochrome p-450 enzyme. J Biol Chem 1985;260:15059-15067.
520 Shen RF, Tai HH: Monoclonal antibodies to thromboxane synthase from porcine lung. Production and application to development of a tandem immunoradiometric assay. J Biol Chem 1986;261:11585-11591.
521 Sun FF, Chapman JP, McGuire JC: Metabolism of prostaglandin endoperoxide in animal tissues. Prostaglandins 1977;14:1055-1074.
522 Needleman P, Minkes M, Raz A: Thromboxanes: Selective biosynthesis and distinct biological properties. Science 1976;193:163-165.
523 Ushikubi F, Nakamura K, Narumiya S: Functional reconstitution of platelet thromboxane a2 receptors with gq and gi2 in phospholipid vesicles. Mol Pharmacol 1994;46:808-816.
524 Hirata M, Hayashi Y, Ushikubi F, Yokota Y, Kageyama R, Nakanishi S, Narumiya S: Cloning and expression of cdna for a human thromboxane a2 receptor. Nature 1991;349:617-620.

525 Raychowdhury MK, Yukawa M, Collins LJ, McGrail SH, Kent KC, Ware JA: Alternative splicing produces a divergent cytoplasmic tail in the human endothelial thromboxane a2 receptor. J Biol Chem 1994;269:19256-19261.

526 Shenker A, Goldsmith P, Unson CG, Spiegel AM: The g protein coupled to the thromboxane a2 receptor in human platelets is a member of the novel gq family. J Biol Chem 1991;266:9309-9313.

527 Offermanns S, Laugwitz KL, Spicher K, Schultz G: G proteins of the g12 family are activated via thromboxane a2 and thrombin receptors in human platelets. Proc Natl Acad Sci U S A 1994;91:504-508.

528 Hirata T, Ushikubi F, Kakizuka A, Okuma M, Narumiya S: Two thromboxane a2 receptor isoforms in human platelets. Opposite coupling to adenylyl cyclase with different sensitivity to arg60 to leu mutation. J Clin Invest 1996;97:949-956.

529 Feletou M, Vanhoutte PM, Verbeuren TJ: The thromboxane/endoperoxide receptor (tp): The common villain. J Cardiovasc Pharmacol 2010;55:317-332.

530 Feletou M, Vanhoutte PM: Endothelium-dependent hyperpolarizations: Past beliefs and present facts. Ann Med 2007;39:495-516.

531 Behm DJ, Ogbonna A, Wu C, Burns-Kurtis CL, Douglas SA: Epoxyeicosatrienoic acids function as selective, endogenous antagonists of native thromboxane receptors: Identification of a novel mechanism of vasodilation. J Pharmacol Exp Ther 2009;328:231-239.

532 Ally AI, Horrobin DF: Thromboxane a2 in blood vessel walls and its physiological significance: Relevance to thrombosis and hypertension. Prostaglandins Med 1980;4:431-438.

533 Katugampola SD, Davenport AP: Thromboxane receptor density is increased in human cardiovascular disease with evidence for inhibition at therapeutic concentrations by the at(1) receptor antagonist losartan. Br J Pharmacol 2001;134:1385-1392.

534 Hunt JA, Merritt JE, MacDermot J, Keen M: Characterization of the thromboxane receptor mediating prostacyclin release from cultured endothelial cells. Biochem Pharmacol 1992;43:1747-1752.

535 Montuschi P, Barnes PJ, Roberts LJ, 2nd: Isoprostanes: Markers and mediators of oxidative stress. Faseb J 2004;18:1791-1800.

536 Ishizuka T, Kawakami M, Hidaka T, Matsuki Y, Takamizawa M, Suzuki K, Kurita A, Nakamura H: Stimulation with thromboxane a2 (txa2) receptor agonist enhances icam-1, vcam-1 or elam-1 expression by human vascular endothelial cells. Clin Exp Immunol 1998;112:464-470.

537 Ishizuka T, Suzuki K, Kawakami M, Hidaka T, Matsuki Y, Nakamura H: Thromboxane a2 receptor blockade suppresses intercellular adhesion molecule-1 expression by stimulated vascular endothelial cells. Eur J Pharmacol 1996;312:367-377.

538 Ashton AW, Ware GM, Kaul DK, Ware JA: Inhibition of tumor necrosis factor alpha-mediated nfkappab activation and leukocyte adhesion, with enhanced endothelial apoptosis, by g protein-linked receptor (tp) ligands. J Biol Chem 2003;278:11858-11866.

539 Nie D, Lamberti M, Zacharek A, Li L, Szekeres K, Tang K, Chen Y, Honn KV: Thromboxane a(2) regulation of endothelial cell migration, angiogenesis, and tumor metastasis. Biochem Biophys Res Commun 2000;267:245-251.

540 Devillier P, Bessard G: Thromboxane a2 and related prostaglandins in airways. Fundam Clin Pharmacol 1997;11:2-18.

541 Schultheiss G, Diener M: Inhibition of spontaneous smooth muscle contractions in rat and rabbit intestine by blockers of the thromboxane a2 pathway. Zentralbl Veterinarmed A 1999;46:123-131.

542 Wilhelmsson L, Wikland M, Wiqvist N: Pgh2, txa2 and pgi2 have potent and differentiated actions on human uterine contractility. Prostaglandins 1981;21:277-286.

543 Palea S, Toson G, Pietra C, Trist DG, Artibani W, Romano O, Corsi M: Pharmacological characterization of thromboxane and prostanoid receptors in human isolated urinary bladder. Br J Pharmacol 1998;124:865-872.

544 Geoffroy J, Benzoni D, Sassard J: Antihypertensive effect of thromboxane a2 receptor blockade in genetically hypertensive rats of the lyon strain. J Hypertens Suppl 1989;7:S272-273.

545 Liel N, Nathan I, Yermiyahu T, Zolotov Z, Lieberman JR, Dvilansky A, Halushka PV: Increased platelet thromboxane a2/prostaglandin h2 receptors in patients with pregnancy induced hypertension. Thromb Res 1993;70:205-210.

546 Martin C, Uhlig S, Ullrich V: Cytokine-induced bronchoconstriction in precision-cut lung slices is dependent upon cyclooxygenase-2 and thromboxane receptor activation. Am J Respir Cell Mol Biol 2001;24:139-145.

547 Hata AN, Breyer RM: Pharmacology and signaling of prostaglandin receptors: Multiple roles in inflammation and immune modulation. Pharmacol Ther 2004;103:147-166.

548 Halushka PV: Thromboxane a(2) receptors: Where have you gone? Prostaglandins Other Lipid Mediat 2000;60:175-189.

549 Dogne JM, Hanson J, Pratico D: Thromboxane, prostacyclin and isoprostanes: Therapeutic targets in atherogenesis. Trends Pharmacol Sci 2005;26:639-644.

550 Yokoyama C, Miyata A, Ihara H, Ullrich V, Tanabe T: Molecular cloning of human platelet thromboxane a synthase. Biochem Biophys Res Commun 1991;178:1479-1484.

551 Feletou M, Huang Y, Vanhoutte PM: Endothelium-mediated control of vascular tone: Cox-1 and cox-2 products. Br J Pharmacol 2011;164:894-912.

552 Tsai MH, Jiang MJ: Rho-kinase-mediated regulation of receptor-agonist-stimulated smooth muscle contraction. Pflugers Arch 2006;453:223-232.

553 Momotani K, Artamonov MV, Utepbergenov D, Derewenda U, Derewenda ZS, Somlyo AV: P63rhogef couples galpha(q/11)-mediated signaling to ca2+ sensitization of vascular smooth muscle contractility. Circ Res 2011;109:993-1002.

554 Tang EH, Vanhoutte PM: Prostanoids and reactive oxygen species: Team players in endothelium-dependent contractions. Pharmacol Ther 2009;122:140-149.

555 Perez-Vizcaino F, Villamor E, Duarte J, Tamargo J: Involvement of protein kinase c in reduced relaxant responses to the no/cyclic gmp pathway in piglet pulmonary arteries contracted by the thromboxane a2-mimetic u46619. Br J Pharmacol 1997;121:1323-1333.

556 Vega A, Chacon P, Alba G, El Bekay R, Martin-Nieto J, Sobrino F: Modulation of ige-dependent cox-2 gene expression by reactive oxygen species in human neutrophils. J Leukoc Biol 2006;80:152-163.

557 Laursen JB, Somers M, Kurz S, McCann L, Warnholtz A, Freeman BA, Tarpey M, Fukai T, Harrison DG: Endothelial regulation of vasomotion in apoe-deficient mice: Implications for interactions between peroxynitrite and tetrahydrobiopterin. Circulation 2001;103:1282-1288.

558 Chen CA, Wang TY, Varadharaj S, Reyes LA, Hemann C, Talukder MA, Chen YR, Druhan LJ, Zweier JL: S-glutathionylation uncouples enos and regulates its cellular and vascular function. Nature 2010;468:1115-1118.

559 Wilson SJ, Cavanagh CC, Lesher AM, Frey AJ, Russell SE, Smyth EM: Activation-dependent stabilization of the human thromboxane receptor: Role of reactive oxygen species. J Lipid Res 2009;50:1047-1056.

560 Kuo C, Campbell LA: Is infection with chlamydia pneumoniae a causative agent in atherosclerosis? Mol Med Today 1998;4:426-430.

561 Liuba P, Karnani P, Pesonen E, Paakkari I, Forslid A, Johansson L, Persson K, Wadstrom T, Laurini R: Endothelial dysfunction after repeated chlamydia pneumoniae infection in apolipoprotein e-knockout mice. Circulation 2000;102:1039-1044.

562 Channon KM, Qian HS, Youngblood SA, Olmez E, Shetty GA, Nepliouevа V, Blazing MA, George SE: Acute host-mediated endothelial injury after adenoviral gene transfer in normal rabbit arteries: Impact on transgene expression and endothelial function. Circ Res 1998;82:1253-1262.

563 Chi D, Henry J, Kelley J, Thorpe R, Smith JK, Krishnaswamy G: The effects of hiv infection on endothelial function. Endothelium 2000;7:223-242.

564 Szklo M, Ding J, Tsai MY, Cushman M, Polak JF, Lima J, Barr RG, Sharrett AR: Individual pathogens, pathogen burden and markers of subclinical atherosclerosis: The multi-ethnic study of atherosclerosis. J Cardiovasc Med (Hagerstown) 2009;10:747-751.

565 Ross R: Atherosclerosis--an inflammatory disease. N Engl J Med 1999;340:115-126.

566 Alexander RW: Theodore cooper memorial lecture. Hypertension and the pathogenesis of atherosclerosis. Oxidative stress and the mediation of arterial inflammatory response: A new perspective. Hypertension 1995;25:155-161.

567 Bhagat K, Vallance P: Inflammatory cytokines impair endothelium-dependent dilatation in human veins in vivo. Circulation 1997;96:3042-3047.

568 Cleland SJ, Sattar N, Petrie JR, Forouhi NG, Elliott HL, Connell JM: Endothelial dysfunction as a possible link between c-reactive protein levels and cardiovascular disease. Clin Sci (Lond) 2000;98:531-535.

569 Sinisalo J, Paronen J, Mattila KJ, Syrjala M, Alfthan G, Palosuo T, Nieminen MS, Vaarala O: Relation of inflammation to vascular function in patients with coronary heart disease. Atherosclerosis 2000;149:403-411.

570 Hingorani AD, Cross J, Kharbanda RK, Mullen MJ, Bhagat K, Taylor M, Donald AE, Palacios M, Griffin GE, Deanfield JE, MacAllister RJ, Vallance P: Acute systemic inflammation impairs endothelium-dependent dilatation in humans. Circulation 2000;102:994-999.

571 Schalkwijk CG, Poland DC, van Dijk W, Kok A, Emeis JJ, Drager AM, Doni A, van Hinsbergh VW, Stehouwer CD: Plasma concentration of c-reactive protein is increased in type i diabetic patients without clinical macroangiopathy and correlates with markers of endothelial dysfunction: Evidence for chronic inflammation. Diabetologia 1999;42:351-357.

572 Gombos RB, Hemmings DG: Differential effects on nitric oxide-mediated vasodilation in mesenteric and uterine arteries from cytomegalovirus-infected mice. Am J Physiol Heart Circ Physiol 2010;299:H1124-1134.

573 Gombos RB, Wolan V, McDonald K, Hemmings DG: Impaired vascular function in mice with an active cytomegalovirus infection. Am J Physiol Heart Circ Physiol 2009;296:H937-945.
574 Gombos RB, Teefy J, Lee A, Hemmings DG: Impact of local endothelial challenge with cytomegalovirus or glycoprotein b on vasodilation in intact pressurized arteries from nonpregnant and pregnant mice. Biol Reprod 2012;87:83.
575 Selinsky C, Luke C, Wloch M, Geall A, Hermanson G, Kaslow D, Evans T: A DNA-based vaccine for the prevention of human cytomegalovirus-associated diseases. Hum Vaccin 2005;1:16-23.
576 Staras SA, Dollard SC, Radford KW, Flanders WD, Pass RF, Cannon MJ: Seroprevalence of cytomegalovirus infection in the united states, 1988-1994. Clin Infect Dis 2006;43:1143-1151.
577 Sia IG, Patel R: New strategies for prevention and therapy of cytomegalovirus infection and disease in solid-organ transplant recipients. Clin Microbiol Rev 2000;13:83-121, table of contents.
578 Griffiths P, Baraniak I, Reeves M: The pathogenesis of human cytomegalovirus. J Pathol 2015;235:288-297.
579 Sinclair J, Sissons P: Latency and reactivation of human cytomegalovirus. J Gen Virol 2006;87:1763-1779.
580 Dupont L, Reeves MB: Cytomegalovirus latency and reactivation: Recent insights into an age old problem. Rev Med Virol 2015.
581 Steininger C: Clinical relevance of cytomegalovirus infection in patients with disorders of the immune system. Clin Microbiol Infect 2007;13:953-963.
582 Jackson SE, Mason GM, Wills MR: Human cytomegalovirus immunity and immune evasion. Virus Res 2011;157:151-160.
583 Rafailidis PI, Mourtzoukou EG, Varbobitis IC, Falagas ME: Severe cytomegalovirus infection in apparently immunocompetent patients: A systematic review. Virol J 2008;5:47.
584 Soderberg-Naucler C: Does cytomegalovirus play a causative role in the development of various inflammatory diseases and cancer? J Intern Med 2006;259:219-246.
585 Koch S, Solana R, Dela Rosa O, Pawelec G: Human cytomegalovirus infection and t cell immunosenescence: A mini review. Mech Ageing Dev 2006;127:538-543.
586 Saffert RT, Penkert RR, Kalejta RF: Cellular and viral control over the initial events of human cytomegalovirus experimental latency in cd34+ cells. J Virol 2010;84:5594-5604.
587 Melnick JL, Adam E, Debakey ME: Cytomegalovirus and atherosclerosis. Eur Heart J 1993;14 Suppl K:30-38.
588 Shimamura M: The contribution of cytomegalovirus to atherosclerotic events after kidney transplantation. J Infect Dis 2013;207:1487-1490.
589 Wu SJ, Villarreal DO, Shedlock DJ, Weiner DB: Synthetic DNA approach to cytomegalovirus vaccine/immune therapy. Adv Exp Med Biol 2015;848:131-148.
590 Fu TM, An Z, Wang D: Progress on pursuit of human cytomegalovirus vaccines for prevention of congenital infection and disease. Vaccine 2014;32:2525-2533.
591 Plotkin SA, Starr SE, Friedman HM, Brayman K, Harris S, Jackson S, Tustin NB, Grossman R, Dafoe D, Barker C: Effect of towne live virus vaccine on cytomegalovirus disease after renal transplant. A controlled trial. Ann Intern Med 1991;114:525-531.

592 Plotkin SA, Huang ES: Cytomegalovirus vaccine virus (towne strain) does not induce latency. J Infect Dis 1985;152:395-397.
593 Plotkin SA, Weibel RE, Alpert G, Starr SE, Friedman HM, Preblud SR, Hoxie J: Resistance of seropositive volunteers to subcutaneous challenge with low-passage human cytomegalovirus. J Infect Dis 1985;151:737-739.
594 Plotkin SA, Starr SE, Friedman HM, Gonczol E, Weibel RE: Protective effects of towne cytomegalovirus vaccine against low-passage cytomegalovirus administered as a challenge. J Infect Dis 1989;159:860-865.
595 Adler SP, Plotkin SA, Gonczol E, Cadoz M, Meric C, Wang JB, Dellamonica P, Best AM, Zahradnik J, Pincus S, Berencsi K, Cox WI, Gyulai Z: A canarypox vector expressing cytomegalovirus (cmv) glycoprotein b primes for antibody responses to a live attenuated cmv vaccine (towne). J Infect Dis 1999;180:843-846.
596 Endresz V, Burian K, Berencsi K, Gyulai Z, Kari L, Horton H, Virok D, Meric C, Plotkin SA, Gonczol E: Optimization of DNA immunization against human cytomegalovirus. Vaccine 2001;19:3972-3980.
597 Griffiths PD, Boeckh M: Antiviral therapy for human cytomegalovirus. 2007.
598 Mocarski Jr E: Betaherpes viral genes and their functions. 2007.
599 Tan BH: Cytomegalovirus treatment. Curr Treat Options Infect Dis 2014;6:256-270.
600 Vaziri S, Pezhman Z, Sayyad B, Mansouri F, Janbakhsh A, Afsharian M, Najafi F: Efficacy of valganciclovir and ganciclovir for cytomegalovirus disease in solid organ transplants: A meta-analysis. J Res Med Sci 2015;19:1185-1192.
601 Matthews T, Boehme R: Antiviral activity and mechanism of action of ganciclovir. Rev Infect Dis 1988;10 Suppl 3:S490-494.
602 Crumpacker CS: Mechanism of action of foscarnet against viral polymerases. Am J Med 1992;92:3S-7S.
603 De Clercq E: Therapeutic potential of cidofovir (hpmpc, vistide) for the treatment of DNA virus (i.E. Herpes-, papova-, pox- and adenovirus) infections. Verh K Acad Geneeskd Belg 1996;58:19-47; discussion 47-19.
604 Biron KK: Antiviral drugs for cytomegalovirus diseases. Antiviral Res 2006;71:154-163.
605 Boeckh M, Murphy WJ, Peggs KS: Reprint of: Recent advances in cytomegalovirus: An update on pharmacologic and cellular therapies. Biol Blood Marrow Transplant 2015;21:S19-24.
606 Sellar RS, Peggs KS: Therapeutic strategies for cytomegalovirus infection in haematopoietic transplant recipients: A focused update. Expert Opin Biol Ther 2014;14:1121-1126.
607 Dropulic LK, Cohen JI: Update on new antivirals under development for the treatment of double-stranded DNA virus infections. Clin Pharmacol Ther 2010;88:610-619.
608 Lischka P, Hewlett G, Wunberg T, Baumeister J, Paulsen D, Goldner T, Ruebsamen-Schaeff H, Zimmermann H: In vitro and in vivo activities of the novel anticytomegalovirus compound aic246. Antimicrob Agents Chemother 2010;54:1290-1297.
609 Price NB, Prichard MN: Progress in the development of new therapies for herpesvirus infections. Curr Opin Virol 2011;1:548-554.
610 Chemaly RF, Ullmann AJ, Stoelben S, Richard MP, Bornhauser M, Groth C, Einsele H, Silverman M, Mullane KM, Brown J, Nowak H, Kolling K, Stobernack HP, Lischka

P, Zimmermann H, Rubsamen-Schaeff H, Champlin RE, Ehninger G: Letermovir for cytomegalovirus prophylaxis in hematopoietic-cell transplantation. N Engl J Med 2014;370:1781-1789.

611 Sellar RS, Ward KN, Thomson KJ, Peggs KS: Evidence for clinical activity of artesunate in multidrug-resistant herpes simplex infection following hsct. Bone Marrow Transplant 2012;47:1482-1483.

612 McGeoch DJ, Cook S, Dolan A, Jamieson FE, Telford EA: Molecular phylogeny and evolutionary timescale for the family of mammalian herpesviruses. J Mol Biol 1995;247:443-458.

613 Jarvis MA, Nelson JA: Human cytomegalovirus persistence and latency in endothelial cells and macrophages. Curr Opin Microbiol 2002;5:403-407.

614 Irmiere A, Gibson W: Isolation and characterization of a noninfectious virion-like particle released from cells infected with human strains of cytomegalovirus. Virology 1983;130:118-133.

615 Cha TA, Tom E, Kemble GW, Duke GM, Mocarski ES, Spaete RR: Human cytomegalovirus clinical isolates carry at least 19 genes not found in laboratory strains. J Virol 1996;70:78-83.

616 Chee MS, Bankier AT, Beck S, Bohni R, Brown CM, Cerny R, Horsnell T, Hutchison CA, 3rd, Kouzarides T, Martignetti JA, et al.: Analysis of the protein-coding content of the sequence of human cytomegalovirus strain ad169. Curr Top Microbiol Immunol 1990;154:125-169.

617 de Jong MD, Galasso GJ, Gazzard B, Griffiths PD, Jabs DA, Kern ER, Spector SA: Summary of the ii international symposium on cytomegalovirus. Antiviral Res 1998;39:141-162.

618 Britt W: Virus entry into host, establishment of infection, spread in host, mechanisms of tissue damage. 2007.

619 Hertel L: Human cytomegalovirus tropism for mucosal myeloid dendritic cells. Rev Med Virol 2014;24:379-395.

620 Shenk TE, Stinski MF: Human cytomegalovirus. Preface. Curr Top Microbiol Immunol 2008;325:v.

621 Kalejta RF: Tegument proteins of human cytomegalovirus. Microbiol Mol Biol Rev 2008;72:249-265, table of contents.

622 Nowlin DM, Cooper NR, Compton T: Expression of a human cytomegalovirus receptor correlates with infectibility of cells. J Virol 1991;65:3114-3121.

623 Viswanathan K, Smith MS, Malouli D, Mansouri M, Nelson JA, Fruh K: Bst2/tetherin enhances entry of human cytomegalovirus. PLoS Pathog 2011;7:e1002332.

624 Soroceanu L, Akhavan A, Cobbs CS: Platelet-derived growth factor-alpha receptor activation is required for human cytomegalovirus infection. Nature 2008;455:391-395.

625 Wang X, Huong SM, Chiu ML, Raab-Traub N, Huang ES: Epidermal growth factor receptor is a cellular receptor for human cytomegalovirus. Nature 2003;424:456-461.

626 Boyle KA, Compton T: Receptor-binding properties of a soluble form of human cytomegalovirus glycoprotein b. J Virol 1998;72:1826-1833.

627 Vanarsdall AL, Johnson DC: Human cytomegalovirus entry into cells. Curr Opin Virol 2012;2:37-42.

628 Chan G, Nogalski MT, Stevenson EV, Yurochko AD: Human cytomegalovirus induction of a unique signalsome during viral entry into monocytes mediates distinct functional changes: A strategy for viral dissemination. J Leukoc Biol 2012;92:743-752.
629 Isaacson MK, Feire AL, Compton T: Epidermal growth factor receptor is not required for human cytomegalovirus entry or signaling. J Virol 2007;81:6241-6247.
630 Chan G, Nogalski MT, Yurochko AD: Activation of egfr on monocytes is required for human cytomegalovirus entry and mediates cellular motility. Proc Natl Acad Sci U S A 2009;106:22369-22374.
631 Vanarsdall AL, Wisner TW, Lei H, Kazlauskas A, Johnson DC: Pdgf receptor-alpha does not promote hcmv entry into epithelial and endothelial cells but increased quantities stimulate entry by an abnormal pathway. PLoS Pathog 2012;8:e1002905.
632 Rossini G, Cerboni C, Santoni A, Landini MP, Landolfo S, Gatti D, Gribaudo G, Varani S: Interplay between human cytomegalovirus and intrinsic/innate host responses: A complex bidirectional relationship. Mediators Inflamm 2012;2012:607276.
633 Feire AL, Roy RM, Manley K, Compton T: The glycoprotein b disintegrin-like domain binds beta 1 integrin to mediate cytomegalovirus entry. J Virol 2010;84:10026-10037.
634 Li J, Lin ML, Wiepz GJ, Guadarrama AG, Bertics PJ: Integrin-mediated migration of murine b82l fibroblasts is dependent on the expression of an intact epidermal growth factor receptor. J Biol Chem 1999;274:11209-11219.
635 Schneller M, Vuori K, Ruoslahti E: Alphavbeta3 integrin associates with activated insulin and pdgfbeta receptors and potentiates the biological activity of pdgf. Embo J 1997;16:5600-5607.
636 Ogawa T, Asai Y, Hashimoto M, Uchida H: Bacterial fimbriae activate human peripheral blood monocytes utilizing tlr2, cd14 and cd11a/cd18 as cellular receptors. Eur J Immunol 2002;32:2543-2550.
637 Topilko A, Michelson S: Hyperimmediate entry of human cytomegalovirus virions and dense bodies into human fibroblasts. Res Virol 1994;145:75-82.
638 Cardone G, Heymann JB, Cheng N, Trus BL, Steven AC: Procapsid assembly, maturation, nuclear exit: Dynamic steps in the production of infectious herpesvirions. Adv Exp Med Biol 2012;726:423-439.
639 Dittmer A, Drach JC, Townsend LB, Fischer A, Bogner E: Interaction of the putative human cytomegalovirus portal protein pul104 with the large terminase subunit pul56 and its inhibition by benzimidazole-d-ribonucleosides. J Virol 2005;79:14660-14667.
640 Stewart M: Molecular mechanism of the nuclear protein import cycle. Nat Rev Mol Cell Biol 2007;8:195-208.
641 Cantrell SR, Bresnahan WA: Human cytomegalovirus (hcmv) ul82 gene product (pp71) relieves hdaxx-mediated repression of hcmv replication. J Virol 2006;80:6188-6191.
642 Britt B: Maturation and egress. 2007.
643 Gibson W, Marcy AI, Comolli JC, Lee J: Identification of precursor to cytomegalovirus capsid assembly protein and evidence that processing results in loss of its carboxy-terminal end. J Virol 1990;64:1241-1249.
644 Plafker SM, Gibson W: Cytomegalovirus assembly protein precursor and proteinase precursor contain two nuclear localization signals that mediate their own nuclear translocation and that of the major capsid protein. J Virol 1998;72:7722-7732.
645 Gibson W: Structure and formation of the cytomegalovirus virion. Curr Top Microbiol Immunol 2008;325:187-204.

646 Muranyi W, Haas J, Wagner M, Krohne G, Koszinowski UH: Cytomegalovirus recruitment of cellular kinases to dissolve the nuclear lamina. Science 2002;297:854-857.
647 Das S, Vasanji A, Pellett PE: Three-dimensional structure of the human cytomegalovirus cytoplasmic virion assembly complex includes a reoriented secretory apparatus. J Virol 2007;81:11861-11869.
648 Das S, Pellett PE: Spatial relationships between markers for secretory and endosomal machinery in human cytomegalovirus-infected cells versus those in uninfected cells. J Virol 2011;85:5864-5879.
649 Landolfo S, Gariglio M, Gribaudo G, Lembo D: The human cytomegalovirus. Pharmacol Ther 2003;98:269-297.
650 Sanchez V, Greis KD, Sztul E, Britt WJ: Accumulation of virion tegument and envelope proteins in a stable cytoplasmic compartment during human cytomegalovirus replication: Characterization of a potential site of virus assembly. J Virol 2000;74:975-986.
651 Sanchez V, Sztul E, Britt WJ: Human cytomegalovirus pp28 (ul99) localizes to a cytoplasmic compartment which overlaps the endoplasmic reticulum-golgi-intermediate compartment. J Virol 2000;74:3842-3851.
652 Rott D, Zhu J, Burnett MS, Zhou YF, Zalles-Ganley A, Ogunmakinwa J, Epstein SE: Effects of mf-tricyclic, a selective cyclooxygenase-2 inhibitor, on atherosclerosis progression and susceptibility to cytomegalovirus replication in apolipoprotein-e knockout mice. J Am Coll Cardiol 2003;41:1812-1819.
653 Hsich E, Zhou YF, Paigen B, Johnson TM, Burnett MS, Epstein SE: Cytomegalovirus infection increases development of atherosclerosis in apolipoprotein-e knockout mice. Atherosclerosis 2001;156:23-28.
654 Burnett MS, Gaydos CA, Madico GE, Glad SM, Paigen B, Quinn TC, Epstein SE: Atherosclerosis in apoe knockout mice infected with multiple pathogens. J Infect Dis 2001;183:226-231.
655 Cheng J, Ke Q, Jin Z, Wang H, Kocher O, Morgan JP, Zhang J, Crumpacker CS: Cytomegalovirus infection causes an increase of arterial blood pressure. PLoS Pathog 2009;5:e1000427.
656 Nerheim PL, Meier JL, Vasef MA, Li WG, Hu L, Rice JB, Gavrila D, Richenbacher WE, Weintraub NL: Enhanced cytomegalovirus infection in atherosclerotic human blood vessels. Am J Pathol 2004;164:589-600.
657 Papadakis KA, Tung JK, Binder SW, Kam LY, Abreu MT, Targan SR, Vasiliauskas EA: Outcome of cytomegalovirus infections in patients with inflammatory bowel disease. Am J Gastroenterol 2001;96:2137-2142.
658 Zhu J, Quyyumi AA, Norman JE, Csako G, Epstein SE: Cytomegalovirus in the pathogenesis of atherosclerosis: The role of inflammation as reflected by elevated c-reactive protein levels. J Am Coll Cardiol 1999;34:1738-1743.
659 Nakase H, Honzawa Y, Toyonaga T, Yamada S, Minami N, Yoshino T, Matsuura M: Diagnosis and treatment of ulcerative colitis with cytomegalovirus infection: Importance of controlling mucosal inflammation to prevent cytomegalovirus reactivation. Intest Res 2014;12:5-11.
660 Halenius A, Hengel H: Human cytomegalovirus and autoimmune disease. Biomed Res Int 2014;2014:472978.
661 Bentz GL, Jarquin-Pardo M, Chan G, Smith MS, Sinzger C, Yurochko AD: Human cytomegalovirus (hcmv) infection of endothelial cells promotes naive monocyte

extravasation and transfer of productive virus to enhance hematogenous dissemination of hcmv. J Virol 2006;80:11539-11555.

662 Yaiw KC, Mohammad AA, Taher C, Wilhelmi V, Davoudi B, Straat K, Assinger A, Ovchinnikova O, Shlyakhto E, Rahbar A, Koutonguk O, Religa P, Butler L, Khan Z, Streblow D, Pernow J, Soderberg-Naucler C: Human cytomegalovirus induces upregulation of arginase ii: Possible implications for vasculopathies. Basic Res Cardiol 2014;109:401.

663 Burns LJ, Pooley JC, Walsh DJ, Vercellotti GM, Weber ML, Kovacs A: Intercellular adhesion molecule-1 expression in endothelial cells is activated by cytomegalovirus immediate early proteins. Transplantation 1999;67:137-144.

664 Shahgasempour S, Woodroffe SB, Garnett HM: Alterations in the expression of elam-1, icam-1 and vcam-1 after in vitro infection of endothelial cells with a clinical isolate of human cytomegalovirus. Microbiol Immunol 1997;41:121-129.

665 Craigen JL, Yong KL, Jordan NJ, MacCormac LP, Westwick J, Akbar AN, Grundy JE: Human cytomegalovirus infection up-regulates interleukin-8 gene expression and stimulates neutrophil transendothelial migration. Immunology 1997;92:138-145.

666 Scholz M, Blaheta RA, Vogel J, Doerr HW, Cinatl J, Jr.: Cytomegalovirus-induced transendothelial cell migration. A closer look at intercellular communication mechanisms. Intervirology 1999;42:350-356.

667 Bruns T, Zimmermann HW, Pachnio A, Li KK, Trivedi PJ, Reynolds G, Hubscher S, Stamataki Z, Badenhorst PW, Weston CJ, Moss PA, Adams DH: Cmv infection of human sinusoidal endothelium regulates hepatic t cell recruitment and activation. J Hepatol 2015;63:38-49.

668 Varani S, Frascaroli G: Analysis of cell migration during human cytomegalovirus (hcmv) infection. Methods Mol Biol 2013;1064:299-313.

669 Rahbar A, Soderberg-Naucler C: Human cytomegalovirus infection of endothelial cells triggers platelet adhesion and aggregation. J Virol 2005;79:2211-2220.

670 van de Berg PJ, Heutinck KM, Raabe R, Minnee RC, Young SL, van Donselaar-van der Pant KA, Bemelman FJ, van Lier RA, ten Berge IJ: Human cytomegalovirus induces systemic immune activation characterized by a type 1 cytokine signature. J Infect Dis 2010;202:690-699.

671 Cheeran MC, Hu S, Yager SL, Gekker G, Peterson PK, Lokensgard JR: Cytomegalovirus induces cytokine and chemokine production differentially in microglia and astrocytes: Antiviral implications. J Neurovirol 2001;7:135-147.

672 Fernandez-Borja M, van Buul JD, Hordijk PL: The regulation of leucocyte transendothelial migration by endothelial signalling events. Cardiovasc Res 2010;86:202-210.

673 Suzuki K, Murtuza B, Suzuki N, Khan M, Kaneda Y, Yacoub MH: Human cytomegalovirus immediate-early protein ie2-86, but not ie1-72, causes graft coronary arteriopathy in the transplanted rat heart. Circulation 2002;106:I158-162.

674 Leskov IL, Whitsett J, Vasquez-Vivar J, Stokes KY: Nad(p)h oxidase and enos play differential roles in cytomegalovirus infection-induced microvascular dysfunction. Free Radic Biol Med 2011;51:2300-2308.

675 Khoretonenko MV, Leskov IL, Jennings SR, Yurochko AD, Stokes KY: Cytomegalovirus infection leads to microvascular dysfunction and exacerbates hypercholesterolemia-induced responses. Am J Pathol 2010;177:2134-2144.

676 Khoretonenko MV, Brunson JL, Senchenkov E, Leskov IL, Marks CR, Stokes KY: Platelets, acting in part via p-selectin, mediate cytomegalovirus-induced microvascular dysfunction. Am J Physiol Heart Circ Physiol 2014;307:H1745-1753.

677 Gombos RB, Brown JC, Teefy J, Gibeault RL, Conn KL, Schang LM, Hemmings DG: Vascular dysfunction in young, mid-aged and aged mice with latent cytomegalovirus infections. Am J Physiol Heart Circ Physiol 2013;304:H183-194.

678 Carr JM, Mahalingam S, Bonder CS, Pitson SM: Sphingosine kinase 1 in viral infections. Rev Med Virol 2013;23:73-84.

679 Machesky NJ, Zhang G, Raghavan B, Zimmerman P, Kelly SL, Merrill AH, Jr., Waldman WJ, Van Brocklyn JR, Trgovcich J: Human cytomegalovirus regulates bioactive sphingolipids. J Biol Chem 2008;283:26148-26160.

680 Hooks JJ, Chin MS, Srinivasan K, Momma Y, Hooper LC, Nagineni CN, Chan CC, Detrick B: Human cytomegalovirus induced cyclooxygenase-2 in human retinal pigment epithelial cells augments viral replication through a prostaglandin pathway. Microbes Infect 2006;8:2236-2244.

681 Ishii I, Friedman B, Ye X, Kawamura S, McGiffert C, Contos JJ, Kingsbury MA, Zhang G, Brown JH, Chun J: Selective loss of sphingosine 1-phosphate signaling with no obvious phenotypic abnormality in mice lacking its g protein-coupled receptor, lp(b3)/edg-3. J Biol Chem 2001;276:33697-33704.

682 Jadeja RN, Rachakonda V, Bagi Z, Khurana S: Assessing myogenic response and vasoactivity in resistance mesenteric arteries using pressure myography. J Vis Exp 2015:e50997.

683 Bevan JA, Osher JV: A direct method for recording tension changes in the wall of small blood vessels in vitro. Agents Actions 1972;2:257-260.

684 Mulvany MJ, Halpern W: Mechanical properties of vascular smooth muscle cells in situ. Nature 1976;260:617-619.

685 Mulvany MJ, Halpern W: Contractile properties of small arterial resistance vessels in spontaneously hypertensive and normotensive rats. Circ Res 1977;41:19-26.

686 Mulvany MJ, Hansen OK, Aalkjaer C: Direct evidence that the greater contractility of resistance vessels in spontaneously hypertensive rats is associated with a narrowed lumen, a thickened media, and an increased number of smooth muscle cell layers. Circ Res 1978;43:854-864.

687 Hemmings DG, Veerareddy S, Baker PN, Davidge ST: Increased myogenic responses in uterine but not mesenteric arteries from pregnant offspring of diet-restricted rat dams. Biol Reprod 2005;72:997-1003.

688 Osol G, Celia G, Gokina N, Barron C, Chien E, Mandala M, Luksha L, Kublickiene K: Placental growth factor is a potent vasodilator of rat and human resistance arteries. Am J Physiol Heart Circ Physiol 2008;294:H1381-1387.

689 Veerareddy S, Cooke CL, Baker PN, Davidge ST: Vascular adaptations to pregnancy in mice: Effects on myogenic tone. Am J Physiol Heart Circ Physiol 2002;283:H2226-2233.

690 Humphreys PW, Joels N: Changes in cardiac output and total peripheral resistance during the carotid sinus baroreceptor reflex in the pregnant rabbit. J Physiol 1977;272:45-55.

691 Tachibana H, Gotoh F, Ishikawa Y: Retinal vascular autoregulation in normal subjects. Stroke 1982;13:149-155.

692 Moss E, Lynagh S, Smith D, Kelly S, McDaid A, Bunton D: A novel system for the investigation of microvascular dysfunction including vascular permeability and flow-mediated dilatation in pressurised human arteries. J Pharmacol Toxicol Methods 2010;62:40-46.

693 Li Q, Chen B, Zeng C, Fan A, Yuan Y, Guo X, Huang X, Huang Q: Differential activation of receptors and signal pathways upon stimulation by different doses of sphingosine-1-phosphate in endothelial cells. Exp Physiol 2015;100:95-107.

694 Klausner JM, Abu-Abid S, Alexander JS, Hanshke-Mineau R, Goldman G, Morel N, Valeri CR, Shepro D, Hechtman HB: Thromboxane modulates endothelial permeability. Mediators Inflamm 1994;3:149-153.

695 Bayat H, Xu S, Pimentel D, Cohen RA, Jiang B: Activation of thromboxane receptor upregulates interleukin (il)-1beta-induced vcam-1 expression through jnk signaling. Arterioscler Thromb Vasc Biol 2008;28:127-134.

696 Kerage D MM, Gombos RB and Hemmmings, DG.: A novel mechanism for vascular tone regulation in arteries by sphingosine 1-phosphate through endothelial barrier control. Submitted to Nature Scientific Reports 2015.

697 Ryu JM, Baek YB, Shin MS, Park JH, Park SH, Lee JH, Han HJ: Sphingosine-1-phosphate-induced flk-1 transactivation stimulates mouse embryonic stem cell proliferation through s1p1/s1p3-dependent beta-arrestin/c-src pathways. Stem Cell Res 2014;12:69-85.

698 Davis MD, Clemens JJ, Macdonald TL, Lynch KR: Sphingosine 1-phosphate analogs as receptor antagonists. J Biol Chem 2005;280:9833-9841.

699 Nakahara T, Iwase A, Nakamura T, Kondo M, Bayasula, Kobayashi H, Takikawa S, Manabe S, Goto M, Kotani T, Kikkawa F: Sphingosine-1-phosphate inhibits h2o2-induced granulosa cell apoptosis via the pi3k/akt signaling pathway. Fertil Steril 2012;98:1001-1008 e1001.

700 Li C, Li JN, Kays J, Guerrero M, Nicol GD: Sphingosine 1-phosphate enhances the excitability of rat sensory neurons through activation of sphingosine 1-phosphate receptors 1 and/or 3. J Neuroinflammation 2015;12:70.

701 French KJ, Schrecengost RS, Lee BD, Zhuang Y, Smith SN, Eberly JL, Yun JK, Smith CD: Discovery and evaluation of inhibitors of human sphingosine kinase. Cancer Res 2003;63:5962-5969.

702 French KJ, Zhuang Y, Maines LW, Gao P, Wang W, Beljanski V, Upson JJ, Green CL, Keller SN, Smith CD: Pharmacology and antitumor activity of abc294640, a selective inhibitor of sphingosine kinase-2. J Pharmacol Exp Ther 2010;333:129-139.

703 Tanfin Z, Serrano-Sanchez M, Leiber D: Atp-binding cassette abcc1 is involved in the release of sphingosine 1-phosphate from rat uterine leiomyoma elt3 cells and late pregnant rat myometrium. Cell Signal 2011;23:1997-2004.

704 Minderman H, Suvannasankha A, O'Loughlin KL, Scheffer GL, Scheper RJ, Robey RW, Baer MR: Flow cytometric analysis of breast cancer resistance protein expression and function. Cytometry 2002;48:59-65.

705 Petrescu AD, Vespa A, Huang H, McIntosh AL, Schroeder F, Kier AB: Fluorescent sterols monitor cell penetrating peptide pep-1 mediated uptake and intracellular targeting of cargo protein in living cells. Biochim Biophys Acta 2009;1788:425-441.

706 Nakase I, Kobayashi NB, Takatani-Nakase T, Yoshida T: Active macropinocytosis induction by stimulation of epidermal growth factor receptor and oncogenic ras expression potentiates cellular uptake efficacy of exosomes. Sci Rep 2008;5:10300.

707 Rabiet MJ, Plantier JL, Rival Y, Genoux Y, Lampugnani MG, Dejana E: Thrombin-induced increase in endothelial permeability is associated with changes in cell-to-cell junction organization. Arterioscler Thromb Vasc Biol 1996;16:488-496.

708 Yu Y, Lv N, Lu Z, Zheng YY, Zhang WC, Chen C, Peng YJ, He WQ, Meng FQ, Zhu MS, Chen HQ: Deletion of myosin light chain kinase in endothelial cells has a minor effect on the lipopolysaccharide-induced increase in microvascular endothelium permeability in mice. Febs J 2012;279:1485-1494.

709 Cooper PH, Mayer P, Baggiolini M: Stimulation of phagocytosis in bone marrow-derived mouse macrophages by bacterial lipopolysaccharide: Correlation with biochemical and functional parameters. J Immunol 1984;133:913-922.

710 Nathan L, Cuevas J, Chaudhuri G: The role of nitric oxide in the altered vascular reactivity of pregnancy in the rat. Br J Pharmacol 1995;114:955-960.

711 Brandes RP, Kim D, Schmitz-Winnenthal FH, Amidi M, Godecke A, Mulsch A, Busse R: Increased nitrovasodilator sensitivity in endothelial nitric oxide synthase knockout mice: Role of soluble guanylyl cyclase. Hypertension 2000;35:231-236.

712 Chakrabarti S, Davidge ST: High glucose-induced oxidative stress alters estrogen effects on eralpha and erbeta in human endothelial cells: Reversal by ampk activator. Journal of Steroid Biochemistry & Molecular Biology 2009;117:99-106.

713 Sanna MG, Liao J, Jo E, Alfonso C, Ahn MY, Peterson MS, Webb B, Lefebvre S, Chun J, Gray N, Rosen H: Sphingosine 1-phosphate (s1p) receptor subtypes s1p1 and s1p3, respectively, regulate lymphocyte recirculation and heart rate. J Biol Chem 2004;279:13839-13848.

714 Catella F, Healy D, Lawson JA, FitzGerald GA: 11-dehydrothromboxane b2: A quantitative index of thromboxane a2 formation in the human circulation. Proc Natl Acad Sci U S A 1986;83:5861-5865.

715 Ashton AW, Mukherjee S, Nagajyothi FN, Huang H, Braunstein VL, Desruisseaux MS, Factor SM, Lopez L, Berman JW, Wittner M, Scherer PE, Capra V, Coffman TM, Serhan CN, Gotlinger K, Wu KK, Weiss LM, Tanowitz HB: Thromboxane a2 is a key regulator of pathogenesis during trypanosoma cruzi infection. J Exp Med 2007;204:929-940.

716 Kawasaki A, Needleman P: Contribution of thromboxane to renal resistance changes in the isolated perfused hydronephrotic rabbit kidney. Circ Res 1982;50:486-490.

717 Yoon N, Dang TQ, Chasiotis H, Kelly SP, Sweeney G: Altered transendothelial transport of hormones as a contributor to diabetes. Diabetes Metab J 2014;38:92-99.

718 Duran WN, Beuve AV, Sanchez FA: Nitric oxide, s-nitrosation, and endothelial permeability. IUBMB Life 2013;65:819-826.

719 Leach L, Taylor A, Sciota F: Vascular dysfunction in the diabetic placenta: Causes and consequences. J Anat 2009;215:69-76.

720 Kerage D, Brindley DN, Hemmings DG: Review: Novel insights into the regulation of vascular tone by sphingosine 1-phosphate. Placenta 2014;35 Suppl:S86-92.

721 Lucke S, Levkau B: Endothelial functions of sphingosine-1-phosphate. Cellular Physiology & Biochemistry 2010;26:87-96.

722 Xiong Y, Hla T: S1p control of endothelial integrity. Curr Top Microbiol Immunol 2014;378:85-105.

723 Adamson RH, Sarai RK, Altangerel A, Thirkill TL, Clark JF, Curry FR: Sphingosine-1-phosphate modulation of basal permeability and acute inflammatory responses in rat venular microvessels. Cardiovasc Res 2010;88:344-351.

724 Minnear FL, Zhu L, He P: Sphingosine 1-phosphate prevents platelet-activating factor-induced increase in hydraulic conductivity in rat mesenteric venules: Pertussis toxin sensitive. Am J Physiol Heart Circ Physiol 2005;289:H840-844.

725 Celia G, Osol G: Mechanism of vegf-induced uterine venous hyperpermeability. J Vasc Res 2005;42:47-54.

726 Sukumaran SK, Prasadarao NV: Escherichia coli k1 invasion increases human brain microvascular endothelial cell monolayer permeability by disassembling vascular-endothelial cadherins at tight junctions. J Infect Dis 2003;188:1295-1309.

727 Darwish I, Liles WC: Emerging therapeutic strategies to prevent infection-related microvascular endothelial activation and dysfunction. Virulence 2013;4:572-582.

728 McVerry BJ, Garcia JG: In vitro and in vivo modulation of vascular barrier integrity by sphingosine 1-phosphate: Mechanistic insights. Cellular signalling 2005;17:131-139.

729 Curry FR, Adamson RH: Vascular permeability modulation at the cell, microvessel, or whole organ level: Towards closing gaps in our knowledge. Cardiovasc Res 2010;87:218-229.

730 Sun X, Singleton PA, Letsiou E, Zhao J, Belvitch P, Sammani S, Chiang ET, Moreno-Vinasco L, Wade MS, Zhou T, Liu B, Parastatidis I, Thomson L, Ischiropoulos H, Natarajan V, Jacobson JR, Machado RF, Dudek SM, Garcia JG: Sphingosine-1-phosphate receptor-3 is a novel biomarker in acute lung injury. Am J Respir Cell Mol Biol 2012;47:628-636.

731 Hemmings DG, Xu Y, Davidge ST: Sphingosine 1-phosphate-induced vasoconstriction is elevated in mesenteric resistance arteries from aged female rats. Br J Pharmacol 2004;143:276-284.

732 Sanchez T, Skoura A, Wu MT, Casserly B, Harrington EO, Hla T: Induction of vascular permeability by the sphingosine-1-phosphate receptor-2 (s1p2r) and its downstream effectors rock and pten. Arteriosclerosis, Thrombosis & Vascular Biology 2007;27:1312-1318.

733 Niessen F, Schaffner F, Furlan-Freguia C, Pawlinski R, Bhattacharjee G, Chun J, Derian CK, Andrade-Gordon P, Rosen H, Ruf W: Dendritic cell par1-s1p3 signalling couples coagulation and inflammation. Nature 2008;452:654-658.

734 Takuwa Y, Okamoto H, Takuwa N, Gonda K, Sugimoto N, Sakurada S: Subtype-specific, differential activities of the edg family receptors for sphingosine-1-phosphate, a novel lysophospholipid mediator. Mol Cell Endocrinol 2001;177:3-11.

735 Sladek SM, Magness RR, Conrad KP: Nitric oxide and pregnancy. Am J Physiol 1997;272:R441-463.

736 Todd ME, Laye CG, Osborne DN: The dimensional characteristics of smooth muscle in rat blood vessels. A computer-assisted analysis. Circ Res 1983;53:319-331.

737 Deutschman DH, Carstens JS, Klepper RL, Smith WS, Page MT, Young TR, Gleason LA, Nakajima N, Sabbadini RA: Predicting obstructive coronary artery disease with serum sphingosine-1-phosphate. Am Heart J 2003;146:62-68.

738 Thompson J, Khalil RA: Gender differences in the regulation of vascular tone. Clin Exp Pharmacol Physiol 2003;30:1-15.

739 Villar IC, Hobbs AJ, Ahluwalia A: Sex differences in vascular function: Implication of endothelium-derived hyperpolarizing factor. J Endocrinol 2008;197:447-462.

740 Taylor SL, Wahl-Jensen V, Copeland AM, Jahrling PB, Schmaljohn CS: Endothelial cell permeability during hantavirus infection involves factor xii-dependent increased activation of the kallikrein-kinin system. PLoS Pathog 2013;9:e1003470.

741 Desvarieux M, Demmer RT, Jacobs DR, Jr., Rundek T, Boden-Albala B, Sacco RL, Papapanou PN: Periodontal bacteria and hypertension: The oral infections and vascular disease epidemiology study (invest). J Hypertens 2010;28:1413-1421.

742 Li C, Samaranayake NR, Ong KL, Wong HK, Cheung BM: Is human cytomegalovirus infection associated with hypertension? The united states national health and nutrition examination survey 1999-2002. PLoS One 2012;7:e39760.

743 Komarova YA, Mehta D, Malik AB: Dual regulation of endothelial junctional permeability. Science's Stke [Electronic Resource]: Signal Transduction Knowledge Environment 2007;2007:re8.

744 Van Sluis GL, Niers TM, Esmon CT, Tigchelaar W, Richel DJ, Buller HR, Van Noorden CJ, Spek CA: Endogenous activated protein c limits cancer cell extravasation through sphingosine-1-phosphate receptor 1-mediated vascular endothelial barrier enhancement. Blood 2009;114:1968-1973.

745 Duran WN, Breslin JW, Sanchez FA: The no cascade, enos location, and microvascular permeability. Cardiovasc Res 2010;87:254-261.

746 Kubes P: Nitric oxide affects microvascular permeability in the intact and inflamed vasculature. Microcirculation 1995;2:235-244.

747 Kubes P, Granger DN: Nitric oxide modulates microvascular permeability. Am J Physiol 1992;262:H611-615.

748 Yuan SY: New insights into enos signaling in microvascular permeability. Am J Physiol Heart Circ Physiol 2006;291:H1029-1031.

749 Di Lorenzo A, Lin MI, Murata T, Landskroner-Eiger S, Schleicher M, Kothiya M, Iwakiri Y, Yu J, Huang PL, Sessa WC: Enos-derived nitric oxide regulates endothelial barrier function through ve-cadherin and rho gtpases. J Cell Sci 2013;126:5541-5552.

750 Hatakeyama T, Pappas PJ, Hobson RW, 2nd, Boric MP, Sessa WC, Duran WN: Endothelial nitric oxide synthase regulates microvascular hyperpermeability in vivo. J Physiol 2006;574:275-281.

751 Thomas DD, Ridnour LA, Isenberg JS, Flores-Santana W, Switzer CH, Donzelli S, Hussain P, Vecoli C, Paolocci N, Ambs S, Colton CA, Harris CC, Roberts DD, Wink DA: The chemical biology of nitric oxide: Implications in cellular signaling. Free Radic Biol Med 2008;45:18-31.

752 Predescu D, Predescu S, Shimizu J, Miyawaki-Shimizu K, Malik AB: Constitutive enos-derived nitric oxide is a determinant of endothelial junctional integrity. Am J Physiol Lung Cell Mol Physiol 2005;289:L371-381.

753 May JM, Qu ZC: Nitric oxide mediates tightening of the endothelial barrier by ascorbic acid. Biochemical & Biophysical Research Communications 2011;404:701-705.

754 May JM, Qu ZC: Nitric oxide mediates tightening of the endothelial barrier by ascorbic acid. Biochem Biophys Res Commun 2010;404:701-705.

755 Wu HM, Huang Q, Yuan Y, Granger HJ: Vegf induces no-dependent hyperpermeability in coronary venules. Am J Physiol 1996;271:H2735-2739.

756 Yuan Y, Granger HJ, Zawieja DC, Chilian WM: Flow modulates coronary venular permeability by a nitric oxide-related mechanism. Am J Physiol 1992;263:H641-646.

757 Boughton-Smith NK, Evans SM, Laszlo F, Whittle BJ, Moncada S: The induction of nitric oxide synthase and intestinal vascular permeability by endotoxin in the rat. Br J Pharmacol 1993;110:1189-1195.

758 Garry PS, Ezra M, Rowland MJ, Westbrook J, Pattinson KT: The role of the nitric oxide pathway in brain injury and its treatment--from bench to bedside. Exp Neurol 2015;263:235-243.

759 Chakrabarti S, Chan CK, Jiang Y, Davidge ST: Neuronal nitric oxide synthase regulates endothelial inflammation. J Leukoc Biol 2012;91:947-956.

760 Cooke CL, Davidge ST: Peroxynitrite increases inos through nf-kappab and decreases prostacyclin synthase in endothelial cells. Am J Physiol Cell Physiol 2002;282:C395-402.

761 Michel T, Li GK, Busconi L: Phosphorylation and subcellular translocation of endothelial nitric oxide synthase. Proc Natl Acad Sci U S A 1993;90:6252-6256.

762 Fukumura D, Gohongi T, Kadambi A, Izumi Y, Ang J, Yun CO, Buerk DG, Huang PL, Jain RK: Predominant role of endothelial nitric oxide synthase in vascular endothelial growth factor-induced angiogenesis and vascular permeability. Proc Natl Acad Sci U S A 2001;98:2604-2609.

763 Fukumura D, Yuan F, Endo M, Jain RK: Role of nitric oxide in tumor microcirculation. Blood flow, vascular permeability, and leukocyte-endothelial interactions. Am J Pathol 1997;150:713-725.

764 Aramoto H, Breslin JW, Pappas PJ, Hobson RW, 2nd, Duran WN: Vascular endothelial growth factor stimulates differential signaling pathways in in vivo microcirculation. Am J Physiol Heart Circ Physiol 2004;287:H1590-1598.

765 Atochin DN, Wang A, Liu VW, Critchlow JD, Dantas AP, Looft-Wilson R, Murata T, Salomone S, Shin HK, Ayata C, Moskowitz MA, Michel T, Sessa WC, Huang PL: The phosphorylation state of enos modulates vascular reactivity and outcome of cerebral ischemia in vivo. J Clin Invest 2007;117:1961-1967.

766 Cohen RA, Weisbrod RM, Gericke M, Yaghoubi M, Bierl C, Bolotina VM: Mechanism of nitric oxide-induced vasodilatation: Refilling of intracellular stores by sarcoplasmic reticulum ca2+ atpase and inhibition of store-operated ca2+ influx. Circ Res 1999;84:210-219.

767 Park SK, Lin HL, Murphy S: Nitric oxide limits transcriptional induction of nitric oxide synthase in cns glial cells. Biochem Biophys Res Commun 1994;201:762-768.

768 Grumbach IM, Chen W, Mertens SA, Harrison DG: A negative feedback mechanism involving nitric oxide and nuclear factor kappa-b modulates endothelial nitric oxide synthase transcription. J Mol Cell Cardiol 2005;39:595-603.

769 Kopincova J, Puzserova A, Bernatova I: L-name in the cardiovascular system - nitric oxide synthase activator? Pharmacol Rep 2012;64:511-520.

770 Nakane M, Hsieh G, Miller LN, Chang R, Terranova MA, Moreland RB, Kolasa T, Brioni JD: Activation of soluble guanylate cyclase causes relaxation of corpus cavernosum tissue: Synergism of nitric oxide and yc-1. Int J Impot Res 2002;14:121-127.

771 Martin E, Lee YC, Murad F: Yc-1 activation of human soluble guanylyl cyclase has both heme-dependent and heme-independent components. Proc Natl Acad Sci U S A 2001;98:12938-12942.

772 Tesfamariam B, Halpern W: Endothelium-dependent and endothelium-independent vasodilation in resistance arteries from hypertensive rats. Hypertension 1988;11:440-444.

773 Feletou M, Huang Y, Vanhoutte PM: Vasoconstrictor prostanoids. Pflugers Arch 2010;459:941-950.

774 Schror K: Thromboxane a2 and platelets as mediators of coronary arterial vasoconstriction in myocardial ischaemia. Eur Heart J 1990;11 Suppl B:27-34.
775 Sparks MA, Makhanova NA, Griffiths RC, Snouwaert JN, Koller BH, Coffman TM: Thromboxane receptors in smooth muscle promote hypertension, vascular remodeling, and sudden death. Hypertension 2013;61:166-173.
776 Karthikeyan VJ, Blann AD, Baghdadi S, Lane DA, Gareth Beevers D, Lip GY: Endothelial dysfunction in hypertension in pregnancy: Associations between circulating endothelial cells, circulating progenitor cells and plasma von willebrand factor. Clin Res Cardiol 2011;100:531-537.
777 Miggin SM, Kinsella BT: Expression and tissue distribution of the mrnas encoding the human thromboxane a2 receptor (tp) alpha and beta isoforms. Biochim Biophys Acta 1998;1425:543-559.
778 Namba T, Sugimoto Y, Hirata M, Hayashi Y, Honda A, Watabe A, Negishi M, Ichikawa A, Narumiya S: Mouse thromboxane a2 receptor: Cdna cloning, expression and northern blot analysis. Biochem Biophys Res Commun 1992;184:1197-1203.
779 Kerage D, Brindley DN, Hemmings DG: Review: Novel insights into the regulation of vascular tone by sphingosine 1-phosphate. Placenta 2013;35 Suppl:S86-92.
780 Zuccarello M, Sasaki T, Kassell NF, Yamashita M: Effect of intracisternal thromboxane a2 analogue on cerebral artery permeability. Acta Neurochir (Wien) 1988;90:144-151.
781 Lai YJ, Pullamsetti SS, Dony E, Weissmann N, Butrous G, Banat GA, Ghofrani HA, Seeger W, Grimminger F, Schermuly RT: Role of the prostanoid ep4 receptor in iloprost-mediated vasodilatation in pulmonary hypertension. Am J Respir Crit Care Med 2008;178:188-196.
782 Camerer E, Regard JB, Cornelissen I, Srinivasan Y, Duong DN, Palmer D, Pham TH, Wong JS, Pappu R, Coughlin SR: Sphingosine-1-phosphate in the plasma compartment regulates basal and inflammation-induced vascular leak in mice. J Clin Invest 2009;119:1871-1879.
783 Fukuhara S, Sakurai A, Sano H, Yamagishi A, Somekawa S, Takakura N, Saito Y, Kangawa K, Mochizuki N: Cyclic amp potentiates vascular endothelial cadherin-mediated cell-cell contact to enhance endothelial barrier function through an epac-rap1 signaling pathway. Mol Cell Biol 2005;25:136-146.
784 Lum H, Jaffe HA, Schulz IT, Masood A, RayChaudhury A, Green RD: Expression of pka inhibitor (pki) gene abolishes camp-mediated protection to endothelial barrier dysfunction. Am J Physiol 1999;277:C580-588.
785 Moy AB, Bodmer JE, Blackwell K, Shasby S, Shasby DM: Camp protects endothelial barrier function independent of inhibiting mlc20-dependent tension development. Am J Physiol 1998;274:L1024-1029.
786 Stelzner TJ, Weil JV, O'Brien RF: Role of cyclic adenosine monophosphate in the induction of endothelial barrier properties. J Cell Physiol 1989;139:157-166.
787 Tuder RM, Cool CD, Yeager M, Taraseviciene-Stewart L, Bull TM, Voelkel NF: The pathobiology of pulmonary hypertension. Endothelium. Clin Chest Med 2001;22:405-418.
788 Schnermann J, Traynor T, Pohl H, Thomas DW, Coffman TM, Briggs JP: Vasoconstrictor responses in thromboxane receptor knockout mice: Tubuloglomerular feedback and ureteral obstruction. Acta Physiol Scand 2000;168:201-207.

789 Ashina K, Tsubosaka Y, Nakamura T, Omori K, Kobayashi K, Hori M, Ozaki H, Murata T: Histamine induces vascular hyperpermeability by increasing blood flow and endothelial barrier disruption in vivo. PLoS One 2015;10:e0132367.

790 Itagaki K, Zhang Q, Hauser CJ: Sphingosine kinase inhibition alleviates endothelial permeability induced by thrombin and activated neutrophils. Shock 2010;33:381-386.

791 Itagaki K, Yun JK, Hengst JA, Yatani A, Hauser CJ, Spolarics Z, Deitch EA: Sphingosine 1-phosphate has dual functions in the regulation of endothelial cell permeability and ca2+ metabolism. J Pharmacol Exp Ther 2007;323:186-191.

792 Komarova YA, Mehta D, Malik AB: Dual regulation of endothelial junctional permeability. Sci STKE 2007;2007:re8.

793 Mao Q, Unadkat JD: Role of the breast cancer resistance protein (bcrp/abcg2) in drug transport-an update. Aaps J 2014.

794 Slobedman B, Cao JZ, Avdic S, Webster B, McAllery S, Cheung AK, Tan JC, Abendroth A: Human cytomegalovirus latent infection and associated viral gene expression. Future Microbiol 2010;5:883-900.

795 Jarvis MA, Nelson JA: Mechanisms of human cytomegalovirus persistence and latency. Front Biosci 2002;7:d1575-1582.

796 Grahame-Clarke C: Human cytomegalovirus, endothelial function and atherosclerosis. Herpes 2005;12:42-45.

797 Kyto V, Vuorinen T, Saukko P, Lautenschlager I, Lignitz E, Saraste A, Voipio-Pulkki LM: Cytomegalovirus infection of the heart is common in patients with fatal myocarditis. Clin Infect Dis 2005;40:683-688.

798 Michaelis M, Doerr HW, Cinatl J: The story of human cytomegalovirus and cancer: Increasing evidence and open questions. Neoplasia 2009;11:1-9.

799 Savva GM, Pachnio A, Kaul B, Morgan K, Huppert FA, Brayne C, Moss PA: Cytomegalovirus infection is associated with increased mortality in the older population. Aging Cell 2013;12:381-387.

800 Salomone S, Waeber C: Selectivity and specificity of sphingosine-1-phosphate receptor ligands: Caveats and critical thinking in characterizing receptor-mediated effects. Front Pharmacol 2011;2:9.

801 Zhu H, Cong JP, Mamtora G, Gingeras T, Shenk T: Cellular gene expression altered by human cytomegalovirus: Global monitoring with oligonucleotide arrays. Proc Natl Acad Sci U S A 1998;95:14470-14475.

802 Miller WE, Zagorski WA, Brenneman JD, Avery D, Miller JL, O'Connor CM: Us28 is a potent activator of phospholipase c during hcmv infection of clinically relevant target cells. PLoS One 2012;7:e50524.

803 Stropes MP, Miller WE: Signaling and regulation of g-protein coupled receptors encoded by cytomegaloviruses. Biochem Cell Biol 2004;82:636-642.

804 Smith MS, Bentz GL, Smith PM, Bivins ER, Yurochko AD: Hcmv activates pi(3)k in monocytes and promotes monocyte motility and transendothelial migration in a pi(3)k-dependent manner. J Leukoc Biol 2004;76:65-76.

805 Zaloudikova M, Herget J, Vizek M: The contractile response of isolated small pulmonary arteries induced by activated macrophages. Physiol Res 2014;63:267-270.

806 Speir E, Yu ZX, Ferrans VJ, Huang ES, Epstein SE: Aspirin attenuates cytomegalovirus infectivity and gene expression mediated by cyclooxygenase-2 in coronary artery smooth muscle cells. Circ Res 1998;83:210-216.

807 Schneider-Schaulies J, Schneider-Schaulies S: Sphingolipids in viral infection. Biol Chem 2015;396:585-595.

808 Huang RT: Sphingolipids of influenza viruses. Biochim Biophys Acta 1976;424:90-97.

809 Miccheli A, Ricciolini R, Lagana A, Piccolella E, Conti F: Modulation of the free sphingosine levels in epstein barr virus transformed human b lymphocytes by phorbol dibutyrate. Biochim Biophys Acta 1991;1095:90-92.

810 Racz A, Veresh Z, Lotz G, Bagi Z, Koller A: Cyclooxygenase-2 derived thromboxane a(2) and reactive oxygen species mediate flow-induced constrictions of venules in hyperhomocysteinemia. Atherosclerosis 2010;208:43-49.

811 Roztocil E, Nicholl SM, Davies MG: Sphingosine-1-phosphate-induced oxygen free radical generation in smooth muscle cell migration requires galpha12/13 protein-mediated phospholipase c activation. J Vasc Surg 2007;46:1253-1259.

812 Hisano Y, Kobayashi N, Yamaguchi A, Nishi T: Mouse spns2 functions as a sphingosine-1-phosphate transporter in vascular endothelial cells. PLoS One 2012;7:e38941.

813 Kim SB, Lee JH, Lee J, Shin SH, Eun HS, Lee SM, Sohn JA, Kim HS, Choi BM, Park MS, Park KI, Namgung R, Park MS: The efficacy and safety of montelukast sodium in the prevention of bronchopulmonary dysplasia. Korean J Pediatr 2015;58:347-353.

814 Margolskee DJ: Clinical experience with mk-571. A potent and specific ltd4 receptor antagonist. Ann N Y Acad Sci 1991;629:148-156.

815 Brinkmann V: Sphingosine 1-phosphate receptors in health and disease: Mechanistic insights from gene deletion studies and reverse pharmacology. Pharmacol Ther 2007;115:84-105.

816 Witt W, Jannasch A, Burkhard D, Christ T, Ravens U, Brunssen C, Leuner A, Morawietz H, Matschke K, Waldow T: Sphingosine-1-phosphate induces contraction of valvular interstitial cells from porcine aortic valves. Cardiovasc Res 2012;93:490-497.

817 Blaukat A, Barac A, Cross MJ, Offermanns S, Dikic I: G protein-coupled receptor-mediated mitogen-activated protein kinase activation through cooperation of galpha(q) and galpha(i) signals. Mol Cell Biol 2000;20:6837-6848.

818 Yao L, Arolfo MP, Dohrman DP, Jiang Z, Fan P, Fuchs S, Janak PH, Gordon AS, Diamond I: Betagamma dimers mediate synergy of dopamine d2 and adenosine a2 receptor-stimulated pka signaling and regulate ethanol consumption. Cell 2002;109:733-743.

819 Zhang M, Yang Y, Yang X, Cai J: Human cytomegalovirus infection is a novel etiology for essential hypertension. Med Hypotheses 2011;76:682-684.

820 Huang PL: Mouse models of nitric oxide synthase deficiency. J Am Soc Nephrol 2000;11 Suppl 16:S120-123.

821 de Figueiredo LF, Mathru M, Solanki D, Macdonald VW, Hess J, Kramer GC: Pulmonary hypertension and systemic vasoconstriction may offset the benefits of acellular hemoglobin blood substitutes. J Trauma 1997;42:847-854; discussion 854-846.

822 Lopez-Lopez G, Moreno L, Cogolludo A, Galisteo M, Ibarra M, Duarte J, Lodi F, Tamargo J, Perez-Vizcaino F: Nitric oxide (no) scavenging and no protecting effects of quercetin and their biological significance in vascular smooth muscle. Mol Pharmacol 2004;65:851-859.

823 Florey O, Haskard DO: Sphingosine 1-phosphate enhances fc gamma receptor-mediated neutrophil activation and recruitment under flow conditions. Journal of Immunology 2009;183:2330-2336.
824 Radu M, Chernoff J: An in vivo assay to test blood vessel permeability. J Vis Exp 2013:e50062.
825 Moitra J, Sammani S, Garcia JG: Re-evaluation of evans blue dye as a marker of albumin clearance in murine models of acute lung injury. Transl Res 2007;150:253-265.
826 Weigert R, Porat-Shliom N, Amornphimoltham P: Imaging cell biology in live animals: Ready for prime time. J Cell Biol 2013;201:969-979.
827 Nussbaum C, Bannenberg S, Keul P, Graler MH, Goncalves-de-Albuquerque CF, Korhonen H, von Wnuck Lipinski K, Heusch G, de Castro Faria Neto HC, Rohwedder I, Gothert JR, Prasad VP, Haufe G, Lange-Sperandio B, Offermanns S, Sperandio M, Levkau B: Sphingosine-1-phosphate receptor 3 promotes leukocyte rolling by mobilizing endothelial p-selectin. Nat Commun 2015;6:6416.
828 Li Y, Xie P, Sun M, Xiang B, Kang Y, Gao P, Zhu W, Ning Z, Ren T: S1pr1 expression correlates with inflammatory responses to newcastle disease virus infection. Infect Genet Evol 2015;37:37-42.
829 Liu J, Zhao J, Lee JF, Gartung A, Jawadi H, Zhang W, Lominadze D, Lee MJ: 3-amino-4-(3-hexylphenylamino)-4-oxobutyl phosphonic acid (w146), a selective antagonist of sphingosine-1-phospahte receptor subtype 1, enhances amd3100-stimulated mobilization of hematopoietic stem progenitor cells in animals. J Biochem Pharmacol Res 2013;1:197-203.
830 Hennessy EJ, Oza V, Adam A, Byth K, Castriotta L, Grewal G, Hamilton GA, Kamhi VM, Lewis P, Li D, Lyne P, Oster L, Rooney MT, Saeh JC, Sha L, Su Q, Wen S, Xue Y, Yang B: Identification and optimization of benzimidazole sulfonamides as orally bioavailable sphingosine 1-phosphate receptor 1 antagonists with in vivo activity. J Med Chem 2015;58:7057-7075.
831 Griffith OW, Kilbourn RG: Nitric oxide synthase inhibitors: Amino acids. Methods Enzymol 1996;268:375-392.
832 Garvey EP, Oplinger JA, Furfine ES, Kiff RJ, Laszlo F, Whittle BJ, Knowles RG: 1400w is a slow, tight binding, and highly selective inhibitor of inducible nitric-oxide synthase in vitro and in vivo. J Biol Chem 1997;272:4959-4963.
833 Thomsen LL, Scott JM, Topley P, Knowles RG, Keerie AJ, Frend AJ: Selective inhibition of inducible nitric oxide synthase inhibits tumor growth in vivo: Studies with 1400w, a novel inhibitor. Cancer Res 1997;57:3300-3304.
834 Srebro DP, Vuckovic SM, Savic Vujovic KR, Prostran MS: Nitric oxide synthase modulates the antihyperalgesic effect of the nmda receptor antagonist mk-801 on carrageenan-induced inflammatory pain in rats. Tohoku J Exp Med 2014;234:287-293.
835 Zhang HQ, Fast W, Marletta MA, Martasek P, Silverman RB: Potent and selective inhibition of neuronal nitric oxide synthase by n omega-propyl-l-arginine. J Med Chem 1997;40:3869-3870.
836 Kojima H, Hirotani M, Nakatsubo N, Kikuchi K, Urano Y, Higuchi T, Hirata Y, Nagano T: Bioimaging of nitric oxide with fluorescent indicators based on the rhodamine chromophore. Anal Chem 2001;73:1967-1973.
837 Kojima H, Nakatsubo N, Kikuchi K, Kawahara S, Kirino Y, Nagoshi H, Hirata Y, Nagano T: Detection and imaging of nitric oxide with novel fluorescent indicators: Diaminofluoresceins. Anal Chem 1998;70:2446-2453.

838 Hernandez F, Peluffo MC, Bas D, Stouffer RL, Tesone M: Local effects of the sphingosine 1-phosphate on prostaglandin f2alpha-induced luteolysis in the pregnant rat. Mol Reprod Dev 2009;76:1153-1164.

839 Jurisicova A, Lee HJ, D'Estaing SG, Tilly J, Perez GI: Molecular requirements for doxorubicin-mediated death in murine oocytes. Cell Death Differ 2006;13:1466-1474.

840 Nagamatsu T, Iwasawa-Kawai Y, Ichikawa M, Kawana K, Yamashita T, Osuga Y, Fujii T, Schust DJ: Emerging roles for lysophospholipid mediators in pregnancy. Am J Reprod Immunol 2014;72:182-191.

841 Johnstone ED, Chan G, Sibley CP, Davidge ST, Lowen B, Guilbert LJ: Sphingosine-1-phosphate inhibition of placental trophoblast differentiation through a g(i)-coupled receptor response. J Lipid Res 2005;46:1833-1839.

APPENDIX

Included in this appendix is the copyright permission (emails/documents) obtained from the authors and journals to use the following figures in my thesis. The articles from which the original figures were obtained from are highlighted in the specific figure legends above.

1. Figures 1.7, 1.8 and 1.9: permission was granted by Dr. Sarah Yuan (author) and Morgan & Claypool Publishers.
2. Figure 1.14: permission was granted by Dr. Teresa Compton and Elsevier
3. Figure 1.15: permission was granted by Dr. Rajiv Khanna and the American Society for Microbiology

UNIVERSITY OF ALBERTA

Daniel Kerage <dkerage@ualberta.ca>

Permission to use your figures in my thesis

3 messages

Daniel Kerage <dkerage@ualberta.ca> Tue, Dec 1, 2015 at 3:45 AM
To: syuan@health.usf.edu

Hi Dr. Sarah Yuan,

My name is Daniel Kerage, a PhD candidate at the University of Alberta, Canada. I have enjoyed reading your work throughout my training. I am writing seeking your permission to use your figures in my thesis. These figures are irresistibly nice, and I could really appreciate if you granted me permission to use them. They are from an online book "Regulation of endothelial barrier function" chapter 4: "The endothelial barrier". I could like to use Figs 14, 16 and 20.
Please let me know whether my request is possible.

Sincerely
Daniel

Yuan, Sarah <syuan@health.usf.edu> Tue, Dec 1, 2015 at 1:31 PM
To: Daniel Kerage <dkerage@ualberta.ca>

Dear Daniel,

I don't have any problem with your using the figures in my book for your thesis as long as you cite or acknowledge the source of publication.

Good luck for your thesis defense.

Sarah Yuan, M.D., Ph.D.
Professor and Chair
Department of Molecular Pharmacology & Physiology
Professor of Surgery
Deriso Endowed Chair in Cardiovascular Disease
University of South Florida Morsani College of Medicine
12901 Bruce B. Downs Blvd., MDC 8
Tampa, FL 33612
813-974-1554 (Administrative Assistant Suzanne McMahon)
syuan@health.usf.edu

From: Daniel Kerage <dkerage@ualberta.ca>
Date: Tuesday, December 1, 2015 at 5:45 AM
To: Sarah Yuan <syuan@health.usf.edu>
Subject: Permission to use your figures in my thesis
[Quoted text hidden]

Daniel Kerage <dkerage@ualberta.ca> Tue, Dec 1, 2015 at 3:46 PM
To: "Yuan, Sarah" <syuan@health.usf.edu>

Great. Yes, the figures will be referenced accordingly. Thank you so much.

Sincerely
Daniel
[Quoted text hidden]

Daniel Kerage <dkerage@ualberta.ca>

Permission to use your figures in my thesis

6 messages

Daniel Kerage <dkerage@ualberta.ca> Mon, Feb 1, 2016 at 4:39 AM
To: cho@morganclaypool.com
Cc: info@morganclaypool.com

Hi Mr. Joe Cho,

My name is Daniel Kerage from the University of Alberta, Canada. I have appreciated and enjoyed reading the work that is published by Morgan & Claypool Publishers throughout my training. I am writing seeking your permission to use the figures published by your company in my PhD thesis. These figures are irresistibly nice, and I could really appreciate if you granted me permission to use them. They are from an online book "Regulation of endothelial barrier function" chapter 4: "The endothelial barrier". I could like to use Figs 14, 16 and 20.

Here is the link to the book: http://www.ncbi.nlm.nih.gov/books/NBK54116/

Please let me know whether my request is possible.

Sincerely

Daniel.

Joe Cho <cho@morganclaypool.com> Mon, Feb 1, 2016 at 5:49 AM
To: Daniel Kerage <dkerage@ualberta.ca>, Jovan Carreon <carreon@morganclaypool.com>
Cc: "info@morganclaypool.com" <info@morganclaypool.com>

Daniel,
Thank you for your kind request and also your feedback regarding Sarah Yuan and Robert Rigor's book. I have cc:Ed here Jovan our Permissions Manager. He can send you the form and walk you through the process for obtaining permission. You certainly will have permission, we would just like to document the details of the new work in which you plan to use these figures. Best of luck to you Daniel and thank you again for your letter,
Joe Cho

Sent from my iPhone
[Quoted text hidden]

Daniel Kerage <dkerage@ualberta.ca> Mon, Feb 1, 2016 at 8:28 AM
To: Joe Cho <cho@morganclaypool.com>
Cc: Jovan Carreon <carreon@morganclaypool.com>, "info@morganclaypool.com" <info@morganclaypool.com>

Great, thanks Joe.

Daniel
[Quoted text hidden]

Daniel Kerage <dkerage@ualberta.ca> Thu, Feb 4, 2016 at 4:02 PM
To: Joe Cho <cho@morganclaypool.com>
Cc: Jovan Carreon <carreon@morganclaypool.com>, "info@morganclaypool.com" <info@morganclaypool.com>

Kindly can I be helped on this, my deadline for thesis submission is getting close.

Thanks
Daniel
[Quoted text hidden]

Jovan Carreon <carreon@morganclaypool.com> Fri, Feb 5, 2016 at 10:26 AM
To: Daniel Kerage <dkerage@ualberta.ca>, Joe Cho <cho@morganclaypool.com>
Cc: info@morganclaypool.com

Dear Daniel Kerage:

Thank you for your email. After reviewing the details of your intended use of figures 14, 16, and 20 from chapter 4 of our title, *Regulation of Endothelial Barrier Function* for academic purposes, I'm pleased to grant you permission to reuse the material in your PhD thesis at University of Alberta, Canada. Please treat this email as an official approval from Morgan & Claypool Publishers. Thank you for your patience, and best of luck with your thesis.

Best regards,

Jovan

--

Jovan Carreon

Editorial Assistant

Morgan & Claypool Publishers

1210 Fifth Ave. Ste. 250

San Rafael, CA 94901

carreon@morganclaypool.com

(415) 785-8003

From: Daniel Kerage [mailto:dkerage@ualberta.ca]
Sent: Thursday, February 4, 2016 3:02 PM
To: Joe Cho <cho@morganclaypool.com>
Cc: Jovan Carreon <carreon@morganclaypool.com>; info@morganclaypool.com
Subject: Re: Permission to use your figures in my thesis

[Quoted text hidden]

Daniel Kerage <dkerage@ualberta.ca> Fri, Feb 5, 2016 at 10:45 AM

To: Jovan Carreon <carreon@morganclaypool.com>
Cc: Joe Cho <cho@morganclaypool.com>, "info@morganclaypool.com" <info@morganclaypool.com>

Thank you Jovan, greatly appreciated.

Daniel
[Quoted text hidden]

UNIVERSITY OF ALBERTA

Daniel Kerage <dkerage@ualberta.ca>

Permission to use your figure for my thesis

9 messages

Daniel Kerage <dkerage@ualberta.ca> Fri, Dec 4, 2015 at 5:37 AM
To: tcompton@wisc.edu

Hi Dr. Teresa Compton,

My name is Daniel Kerage, a PhD candidate at the University of Alberta, Canada. I have enjoyed reading your work throughout my training. I am writing seeking your permission to use your figure in my thesis. It is a very nice figure and I could really appreciate if you granted me permission to use it.

The figure is from "**Receptors and immune sensors: the complex entry path of human cytomegalovirus**-2004", and I could like to use Figure 1.

Please let me know whether my request is possible, with the promise to reference the figure accordingly.

Sincerely
Daniel.

Mail Delivery Subsystem <mailer-daemon@googlemail.com> Fri, Dec 4, 2015 at 5:37 AM
To: dkerage@ualberta.ca

Delivery to the following recipient failed permanently:

tcompton@wisc.edu

Technical details of permanent failure:
Google tried to deliver your message, but it was rejected by the server for the recipient domain wisc.edu by smtp.wiscmail.wisc.edu. [144.92.197.138].

The error that the other server returned was:
550 5.1.1 unknown or illegal alias <http://kb.wisc.edu/wiscmail/page.php?id=3998#alias>: tcompton@wisc.edu

----- Original message -----

DKIM-Signature: v=1; a=rsa-sha256; c=relaxed/relaxed;
d=ualberta-ca.20150623.gappssmtp.com; s=20150623;
h=mime-version:date:message-id:subject:from:to:content-type;
bh=v08RO/yH+NDnZh8YUNJlxZzBkazFm70XUw2dOvm1h4U=;
b=yZY5xHelyMhLfd5AbXH6i59d2Czfn5/kCzFoN2+kdMq/ktc4NhthzfJmPs9LmwkvlT
sXqPkUHW4CaOpnJ1OTzW3blHradyx75SClR5EzZYrx6TJwQlYpWF2LhGFmui7Zl7hv5
PGNOyolLNsfrXRECvLtHQ5MRC+PoBnh7b+KKbjuy8kQGO6mbTzAMdEuEMJ100+/TkPeE
DfzJr1xwF/ilK6n1EMM6Z97lQStoDo7HdAKmxv5stbZPGhl8rsNJDXDqXTtXeo3wdlgZ
hMti6UtMnAqNkpwawlGgbTAaNLX3hq9DtJThzhtnVsqrPcIztRAPmPtxT1FDgAANlSJg
/gOw==
X-Google-DKIM-Signature: v=1; a=rsa-sha256; c=relaxed/relaxed;
d=1e100.net; s=20130820;
h=x-gm-message-state:mime-version:date:message-id:subject:from:to
:content-type;

bh=v08RO/yH+NDnZh8YUNJlxZzBkazFm70XUw2dOvm1h4U=;
b=cek7Z96AVsqe1O+Q55rAnZjMbF037b31KVYa+o3hkM9azdSM6tM4j20VognloWbGRA
44AvH7HrJclkhqv7JdgMPgSV2yUNyth+uEtcNJaYYH5SgVr9mdlkNnMtclbp9nnoblW4
eB8xHAXELf2+WQFDNz5ynkWRWYo4PxwZtoim+mobdZ5ztVx+QdfSa8+43LqLXVbRxyac
iJeZoTYLx9LE9rpZc0jsh0y5przDTPglmkTXl3JweyAeQwu9p9fB6e9NfqrLD/5lB09X
ujJeTl8a6vaK1xLp4ul0kldpTVlln74DqUotZxSou6iAOzVJSSyMAU8P7SIRWciGVAtt
bKHg==
X-Gm-Message-State: ALoCoQm6mDB+cH+dC72f+1TvAvUiEFdenMDjQ5pFeCSdNTMBgKc
7mKOA75TmreCpdxgVn/KjnY3u
MIME-Version: 1.0
X-Received: by 10.13.204.198 with SMTP id o189mr10695871ywd.288.1449232663658;
Fri, 04 Dec 2015 04:37:43 -0800 (PST)
Received: by 10.129.75.206 with HTTP; Fri, 4 Dec 2015 04:37:43 -0800 (PST)
Date: Fri, 4 Dec 2015 05:37:43 -0700
Message-ID: <CAGjFe=hdatvYeWnk2bJaPyUxJYi1DeqLpNv0T5VC2WngbdG2zw@mail.gmail.com>
Subject: Permission to use your figure for my thesis
From: Daniel Kerage <dkerage@ualberta.ca>
To: tcompton@wisc.edu
Content-Type: multipart/alternative; boundary=001a114f1a4a1d8f87052611c61d

Hi Dr. Teresa Compton,

My name is Daniel Kerage, a PhD candidate at the University of Alberta, Canada. I have enjoyed reading your work throughout my training. I am writing seeking your permission to use your figure in my thesis. It is a very nice figure and I could really appreciate if you granted me permission to use it.

The figure is from "*Receptors and immune sensors: the complex entry path of human cytomegalovirus*-2004", and I could like to use Figure 1.
[Quoted text hidden]

Daniel Kerage <dkerage@ualberta.ca> Fri, Dec 4, 2015 at 5:43 AM
To: teresa.compton@biogenidec.com

Hi Dr. Compton,

Please see my email below it bounced when I sent to your previous station.

Thanks
Daniel
---------- Forwarded message ----------
From: **Daniel Kerage** <dkerage@ualberta.ca>
Date: Fri, Dec 4, 2015 at 5:37 AM
Subject: Permission to use your figure for my thesis
[Quoted text hidden]

Mail Delivery Subsystem <mailer-daemon@googlemail.com> Fri, Dec 4, 2015 at 5:43 AM
To: dkerage@ualberta.ca

Delivery to the following recipient failed permanently:

teresa.compton@biogenidec.com

Technical details of permanent failure:
Google tried to deliver your message, but it was rejected by the server for the recipient domain biogenidec.com by us-smtp-inbound-2.mimecast.com. [205.139.110.242].

The error that the other server returned was:
550 Invalid Recipient - https://community.mimecast.com/docs/DOC-1369#550

----- Original message -----

DKIM-Signature: v=1; a=rsa-sha256; c=relaxed/relaxed;
d=ualberta-ca.20150623.gappssmtp.com; s=20150623;
h=mime-version:in-reply-to:references:date:message-id:subject:from:to
:content-type;
bh=3E4SNgYKnJk01DFy2bzg3OAhQzSdTK7C2tw3IbaR6fg=;
b=XhZR1MrJuFU0THy7NVXv6epN1x815kXLqxMMvjAN5WRcbEDwBB4yLF2+dl4J2Zg/nO
Q2ulMYYAe53SRAuYDGAePeOOKvkfQ8itT6aTV+Y7pqWsBauoeAqzycuje2HN0IzeglW+
OSIEFueQ45KAChf1Uus4bxNTGYR3lHUezXAZ24w4qn0cw4ixXRlUCgMxbhW90nUhAHze
erKAESdnp+bXKt/zWeNmpHy7vnGKKQ036gD7Sv37ouUWsXKd6VTWuvdFHKDkX9N8Mb4w
BkOFvP4tv2eGhM1x+KoWmBJXnivxttjFSaQQCxFb8yJVgDPq5L1NjsnE6BE9vQkIX6gs
O8DQ==
X-Google-DKIM-Signature: v=1; a=rsa-sha256; c=relaxed/relaxed;
d=1e100.net; s=20130820;
h=x-gm-message-state:mime-version:in-reply-to:references:date
:message-id:subject:from:to:content-type;
bh=3E4SNgYKnJk01DFy2bzg3OAhQzSdTK7C2tw3IbaR6fg=;
b=glkZCgwezSNveBChqBYbR6F4s2lmqd+bXvEBjSF2VcuNJFJvAEO5/0PUAG6Szxnef3
j37hNevMfsIYRp1TeFO8Od4YqVPruQpUSOkvNglDggWgsjdy/yI9FAhDmm9VEPAfc4q0
c8gZZzKQ76rKVC/sMtPGaIZ171Zdi0+wGcUz0jmIh2TmAj3zMJ+RNRbCnsItHmQGYdY8
1lqsM05lozkVqxVKhiHT3hsHkOSTxQbAgfsPbTs9gQ103MPY5/ezoTyigBm/CiqvSJ60
TOLpxvX17jXP+lnrJ3+vRzgYMI2mupq+7hlwcZVxc3eso1rzvtHO11FyMZajxzcpY/pO
fX7g==
X-Gm-Message-State: ALoCoQm7xb2yMPHE0Qs2uAadtcWFAApnvZ4SBvdEBV01EjDXZ76gAwg7fTZV
nw/moXmPHWAzNKQf
MIME-Version: 1.0
X-Received: by 10.13.247.129 with SMTP id h123mr12041689ywf.321.1449233027812;
Fri, 04 Dec 2015 04:43:47 -0800 (PST)
Received: by 10.129.75.206 with HTTP; Fri, 4 Dec 2015 04:43:47 -0800 (PST)
In-Reply-To: <CAGjFe=hdatvYeWnk2bJaPyUxJYi1DeqLpNv0T5VC2WngbdG2zw@mail.gmail.com>
References: <CAGjFe=hdatvYeWnk2bJaPyUxJYi1DeqLpNv0T5VC2WngbdG2zw@mail.gmail.com>
Date: Fri, 4 Dec 2015 05:43:47 -0700
Message-ID: <CAGjFe=g7XO9+gd+NkeRDUS+nAvg6bWa-wbi01=AAktvsUfiwWg@mail.gmail.com>
Subject: Fwd: Permission to use your figure for my thesis
From: Daniel Kerage <dkerage@ualberta.ca>
To: teresa.compton@biogenidec.com
Content-Type: multipart/alternative; boundary=94eb2c0826e4d20925052611dbeb

Hi Dr. Compton,

Please see my email below it bounced when I sent to your previous station.

Thanks
Daniel
---------- Forwarded message ----------
From: Daniel Kerage <dkerage@ualberta.ca>
Date: Fri, Dec 4, 2015 at 5:37 AM
Subject: Permission to use your figure for my thesis

To: tcompton@wisc.edu

Hi Dr. Teresa Compton,

My name is Daniel Kerage, a PhD candidate at the University of Alberta, Canada. I have enjoyed reading your work throughout my training. I am writing seeking your permission to use your figure in my thesis. It is a very nice figure and I could really appreciate if you granted me permission to use it.

The figure is from "*Receptors and immune sensors: the complex entry path of human cytomegalovirus*-2004", and I could like to use Figure 1.
[Quoted text hidden]

Daniel Kerage <dkerage@ualberta.ca> Fri, Dec 4, 2015 at 5:48 AM
To: teresa.compton@biogenidec.com

---------- Forwarded message ----------
From: **Daniel Kerage** <dkerage@ualberta.ca>
[Quoted text hidden]

Mail Delivery Subsystem <mailer-daemon@googlemail.com> Fri, Dec 4, 2015 at 5:48 AM
To: dkerage@ualberta.ca

Delivery to the following recipient failed permanently:

teresa.compton@biogenidec.com

Technical details of permanent failure:
Google tried to deliver your message, but it was rejected by the server for the recipient domain biogenidec.com by us-smtp-inbound-1.mimecast.com. [205.139.110.242].

The error that the other server returned was:
550 Invalid Recipient - https://community.mimecast.com/docs/DOC-1369#550

---- Original message ----

DKIM-Signature: v=1; a=rsa-sha256; c=relaxed/relaxed;
d=ualberta-ca.20150623.gappssmtp.com; s=20150623;
h=mime-version:in-reply-to:references:date:message-id:subject:from:to
:content-type;
bh=YyKD8nCEk75Ux1xHlFt8El5Zkcy5G5OnfZ+FO0b/KRI=;
b=E8ElSi3vRtYjhtfQqo06Dj6ET4trOv2b8ON3AGSpRAtlwHh7OAPEWfktnDgw1lwnzG
VnLjJ+A/Gony9BU/5EocyLnKliiqBqmQ0ey2L6+BI8Vy0Qk8MOPwaE4iCpZqzz/k8JWZ
3soTi8y7+nMEIplYXmCdBDfQ4RbLj3dExtjf3sJkfi8utkFeW8GYdu7uJ+m+cxpF8lwT
DMJczigmwg2vsMBs2/CdhIy7xjREwKcIVzFrsFu71yPOXHYjzKaD4PXJ+BT6J1IJjhz5
XhF96rXwfKTH1EiuqVKe4i+YXKTNAbC3SPBWEGr/hECtqoSEYM6C11YVhK2S2gHBBp4G
j8Bw==
X-Google-DKIM-Signature: v=1; a=rsa-sha256; c=relaxed/relaxed;
d=1e100.net; s=20130820;
h=x-gm-message-state:mime-version:in-reply-to:references:date
:message-id:subject:from:to:content-type;

bh=YyKD8nCEk75Ux1xHlFt8El5Zkcy5G5OnfZ+FO0b/KRI=;
b=Y7V0QiJyOXM/O/YIf9eizICDrKUqI8jfh13UJX0e5CnorsZKjznRcJzJogtmCIDxkO
f9RsJSVSYskjLXyPdGRIK9xyEe39a2PZQIO56zbrOXwJBjJLEzP2QV5fT+TPKLDrRdF1
WebIfp5GzxkQK9YN+n0VxH953iIP2O2Xyq4xLIoLXxwkd+P/VV4pvMZAQt7ezaXzwHwM
1gv8rFeyIKRIaAYB6XXK6FIjhamb1UoJ8FC7P1OCsSqDeGIZbYmrCRK05IDmFzEKzIFn
syqp0+tneRWEAQz/qYmPPXM/F0OrbI7cN0CTNP8iSuV13IFIrdhJNI+yJP+PEoWYXfS9
mfTA==
X-Gm-Message-State: ALoCoQmRMvhEJuXiEgnlddSahlfTWp99tKSWdNAn8issempmViXV3R2+
cVMbANlxrPyn40P/yA5k
MIME-Version: 1.0
X-Received: by 10.13.247.129 with SMTP id h123mr12060836ywf.321.1449233315318;
Fri, 04 Dec 2015 04:48:35 -0800 (PST)
Received: by 10.129.75.206 with HTTP; Fri, 4 Dec 2015 04:48:35 -0800 (PST)
In-Reply-To: <CAGjFe=g7XO9+gd+NkeRDUS+nAvg6bWa-wbi01=AAktvsUfiwWg@mail.gmail.com>
References: <CAGjFe=hdatvYeWnk2bJaPyUxJYi1DeqLpNv0T5VC2WngbdG2zw@mail.gmail.com>
<CAGjFe=g7XO9+gd+NkeRDUS+nAvg6bWa-wbi01=AAktvsUfiwWg@mail.gmail.com>
Date: Fri, 4 Dec 2015 05:48:35 -0700
Message-ID: <CAGjFe=jyTAbRuq8qEZYNMpCC=0JSU7FsO2SPXnwcy2SzDO3DwQ@mail.gmail.com>
Subject: Fwd: Permission to use your figure for my thesis
From: Daniel Kerage <dkerage@ualberta.ca>
To: teresa.compton@biogenidec.com
Content-Type: multipart/alternative; boundary=94eb2c0826e4f4f8b2052611ec6b

---------- Forwarded message ----------
From: Daniel Kerage <dkerage@ualberta.ca>
Date: Fri, Dec 4, 2015 at 5:43 AM
Subject: Fwd: Permission to use your figure for my thesis
To: teresa.compton@biogenidec.com

Hi Dr. Compton,

Please see my email below it bounced when I sent to your previous station.

Thanks
Daniel
---------- Forwarded message ----------
From: Daniel Kerage <dkerage@ualberta.ca>
Date: Fri, Dec 4, 2015 at 5:37 AM
Subject: Permission to use your figure for my thesis
To: tcompton@wisc.edu

Hi Dr. Teresa Compton,

My name is Daniel Kerage, a PhD candidate at the University of Alberta, Canada. I have enjoyed reading your work throughout my training. I am writing seeking your permission to use your figure in my thesis. It is a very nice figure and I could really appreciate if you granted me permission to use it.

The figure is from "*Receptors and immune sensors: the complex entry path of human cytomegalovirus*-2004", and I could like to use Figure 1.
[Quoted text hidden]

Daniel Kerage <dkerage@ualberta.ca> Mon, Feb 1, 2016 at 4:53 AM
To: teresacompton@yahoo.com

Hi Dr. Compton,

I have been trying to reach out to you using your previous contacts with little success, I just found your yahoo email address from Linkedn I hope it is the right one.

Please see my request below and advice accordingly.

Thanks
Daniel.

---------- Forwarded message ----------
From: **Daniel Kerage** <dkerage@ualberta.ca>
Date: Fri, Dec 4, 2015 at 5:37 AM
Subject: Permission to use your figure for my thesis
To: tcompton@wisc.edu

[Quoted text hidden]

Teresa Compton <teresacompton@yahoo.com> Mon, Feb 1, 2016 at 8:13 AM
To: Daniel Kerage <dkerage@ualberta.ca>

Dear Daniel,

Yes, you may use the figure. I wish you all success in your career. Good luck with your thesis defense.

With best regards,
Teresa

Teresa Compton, Ph.D.
Teresacompton@yahoo.com
mobile: 608-347-9201
www.linkedin.com/in/teresacompton/

From: Daniel Kerage <dkerage@ualberta.ca>
Date: Monday, February 1, 2016 at 6:53 AM
To: Teresa Compton <teresacompton@yahoo.com>
Subject: Fwd: Permission to use your figure for my thesis
[Quoted text hidden]

Daniel Kerage <dkerage@ualberta.ca> Mon, Feb 1, 2016 at 9:31 AM
To: Teresa Compton <teresacompton@yahoo.com>

Great, thank you so much.

Daniel
[Quoted text hidden]

Copyright Clearance Center RightsLink®

My Orders My Library My Profile

Welcome dkerage@gmail.com Log out | Help

My Orders > Orders > All Orders

License Details

Thank you very much for your order.

This is a License Agreement between Daniel Kerage ("You") and Elsevier ("Elsevier"). The license consists of your order details, the terms and conditions provided by Elsevier, and the payment terms and conditions.

Get the printable license.

License Number	3800161226286
License date	Feb 01, 2016
Licensed Content Publisher	Elsevier
Licensed Content Publication	Trends in Cell Biology
Licensed Content Title	Receptors and immune sensors: the complex entry path of human cytomegalovirus
Licensed Content Author	Teresa Compton
Licensed Content Date	January 2004
Licensed content volume number	14
Licensed content issue number	1
Number of pages	4
Type of Use	reuse in a thesis/dissertation
Portion	figures/tables/illustrations
Number of figures/tables/illustrations	1
Format	electronic
Are you the author of this Elsevier article?	No
Will you be translating?	No
Original figure numbers	Figure 1
Title of your thesis/dissertation	Probing the role of S1P in vascular tone control and the impact of CMV infection
Expected completion date	Feb 2016
Estimated size (number of pages)	1
Elsevier VAT number	GB 494 6272 12
Price	0.00 USD
VAT/Local Sales Tax	0.00 USD / 0.00 GBP
Total	**0.00 USD**

BACK

UNIVERSITY OF ALBERTA

Daniel Kerage <dkerage@ualberta.ca>

Permission to use your figure in my thesis

3 messages

Daniel Kerage <dkerage@ualberta.ca> Fri, Dec 4, 2015 at 5:20 AM
To: rajiv.khanna@qimr.edu.au

Hi Dr. Rajiv Khanna,

My name is Daniel Kerage, a PhD candidate at the University of Alberta, Canada. I have enjoyed reading your work throughout my training. I am writing seeking your permission to use your figure in my thesis. It is a very nice figure and I could really appreciate if you granted me permission to use it.

The figure is from "Immunobiology of Human Cytomegalovirus: from Bench to Bedside-2009", and I could like to use Figure 3.

Please let me know whether my request is possible, with the promise to reference the figure accordingly.

Sincerely
Daniel

Rajiv Khanna <Rajiv.Khanna@qimrberghofer.edu.au> Sat, Dec 5, 2015 at 12:22 AM
To: Daniel Kerage <dkerage@ualberta.ca>

Dear Daniel

I have no objection in reproducing the figure for your thesis.

Cheers

Rajiv

Prof. Rajiv Khanna PhD FAHMS | Coordinator, QIMR-CIVD
Editor-in-Chief, Clinical and Translational Immunology
Senior Principal Research Fellow (NH&MRC)
Group Leader, Tumour Immunology Laboratory
QIMR Berghofer Medical Research Institute
t +61 7 3362 0385 | **m** +61 448 848 202 | **f** +61 7 3845 3510
rajiv.khanna@qimr.edu.au| http://www.qimr.edu.au/
300 Herston Road, Herston QLD 4006
Locked Bag 2000 Royal Brisbane Hospital, QLD 4029

From: Daniel Kerage [dkerage@ualberta.ca]
Sent: Friday, 4 December 2015 10:20 PM
To: Rajiv Khanna
Subject: Permission to use your figure in my thesis

[Quoted text hidden]

Daniel Kerage <dkerage@ualberta.ca> Sat, Dec 5, 2015 at 12:51 AM
To: Rajiv Khanna <Rajiv.Khanna@qimrberghofer.edu.au>

Great, thank you so much.

Daniel.

[Quoted text hidden]

Daniel Kerage <dkerage@ualberta.ca>

Case #00097033 - Requesting Permission to Reuse a Figure [ref:_00D30oeGz._500a0132CGp:ref]

1 message

customercare@copyright.com <customercare@copyright.com> Mon, Feb 1, 2016 at 9:29 PM
To: "dkerage@ualberta.ca" <dkerage@ualberta.ca>

Dear Daniel,

Thank you for contacting CCC's Rightslink service.

If you see the said message after you have filled out the Rightslink order page and clicked 'Quick Price', then, yes, this grants permission for the re-use without having to complete a Rightslink order. As proof of permission, I would suggest you print a copy of the order page or a screen shot of which for documentation.

I hope this is helpful. Should you have further questions or require assistance, please feel free to let me know.

Kind regards,
Hanna

Hanna Lao
Customer Account Specialist
Copyright Clearance Center
222 Rosewood Drive
Danvers, MA 01923
www.copyright.com
+1.855.239.3415

Facebook - Twitter - LinkedIn

ref:_00D30oeGz._500a0132CGp:ref

---------- Original Message ----------
From: Daniel Kerage [dkerage@ualberta.ca]
Sent: 2/1/2016 1:29 PM
To: customercare@copyright.com
Subject: Requesting Permission to Reuse a Figure

Hi,

I was in the process of requesting permission to use a figure from " Immunobiology of Human Cytomegalovirus: from Bench to Bedside" for my doctoral thesis, and I received the following message. I wanted to confirm that this is regarded authorization before I use Fig 3 in my thesis.

ASM (American Society for Microbiology) authorizes an advanced degree candidate to republish the requested material in his/her doctoral thesis or dissertation. If your thesis, or dissertation, is to be published commercially,

then you must reapply for permission.

Please let me know ASAP.

Thanks with appreciation.

Daniel.

ref:_00D30oeGz._500a0132CGp:ref